Functional Characterization of GYF-Domain Containing Proteins

Dissertation zur Erlangung des akademischen Grades des Doktors der Naturwissenschaften (Dr. rer. nat.)

eingereicht im Fachbereich Biologie, Chemie, Pharmazie der Freien Universität Berlin

vorgelegt von Diplom-Biologin

Gesa Ines Albert

aus Tübingen

im November 2011

Diese Arbeit entstand im Zeitraum vom August 2007 bis November 2011 am Leibniz-Institut für Molekulare Pharmakologie (FMP), Berlin und der Freien Universität Berlin unter Anleitung von Prof. Dr. Christian Freund.

Erstgutachter: Prof. Dr. Christian Freund
Protein Engineering Group
Leibniz-Institut für Molekulare Pharmakologie (FMP) und
Freie Universität Berlin
Robert-Rössle-Str. 10
13125 Berlin

Zweitgutachter: Prof. Dr. Dominik N. Müller
Department of Experimental Medicine I
Nikolaus-Fiebiger-Center for Molecular Medicine
Friedrich-Alexander-Universität Erlangen-Nürnberg
Glückstraße 6
91054 Erlangen

Disputation am 20.01.2012

Für meine Familie und meine Familie im Herzen

“What happens when you lose everything
You just start again, you start all over again”

Maximo Park (Lyrics from “Apply Some Pressure”)

Table of Contents

Table of Figures

Summary

GYF-domains (standing for a conserved glycine, tyrosine, phenylalanine motif) are small adapter domains that interact with proline-rich sequences (PRS) of other proteins. Two subfamilies have been described so far that both differ in the binding behavior of the respective GYF-domain. The CD2BP2-type subfamily is named after the first GYF protein discovered, the CD2 binding protein 2. This protein was found as binding partner of the T cell adhesion molecule CD2. Independent work showed an involvement of CD2BP2 in nuclear mRNA splicing. The Smy2-type subfamily is named after the yeast suppressor of myosin 2-66. The human and mouse ortholog of Smy2 is called Grb-10 interacting GYF protein 2 (GIGYF2). Here, very little was known about the function at the beginning of this study.

The aim of this study was to characterize the two proteins GIGYF2 and CD2BP2 in different cell lines and mouse organs for a better understanding of their functional implications within the cell. Also, a conditional CD2BP2 knockout (KO) mouse was generated to primarily address the question of whether or not mice can survive without CD2BP2.

Expression analyses by a newly generated antibody against the GIGYF2 GYF-domain were performed to show the specificity of the antibody. The localization of GIGYF2 was addressed with nuclear and cytoplasmic extracts of human HeLa and rat pc12 cells, showing a cytoplasmic localization of the protein. GIGYF2 showed a ubiquitous protein expression in different mouse organs of C57BL/6 (BL6) mice with the least amounts in the kidney. Novel potential interaction partners suggested by pull-down in combination with SILAC-MS analyses were confirmed by immunofluorescence co-localization studies. Analyses in HeLa cells and the neuronal cell lines SH-SY5Y and Neuro2a showed the localization of GIGYF2 to the ER and Golgi in living cells and its co-localization with the COPII vesicle component Sec31 in fixed cells. Also, GIGYF2 was stress-dependently recruited into cytoplasmic stress granules (SGs), where it co-localized with the SG marker TIA-1. A stress-dependent co-localization with TIA-1 could also be observed in neurites of SH-SY5Y cells.

Expression analyses of CD2BP2 in mouse organs showed a ubiquitous expression at the mRNA level whereas it was mainly expressed in hematopoietic organs at the protein level. A more detailed analysis in immune cells revealed the presence of CD2BP2 in mature B and T cells, dendritic cells and macrophages. Studies in developing T cells showed the expression of CD2BP2 at double negative stage 1 (DN1) and subsequent stages.

For the generation of a conditional CD2BP2 KO mouse, a targeting vector was cloned and electroporated into 129 and BL6 strain derived murine stem cells (ES cells). Positive clones were injected into morulae and implanted into foster mothers. Only 129-derived ES cell clones gave rise to high chimeric offspring. Germline transmitted founder mice were bred with PGK- Cre deleter mice for the induction of the KO. Breedings of $CD2BP2^{+/-}$ mice resulted in no homozygous KO. Analysis of timed matings showed embryonic lethality of CD2BP2 null mice before embryonic day 10.5.

From this study, we strongly favor the hypothesis that GIGYF2 is involved in the assembly or regulation of ribonuclear protein complexes. Future studies should focus on its involvement in the transport of mRNA from the cell soma to neurites within neuronal cells.

Mice cannot survive without CD2BP2. The predominant hematopoietic expression in adult mice speaks for a major function in the immune system. Why this gene, which is expressed in all organs at RNA level, is down regulated at the protein level needs to be addressed in future studies. Also, the reason for the lethality during embryonic development will help to understand the function of this GYF-domain containing protein in more detail.

Zusammenfassung

GYF-Domänen, die nach einem konservierten Glycin, Tyrosin, Phenylalanin Motiv benannt sind, sind kleine Adapterdomänen, die mit prolinreichen Sequenzen anderer Proteinen interagieren. Bisher wurden zwei Unterklassen beschrieben, die sich im Bindungsverhalten der GYF-Domäne unterscheiden. Die CD2BP2-Typ Unterfamilie wurde nach dem CD2 bindenden Protein 2 (CD2BP2) benannt, in dem die erste GYF-Domäne identifiziert wurde. CD2BP2 erkennt die zytoplasmatischen prolinreichen Sequenzen des T Zell Adhesionsmoleküls CD2. Weitere Studien zeigten eine Beteiligung von CD2BP2 an splißosomalen Prozessen im Zellkern. Die Smy2-Typ Unterfamilie wurde nach dem Hefeprotein „Suppressor of myosin 2-66“ (Smy2) benannt. Ein zu Smy2 humanes und murines Ortholog ist das „Grb-10 interacting GYF protein 2“ (GIGYF2). Über dieses Protein war zu Beginn dieser Arbeit sehr wenig bekannt.

Im Rahmen dieser Arbeit sollten die beiden Proteine CD2BP2 und GIGYF2 in verschiedenen Zelllinien und Organen der Maus im Bezug auf ihre zelluläre Funktion charakterisiert werden. Weiterhin wurde eine konditionelle CD2BP2 Knockout (KO) Maus generiert, um die primäre Frage zu beantworten, ob Mäuse ohne CD2BP2 lebensfähig sind.

Die Spezifität eines neu hergestellten Antikörpers gegen die GYF-Domäne von GIGYF2 wurde mittels Expressionsanalysen bewiesen. Für die Untersuchung der zellulären Lokalisation von GIGYF2 wurden nukleare und zytoplasmatische Zellextrakte aus humanen HeLa Zellen und aus Ratten pc12 Zellen eingesetzt. Beide Zelltypen zeigten eine hauptsächlich zyoplasmatische Expression des Proteins. Untersuchungen an Zelllysaten verschiedener C57BL/6 (BL6) Mausorgane wiesen auf eine ubiquitäre Expression von GIGYF2 in Mausorganen hin. Am geringsten wurde das Protein in der Niere exprimiert. Vorangegangene Pull-down-Experimente in Kombination mit der massenspektrometrischen Analyse der Bindungspartner (SILAC-MS) hatten neue potentielle Interaktionspartner von GIGYF2 hervorgebracht, die mittels Kolokalisationsstudien genauer untersucht wurden. Studien in lebenden HeLa Zellen, den neuronalen Zelllinien SH-SY5Y und Neuro2a zeigten, dass GIGYF2 innerhalb der Zelle im ER und dem Golgi Apparat lokalisiert ist. In fixierten Zellen kolokalisierte GIGYF2 mit dem COPII Vesikel Protein Sec31 und wurde stressinduziert in zytoplasmatische „stress granules“ (SG) rekrutiert. Diese stressinduzierte Kolokalisation mit dem SG Markerprotein TIA-1 wurde auch in Neuriten von SH-SY5Y Zellen beobachtet.

CD2BP2 Expressionsanalysen in verschiedenen Mausorganen zeigten eine ubiquitäre Expression auf mRNA Ebene wohingegen CD2BP2 auf Proteinebene hauptsächlich in hämatopoetischen Organen gefunden wurde. Eine detaillierte Expressionsanalyse in Immunzellen detektierte CD2BP2 in reifen B und T Zellen, Dendritischen Zellen und Makrophagen. In unreifen T Zellen wurde CD2BP2 schon im frühesten Entwicklungsstadium, der doppelt negativen Phase 1, gefunden.

Zur Herstellung einer konditionellen CD2BP2 KO Maus wurde ein Zielvektor kloniert, der in murine Stammzellen der Stämme 129 und BL6 elektroporiert wurde. Daraus resultierende positive Klone wurden in Morulae injiziert und in Leihmütter implantiert. Nur die Stammzellklone des 129er Stamms führten zu hochchimären Mäusen. Mäuse, die den Zielvektor durch Keimbahntransmission in ihrem Genom integriert hatten, wurden für die Induktion des KO mit PGK-Cre Mäusen verpaart. Die Verpaarung von $CD2BP2^{+/-}$ Mäusen erbrachte keine homozygoten CD2BP2 KO Mäuse. Bei zeitlich kontrollierten Verpaarungen starben CD2BP2 KO Mäuse vor dem Embryonaltag 10,5.

Die Ergebnissen dieser Studie legen nahe, dass GIGYF2 in die Assemblierung oder Regulation von ribonuklären Proteinkomplexen involviert ist. In zukünftigen Studien sollte weiterhin die Funktion von GIGYF2 bei dem neuronalen Transport von mRNA vom Zellsoma in Neuriten untersucht werden.

Für Mäuse ist CD2BP2 offensichtlich ein essentielles Gen. Die hauptsächliche Expression von CD2BP2 in hämatopoetischen Organen adulter Mäuse spricht für eine späte Hauptfunktion im Immunsystem. Der Grund für die unterschiedliche Expression von CD2BP2 auf mRNA und Protein Ebene muß in zukünftigen Studien untersucht werden.

Der Grund für die embryonale Letalität des GYF-Domänen Proteins CD2BP2 sollte helfen, wichtige, an dieses Protein gekoppelte Prozesse innerhalb des Organismus genauer zu verstehen.

1 Introduction

GYF-domain proteins are thought to play a role in the adaptive immune system and mRNA surveillance, although the precise functions and mechanisms are still unknown.

The immune system helps the body to combat exogenous pathogens. Bacteria, viruses and other intruders are destroyed by two different immune answers of the immune system, the *innate* and the *adaptive* immune response [1]. The CD2 adhesion molecule is a surface receptor expressed on T cells. The GYF-domain of CD2BP2 binds to the proline-rich sequences (PRS) of the CD2 intracellular tail [2, 3].

The maturation of pre-mRNA, in which introns are cleaved off in an ATP-dependent process, takes place in the nucleus. Mature mRNA is subsequently transported to the cytoplasm, used for protein expression and finally degraded there. CD2BP2 was found as a member of the U5 snRNP but was absent in the catalytically active splicing complex [4].

Animal models offer a broad opportunity of analyses that cannot be addressed by any other technique. Specific alterations of genes or gene segments allow observations of complex features from different cell types or organs. “Cells have no blood pressure” [5] describes literally the limitations of cell culture analyses. Here, targeted knockout analysis has been performed to address the questions of whether or not mice can survive without CD2BP2.

Besides some potential interaction partners, little is known about the human GYF-domain protein GIGYF2. Splicing in the nucleus was speculated to be the major function of the protein [6]. Basic functional analyses of GIGYF2 will be described here to investigate the cellular interaction and localization in the cell.

In this introduction, I will review the principles of protein-protein interactions carried out by proline-rich sequences (PRS) and their interaction partners, and the structural information that can be drawn from the interaction. Background information about cellular systems in which putative functions of GYF proteins have been described follows. These are the immune system, mRNA splicing and the formation of cytoplasmic granules and transport via COPII vesicles. Finally, the history and technical development of targeted mouse mutations will be reviewed here.

1.1 Molecular Interactions of GYF domains

Protein-protein interactions are key elements of cellular behavior, and are often mediated by short peptide motifs. PRS are abundant recognition motifs in eukaryotes. Several protein domains are known to interact with PRSs. Src homology 3 (SH3) [7, 8], domains with conserved Trp-Trp motives (WW) [9, 10], Enabled/VASP homology (EVH1) [11, 12], Ubiquitin E2 variant (UEV) [13], Profilin [14] and the domains with conserved Gly-Tyr-Phe motifs (GYF) [2, 3] all interact with particular motifs comprising several prolines.

While SH3 domains have the highest distribution in mice and human proteins with 163 and 332 domain variants, respectively, there are only a few GYF domain proteins discovered thus far (Table 1.1).

ORGANISM	SH3	WW	EVH1	GYF
Saccharomyces cerevisiae/ Schizosaccharomyces pombe	25	5	1	5
Caenorhabditis elegans	66	18	2	0
Drosophila melanogaster	90	27	5	2
Mus musculus	163	39	16	3
Homo sapiens	332	80	20	3

Table 1.1 **Distribution of SH3, WW, EVH1 and GYF domains within eukaryotes**. SH3 domains form the family with the highest distribution, whereas there are only few GYF domain proteins found yet (Adapted from [12, 15]).

Several studies showed the implication of PRS on the regulation of the catalytic activity of proteins, on signaling pathways and on the specific localization of proteins to certain subcellular compartments [16-19]. In addition to these functions, PRS are important for coordinate assembly of large protein complexes [20].

PRSs preferentially form polyproline type II helices (PPII), a left-handed transient helix with a periodicity of 3 (Figure 1.1). The interaction between proline-recognition domains (PRDs) and their targets is mostly characterized by low affinity and moderate specificity, which favors transient binding [12, 20-23]. PRDs often bind to unstructured regions of a protein leading to conformational changes [24]. Although the binding is transient, it is still specific.

All interactions of PRSs and PRDs are mediated by charge-complementarity between charged residues of the domain (shown in green in Figure 1.1) and positively charged residues of the PRSs (shown in red). The specificity region within a domain family is less conserved than residues outside the binding pocket [7, 20]. While the GYF and WW domains form one prominent hydrophobic pocket the SH3 domain forms two more shallow hydrophobic

grooves. That is why the binding motif of GYF and WW domains comprises a x-P-P-x sequence whereas the SH3 domain converges on the motif P-x-x-P.

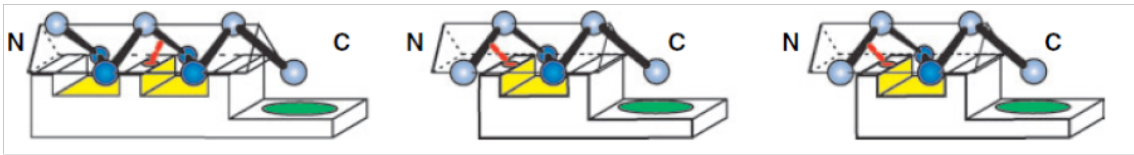

Figure 1.1. **Cartoon of the three PRD domains SH3 (left), WW (middle) and GYF (right), bound to their proline-rich ligands**. Prolines of the ligands (dark blue) bind to aromatic residues of the domain that form an aromatic cradle (yellow). The green patch symbolizes negatively charged residues of the domain. The red line indicates a conserved hydrogen bond [12] [23].

1.2 The GYF-domain Family

Yeast-two hybrid screens with an activated T cell library first discovered the interaction between the T cell adhesion molecule CD2 and the CD2 binding protein 2 (CD2BP2) [2, 3]. The human protein CD2BP2 (KIAA1178 or U5-52K) consists of 341 amino acids (AA) and has a molecular weight of 37 kD. Because of its acidic nature (pI of 4.49), it has an apparent molecular weight of 52 kD in an SDS-PAGE. Several serine phosphorylations (position 46, 49, 118, 194 and 195) could also influence the running behavior [15].

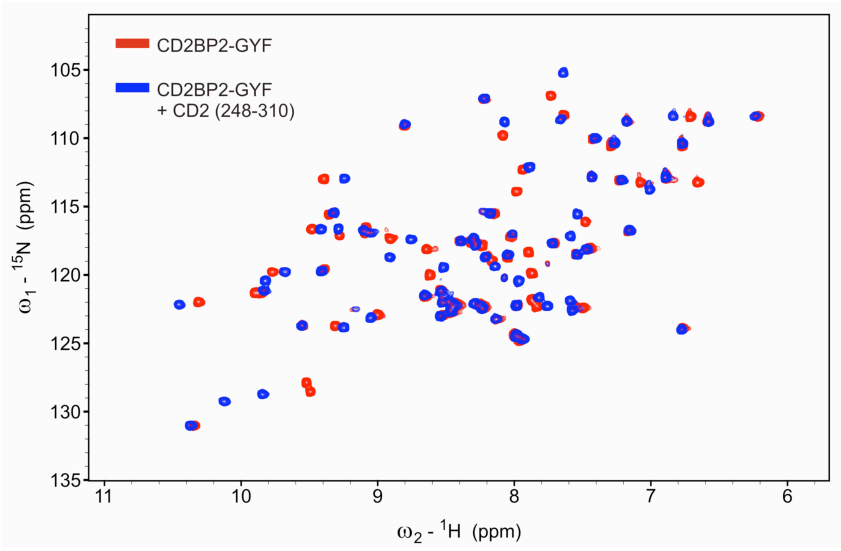

Figure 1.2. **^{15}N-^{1}H NMR correlation spectrum of the CD2BP2 GYF-domain** (AA 256-341) before (red) and after (blue) addition of equimolar amounts of the cytoplasmic CD2-tail (AA 221-282). The ^{15}N-^{1}H correlation spectrum shows the chemical shift changes in the labeled CD2BP2 GYF-domain (AA 256-341) upon addition of equimolar amounts of unlabeled CD2 peptide (AA 221-282). The CD2-fragment has two PPPGHR regions that mediate this interaction. Adapted from [3].

An NMR spectrum revealed that the PRS of the CD2 tail interact with the conserved GYF-domain fold in the C-terminus of CD2BP2 (Figure 1.2).

Based on the CD2 binding sequence, novel recognition motifs were identified that share a R/K/G x x PPG x (R/K) sequence. This subgroup is now classified as CD2BP2-type GYF domain family [6, 25]. Peptide substitution analyses determined two possible binding

consensi of this subfamily. Interactions such as the CD2/ CD2BP2 require positively charged residues flanking the PPG core (PPG x (R/K)) while negatively charged amino acids (AA) surrounding the binding site are disfavored. On the other hand, random approaches using phage display converged on a PPGW motif that is rarely present in natural proteins. However, a somewhat more relaxed consensus containing F/Y/M/L directly C-terminal to the PPG core motif is frequently present in eukaryotic proteins and presumably represents a larger class of natural ligands [22].

BLAST searches with the CD2BP2-GYF sequence as template revealed GYF-domains in proteins of different species. The majority of GYF-domain containing proteins contain an aspartate instead of a tryptophan at position 22 of the GYF-domain and the loop between β1 and β2 is shorter (Figure 1.3). This subfamily was defined as Smy2-type subfamily, named after the yeast protein suppressor of myosin 2-66 (Smy2) and binds to the ligand consensus motif PPGϕ where ϕ can be any hydrophobic AA except for tryptophan [22].

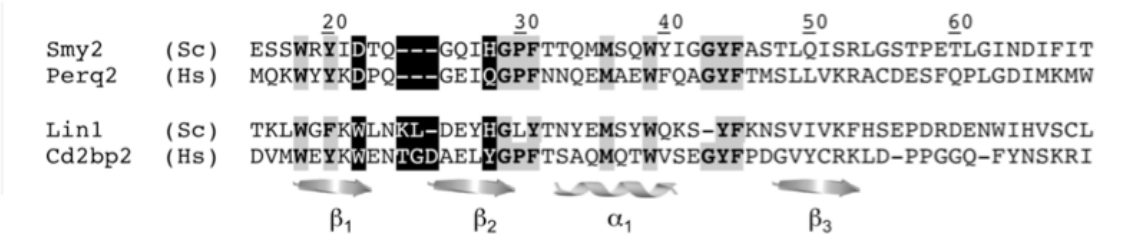

Figure 1.3. **Comparison of the SMY2-type (top) and CD2BP2-type subfamily of GYF-domain proteins.** The GYF-domain of the Smy2-type family (here represented by the yeast proteins Smy2 and the human ortholog Perq2 (GIGYF2)) and CD2BP2-type family (with the yeast protein Lin1 and the human ortholog CD2BP2) feature differences that result in different binding behavior. The Smy2-type family has an aspartate instead of a tryptophan at position 22 and a shorter loop between the β_1 and β_2 [26].

In summary, the GYF-domain family shows the characteristics of PRS-dependent interactions, where residues flanking the core motif contribute to specificity. The family can be further discriminated into two different subfamilies that often mediate similar binding functions. The CD2BP2-type family preferentially binds either to the motif PPPGx (R/K) or PPGW, the Smy2-type family binds to the motif PPGϕ. The PPGW and PPGϕ motifs are independent of charge but dominated by hydrophobic interactions. The CD2BP2-type subfamily is present in evolutionary distant species and its GYF domain is conserved from yeast to men. A similar conservation is seen for Smy2-type GYF domains, indicating an early separation in evolution for the two subfamilies [27].

1.3 The Role of GYF-domains in the Immune System

The first line of defense is the innate immune system, which is already fully developed at birth. Several mechanisms have been developed that combat invaders in a non-specific manner. Natural killer cells as members of the innate immune system defend pathogens by the release of cytolytic proteins that cause cell death of the targeted cell by apoptosis. The complement system marks (opsonizes) pathogens for subsequent phagocytosis by macrophages, neutrophils and DCs. These cells invaginate pathogens directly and present digested parts on their surface. DCs mature and migrate into peripheral immune organs where they present their antigens to T and B cells. Thus, macrophages, neutrophils and DCs serve as messengers between the innate and the adaptive immune system. Together with B cells of the adaptive immune response, they act as antigen presenting cells (APC). Presentation of antigens activates T cells that recognize antigens specific to their T cell receptor (TCR). The adaptive immune response forms an immunological memory, which can sustain a lifelong immunity against further exposure to that particular disease.

All immune cells derive from the bone marrow (BM), where the maturation of B cells takes place as well. The hematopoietic stem cell can differentiate either into common myeloid progenitor or common lymphoid progenitor (CLP) cells. The first cell type gives rise to granulocytes and macrophage progenitors as well as megacaryocytes and erythrocyte progenitors. The latter cells differentiate into B, T and natural killer (NK) cells.

T cells migrate into the thymus where they complete their maturation. Because of this function in lymphocyte development (B and T cell development), the bone marrow and thymus are defined as primary lymphoid organs. Upon antigen activation T cells differentiate into antigen-specific effector cells while B cells become antibody-producing plasma cells. The adaptive immune response takes place in secondary lymphoid organs such as spleen, lymph node (LN) and mucosa-associated lymphoid- tissue (MALT).

B cells can activate T cells by presenting internalized and processed antigen fragments that were previously bound to a B cell receptor (BCR). The major histocompatibility complex II (MHCII) is expressed on various cells of the immune system and defines a molecular complex that is assembled in the ER and loaded with a placeholder peptide for its transport into lysosomes. Here, the replacement with antigens takes place. The latter derive from extracellular pathogens, which were engulfed by APC. The TCR interacts with the peptide-bound MHCII, which leads to the activation and clonal expansion of cluster of differentiation (CD) 4 T cells. Activated T cells produce cytokines, which activate B cells, leading to their differentiation into antibody-producing plasma cells [1, 28, 29].

T cells can be divided into two subsets that are defined by their surface receptors. CD8 expressing T cells are also called cytotoxic T cells and become activated by pathogenic particles that are presented by the major histocompatibility complex I (MHCI). MHCI are expressed on almost all cells in the body. The receptor assembly takes place in the ER.

Pathogens that are processed in the cytosol are transported to the ER and loaded on the receptor that is only stable in its peptide-bound form. The MHCI presents mostly cytoplamic peptides including invasive pathogens such as virus particles. Upon activation, cytotoxic T cells kill the infected cells or induce apoptosis by secretion of cytokines. The other T cell subclass, CD4-expressing T cells can be further classified into two major subclasses. Both types combat bacterial infections by recognizing peptides presented by the MHCII receptor. Intracellular bacteria such as *M. lepra* infect macrophages and reside in their lysosomes. T_H1 cells can activate these macrophages and induce the fusion of their lysosomes. They also secret cytokines and thereby activate additional immune cells leading to the induction of an immune response. B cell activation is carried out by T_H2 cells [1].

1.3.1.1 T cell development

The development of T cells takes place in the thymus. Within the thymus, T cell development can be divided into different stages. T cell precursors lack the surface expression markers CD4 and CD8. These cells are called double negative (DN) and are characterized by the expression of the surface receptors CD44 and CD25 [30]. The four maturation steps that lead to double positive (DP) cells are called DN one to four. In the first, most immature stage (DN1), CD44 expressing cells still have the capacity to develop into T, B and NK cells but not into other hematopoietic lineages [31]. The upregulation of CD25 defines the second stage (DN2, $CD25^+$ $CD44^+$) of T cell maturation. Here, the cells loose the potential of becoming B, and NK cells [31]. T cell commitment takes place in DN3 that is crucially dependent on Notch-1 signaling. The DN4 stage is defined by the down-regulation of CD44, leading to CD25 single positive cells (DN4). The double negative stages are followed by the co-expression of the CD4 and CD8 receptors in the double positive (DP) stage. Here, the T cell receptor rearranges leading to allelic exclusion and the differentiation into αβ or γδ T cell lineages [32]. The final maturation of the αβ lineage is defined by the expression of either CD4 or CD8 receptors. Again, Notch-signaling influences the maturation as can be seen for B cell versus T cell lineages, at the αβ versus γδ lineage commitment and the $CD4^+$ versus $CD8^+$ stage [33, 34]. Mature CD4 and CD8 T cells express the T cell receptor and several other co-receptors that are necessary for the propagation of the T cell receptor signal.

1.3.1.2 The CD2 molecule

The CD2 adhesion molecule is expressed on mature T cells, but also on thymocytes, NK cells and a subset of thymic B cells [35, 36]. In humans it interacts with CD58 (LFA3) [37], a surface molecule that is present on hematopoietic (lymphocytes, granulocytes, myeloid cells, erythrocyte) and non- hematopoietic (fibroblasts) cells [38]. The murine interaction partner of

CD2 is CD48 [39], which mainly occurs on T cells, monocytes, endothelial and B cells [40, 41].

Interactions of CD2 with its counterparts hCD58 or mCD48 induces several changes within the cell such as Ca^{2+} flux [42, 43], tyrosine phosphorylation and production of IL-2 and IFNγ [44]. It also promotes and enhances the adhesion between T cells and APC or NK cells [45]. CD2 activation can initiate the reversal of the anergic state [46] and enhance the susceptibility of activated T cells for IL-12 [47]. The CD2 adhesion molecule can function as co-stimulatory molecule by activating lymphocytes that deliver intracellular signals. Overall, CD2 activation induces a remodeling of the cytoskeleton [48].

Several segments of CD2 are involved in different signaling pathways [43] but still, the function of the CD2 *in vivo* is not completely understood. CD2 knockout mice display a normal repertoire of lymphocytes and can raise an effective immune response [49] whereas CD48 null mice show impaired $CD4^+$ T cell activation [50]. In view of this, other surface receptors might compensate CD2 deficiency whereas CD48 seems to interact with several surface receptors with functions that cannot be compensated.

1.3.1.3 CD2BP2 and the immune system

Nishizawa et al. demonstrated the interaction of the his-CD2BP2-GYF domain (AA 256- 341) with a GST-tagged cytoplasmic tail fragment (AA 221- 282) of CD2 (Figure 1.2) [3]. Deletion studies showed that the PPPGHR motif of the CD2 tail is necessary for CD2BP2-binding. This motif corresponds to the motif essential for CD2-stimulated IL-2 production. In accordance, overexpression of the CD2BP2-GYF domain in a human $CD4^+$ T cell line (Jurkat cells) led to enhanced IL-2 production (150-200 %) whereas anti-sense DNA decreased the production by 50 %.

To better understand the role of CD2BP2 in T cell signaling, our group performed co-localization and knockdown studies in human HeLa and peripheral blood mononuclear cells (PBMCs) [51]. The overexpression of CD2BP2 and CD2 in HeLa cells showed no co-localization. CD2 was observed at the cell membrane whereas CD2BP2 localized to the nucleus. 40-60 % siRNA knockdown of stimulated versus unstimulated PBMCs showed no effect on the expression level of IFNγ, IL-2 or IL-10.

1.4 The Role of CD2BP2-GYF in Spliceosome Assembly

Complexes consisting of RNA and proteins named ribonucleoproteins (RNP) play a pivotal role in numerous processes within the cell. Often, they are involved in the regulation of splicing.

Splicing is performed by small nuclear ribonuclear particles (snRNPs) U1, U2, U4/ U6 and U5 [52]. Each snRNP has one snRNA (the U4/ U6 complex has two), and a variable number of complex-specific proteins. The splicing process can be divided into several steps. The cycle starts with ATP-independent binding of the U1 to the 5' splice site (SS) and the U2 snRNP associates with the branch point leading to complex A. Next, the tri-snRNP complex, consisting of U4/ U6 and U5 snRNP is recruited into the cycle, forming complex B. Numerous structural rearrangements take place during the next maturation step, and the U1 and U4 leave the complex. This leads to the catalytically activated complex B*. The first catalytic step generates complex C. After the second catalytic step, the entire spliceosomal complex dissociates and the mRNA is released in form of an mRNP. The snRNP complexes are recycled to start the next round of splicing.

1.4.1.1 CD2BP2 and Splicing

The group of Reinhard Luehrmann identified a protein, running at the height of 52 kD in SDS-PAGE, as a constituent of the U5 snRNP, and called it U5-52K [53]. Sequence alignments and homology studies confirmed U5-52K to be identical with CD2BP2. A first study showed the phosphorylation of CD2BP2 upon tri-snRNP formation in an ATP-dependent manner [53]; a successive study could not confirm the presence of CD2BP2 in tri-snRNPs [4].

U5 snRNPs mediate important steps during splicing assembly by enhancing the first catalytic step of splicing. The complex is essential for the second splicing step and the maturation and dissociation of the cycle. Sucrose gradient studies showed that CD2BP2 is present in the 20S fraction containing the U5 snRNP, but is absent in the 25S tri-snRNP fraction. Therefore, the function of CD2BP2 is thought to be more related to the complex's assembly than to a catalytic function [4].

Yeast-two hybrid studies with CD2BP2 as a bait discovered two novel binding partners, U5-15K and 102K (Prp6/ Prp1). Studies in human HeLa cells confirmed that the N-terminal region of CD2BP2 interacts with 102K (Prp6/ Prp1) [4].

S. pombe Prp1 (homologous to human 102K) as part of the U5 snRNP interacts with the U4/ U6 protein Prp31. Their interaction is essential for the assembly of the U4/ U6.U5 tri-snRNP complex. Recently it was shown that *S. pombe* Prp1 and the human ortholog 102K as well as Prp31 are phosphorylated by the dual specific Cdk like serine/ threonin kinase Prp4 at several threonines in the conserved N-terminus. This phosphorylation is essential for the stable

formation of complex B [54, 55]. The *Saccharomyces cevervisiae (S. cevervisiae)* ortholog Prp6 is the only ortholog in eukaryotes without these conserved residues. The Prp4 kinase is not expressed in *S. cevervisiae*. Accordingly, phosphorylation seems to influence mRNA splicing in most species and might have a regulatory function during assembly.

The U5-15K protein is an essential splicing protein that is specific to the U5 snRNP. Knockout studies in *S. cevervisiae* showed that the yeast ortholog Dib1 is lethal, in contrast to the *S. cevervisiae* ortholog of CD2BP2, Snu40 [56]. Also, disruption of DML1, the ortholog of U5-15K in *Caenorhabditis elegans* (*C. elegans*) by RNA interference leads to embryonic lethality during gastrulation [57]. Even though U5-15K binds CD2BP2 at the GYF-domain containing C-terminal region, it lacks PRS. Structural analyses demonstrated that it binds the GYF domain on a second binding site opposite the PRD [4].

With the information from the splicing related interaction partners of CD2BP2, an interaction network can be proposed (Figure 1.4). The N-terminal region of CD2BP2 interacts with U5-102K (Prp6) via an unknown binding motif [6]. Prp6 is regulated by Prp4 kinase, which is a key regulator of complex B formation.

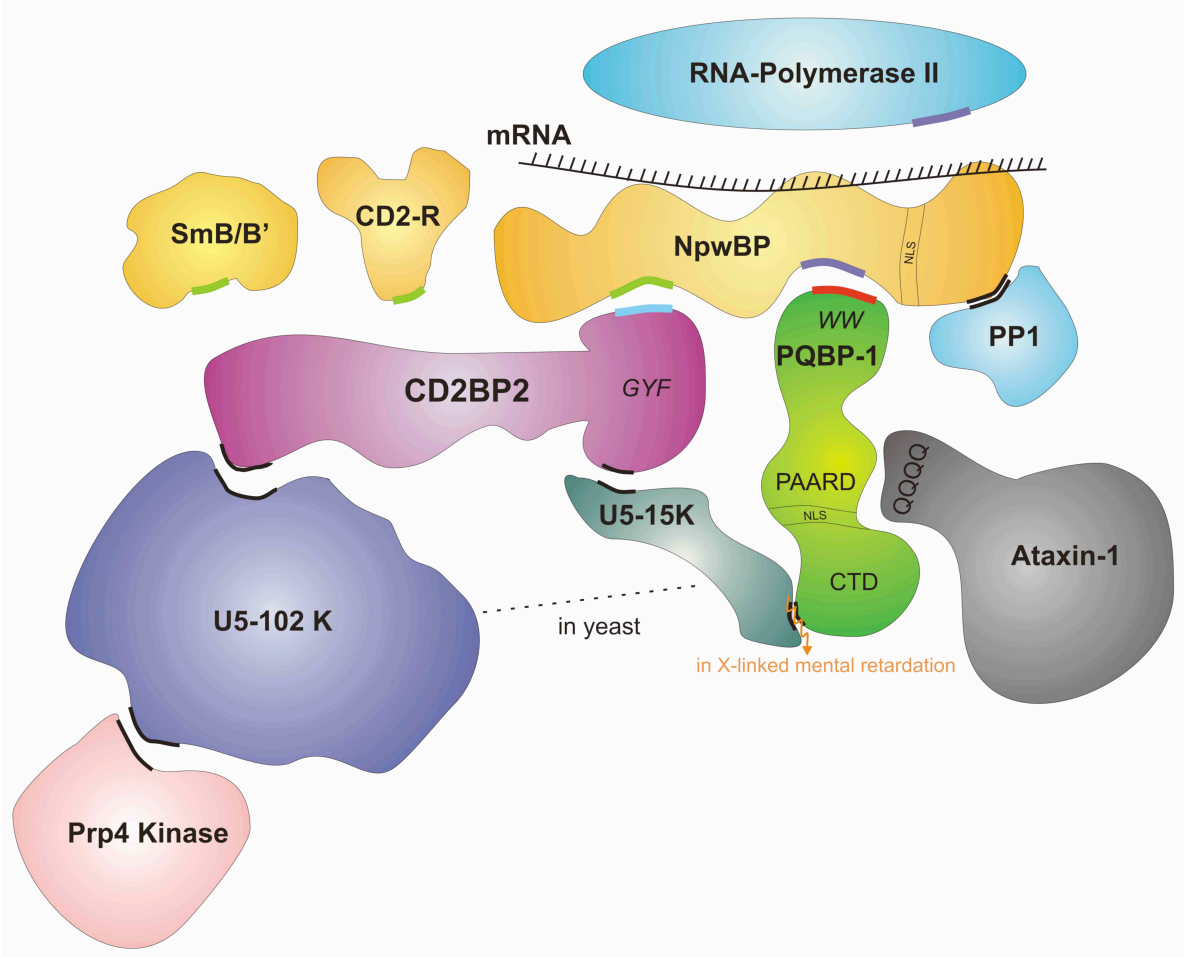

Figure 1.4. **Hypothetic protein interaction network of CD2BP2**. PRS with a GYF recognition motif are shown in green, the ones binding to WW domains in lilac. PRD of the GYF domain is shown in blue of WW in red, respectively. All unknown interaction sites are shown in black.

The C-terminal GYF domain of CD2BP2 interacts with the PRS of the cytoplasmic tail of CD2 *in vitro*, the SH3 domain of Fyn competes for the same binding site [27]. This PRD can also bind to SMB/B', a spliceosomal protein that is present in all snRNPs and to the RNA-binding protein "Npw38 binding protein" (NpwBP) [58]. The binding site opposite to the PRD within the GYF domain interacts with the U5 specific protein U5-15K that also interacts with the polyglutamine-binding protein 1 (PQBP-1).

Frame shift mutations in X-linked mental retardation can abolish a U5-15K: PQBP-1 interaction [59]. The PRS of NpwBP and the RNA-Polymerase II both bind to the N-terminal WW-domain of PQBP-1 [60].The serine/ threonine phosphatase protein phosphatase1 (PP1) regulates the phosphorylation status of NpwBP [61]. Ataxin-1 favorable binds PQBP-1 when there are pathologically enriched polyQ repeats [60]. We speculate that there exist an indirect interaction of CD2BP2 and PQBP-1 via the direct interaction partners NpwBP and U5-15K.

In an in vitro splicing assay, high amounts of CD2BP2 inhibited splicing at the stage of complex A formation [58].

1.5 The GYF-domain protein GIGYF2

The growth factor receptor-bound protease 10 (Grb10) interacting GYF protein 2 (GIGYF2) (also called PERQ amino acid-rich with GYF domain containing protein 2 (PERQ2)) belongs to the family of Smy2-type GYF domains and shares the same structural characteristics such as a preference for binding the PPG(F/I/L/V) motif. A yeast-two hybrid screen revealed an interaction between GIGYF2 and the binding motif PPG(F/I/L/V). Spot analyses allowed a more detailed analysis of the binding motif and entailed the classification as a Smy2-type GYF domain. In subsequent yeast-two hybrid screens with human GIGYF2 (PERQ2) as bait, several new potential interacting partners were found, such as the splicing-related proteins, snRNP-N, SMN and U1snRNP C, the SWAN protein and the two proteins known to bind CD2BP2, SmB/B' and NPwBP. Nuclear localization and an involvement in splicing was hypothesized because of these nuclear, spliceosomal interaction partners [6].

The murine GIGYF2 and the very homologous GIGYF1 (PERQ1) were found as interaction partners of the N-terminal region of Grb10 [62]. The murine Grb10, in contrast to the human Grb10 contains a GYF binding motif. Grb10 belongs to the family of putative adaptor proteins and binds to activated tyrosine kinase receptors such as insulin and insulin growth factor-1 (IGF-1) [63-65]. The activity of Grb10 seems to be phosphorylation dependent and several serine and tyrosine phosphorylation sites have been described [66, 67]. Disruption of the GYF domain leads to loss of Grb10 binding. Three potential tyrosine phosphorylation sites, a proline-rich region, a bipartite NLS motif and large glycine and glutamine stretches in the C-terminus were assigned to the murine GIGYF2. RNA expression was mainly detected

in the heart and liver with somewhat lower expression in kidney and brain and barely detectable in the lung [62].

Mutations in GIGYF2 were linked to familial Parkinson's disease (PD) [68]. The PARK11 locus lying on chromosome 2q36-37 has been discovered by whole-genome linkage analyses in a population of patients suffering from PD that have a least one first-degree affected relative [69-71]. Two different populations of Caucasian patients with familial PD and their population-matched controls were sequenced and screened for mutations in GIGYF2 as potential candidate gene. They found 7 heterozygous AA changes in 12 unrelated index cases with PD that where not present in the controls. The mutations occurred in highly conserved AA blocks and could all be detected in several consecutive generations. From these data, GIGYF2 was suggested as candidate gene for PD.

The study caused a vivid debate within the community focusing on neurodegenerative disorders of whether or not GIGYF2 can be considered as candidate gene for PD. 13 studies from different groups all over the world contributed by analyzing different populations [72-84]. Finally, in 2010, a follow-up study in a French population, similar to the first one showed no association between GIGYF2 and PD [85].

In 2009, the Smith lab published the generation of a GIGYF2 knockout mouse, created by a 129Ola ES cell derived gene trap vector from BayGenomics [86]. All analyses were performed in a C56BL/6-Tyr ^{cBRD}/ 129 Ola mixed background. Embryos resulting from heterozygous matings showed normal Mendelian distribution between embryonic day (E) 17.5- 18.5 and normal growth and anatomy. The lethality of the homozygous knockout (KO) mice rose during the first postnatal day up to 85 % due to lack of feeding, while the survivors showed normal motility and histology. Beginning with 15 months of age, heterozygous mice develop mild motor dysfunctions. On the histological level, these mice exhibited abnormalities in the central nervous system (CNS). The substantia nigra, the area that is mostly affected by PD, showed no abnormalities. In summary, the data obtained from the gene trap knockout analyzed in a mixed genetic background showed a mild neurodegenerative like phenotype but no obvious link to PD.

1.5.1 **Smy2-type GYF-domain containing proteins exert their function in the cytoplasm**

In localization studies of yeast cells, Georgiev et al. could show the co-localization of the GIGYF2 ortholog, Smy2 with Dcp2 [87]. This catalytic subunit of the Dcp1-Dcp2 decapping enzyme complex [88] is a well-known marker for processing bodies (P-bodies) [89].

P-bodies and stress granules (SG) both belong to a recently found family of RNA granules called mRNA silencing foci. They contain mRNAs that are temporally or constantly excluded from the translation machinery [90]. P-bodies can steadily be detected in the cytoplasm of cells but the size can be induced by different factors such as global translation silencing or hypoxic stress [91, 92]. Several decay machineries like the deadenylation or the RNA-induced

silencing complex (RISC) stall mRNA within P-bodies. The deadenylation of the 3'polyadenosine (poly-A tail) is catalyzed by the deadenylase CCR4p/ Pop2p/ Not complex and leads to 3' to 5' degradation or decapping by Dcp1p/ Pcp2p enzymes and the exonuclease Xrn1p [93]. The RISC complex can inactivate or reduce the expression of certain mRNAs that are targeted by two different kinds of non-coding RNAs. The small interfering RNAs (siRNAs) or microRNAs (miRNA) recognize specific untranslated regions in mRNAs and silence them either by translation repression or mRNA decay. Both RNAs are transcribed in the nucleus by the RNA-polymerase II and form hairpin structures that are exported into the cytoplasm. The RNase-III enzyme Dicer cleaves pre-mi and siRNAs into 19-23 bp fragments, which are loaded into the RISC complex. Two mechanisms lead to the process of RNA interference. In the first mechanism, the targeted mRNA can be cleaved by the endonuclease Argonaut2 (Ago2) that recognizes siRNAs that specifically base-pair with mRNA. In the second, miRNA base pairing induces the deadenylation of mRNA and thereby its repression. This base pairing is not entirely complement but requires a seed region of about 8 bases for binding [94-98].

mRNA that accumulates within P-bodies is needed for assembly and stability [99] and does not necessarily become degraded but can return to translation with a mechanism not understood yet [91, 100]. This mechanism allows the temporal or spatial protein expression that is important in different cell systems such as neurites of neuronal cells.

In contrast to P-bodies, SG form only upon stress induction, when translation initiation is impaired. This highly conserved process can be induced by decreased translation initiation rates during stress [101], drugs blocking translation initiation [102], knockdown of specific initiation factors [103] or overexpression of RNA-binding proteins that repress translation [104-107]. Inversely, trapping mRNA in polysomes with drugs that block ribosome elongation can block the formation of stress granules [108, 109]. From the composition of stress granules, it can be concluded that they contain mRNAs stalled in the process of translation initiation. Typical stress granule markers are poly$(A)^+$ mRNA, 40S ribosomal subunits, elongation initiation factor 4 E (eIF4E), eIF4G, eIF4A, eIF4B, poly (A) binding protein-1 (PABP-1), eIF3 and eIF2 as well as protein components including RNA helicases, translation and stability regulators, and factors involved in cell signaling [101, 110-114]. Stress granules have also been discovered under *in vivo* conditions in neuronal cells in the context of neurodegeneration [115-117]. Acute stress needs quick adaption by the cell, which can be realized by post-translational modifications (PTM) of several proteins, such as the phosphorylation of the translation initiation factor eIF2α. The translation initiation complex can be phosphorylated by eIF2α K1/ HR1 upon induction of oxidative stress (such as arsenite [118]) and subsequently be recruited to SG [105, 110, 119]. Disruption of SG assembly has no influence on translation silencing, therefore SG are rather the consequence than the cause of translation inhibition upon stress [90].

SG and P-bodies exhibit common features such as an enhanced formation upon stress induction [92]. They share certain proteins, one third of the components present in SG granules can also be found in P-bodies [109] and they can fuse and give rise to a hybrid structure positive for Dcp1a and TIAR [120]. Major differences are that SG contain polyadenylated transcripts while P-bodies comprise deadenylated mRNA and no PABP-1. Accordingly, SGs have no components of the decapping machinery whereas translation initiation factors and small ribosomal subunits are not present in P-bodies [92, 120].

The transport of proteins between different membrane compartments within the cell is important for their function and identity. Small membrane vesicles allow the transport of cargo proteins to their specific destination. The folding of newly synthesized proteins takes place in the Endoplasmatic Reticulum (ER), which is the starting point of the secretory pathway. From here, they are transported by the coat protein complex II (COPII)- coated vesicles to the Golgi-Apparatus and other donor organelles [121]. The highly conserved COPII consists of five core proteins, the small guanosine triphosphate (GTPase) Sar1p [122] and the subcomplexes Sec23/ Sec24 and Sec13/ Sec31 [123]. Sar1p initiates vesicle formation. Upon GTP binding, it translocalizes from the cytosol to the membrane of the ER and recruits all the other factors necessary to bend the membrane [124] and molecular switch. Sar1p activation is driven by the guanine nucleotide exchange factor (GEF) Sec1p that is only present at the membrane of the ER [123, 125, 126]. The hydrolyzed form of Sar1p binds to the heterodimer Sec23/ 24 forming the pre-budding complex. Subsequently, the heterotetramer Sec13/ 31 is recruited to the outer shell of the coat and all cargo subcomplexes combine with each other and pinch off as COPII vesicle [126]. The mature COPII vesicle loses its coat and undergoes tethering, docking and fusion to the Golgi membrane [127]. *In vitro* studies showed that the five core proteins serve as minimum requirement for vesicle formation [128, 129] whereas *in vivo,* the situation is more complicated with additional protein factors necessary for successful COPII formation and budding [130-132]. Sec23p, for example, stimulates hydrolysis of Sar1p, and thereby acts as a GTPase activator protein (GAP). Sec24p is a multivalent cargo adaptor that has three independent protein recognition sites (A, B and C) necessary for ER export. Mutations in any of these binding sites can lead to blockage of ER-to-Golgi transport or even lethality. The blockage seems to be caused by defects in COPII vesicle formation [133, 134]. Two independent studies screened several mutant yeast strains for suppressor genes, that, when overexpressed, overcome these phenotypical changes. Both discovered the GYF-domain containing protein Smy2 as potent high copy number suppressor. Because Smy2 is not incorporated into COPII vesicles, it is no bona fide cargo protein but rather acts as general accessory protein that promotes flux of proteins in the early secretory pathway [134, 135].

1.6 Targeted Mouse Mutations

Gene deletions in animal models or overexpression of human genes in rodents can be used for phenotypical analyses and to screen for therapeutic treatments in humans. Before these techniques were available, data were mostly collected from spontaneous mutations in patients or animals but it was difficult to find the direct genetic link.

The generation of a genetically modified animal model mostly derives from two different motivations. Either from the cellular point of disease where a hereditary disease can be correlated to a specific gene. In this case, the cDNA is sequenced and the anatomical distribution of the gene and protein expression is known. To gain a better understanding of the disease and potential treatments, targeted gene mutations then reveal the functional context of the gene.

On the other hand, structural analyses often give insights into the molecular context of a given protein but the cell culture system limits further functional or phenotypical analyses. Here, again, an animal model helps to understand the function of a gene in a multicellular context.

1.6.1 **The history of targeted gene transfer**

Spontaneous mutations in animals were used as very first models to analyze human diseases. Microinjections developed into a standard technique in a remarkably short time in the field of mammalian genetics. In 1974, purified viral SV40 DNA was, for the first time, injected into the blastocoel of mouse blastocyts (3.5 day old pre-implantation embryos) [136]. Viral DNA sequences could be found in the somatic tissue of newborn animals, suggesting that the sequence was inserted into the genome of the embryonic cells. In addition, in 1976, Jaenisch discovered that the Moloney murine leukemia virus (MMLV) could be introduced into the germline of mice after viral infection of pre-implanted embryos. In 1980, the microinjection of the cloned Thymidine Kinase (TK) of herpes simplex virus (HSV) into the nuclei of cultivated fibroblasts resulted in stable incorporation and expression of the TK gene in 5-20% of recipient cells [137, 138]. The first successful integration of a cloned gene into somatic tissue of a mouse gene by injection into the pronucleus of a mouse oocyte was reported in 1980 by Gordon et al. Shortly thereafter, several groups were successful in the integration of cloned genes into somatic tissues and germline cells using this technique [139-143]. Especially in neurodegenerative disease, transgenic mice contributed substantially to the development of new therapeutic treatments [144]. One drawback of transgenic models is, that they are not targeted; meaning the exact integration locus into the genome is unclear.

The combination of Martin Evans, Marco R. Capecchi and Oliver Smithies' studies led to the generation of targeted gene transfer via homologous recombination of genes. This groundbreaking work was rewarded the Nobel Prize in 2007.

The Evans lab set the basis for this success by establishing conditions to cultivate and manipulate murine embryonic stem cells (ES cells) [145]. Early stem cells are defined as pluripotent cells that can give rise to any cell in developing organisms except for extraembryonic tissue. Later on, the lab was able to inject manipulated ES cells into blastocysts leading to chimeric mice and finally to successful germline transmission [146]. Chimeric mice consist of cells from two different individual and thus carry genetic information from two different backgrounds, in this case from the manipulated ES cells and the recipient blastocyst. If the manipulated cells generate germ cells, they can transmit the altered gene to the next generation, a process called germline transmission. The condition (passage number, differentiation stage, euploidy, health status), background and handling of ES cells influence this critical step enormously and are a limiting step in the generation of knockout mice.

Joshua Lederberg determined the principles of homologous recombination, or the genetic recombination of two similar or identical strains of DNA, in bacteria. For his work he received the Nobel Prize in 1958. Capecchi and Smithies were independently able to apply homologous recombination to the mammalian system.

Gene targeting via homologous recombination is defined as homologous recombination between DNA sequences that result in changes in the endogenous gene, either by the specific deletion or introduction of gene segments. The Capecchi lab showed, for the first time, successful gene targeting by homologous recombination into cell lines [147]. Smithies and co-workers managed the recombination of a plasmid into the β-globulin gene in human erythro-leukemia cells [148].

With the help of the Evans Lab, Capecchi and Smithies could transfer their knowledge about gene targeting into murine ES cells. Now, they could show that it was possible to either repair cells (for example the introduction of the Hypoxanthin-Phosphoribosyl-Transferase (HPRT) gene) or introduce genes (for example the neomycin (neo) cassette) by gene targeting [149, 150].

Homologous recombination is a rather infrequent event. Capecchi determined the efficiency of successful recombination in murine ES cells as 1 in 1000. Experiments with positive and negative selection markers were performed to improve the statistics. Cells treated with G418 (Geneticin™) die because G418 blocks polypeptide synthesis. Successfully recombined cells expressing neomycin (aminoglycoside phosphotransferase) could survive the selection process. The neo cassette needs to be localized within the area of homologous recombination to serve as a positive selection marker. To avoid non-homologous integration into the genome, a negative selection marker is placed outside the recombination region. The previously mentioned herpes simplex virus derived Thymidine Kinase is often used as such. Cell treatment with Ganciclovir, a toxic Thymidine analog that inhibits transcription, negatively selects randomly integrated DNA [151].

With the development of efficient screening methods, all requirements for the generation of knockout mice were assembled, namely cultivation of manipulated ES cells and germline transmission, methods for specific gene transfer into ES cells and finally the enrichment of positive ES cell clones.

Several labs participated in the race for the first knockout mouse including the Labs of Capecchi and Smithies [152-155] leading to the first knockout mice in 1989. Since then, hundreds of strains with one to several modifications have been created. Recently, the International Knockout Mouse Consortium (IKMC) was created by the merging of several national and international companies and consortia with the aim to "mutate all protein-coding genes in the mouse using a combination of gene trapping and gene targeting in C57BL/6 mouse embryonic stem (ES) cells" [156] .

1.6.2 **Conditional gene targeting**

The knockout technique has several limitations. Deletions of essential genes that lead to embryonic lethality cannot be analyzed further. Additionally, the maintenance of the positive selection marker can influence the expression and behavior of the targeted gene or a neighboring one [157, 158]. Site-specific recombination (SSR) can circumvent these limitations by the introduction of null mutations only in specific cells or organs *in vivo* [159]. The bacteriophage P1 has a segmented genome in which each segment is flanked (floxed) with loxP sites (locus of crossover (x) in P1). Expression of the enzyme Cre- recombinase leads to specific recombination of two loxP sites and excision of the floxed gene segment, leaving one loxP site inside the genome [160].

The yeast-derived FRT system is based on the same mechanism. Flip recombinase recognition target sites (FRT sites) flank gene segments, which can be excised in the presence of the Flip-recombinase (named after the ability to invert or "flip" DNA segments in *S. cerevisiae*) [161].

The Cre- and Flip-recombinases belong to the λ-integrase family that can perform strand cleavage, exchange and ligation of DNA segments [162]. Their recognition sites are built the same way (Figure 1.5), containing two 13 bp palindrome sequences (inverted repeats) that are separated by a 8 bp asymmetric core (spacer) [163]. The unique feature of both recombinases is that they need no co-factors, which makes them the perfect tool for site-specific modifications. Flanking the neo cassette with FRT sites while the gene segment of interest is floxed by loxP sites is meanwhile regularly used for the creation of conditional targeting vectors. The selective expression of the Flip recombinase leads to the excision of the marker, leaving the floxed gene intact. The asymmetric spacer region of the recombination site carries out cleavage, exchange and ligation [164]. Therefore, the same orientation of the two spacer regions are essential for successful recombination [165].

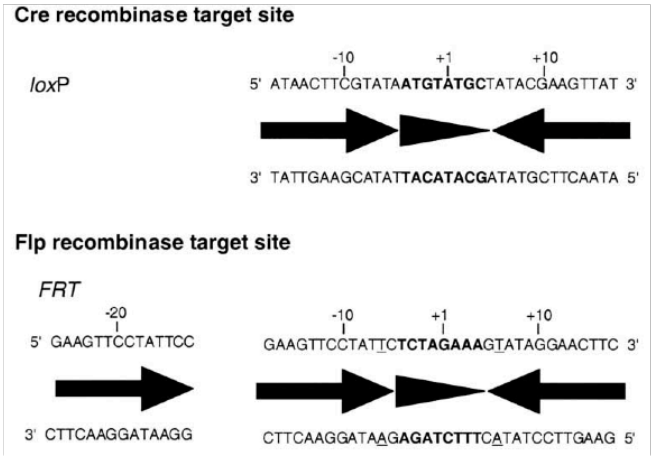

Figure 1.5. **Structure and sequence of loxP and FRT sites**. Typically for members of the λ-integrase family they have two palindrome sequences (inverted repeats) that are separated by a spacer sequence [159]

Activation of these recombination systems in specific cells leads to tissue-specific [166] targeting allowing the analysis of gene modifications that are restricted to certain cell types. The process of cell site-directed gene inactivation is called conditional gene targeting. The Rajewsky group was the first who showed the conditional deletion of the DNA polymerase β-gene segment in T cells of mice [166].

Inducible knockout mice can be generated by breeding floxed mice with deleter strains that express the Cre-recombinase under an inducible promoter such as the promoter of the mouse Mx1 gene [167]. This gene serves as defense mechanism upon viral infection and is silent in healthy mice. The administration of interferon α (IFN-α), β or synthetic double-stranded RNA (polyinosinic poly-cytidylic acid (pI-pC)) activates the gene transiently and can thereby induce the knockout. This leads to the excision of the gene within days and allows the analysis of the knockout at any developmental state.

1.6.3 **The knockout workflow**

Even though generation of a knockout mouse is quite complex, once the basic principles are clear, the workflow is more comprehensive. Figure 1.6 summarizes the individual steps of the workflow.

First, the targeting vector is cloned, containing a positive and negative selection marker, and, in case of a conditional knockout, loxP and FRT sites that flox the gene of interest and flank the positive selection marker. This vector is subsequently electroporated into murine ES cells. The most common ES cell line derives from the inbred line 129, but C57BL/6 ES cell lines become increasingly popular. Cells are selected and screened for successful homologous recombination events. Positive clones are then injected into appropriate blastocysts and implanted into pseudo pregnant mice. Part of the offspring are chimeric, meaning that they contain a mosaic of genetically modified cells and cells deriving from the recipient mother.

The DNA from both ES cells and recipient mother should result in different coat color of the offspring. The 129-derived mouse strain, for example, has an agouti coat color in contrast to the black coat of recipient C57BL/6 mice; therefore, chimeras exhibit a variegated coat color. The chimeric mice are then bred with WT C57BL/6 mice. If the germ cells derive from genetically modified cells, germline transmission will lead to the creation of a novel founder strain.

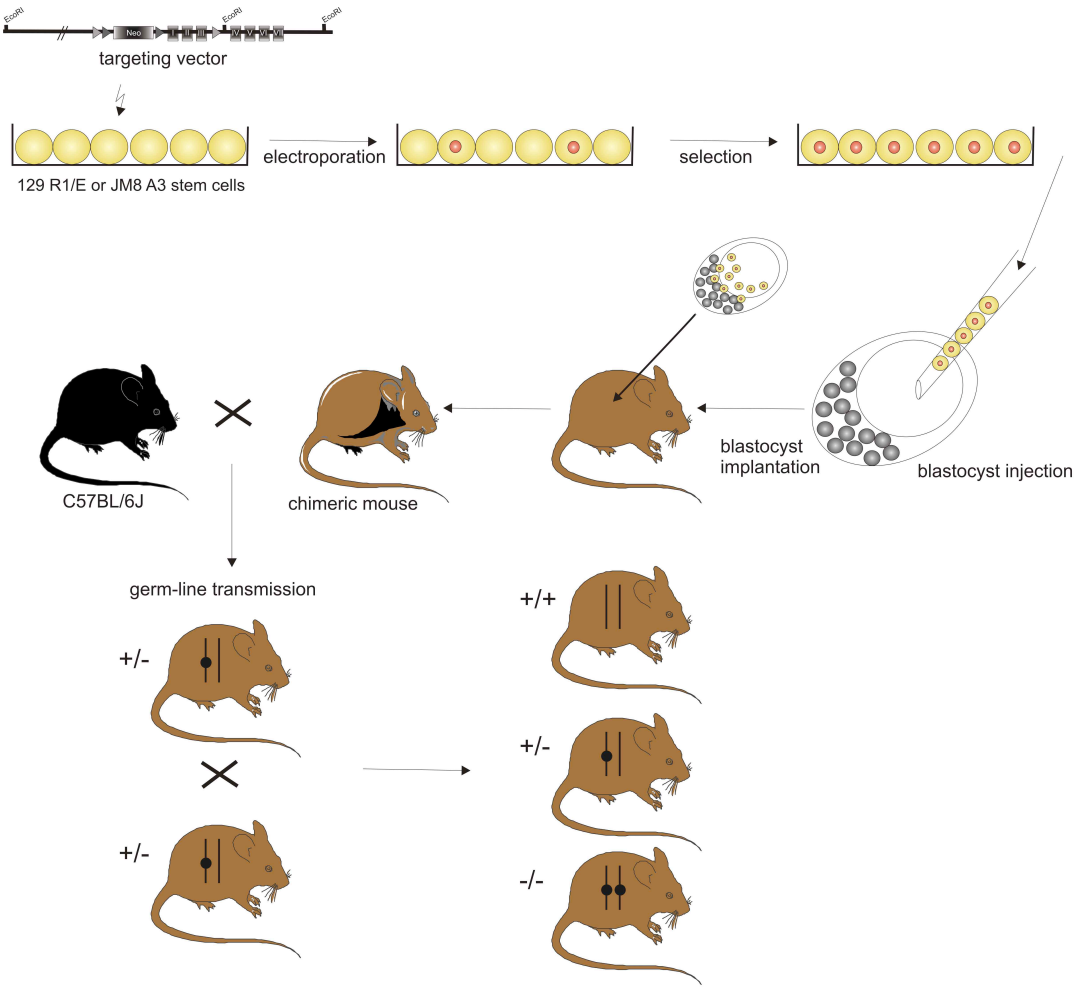

Figure 1.6. **Knockout work flow** from the generation of the targeting vector and its electroporation into ES cells, to the screening for positive clones, their injection into blastocysts, the implantation into a foster mother, the germline transmission an finally the knockout breeding

1.6.3.1 129 versus BL6 ES cells

For historical and technical reasons, the targeting vector is mostly electroporated into the 129 strain-derived ES cells. The major advantages of these very stable cells are that they grow well in culture and remain viable throughout the electroporation and implanting process. This is important for a high success rate of germline transmission. Also, 129 ES cells colonize a large portion of the developing embryo and therefore enhance the chances for highly chimeric mice, meaning that many of the cells in the body are formed from the manipulated cells.

The disadvantage over C57BL/6 cells is that the mice deriving from the 129 strains are not good breeders. Also, they show abnormal behavior [168], anatomy [169], immunology [170], neurobiology and physiology [171]. C57BL/6 mice, in contrast, are well-characterized inbred strains that have been used for the mouse genome-sequencing project (Welcome Trust, Sanger Institute). Mouse strains that have been crossed for 20 or more consecutive generations with sister-brother matings are considered as inbred [172]. This strict definition is important for the reproducibility of experiments and to allow all researchers worldwide to compare their results with others from the same genetic material.

C.C. Little established the C57BL/6 inbred strain in the 1920s. Due to separation of breeding stocks, two sublines emerged from this strain in the 1940s and 50s that are called C57BL/6J and N [173]. Mice derived from the two different sublines show phenotypic differences [174]. This is due to slightly different genetic backgrounds as can be analyzed by comparing their single nucleotide polymorphisms (SNP). They differ in at least 11 SNP loci, which have an impact on their phenotype [175].

Electroporation into BL6 ES cells could overcome the drawbacks of mixed backgrounds and time-consuming back crossing into pure strains. However, they have lower germline transmission rates, and, the degree of chimerism, which can, to a certain degree, be estimated by the amount of agouti coat color in 129/ BL6 chimeras, can not be measured with normal BL6 cells because of the black coat color. To receive pure BL6 background, mice need to be crossed back for at least 10 generations with WT BL6 mice. This congenic breeding strategy is very time consuming and inefficient. To overcome this limitation, marker assisted selection protocols (MASP) have been developed in which littermates are screened for polymorphisms that are characteristic for the recipient strain. Mice positive for these markers are selected and used for the next breeding. This process, called speed congenic, accelerates breeding from 3 to 4 years down to 1 or 2 years [176]. Because of all of these disadvantages scientists are looking for BL6 lines that show better germline transmission and phenotypical distinctions. The Jackson Laboratory developed an albino BL6J strain [177]. These mice show mutations in the tyrosinase gene. Deletions lead to the absence of pigments in skin, hair and eyes. This allows the identification of recipient blastocyts by coat color. Pettitt and colleagues created a BL6/N mouse from JM8 ES cells where the agouti locus was repaired so that these mice have agouti coat color and showed good germline transmission rates [171]. Still, these strains have not yet taken hold in the community and need to be analyzed further.

1.7 The Aim of this Study

GYF-domain containing proteins are small adaptor domains that mediate interactions with proline-rich sequences (PRS) of other proteins. Two different kinds of subfamilies have been discovered that contain proteins with similar binding behavior. This study aimed to investigate functional characteristics of the two proteins GIGYF2 and CD2BP2, both representing one subfamily.

Molecular and cellular informations about GIGYF2 are sparse and asked for a basic functional characterization of the protein. Here, the aim was to analyze the localization of GIGYF2 and identify new interaction partners. For both proteins, GIGYF2 and CD2BP2, specific antibodies against the full length protein or the GYF-domain were to be generated. With this tool at hand, GIGYF2 was to be investigated considering its localization within cell lines and mouse organs. Potential interaction partners from pull-down SILAC-MS studies of GIGYF2 were to be confirmed by immunofluorescence- based co-localization studies. In the light of new data from other groups that indicated a neuronal function of the protein, the interaction studies performed in human HeLa cells were to be confirmed in neuronal cells.

CD2BP2 was first discovered as cytoplasmic interaction partner of the CD2 adhesion molecule. Subsequent studies showed a nuclear localization in HeLa cells in accordance with a function in mRNA splicing. While previous studies confirmed the splicing-related role of CD2BP2 with pull-down SILAC-MS studies and *in vitro* splicing assays, the role in the immune system was not elusive, yet.

This study was meant to address the immune-related function by characterizing CD2BP2 in hematopoietic cells and the generation of a conditional KO system.

For analyses of the immune system, the mouse was to be chosen as model system. Expression studies comparing mRNA and protein levels of CD2BP2 were to be preformed to understand the organ-related function of CD2BP2. Further, more detailed expression studies of CD2BP2 in immune cells were to be carried out.

For the generation of a conditional knockout mouse, a CD2BP2 targeting vector had to be cloned and inserted into 129 and C57BL/6 derived murine embryonic stem cells (ES cells). Homologous recombined ES cell clones had to be implanted into foster mothers for the generation of chimeric mice. In case of successful germline transmission of the targeting vector the aim was to establish a genotyping strategy that would allow unequivocal determination of the different genotypes. Different breeding strains were to be established. The induction of the knockout was to be induced by breeding with Cre-recombinase expressing mice. A central question of this study was, if homozygous CD2BP2 null mice would be viable.

2 Material and Methods

2.1 Material

2.1.1 DNA constructs

Name	Vector	Cloned by	Species	Restriction sites
GIGYF2-EYFP (cDNA HJ03496)	pEYFP-C1 (Clontech)	Michael Kofler	Human	NcoI-HindIII
His-CD2BP2 NM_006110.2	pFastBacT1 (Gibco)	Michael Kofler	Human	BamHI-HindIII
His-GIGYF2-GYF (O75137)	pGADT7 (Clontech)	Michael Kofler	Human	BsmHI-XHoI
pPNT4-CD2BP2	pPNT-4	Gesa Albert	Mouse	KpnI
pZErO®-2-CD2BP2-HindIII-loxP	pZErO®-2	Gesa Albert	Mouse	HpaI
pZErO®-2-HindIII-5'homology_3'homology	pZErO®-2	Gesa Albert	Mouse	HindIII

Table 2.1 **Cloned DNA constructs**

2.1.2 Commercially available DNA constructs

Name	Resistance	Company
Endo-marker	pEYFP-Endo	BD bioscience Clontech
ER marker	pECFP-ER	BD bioscience Clontech
Golgi marker	pEYFP-Golgi	BD bioscience Clontech
pCR 2.1-TOPO® TA	Amp and Kan	invitrogen
pCR®-Blunt II-TOPO®	Kan and Zeocin	invitrogen
pPNT-4	neo	GSF research Centre, Munich, Germany
pZErO®-2	Kan	invitrogen

Table 2.2. **Commercially available DNA constructs**

2.1.3 **DNA-Primer**

All DNA primers were diluted in Aqua Bidest. Primer stocks were reconstituted to 50 µM. Working solutions were diluted to 25 µM. Primer design has been performed with Primer 3 [178]. Primers were purchased from Biotez (Berlin, Germany).

Name	**Sequence (5' to 3')**
3´probeA_reverse	TCTGCCCCCTCCTTGGTGTTATC
3´probeA_sense	GGGCTTGGTGGTGGGTATTTGA
3´probeB_reverse	GGCTGCCCCTGTCAACTG
3´probeB_sense	TATCCAGCCTTATCTCCCACTCG
3'_external_f	GGGAGGATTGGGAAGACAAT
3'_external_r	GCCTCCTGGAGACAGATGAG
3' end of 3'homology	GCTTTTAGGTGAAGTATAAACTTGG
3'end of 5'homology	GAAAACCCTGGAGGAGAAAG
3'external_B_f	CCGAAGCGTTAACATAACTTCG
3'external_B_r	TGGTGGGGTGAAAACTTAGG
3'external_C_r	CCTCCCACAGCCCTCTACT
3'externalal_C_f	AAATTGCATCGCATTGTCTG
5´probe_reverse	ACCAGCCGCAAAAAAGCAATCA
5´probe_sense	GAAACCCCATCTCAGTAAT
5' end of 3'homology	GGACAGCAAGGGGGAGGATT
5'end of 5'homology	TATGACCATGATTACGCCAA
5'external_B_f	TCAGGAAGGAATGACCATGA
5'external_B_r	TACCGGTGGATGTGGAATGT
5'probe_A_forward	AGCACACCACGTCCTTATCC
5'probe_A_reverse	GGAGCTACCGAACTCAACCA
5'probe_B_forward	GTCTGGAGCATGCGCTTTAG
5'probe_b_reverse	CAGAAAGCGAAGGAGCAAAG

5'probe_C_forward	AGGTCGCTACGTGGTATTCG
5'probe_C_reverse	GCGAGGACAGATCGCTAAAG
5104_forward_positive_clo	AAAGATTTGTGTACAGATCCTGGAG
5105_reverse_positive_clo	AGAATTTCTTACAAACTTCCACCAG
as20cre (PGK Cre)	GTGGCAGATGGCGCGGCAACACCATT
as23	CTCGAGGATAACTTGTTTATTGC
as29	CTAATGTTGTGGGAAATTGGAGC
cDNA_cd2bp2_f	GGCAAAGGGAGAAAGGGGCCT
cDNA_cd2bp2_r	CTCCTCAGCGAACATGTC
Cre_for	GAACGCACTGATTTCGACCA
Cre_rev	AACCAGCGTTTTCGTTCTGC
Deleter1	CGCCATCCACGCTGTTTTGACC
Deleter2	CAGCCCGGACCGACGATGAAG
extern_forward	AGTAGCCAGGGCTAGGAAGG
extern_reverse	GGGGAACTTCCTGACTAGGG
hindIII-loxP_forward	TTTTTGTTAACATAACTTCATATAATGTATGCATATCGAAG
hindIII-loxP_reverse	AAAAAGTTAACGAATTCATAACTTCATATAGCATACATTAT
Intern_5'probe_F	TAGATTGGGCTGGGTTCTTG
Intern_5'probe_R	CTGATCCCCTTTCTGCTGAG
loxP_Primer_forward	GGCAAGCACTCTTTAAGCAG
loxP_Primer_reverse	TTACAAACTTCCACCAGGGC
p_cre_A_forward	CTTCTGTGGCCGTAAAGCTC
p_cre_A_reverse	CTCCATCCTGAAGGCTTGTC
p_cre_B_forward	AATGGGAGAAAACCCTGGAG
p_cre_B_reverse	AAAGTGGCCTTCCTCCATCT
P_cre_C_forward	GGTTTGAGTTGTTCCCCAGA
P_cre_C_reverse	GCCTTCCTCCATCTCTTCCT

P_cre_D_forward	GGCGTTGAGGTTTGAGTTGT
P_cre_D_reverse	AAAGTGGCCTTCCTCCATCT
P_flip_A_forward	GGTTTGAGTTGTTCCCCAGA
p_flip_A_reverse	AACCCAGGAGTCATTTGCAC
p_flip_B_forward	GGCGTTGAGGTTTGAGTTGT
p_flip_B_reverse	AACCCAGGAGTCATTTGCAC
p_loxP_PpNT	GTATAGCATACATTATACGAAGTTATCGAAGTT
P_neo_naumann_ forward	GATCTCCTGTCATCTCACCTG
P_neo_naumann_reverse	CATCGCCATGGGTCACGACGA
p_neo_new_f	CATTCTGCACGCTTCAAAAG
p_neo_new_r	TGTCTGTTGTGCCCAGTCAT
P_nested_forward	AGACAATCGGCTGCTCTGAT
P_nested_reverse	AGTGACAACGTCGAGCACAG
p_ZERO_5082	GAATACTCAAGCTATGCATC
p_ZERO_5083	CAGTTGGATGGAGAAATCTT
p_ZERO_5084	TTCCTGGTGCATGAGGTAGG
p_ZERO_5085	CAGGAGAAGGAGCGGCAGAA
p_ZERO_5086	TCCTTTCCCCTCTCCACAGC
p_ZERO_5087	ACCCCCAAAAGGAGTCACAG
Pneo_forward	CTTTGCTCCTTCGCTTTCTG
Pneo_reverse	AGTGACAACGTCGAGCACAG
pZERO_5088	ATTCACAATGGGAGAAAACC
pZERO_5089	TACATGCAAACGGAAGCCCG
pZERO_5090	ACGTAGGGGAACCTGACTCC
pZERO_5091	CAAGCACTCTTTAGACAGTG
pZERO_5092	GCACTCCTGGAGGGACTTTT
pZERO_5093	TCTGTCCTCTCTGTTCTTACAG

pZERO_5094	CCTTGAAATCCTATTGAGAG
se19cre (PGK Cre)	GCCTGCATTACCGGTCGATGCAACGA
TB96	GGCCAGCTAAACATGCTTCATCGTC
TB98	CTTTAACCCTGATCCTGGCAATTTCG
WT_forward	CTCAGCAGAAAGGGGATCAG
WT_reverse	AACCCAGGAGTCATTTGCAC

Table 2.3. **DNA-primer shown in 5' to 3' direction**

2.1.4 DNA and proteins Markers

Name	Application	Company
1 kb DNA ladder	DNA marker	New England Biolabs
100 bp DNA ladder	DNA marker	New England Biolabs
Mark12™	Protein marker	invitrogen
SeeBlue®Plus2 prestained	Protein marker	invitrogen

Table 2.4. **DNA and protein markers**

2.1.5 Buffers and Media

Name of the Buffer/ Medium	Protocol
10 x Eri-Lysis buffer	1,55 M NaH_4Cl 10 mM $NaHCO_3$ 10 mM EDTA
2YT Medium	6 g/L tryptone 10 g/L yeast extract 5 g/L NaCl
Annealing Buffer (10x) for DNA oligomeres	100 mM Tris pH 7.5 1 M NaCl 10 mM EDTA

Blotting buffer for Western blot	48 mM Tris 38 mM Glycin 20 % Methanol 1,3 mM SDS
Coomassie gel staining buffer	0,25 % Coomassie®brillian blue R250 10% Acetic Acid 40 % Methanol Filtration
Destaining buffer for Coomassie gels	10 % Acetic Acid 30 % Methanol
ES cell lysis buffer	50 mM Tris pH 8 100 mM EDTA 100 mM NaCl 1% SDS
ES cell Medium	500 mL Invitrogen Knockout-DMEM 2.5 mL Penicillin 2.5mL Streptomycin 2-4 mM Glutamine 5 mL 100x non-essential amino acids 0.1 mM 2-mercaptoethanol 20% FCS (ES-cell tested), heat inactivated for 20 min, 60°C 1000U/ mL LIF
FACS Sorting buffer	PBS + 5 % FCS + 0,5 M EDTA
MEF Medium	500 mL DMEM 2.5 mL Penicillin 2.5mL Streptomycin 2-4 mM Glutamine 5 mL 100x non-essential amino acids 0.1 mM 2-mercaptoethanol 10% FCS, heat inactivated for 20 min, 60°C

Freezing Medium for ES cells	ES-cell Medium 20 % DMSO
G418 (100 mg/mL)	720 µL in 200 mL Medium
Ganciclovir (10x)	216 µL in 200 mL Medium
Hybridizing buffer for Southern blot	Hybridizing Buffer was prepared Pre- Hybridizing Buffer without Denhard's
Intracellular FACS buffer	PBS pH 7.4 + 0.1% FCS
LB Medium	10 g/L tryptone 5 g/L yeast extract 5g/L NaCl
MAF Medium	500 mL DMEM 10% FCS 1% P/S
OLB buffer for Southern blot	100 µL solution A 250 µL solution B 150 µL solution C
PBS	137 mM NaCl 2.7 mM KCl 8.1 mM Na_2HPO_4 1.76 mM KH_2PO_4
Pre- Hybridizing buffer for Southern blot	10 mL water 3.75 mL 20x SSC 750 µL 100x Denhard's 340 µL 10x SDS 300 µL salmon sperm DNA
RIPA Buffer	50 mM Tris pH 7.5 150 mM NaCl 1mM EDTA 1% NP-40 0.1% SDS

Running buffer for SDS-PAGE	25 mM Tris 19 mM Glycin 0,1 % SDS (m/v)
Running gel for SDS-PAGE	5% AMBA 37,5:1 (m/v) 375 mM Tris-HCl 0,1 % SDS (m/v) 0,1 % TEMED (v/v) 0,0375 % APS (m/v)
S.O.C. Medium	2% Tryptone 0.5% Yeast Extract 10 mM NaCl 2.5 mM KCl 10 mM $MgCl_2$ 10 mM $MgSO_4$ 20 mM glucose
SDS-loading buffer	170 mM Tris-HCl 3 mM EDTA 0,2 % Bromphenol blue (m/v) 10 % SDS (m/v) 30% Glycerol 150 mM DTT
SILAC lysis buffer	PBS with 1% NP-40 5 mM EDTA 1 mM DTT 1 mM PMSF 1 µM Pepstatin A 2 mM sodium orthovanadate 2 Protease Inhibitor Cocktail tablets per 15ml
Solution A for hybridization buffer	1mL solution O 18 µL b-Mercaptoethanol 5 µL dGTP (0.1 M)

	5 µL dTTP (0.1M)
Solution B for hybridization buffer	2 M HEPES pH 6.6
Solution C for hybridization buffer	Random Hexamere in TE-buffer (90 U/mL)
Solution O for hybridization buffer	1.25 M Tris pH 8 125 mM $MgCl_2$
SSC Buffer (x 20)	3M NaCl 300 mM Sodium Citrate pH 7
Stacking gel for SDS-PAGE	7,5 % to 17 % Acrylamid/N,N'-methylen-bis-acrylamid (AMBA) 37,5:1 (m/v) 375 mM Tris-HCl 0,1 % SDS (m/v) 0,1 % TEMED (v/v) 0,0375 % APS (m/v)
TBS (-T)	500 mM Tris HCl pH 7.4 150 mM NaCl (0,05 % Tween)
TE buffer	10 mM Tris pH 7.5 1mM EDTA
Transfection Medium	10 mM HEPES in PBS
0.1% Chicken Trypsin	475 mM PBS 0.1 g EDTA 0.5 g D-glucose 5 mL chicken serum 20 mL 2.5 % trypsin Sterile filtered through 0.22 µM filter, stored in aliquots at -20°C

Table 2.5. Name and protocols of buffers and media

2.1.6 **Bacteriophage P1 artificial chromosome library**

A mouse genomic DNA bacteriophage P1 artificial chromosome (PAC) library RPCI-21 [179] was used to screen for genomic DNA. It was obtained from the Deutsches Ressourcenzentrum für Genomforschung GmbH (RZPD, Berlin, Germany). The library had

been generated as follows: Female 129S6/SvEvTac mouse spleen genomic DNA (partially MboI digested) was cloned into the BamHI sites of the vector pPAC4. PAC clones were transformed into *E. coli* and gridded onto nylon hybridization membranes. The library has an average insert size of 137 kb.

2.1.7 **Antibodies**

Name	**Species**	**Application**	**Company**
Alexa Fluor 647® anti-mouse CD62L (MEL-14)	Rat	Flow Cytometry	BioLegend
Allophycocyanin-conjugated $F(ab')_2$ Fragment Donkey anti-Rabbit IgG	Donkey	Flow Cytometry	Jackson ImmunoResearch
APC anti-mouse CD19 (6D5)	Rat	Flow Cytometry	BioLegend
APC anti-mouse CD4 (GK1.5)	Rat	Flow Cytometry	BioLegend
APC anti-mouse CD45R/B220 (RA3-6B2)	Rat	Flow Cytometry	BioLegend
APC anti-mouse CD8q (53-6.7)	Rat	Flow Cytometry	BioLegend
Beta-tubulin (ab11307)	Mouse	Western blot	abcam
Biotin anti-mouse CD4 (GK 1.5)	Rat	Flow Cytometry	BioLegend
Biotin anti-mouse CD8a (53-6.7)	Rat	Flow Cytometry	BioLegend
CD2BP2	Rabbit	Western blot Co-precipitation	self-made
CD2BP2 (ab32899)	Goat	Western blot	abcam
GAPDH (14C10)	Rabbit	Western blot	New England Biolab
GIGYF2	Rabbit	Western blot Immunofluoresence	self-made
LDH-A (N-14) (sc-27230)	Goat	Western blot	Santa Cruz
Pacific Blue™ anti-mouse CD11b (M1/70)	Rat	Flow Cytometry	BioLegend
Pacific Blue™ anti-mouse CD11c (N418)	Rat	Flow Cytometry	BioLegend
Pacific Blue™ anti-mouse F4/80 (Cl:A3-1)	Rat	Flow Cytometry	BioLegend
PE anti-mouse CD2 (RM2-5)	Rat	Flow Cytometry	BioLegend

PE anti-mouse CD3 (17A2)	Rat	Flow Cytometry	BioLegend
Rabbit polyclonal IgG (ab27472)	Rabbit	Flow Cytometry	abcam
Sp1 (sc-59)	Goat	Western blot	Santa Cruz

Table 2.6. **Commercially available and self-made antibodies.** Number in brackets either referred to the order number or the number of the cell clone.

2.1.8 **Bacteria**

2.1.8.1 E.coli BL21 (DE3) pLysS

For protein expression, carries a T7 RNA-Polymerase gen.

Genotype: BL21 (DE3) pLysS F—, *ompT hsdS*B(rB— mB—) *gal dcm* (DE3) pLysS [CamR] (Novagen)

2.1.8.2 E.coli XL1-Blue

For molecularbiological methods.

Genotype: F'::Tn 10 proA+ B+ lacIq Δ(lacZ)M15/recA1 endA1 gyrA96 (Nalr)

thi hsdR17 (r− k m+k) glnV44 relA1 lac

(Stratagene)

2.1.8.3 Top10

For cloning of large constructs, mostly used for mouse cloning.

Genotype: F– *mcr*A Δ(*mrr-hsd*RMS-*mcr*BC) Φ80*lac*ZΔM15 Δ*lac*X74 *rec*A1 *ara*D139 Δ(*ara leu*) 7697 *gal*U *gal*K *rps*L (StrR) *end*A1 *nup*G (invitrogen)

2.1.8.4 Cell lines

Name	Species	Growing condition	Medium
HeLa S3	Huma	confluent	DMEM
Neuro2a	Mouse	confluent	DMEM
pc12	Rat	confluent	DMEM
SH-SY5Y	Human	confluent	DMEM/Ham's F12 (1: 1)

Table 2.7. **Cell lines used in this study**.

2.1.8.5 Murine ES cells

Name	Origin
JM8.A3.N1	C57BL/6
R1/E	129

Table 2.8. Murine ES cells for the generation of knockout mice

2.1.8.6 Mouse strains

Name	Remarks	Supplier
C57BL/6J	The C57BL/6J inbred strain was created by Dr. CC Little from the mating of female 57 with male 52 from Miss Abbie Lathrop's stock. The same cross gave rise to the C57L and C57BR strains. Generation F226pF227 (02-JAN-10)	Jackson Laboratory
C57BL/6JOlaHsd	In 1974, from Jackson Laboratory to Laboratory Animals Centre, Carshalton. To OLAC (now Harlan UK) in 1983. In 1997 to Harlan Laboratories, Netherlands.	Harlan Laboratories
Flipo mouse (CAGGs-Flpo)	(CAGGs-Flpo) [180]	Konstantinos Anastassiadis, TU Dresden, Germany
PGK-Cre	Cre is driven by the early acting PGK-1 promoter [181]	Konstantinos Anastassiadis, TU Dresden, Germany

Table 2.9. **Name and origin of the mouse strains used**.

2.1.9 **Consumables**

All consumables were purchased from Roth, Sigma Aldrich, Greiner or Hartenstein unless noted otherwise.

2.1.10 **Instruments**

Name	**Producer**
ÄKTA™-Purifier	GE Healthcare
Centrifuge 5415R/D	Eppendorf
Centrifuge 5810R	Sarstedt
Centrifuge Avanti J-25	Beckman Coulter
Electrophorese systems for agarose gels	Owl Separation Systems
Geiger counter	berthold
Gel documentation system	Intas GmbH
Gene Pulser Ecell™	Bio-Rad Laboratories
Gene Pulser electroporator #165-2661	Bio-Rad Laboratories
Homogenizer 91-PCS24	Peqlab
Microwave R-239	Sharp
Multitron II Stackable Incubator Shaker	Infros AG Battningen
Nanodrop Spectrometer	Peqlab
PCR cycler	G-Storm
PCR cycler Epgradient	Eppendorf GmbH
pH-Meter	Knick Elektronische Mess-geräte GmbH & Co. KG
Phosphoimager 830	Storm
Power Supply Power Pac 300	Bio-Rad Laboratories
Profinia	Bio-Rad Laboratories
Scale EW1500	EW 1500 Kern & Sohn GmbH
Scale TP-214	Denver Instrument
SDS-PAGE Mini-Protean II	Bio-Rad Laboratories
Sonifier W250D	Branson Ultrasonics

TaqMan PCR cycler	Applied Biosystem 5700 Fast
Thermomixer comfort	Eppendorf GmbH
Water bath	Memmert
Water purifier arium®	Sartorius Stedim Biotech
XCell SureLock™ Mini-Cell	Invitrogen

Table 2.10. **Instruments used in this study.**

2.1.11 **Kits**

Name	**Catalog Number**	**Producer**
PCR/DNA Clean-up Kit (Gene Matrix)	E3520-01	roboklon
Pure link Midi Kit	K2106-15	invitrogen
QIAEXII Gel Extraction Kit	20021	Qiagen
Qiaquick PCR purification Kit	28106	Qiagen

Table 2.11. **KITs**

2.1.12 **Software**

Name	**Supplier**
ClustalW	http://www.ebi.ac.uk/Tools/msa/clustalw2/
Corel Draw	Corel
EndNote X4	EndNote
FlowJo	FlowJo
ImageQuant v5.1	GE Healthcare
LSM Image Browser Software	Zeiss
Molecular Toolkit	http://www.vivo.colostate.edu/molkit/
Odyssey Infrared Imaging System Software	licor
Office 98	Microsoft

Primer 3	http://frodo.wi.mit.edu/primer3/
Pyrat V1.6 Build 109	Scionics Computer Innovation
Vector NTI	invitrogen

Table 2.12. **Software used for this study**

2.2 DNA and RNA methods

2.2.1 DNA restriction digest

For DNA digest, 100 ng to 1 µg DNA was digested with the according enzymes and buffers for 1h at 37°C. DNA for Southern blot analysis was digested overnight.

2.2.2 Polymerase Chain Reaction

Polymerase chain reaction (PCR) allows the specific amplification of DNA-fragments with the termostabile Taq polymerase. The specificity is achieved by using specific forward (5' to 3') and reverse (3' to 5') primers.

PCR reactions were performed with OptiTaq Polymerase (roboklon). The PCR cycles used are listed in Table 2.13.

Name	Initialization	Denaturation	Annealing	Elongation	Final elongation	Number of cycles
Colony PCR	94°C 2 min	94°C 15 sec	58°C 15 sec	72°C 45 sec	72°C 5 min	25
Cre CBO	95°C 2 min	95°C 30 sec	60°C 30 sec	72°C 30 sec	72°C 30 min	36
External	95°C 2 min	95°C 30 sec	60°C 30 sec	72°C 4 min	72°C 7 min	35
Mousetail 56	95°C 2 min	95°C 15 sec	56°C 25 sec	72°C 30 sec	72°C 7 min	35

Table 2.13. **PCR cycles.** Number of cycles referrers to denaturation to elongation step.

2.2.3 DNA- Ligation

Table 2.14 shows the pipetting scheme for blunt and sticky end ligation.

Vector, linearized, CIPed (25 ng)	1 µL
DNA Fragment (Insert)	1-5 µL (see formula 2.1.1)
10x ligation buffer	1 µL
T4 DNA Ligase (4u/µL)	1µL

Water	Ad 10 µL

Table 2.14 **Ligation scheme for sticky and blunt end ligation**

The amount of insert was calculated by:

$$X \text{ ng insert} = \frac{(10) \times (Y \text{ bp DNA Fragment}) \times (25 \text{ ng linearized vector})}{(Z \text{ bp vector})}$$

2.2.4 **Annealing of DNA-Oligomers**

100 ng of each oligo in a final volume of 50 µL was boiled for 5 min and slowly cooled down to 75°C for 30 min.

2.2.5 **Chemical DNA Transfection**

DNA and competent *E. Coli* bacteria were combined, incubated on ice for 30 min, heat shock at 42°C for 45 sec and chilled on ice for 2 min. Cells were resuspended in 250 µL warm S.O.C. medium and was shaken at 37°C for 1h at 350 rpm. For selection, cells were spread on agar plates with the according antibiotics and incubated overnight at 37°C.

2.2.6 **DNA Transfection via Electroporation**

To improve electroporation efficiency, samples were desalted with viva spin microcolumns and resuspended with water. DNA and electrocompetent *E. Coli* bacteria were mixed in a pre-chilled electroporation cuvette. Cells were permeabelysed by applying and electroshock. Afterwards, cells were resuspended in 1 mL warm LB- medium and was shaken at 37°C for one hour with 350 rpm. For selection, cells were spread on agar plates with the according antibiotics and incubated overnight at 37°C.

2.2.7 **siRNA knockdown via Electroporation**

Knockdown of GIGYF2 was performed via electroporation. $1x10^6$ cells were centrifuged at 1000x g for 10 min and resuspended in Nucleofectin V solution (Amaxa). siRNA (Qiagen) was added and electroporated with Programm T-24 (Amaxa). 500 µL fresh medium was added and cells were plated into 6-well plates. Cell lysis was performed the next day.

siRNA-GIGYF2:

sense: r(GCA UGA AUU UAU ACG CUC A)dTdT

antisense: r(UGA GCG UAU AAA UUC AUG C)dTdT

2.2.8 **Colony PCR**

Colony PCR allows to test for successfully integrated DNA inserts into a vector. Bacteria colonies were picked from agar plates and resuspended in 10 µL water. Samples were boiled for 5 min, centrifuged for 3 min full speed and placed on ice. 1 µL was used per PCR approach.

2.2.9 **Colony Hybridization**

Colony Hybridization allows to test for successfully integrated DNA inserts into a vector. A positively charged nylon membrane was cut in the size of an agar plate and a raster with rising number was used to mark the different clones. A replicate plate was marked in the same way at the bottom of the plate. Colonies were picked from the original plate, transferred to the nylon membrane and afterwards to the replicate plate. Both plates were incubated overnight at 37°C.

The membrane was incubated for 5 min, first in denaturation solution, in neutralizing solution and finally in 2X SSC. Radioactive marked DNA probes (mostly the insert of interest) were used to detect positive clones on the membrane. The according clones were amplified from the replicate plate.

2.2.10 **DNA purification via Phenol/ Chloroform extraction**

DNA in lysis buffer was mixed with the same volume of Phenol/Chloroform/Isoamyl alcohol (25:24:1 v:v:v) and centrifuged at full speed for 5 min at RT. Supernatant was transferred to fresh tube and mixed with same volume of Chloroform/Isoamyl alcohol (24:1) and centrifuged with same parameters. All steps were performed with heavy 2 mL Phase Lock tubes.

2.2.11 **Precipitation of small amounts of DNA with Isopropanol**

DNA was precipitated with 500µL 100 % Isopropanol and centrifuged at full speed for 30 min at 4°C. Supernatant was discarded and pellet was washed with 70 % Ethanol. Samples were centrifuged for 15 min with full speed at 4°C. Pellets were dried and resuspended in water or TE-buffer.

2.2.12 **Precipitation of large amounts of DNA with Isopropanol**

DNA was precipitated with 500µL 100 % Isopropanol and slowly mixing of the tube until a white DNA strand could be seen. Either, the liquid was cautiously soaked and 70% ethanol was added or the DNA strand was fished with a yellow pipet tip and transferred to a fresh

tube with 70% ethanol. The same step was repeated with 95 % ethanol. DNA was resolved in TE-buffer and resolved over night at 56°C in a humidity chamber.

2.2.13 **DNA Sequencing**

DNA for sequencing was send to SeqLab in Göttingen, Germany. The DNA was delivered according to the requests demanded by the company.

2.2.14 **Generation of probes for Southern blots**

Several DNA oligomeres were clone for hybridization in PAC DNA screening, Southern blot or Colony PCR. The 5' and 3'external probes for Southern blots were generated by amplification of WT mouse DNA with the following primers:

5'probe sense: 5'GAAACCCCATCTCAGTAAT'3

5'probe reverse: 5'ACCAGCCGCAAAAAAGCAATCA'3

3'probe sense: 5'TATCCAGCCTTATCTCCCACTCG'3

3'probe reverse: 5'GGCTGCCCCTGTCAACTG'3

Leading to a fragment of 234 bp for the 5'probe and 355 bp for the 3'probe.

The PCR fragments were cloned into pCR 2.1-TOPO® TA. This vector is covalently linked with Topoisomerase I. The Topoisomerase adds a single deoxyadenosine to the PCR insert, the vector has an overhanging deoxythymidin, allowing efficient ligation of the insert and vector. For the generation of clean probes, the vector was digested with EcoRI and DNA fragments were purified via gel purification.

For the screening of PAC DNA a 213 bp fragment of CD2BP2 cDNA was amplified with the following primers:

Forward primer: 5'GGCAAAGGGAGAAAGGGGCCT'3

Reverse primer: 5'CTCCTCAGCGAACATGTC'3

2.2.15 **Radioactive Labeling with Rediprime**

Labeling with "Rediprime II Random Primer Labeling system" (GE healthcare) has been performed according to the Manufactures Protocol.

2.2.16 **Radioactive double labeling with random hexameres**

DNA labeling via *in vitro* transcription works as follows. Random hexamere bind to one denaturated single-stranded DNA strand. The Klenow fragment (large subunit of DNA

polymerase I, *E.coli*) fills up the gaps with different NTPs [182], thereby, [alpha-^{32}P]dCTP and dATP (Hartmann Analytik, Germany) is integrated leading to a radioactive probe.

For the generation of radioactive probes, 1 µL DNA (50 ng/µL) was boiled for 5 min and chilled on ice. Labeling was performed according to Table 2.15 and incubated for 3 h at 30°C.

DNA	**1µL**
OLB-buffer	10 µL
^{32}P-CTP (30µCi)	3 µL
^{32}P-ATP (30µCi)	3 µL
DNA Polymerase 1, Large (Klenow) Fragment	1µL
Water	Ad 30 µL

Table 2.15 **Pipetting scheme for radioactive double labeling**

2.2.17 **DNA purification**

All DNA fragments were purified with EURx BlueMatrix PCR clean up DNA purification Kit according to the Manufactures Protocol.

2.2.18 **Southern blotting**

The Southern blot serves as a method to detect specific DNA fragments [183]. First, the DNA is digested, then loaded on an agarose gel and then blotted on a positively charged nylon membrane. The DNA fragments of interest are captured by small radioactive labeled DNA probes.

Genomic DNA was digested with the according enzymes overnight and separated with a 0.7 % agarose gel at 80 V for 3 to 4 hours. The Southern blot was built up as follows. A tray was filled with 0.4 M NaOH and covered with a glass plate. Two Whatman papers covered the plate and both ends of the paper were placed into the 0.4 M NaOH solution. The agarose gel was put bottom up on the Whatman paper, followed by a positively charged nylon membrane and another Whatman paper. Green towels were put on top to create an osmotic gradient fixed by a glass plate and weights. Southern

blotting was performed overnight. The next day, the membrane was washed two times with 2x SSC.

The membrane was incubated for at least 6 hours with pre-hybridizing solution. Radioactive probes were incubated overnight in hybridizing solution. Afterwards, the membrane was

washed with 2XSSC, 0.2% SDS until no radioactive signal could be measured in the washing buffer. Membranes were incubated on phospho-imager plates and detected the next day.

2.2.19 **Production of salmon sperm DNA for Southern blotting**

Salmon sperm is meant to block unspecific binding of labeled probes and thereby reducing the background.

1 g salmon sperm DNA was dissolved in 100 mL 0.4 M NaOH and stirred overnight at RT. DNA was denaturated by boiling 45 min. Chilled DNA was set to pH 7 and centrifuged at 2000 rpm for 10 min. The denaturation was performed by adding two volumes of 95% EtOH and incubation at -20°C for 1 h. After centrifugation, pellet was washed with 70% EtOH. EtOH free DNA was resuspended in TE buffer with a final concentration of 10 mg/mL and stored in aliquots at -20°C.

2.2.20 **RNA extraction from mouse organs**

Organs were extracted and immediately snap frozen with liquid nitrogen. For extraction, tissue was mixed with 700 µL Qiazol®. Samples were homogenized with 5 2.8 diameter ceramic beads for 20 sec, 5000 rpm in a homogenizer (SeqLab). After 5 min incubation at RT, samples were mixed with 140 µL chloroform, incubated for 3min at RT and centrifuged at 12 000 x g, 15min at 4°C. Samples were transferred into fresh tubes, mixed with same volume of 70% Ethanol and transferred on RNeasy Mini columns (Qiagen). Columns were centrifuged for 15 sec at 8 000 x g at RT. Flow through was mixed with 350 µL RWI buffer and centrifuged.

For DNA depletion, samples were treated with 70 µL RDD-Buffer with 10 µL DNase and incubated for 15 min at RT. Columns were one time washed with 350 µL RWI-buffer and centrifuged for 20 sec at 8 600 x g at RT and again washed with 700 µL RPE buffer, centrifugation lasted 2 min at 8 600 x g. RNA was eluted by applying 30 µL RNase free water onto the column, one min incubation and centrifugation for one min with full speed at RT. RNA concentration was determined at the Nano Drop (peqlab).

2.2.21 **Reverse Transcription**

2 µg RNA was reversely transcribed with the High Capacity RNA-to-cDNA Kit according to the manufactures protocol.

2.2.22 **Real-Time PCR with TaqMan® Probes**

TaqMan PCR® allows a more specific quantitation than regular qRT-PCR. The principles rely on the exonuclease activity of the Taq polymerase. A specific probe with a fluorophore, covalently coupled to the 5' end and a quencher at the 3' end base pairs with a DNA fragment in between the forward and reverse primers. As long as the quencher is in close proximity to the fluorophore, it is constantly blocked and unable to emit fluorescence. When the amplification takes place, the polymerase cleaves off the fluorophore leading to fluorescence, which can be measured. Accordingly, the detected fluorescence is directly proportional to the fluorophore release after strand-amplification [184].

For expression normalization, cDNA samples were measured with the reference gene eukaryotic 18S rRNA (GenBank accession number: X03205). Standard curve was evaluated by mixing 5 µL of all samples and five time dilution 1:10.

CD2BP2 cDNA levels were measured in duplicates using the following primers and probes (spanning exon 5 to 6):

Forward: 5'GAG GAA GTA GCA GAG GGT GAA CTG'3

Reverse: 5'CAG GCC ATC TCC TGC TGA CT'3

Probe: Fam-AAA CCC CAA CCC CTA CCC AAA GAG AGG-Tamra

2.3 Protein Analysis

2.3.1 **Protein Expression in *Escherichia Coli***

BL21 (DE3) pLysS cells were transfected with his-GIGYF2-GYF-pGADT7. Clones were used to inocculat 3 mL 2YT-medium supplemented with amp at 37°C. Preculture was grown overnight and used for the inocculation of 50 mL 2YT-medium with amp. At an OD of 0.6, protein expression was induced by 1mM Isopropyl-β-D-thiogalactopyranosid (IPTG). After 3.30h, cells were centrifuged and pellet was frozen at -80° for further usage.

2.3.2 **Protein Expression of his-CD2BP2 in SF9 Insect cells**

The ovary cell line *Spodoptera frugiperda* was transfected with the human his tagged construct of human his-CD2BP2 (NM_006110.2) for protein expression. Sindy Blank in our lab has performed the expression and purification of CD2BP2.

2.3.3 **Bradford Assay**

The Bradford Assay is photometric technique to measure protein concentration [185].

Protein concentration was determined by creating a standard curve with rising amounts of BSA (1, 2, 5, 10, 15 µg/µL). Between 1 µL protein samples was measured at 595 nm with 99 µL water and 900 µL Bradford solution (1:5 dilution). Concentration was evaluated via linear regression.

2.3.4 **Protein extraction from mouse organs**

10-12 weeks old C57BL/6J mice were sacrificed by cervical dislocation. Organs were extracted and immediately snap frozen into liquid nitrogen.

Proteins were extracted by mixing with 5 ceramic beads (2.8 mm diameter) in 500 µL RIPA-buffer with protease inhibitors in a homogenizer. They were mixed for 15 sec twice and incubated on ice for 30 min. Samples were centrifuged for 10 min at 16 000x g at 4°C. Supernatant was transferred into a fresh tube and protein concentration was determined via Bradford assay.

2.3.5 **Pull-down**

For the pull-down, glutathione beads were loaded with 5 mg GST-fusion protein per mL of matrix and washed 3 times with PBS. 25 µL of the protein-loaded slurry were resuspended with an equal volume of PBS and incubated with 1-1.5 mL cell lysate over night at 4 ºC. In the GIGYF2-GYF pull-downs, the peptide PD2 (HVGPPPGLEVQ) was added. The GST-beads were centrifuged for 5 min at 500 x g at 4 °C, the supernatant removed, and the beads washed 3 times with 1 mL PBS. For the SILAC pull-down, beads of the labeled and unlabeled sample were combined in a ratio of 1:2 labeled to unlabeled sample. Combined beads were centrifuged for 5 min at 500 x g at 4 °C and the supernatant was removed. Proteins were eluted with SDS-loading buffer and the sample was boiled for 5 min at 95 °C. Samples were separated on 4-20% Tris-Glycine gradient gels.

2.3.6 **Immunoprecipitation with agarose beads**

The precipitation of endogenous protein from lysate with antibodies from rabbits was performed with agarose-coupled Protein G beads (Invitrogen). 30 µL of protein G bead slurry was washed three times with 1 mL TBS at 1000 x g to remove residual ethanol. Beads were incubated with different antibody concentrations for 2 to 3 h at 4°C on a rotating wheel. To remove uncoupled antibody, the mixture was washed three times with TBS. Different amounts of cell lysates were added to the mixture and incubated over night at 4°C on a

rotating wheel. The next day, samples were washed three times with TBS-T. Proteins were eluted with 40 µL SDS-loading buffer.

2.3.7 **Cell fractionation**

HeLa and pc12 cells were separated with NE-PER Nuclear and Cytoplasmic Extraction Kit™ (PIERCE) according to the manufactures' protocol with same changes. After addition of buffer CERII, cells were centrifuged at 800x g for 10 min. The nuclear fraction was extracted with RIPA buffer.

2.3.8 **SDS-PAGE**

The sodium dodecyl sulfate polyacrylamide gel electrophoresis (SDS-PAGE) separates proteins according to their electrophoretic mobility. Proteins or cell lysates are mixed with SDS-buffer, an anionic detergent which denaturates the protein and applies negative charges to each protein in relation to its mass. SDS-PAGEs were either performed with self-made protein gels or w 4-12 % Bis-Tris gradient gels (invitrogen). Gels were run at 140 V until loading front left the stacking gel and set to 180 V in the running gel.

2.3.9 **Coomassie® Staining**

Coomassie®brilliant blue R250 forms complexes with proteins and can therefore be used to detect protein bands in a SDS-gel. The detection limit of this staining method is about 50 ng. Incubating the proteins gels for at least 30 min in Coomassie-buffer performed staining. Gels were destained until bands were detectable.

2.3.10 **Western blot**

Proteins, separated via SDS-gels can further be blotted onto positively charged nitrocellulose membranes for immunodetection with specific antibodies.

All blots were performed in a tank-blotting chamber (invitrogen) at 30V for 90 min. Incubating the membrane with 5% TBS milk solution blocked unspecific proteins. First and secondary antibody were diluted in 5% TBS-T milk solution, the first antibody for one hour up to overnight at 4°C, the secondary antibody for 45 min at RT. Both were washed three times with TBS-T. Western Blots were analyzed with Odyssey®Infrared-Scanner.

2.3.11 **Mass spectrometry**

For the detection of proteins, Proteins were separated via SDS-PAGE and Coomassie stained. Protein bands of interest were cut out of the gel and digested in the gel with trypsin. Bands

were incubated with 100 µL washing solution for 10 min at 30°C, 750 rpm. 100 µL equilibration-buffer was added and incubated for 10 min at 30°C, 750 rpm. Adding 50 µL of acetonitril (ACN) dehydrated the bands. They were dried in a speed Vac for about 10 min. Dried bands were digested with trypsin over night at 37°C, 300 rpm. The next day, digest was stopped and incubated in an ultrasound bad for 10 min. Supernatant was transferred into MS vial. 20 µL ACN was added to the bands and mixed with the other supernatant. All supernatant were concentrated in a speed vac. Residual was solubilized with 6 µL ACN/0,1 % TFA and stored at -20°C until measurement.

All mass spectrometry (MS) analysis were performed at the AG Krause at the FMP in Berlin and measured by Michael Schuemann.

2.3.12 **SILAC Pull-down MS**

HeLa cells were cultured in defined SILAC DMEM (I nvitrogen) supplemented with ^{15}N-lysine, ^{15}N-arginine and 10% (v/v) dialyzed FCS. Labeled SILAC medium was prepared by adding $^{13}C_6$-arginine and $^{13}C_6$-lysine (Cambridge Isotope Laboratories, Andover, MA). For unlabeled medium normal ^{12}C amino acids were used. Cells were cultured for 8 days in SILAC media. After washing with PBS, preparation of the cytoplasmic fraction was performed as described in 2.3.7. The pull-down process is described in 2.3.5. The processed MS/MS spectra and MASCOT server (version 2.0, Matrix Science Ltd, London, UK) were used to search in-house against the UniProt/Swiss-Prot database (release 56.0 of July 22nd, 2008, contains 392,667 sequence entries, comprising 141,121,034 amino acids). A maximum of two missed cleavages was allowed, and the mass tolerance of precursor and sequence ions was set to 100 ppm and 0.05 Da, respectively. Acrylamide modification of cystine, methionine oxidation, $^{13}C_6$-arginine, and $^{13}C_6$-lysine were considered as possible modifications. A protein was accepted as identified if the total MASCOT score was greater than the significance threshold and at least two peptides appeared the first time in the report and were the first-ranking peptides.

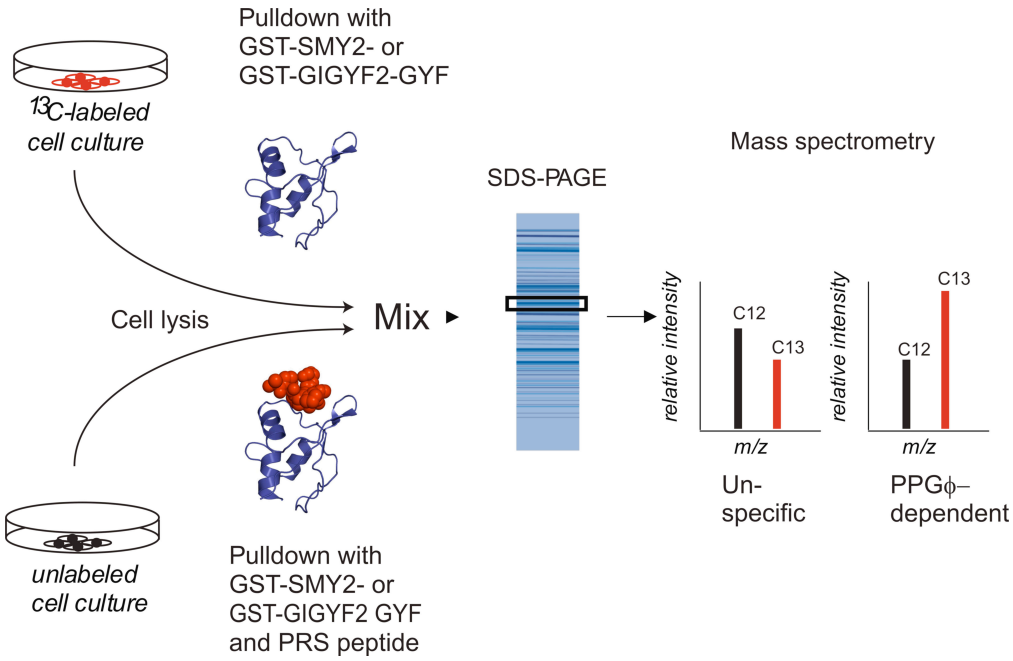

Figure 2.1. **Schematic drawing of SILAC pull-downs and MS analyses**. HeLa cells were cultured in ^{13}C-arginine/^{13}C-lysine labeled medium unlabeled medium. Pull-downs were performed either with competing peptide (labeled medium) or without, combined and analyzed by 1D-PAGE. ^{13}C enrichment in MS spectra was indicative for specific binding partners.

Quantification was carried out by MSQUANT open-source software (Peter Mortensen and Matthias Mann, http://msquant.sourceforge.net/) and was based on calculations of isotope intensity ratios of at least two arginine- or lysine-containing tryptic peptides with individual MASCOT score indicating identity. Additional criteria were that no interfering mass peaks were observed and that peptides contained neither missed cleavage sites nor methionine oxidation. Relative protein ratios were calculated by averaging over all peptides. Standard deviations of the quantification for individual proteins were obtained from MSQUANT. Analytical reproducibility was determined by multiple LC-MS measurements of selected samples showing that the experiment-to-experiment deviation of $^{13}C/^{12}C$ ratios are less than 25% (peptide score indicates identity or homology). Based on decoy database searches the false positive rate was estimated to be ≤ 1%. The entire workflow of SILAC pull-down MS is shown in Figure 2.1.

2.3.13 **Staining of immune cells for cell sorting**

Thymus, Spleen, mesenterial and medial lymph nodes from C57BL/6 mice were used for analysis. Immune cells were extracted by sieving the organs through 40 µM cell strainer. Spleen cells were resuspended in Eri-lysis buffer and incubated for 5 min at RT. Cells were washed twice with FACS sorting buffer. $1x10^6$ cells in 100 µL were blocked for 30 min at 4°C in the according normal serum, followed by the antibody staining for 30 min at 4°C. After washing, cells were resuspended in FACS buffer and sorted at the Cell sorting facility, Max-Dellbrück Center for Molecular Medicine, Berlin.

2.3.14 **Extracellular and intracellular staining of immune cells**

C57BL/6 mice were used for cell analysis. Thymus, Spleen, mesenterial and medial lymph nodes were extracted, washed with FACS buffer and mashed through a 40 μM cell strainer. Femoral bone marrow was extracted via flushing with FACS buffer and filtering through a 40 μM filter.

Single cell suspension was washed with 50 mL FACS buffer at 300x g for 10 min, 4°C. For some analysis, spleen and thymus was incubated with Eri-lysis buffer for 5 min at RT and washed again with 50 mL FACS buffer. Cells were counted and $1x10^6$ to $1x10^7$ cell were stained with 100μL extracellular antibody. After incubation for 15 min at 4°C in the fridge, cells were washed with 1 mL FACS buffer. After washing with 1 mL FACS buffer, cells were permeabilized with 70 μL Cytofix/ Cytoperm (BD) for 10 min at RT in the dark. All subsequent washing and incubations steps were performed with 1x Cytofix/ Cytoperm washing buffer. After washing, cells were incubated with 5% normal goat serum for 30 min at 4°C. $1x10^6$ cells were stained with 100 μL intracellular antibody for 15 min at 4°C and afterwards washed with 1 mL washing buffer. If necessary, samples were stained with 100 μL secondary antibody for 15 min at 4°C and finally resuspended in 200-300 μL FACS buffer.

2.3.15 **Antibody competition assay**

To test the specificity of the rabbit anti-CD2BP2 in intracellular flow cytometry, Thymus and spleen of a 9 weeks old BL6 male was used. Because BSA has a bout double the molecular weight of CD2BP2 (69 kD and 38 kD respectively), they were titrated starting from a concentration of 1:5, 1:10, 1:25 and 1:50. The protein was added to the antibody and incubated for 30 min; the rest of the staining was performed as described in 2.3.14. The CD2BP2 positive control was added in a concentration of 1:100.

2.3.15.1 MACS Sorting

The thymus from five weeks old male BL6 mice was used for this analyzes. Two to four thymus where pooled together, washed and depleted of erythrocytes by incubating the cells for 5 min with Eri-Lysis buffer at RT. 1x 106 cells were stained in 100 μL FACS buffer. Blocking was performed with 1:200 Fc block for 10 min at 4°C. Anti-biotin CD4 and CD8 (1:200) were directly applied to the cells and incubated for 10 min at 4°C. After washing, 160 μL FACS buffer with 1:200 Pc block and 40 μL anti-biotin beads was applied to the cells for 15 min at 4°C. Meanwhile incubation, LS Columns (Millipore) that were packed with ferromagnetic spheres where equilibrated three times with 3 mL FACS buffer. Cells were resuspended in 2 mL FACS buffer and applied to the column. After loading, the column was washed with 6 ml buffer. Supernatant was collected and used for CD4 CD8 positive cell depleted analyses.

2.3.15.2 FACS Measurement

All flow cytometric measurements have been performed at the instrument FACS Diva II (BD bioscience). Before measurement of the samples, all lasers were compensated with compensation controls. The instrument was flushed with FACS clean (BD) during measurements.

2.4 Cell lines

2.4.1 **Maintaining adherent cell lines**

Cells were maintained in the according media with supplements at 37°C under 5% CO_2/ 95% air. Medium was exchanged every second day. When cells reached confluency of 70-80%, they were washed once with PBS and incubated with trypsin for 5 min at 37°C. Loose cells were washed with FCS containing medium and centrifuged for 5 min, 1000x g. One third of the cells were transferred to a new cell culture flask and supplemented with fresh medium.

2.4.2 **Maintaining suspension cell lines**

Cells were kept as suspension cells in the according medium at 37°C under 5% CO_2/ 95% air. Every second day, 1 mL cell suspension was transferred to a new cell culture flask and supplemented with fresh medium.

2.4.3 **Coating of Cover Slips**

1.668 g Boric Acid was dissolved in 180 mL water and the pH was set to 8.3. 90 mg Poly-Ornithine was added and sterile filtered. Autoclaved cover slips were distributed into 6-well plates, covered with 1 mL Poly Ornithine solution, and incubated under the hood. After 1 h, the slips were washed three times with sterile water and dried under the hood over night. The next day, cover slips were either used directly or wrapped with parafilm and stored at 4°C up to 4 weeks.

2.4.4 **Transfection of adherent cells**

Cells were either grown in 10 cm petri dished or on Poly-Ornithine coated cover slips until 60-80% confluent. Transfection was performed with fuGENE 6 according to the manufacturer's protocol. For western blot analysis or Immunofluorescence, cells were harvested 24 to 48 h post transfection.

2.4.5 **Confocal laser scanning microscopy**

For endogenous protein staining 1 x 10^4 HeLa S3 cells were grown on glass cover slips pre-coated with poly-L-ornithine and fixed with 4% paraformaldehyde. For permeabilization, cells were treated with -20 °C methanol. After washing three times with PBS, first and secondary antibodies where incubated in PBS with 0.2 % fish gelatine. Stained cells were mounted in mowiol (Roth). All cells were analyzed by confocal microscopy (LSM 510 Meta, Carl-Zeiss) with an 100x/1.3 objective and excitation with the following sources: An Argon-Laser at 458 nm for CFP, an Argon-Laser at 514 nm for YFP, an Argon-Laser at 488 nm for cy2 and a Helium-Neon-Laser at 543 nm for cy3. Images were processed using Zeiss LSM Image Browser and Corel Draw (Corel Corporation, Ottawa, Canada).

2.4.6 **Generation of Murine Adult Fibroblasts (MAF)**

A piece of clipped mouse ear that was normally used for genotyping was used for the generations of MAFs. The earpiece was dipped twice into 70 % ethanol and once into sterile PBS under the sterile bank. The ear peace was transferred into a fresh tube and 300 µL Collagenase2 (PAA) was added. With eye surgical scissors, the piece was diced into very small pieces. After incubation for 2-3 hours at 37°C and several mixing steps, the mixture was plated into 6 well plates and filled up with MAF-medium. Medium was changed the next day.

2.4.7 **Protein purification via ion exchange chromatography**

His-tagged proteins were purified by immobilizing the hexahistidine-peptide to Ni^{2+} or Co^{2+} coupled agarose. 10 mM imidazol was used for the equilibration and washing steps. For elution, the imidazol concentration was linear raised up to 400 mM.

2.5 Generation of polyclonal antibodies in rabbit

Purified proteins were sent to BioGenes (Berlin, Germany) for immunization of rabbits. Two rabbits were immunized with the according protein once a week for three consecutive weeks. In the forth week, serum was taken and tested for specificity the lab. This was repeated three times until the serum of the animals showed specific bands in Western blots.

2.6 Excision test of loxP sites in EL350 cells

The recombination of the loxP sites in the final pPNT-FRT4-CD2BP2 vector was tested in EL350 cells that express the cre-recombinase upon induction via L-arabinose [186].

Therefore, LB medium was inoculated with EL350 cells (kindly provided by Chiara Perrod, AG Rosenbauer at the MDC in Berlin) and grown over night at 30°C.

The next day, the cells were induced with 1:100 10 % L-arabinose at OD600. Bacteria were grown for one more hour, chilled on ice for 20 min and centrifuged for 10 min at 1000x g. Cells were made competent by washing 3 times with 10% ice cold glycerol. At the end, pellets were resuspended with 50% glycerol. Aliquots were snap frozen and stored at -80°C.

The pPNT-FRT4-CD2BP2 vector and a control vector was electroporated into the competent EL350 bacteria, incubated for 1h at 30°C and plated on amp agar plates. The next day, about 20 colonies are replated on kan and amp agar plates. About five colonies grown on amp plates were used for an over night culture. DNA was extracted and digested with EcoRI and AgeI.

2.7 Stem cell culture

2.7.1 **Mouse embryonic fibroblasts (Feeder Cells)**

Fetuses were harvested between day 12.5- 14.5 of gestation. Time of gestation was confirmed by weighing of the fetuses. Head, liver and blood clogs were removed and corpus was washed with 1- 2 mL PBS. Tissue was transferred into a fresh 60 mm dish and minced with 2 mL trypsin.

After incubation, the tissue was pipetted vigorously until it is a single cell suspension. Cells were spread into two 25 cm^2 flaks (passage 0). Cells were split every 3 to 4 days during early passages (P1-6), then every week. Back-up cells were frozen at Passage 2.

For stem cell screening, heterozygous neomycin mice were used. Cells were radiated with UV light (5000 rad) for inactivation.

2.7.2 **Electroporation of murine Stem Cells**

129 R1 (passage 12) and BL6 JM8 (passage 18) stem cells were thawed five days before the electroporation and splitted twice. Cells were kept on a layer of inactivated feeder cells. For the elctroporation 6 Mio cells we re washed with PBS and incubated with chicken trypsin at 37°C until colonies became single cells. Trypsination was stopped with feeder medium and cells were centrifuged for 5 min, 300x g. 1x 10^7 cells were resuspended in 500 µL transfection medium and mixed with 25 µg linearized vector in a 4 mm cuvette (biorad). Electroporation was applied with 250 V, 500 µF at high capacity. Cells were incubated on ice for 10 min, resuspended in ES-Medium and spread on 8-10 10 cm plates that were coated with inactivated feeder cells.

2.7.3 **Positive and negative stem cell selection**

Positive selection started 24 h after electroporation with the supplementation of 300 µg/mL G418. After 72h, the negative selection started by the additional supplementation of ganciclovir. Supplementation stopped with the start of clone picking which started 6 days after the electroporation.

2.7.4 **Picking of stem cell colonies**

Before picking, the stem cells were washed with 5 mL warm ES-cell medium. Colonies were picked under the microscope, soaked with 10 µL medium and transferred into a round-bottom 96 well plate. Two plates were picked in parallel and one plate was exchange against the other one after picking of 24 colonies. Colonies were separated with 30 µL chicken trypsin that was incubated for 30 min at 37°C or until cell were floating in the wells. Adding 60 µL of ES-cell medium stopped trypsination. Cells were resuspended 10-20 times to ensure separation. Finally, the 96 well plates were supplemented with 100 µL inactivated feeder cells per well. Medium was exchanged every day until cells were dense enough for back-up plates.

2.7.5 **Splitting of ES-cell for genotyping and back-up plates**

The FCS was removed by washing the cells with 100 µL PBS. Colonies were separated by incubation with 25 µL chicken trypsin at 37°C until cell were floating. Cells were resuspended in 125 µL ES-cell medium and 50 µL cells were distributed into 3 96 well plates, respectively. Back-up plates were supplemented with 100 µL feeder-cells, genotyping cells with 100 µL ES-cell medium.

2.7.6 **Freezing of ES-cell back-up plates**

Cells were washed with 100 µL PBS, separated with 25 µL trypsin and incubated for 9 min at 37°C. 75 µL ES-cell medium stopped the trypsination. 100 µL separated cells were thoroughly mixed with 100 µL freezing medium on ice. Plates were covered with 50 µL paraffin oil and deep-frozen.

2.7.7 **Expansion of genotyping plates and DNA extraction**

Cells were grown in 96 well plates until 100 % confluence and expanded to 4 24 well plates, that were coated with 0.1% gelatin. After at most one week or cell medium is yellow, cells were lysed with 500 µL ES cell lysis buffer with Proteinase K.

For DNA extraction, 500 µL isopropanol was added and plates were shake until DNA filament became visible. Fluids were aspirated and DNA washed with 500 µL 70% ethanol.

DNA was “fished” with a pipette tip and resuspended in 120 µL TE-buffer in a 96 well plate. The plates were incubated in a mosty chamber at 37°C over night to resolve DNA completely.

2.7.8 **Mouse genotyping**

Small ear clips or tail biopsies were incubated with 500 µL QuickExtract DNA Extraction Solution (Biozym), vortexed for 15 sec, incubated for 6 min at 65°C, vortexed again 15 sec and incubated at 95°C for 2 min. The mastermix for PCR prepared as shown in Table 2.16 with OptiTaq polymerase and the according buffers.

Name	**Amount in µL**
DNA	2-5
10x buffer C	1,5
dNPT mix (2.5 mM each)	1,2
Forward primer	0,3
Reverse primer	0,3
OptiTaq	0,3
H_2O	Ad 15

Table 2.16. **Mastermix for genotyping PCR**

After PCR, the samples were stored at -20°C. 3 to 5 µL was used per PCR sample. In Table 2.17, genotyping PCRs with expected sizes are shown.

Name	**Sequence**	**Annealing Temperature**	**PCR program**	**Size**
3’external	5'gggaggattgggaagacaat'3 5'gcctcctggagacagatgag'3	58 °C	External	Neo: 4060 bp
3’external_B	5’ccgaagcgttaacataacttcg’3 5’tggtggggtgaaaacttagg’3	58- 60°C	External	Neo: 2120 bp Flox: 2120 bp
5’external_B	5’tcaggaaggaatgaccatga’3 5’aacccaggagtcatttgcac’3	58- 60°C	External	Neo: 4103 bp

Flip_B	5’ggcgttgaggtttgagttgt’3 5’aacccaggagtcatttgcac’3	56 °C	Mousetail 56°C	WT: 265 bp Neo: 2011 bp Flox: 332 bp
Cre_A_f Cre_A_r	5’cttctgtggccgtaaagctc’3 5’ctccatcctgaaggcttgtc’3	56°C	Mousetail 56°C	WT: 2138 bp Neo: 3949 bp Flox: 2232 bp Cre: 423 bp
Cre-Deleter (CBO)	5’cgccatccacgctgttttgacc’3 5’cagcccggaccgacgatgaag’3	60°C	Mousetail cre birchmayer	Cre+: 489 bp
Flip_B_f 3’external_B_r	5’ggcgttgaggtttgagttgt’3 5’tggtggggtgaaaacttagg’3	60°C	External	WT: 3862 bp Neo: 5672 bp Flox: 3974 bp KO: 2146 bp
p_loxP_PpNT 5’external_r	5'gtatagcatacattatacgaagttatcgaagtt'3 5'ggggaacttcctgactaggg'3	56°C	Mousetail 56°C	Neo: 266 bp
P_ZERO_5088 Flip_B_r	5’attcacaatgggagaaaacc’3 5’aacccaggagtcatttgcac’3	56°C	Mousetail 56°C	WT: 378 bp Neo: 2144 bp Flox: 445 bp
WT_new_A_f WT_new_A_r	5’ggtttgagttgttccccaga’3 5’gctcttctctctgagtcctgct’3	60°C	Mousetail 60°C	WT: 325 bp
WT_new_B_f WT_new_B_r	5’tttgagttgttccccagagc’3 5’gctcttctctctgagtcctgct’3	60°C	Mousetail 60°C	WT: 303 bp
WT_new_C_f WT_new_C_r	5’ccccagagctccagatctaa’3 5’gctcttctctctgagtcctgct’3	60°C	Mousetail 60°C	WT: 311 bp

Table 2.17. **Mouse genotyping DNA primers**

2.7.9 **Mouse housing and handling**

All animals were kept under specific pathogen free (SPF) conditions in the mouse house of the MDC, Berlin, Germany according to recommendations of the Federation of European Laboratory Animal Science Associations (FELASA) with food and water provided *ad libitum* in air conditioned rooms at 22-23 °C with a standard 12 h light/dark cycle. Cutting of mousetail biopsies and sacrifices were approved by the Landesamt für Gesundheit und Soziales (LAGeSo), Berlin Germany (O- 0078/11) or the MDC (X 9005/11) and performed by the staff of the animal facility.

Mice were exclusively handled by people certificated to perform animal experiments. Mice were tattooed within the first week after birth and mouse tail biopsies were cut in this process. Pups were weaned after 21 days and if necessary, ear clips were taken.

Breeding was started after six weeks of age of the male and 8 weeks of age for female mice and either set up with one male and one female or one male and two females.

Female in plug breedings were tested every day for positive plug, this was considered as embryonic day 0.5.

Cervical dislocation was performed without previous anesthesia to avoid additional stress for the animal. If the animals were sacrificed with isoflurane, the according amount of the halogenated ether was saturated in a glass chamber before the animal was put in.

3 Results

3.1 Functional characterization of the protein GIGYF2

Little was known about the cellular localization or function of the GYF-domain containing protein GIGYF2. Most of the potential interaction partners found by yeast-two-hybrid screening [22] are localized to the nucleus. Because of this and the predicted NLS, GIGYF2 was expected to fulfill a nuclear function. To better analyze the role of GIGYF2 within the cell, we generated a polyclonal antibody raised against the GYF-domain of GIGYF2. With this antibody localization studies in several cell lines and mouse organs have been performed.

3.1.1 Generation and characterization of anti-GIGYF2-GYF

The GYF-domain of GIGYF2 was expressed and purified as described in the Method part. The his-tagged protein was purified via ion exchange chromatography and used for immunization of rabbits. The protein was coupled with a carrier-peptide GIGPEVPDDEDF (KLH) to enhance immunogenicity (at BioGenes, Berlin, Germany). The specificity of the antiserum was analyzed in overexpression and knockdown studies and by MS.

Knockdown with GIGYF2 siRNA led to a reduction of GIGYF2 expression in HeLa cells. This can be seen by a reduced immunoreactive band against GIGYF2 in the Western blot shown in Figure 3.1 A. The sample with the knockdown shows reduced intensity of a band at 150 kD, which correlates with the size of GIGYF2. Overexpression of GIGYF2-YFP in HeLa cells led to an additional higher band as shown in the Western blots in Figure 3.1. B.

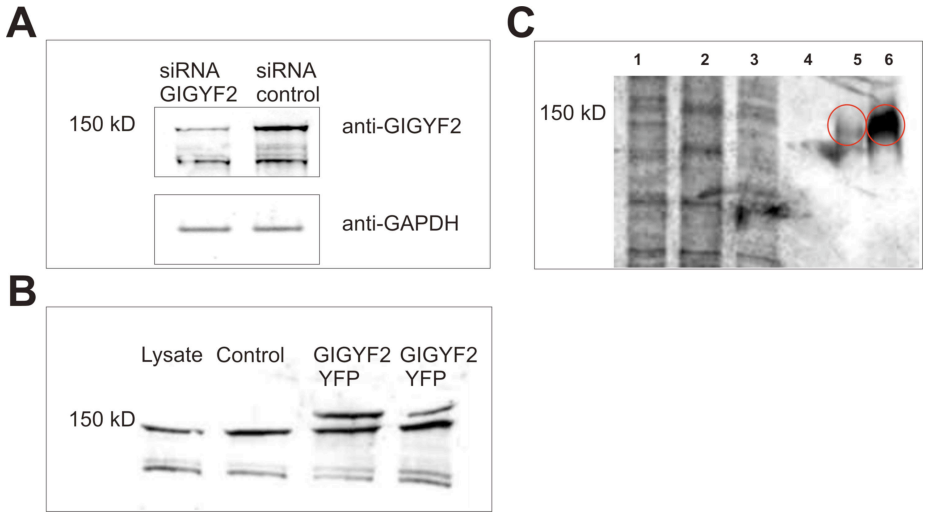

Figure 3.1 **Western blots confirming specific recognition by antibodies in the serum**. Specificity of antiserum was further analyzed in overexpression and knockdown studies and MS. Knockdown of GIGYF2 protein in HeLa cells leads to a weaker immunoreactive band of the antibody serum compared to the control in shown in A. Overexpressed GIGYF2-YFP was recognized by the antibody serum in Western blot (B). Anti-GIGYF-GYF can precipitate endogenous GIGYF2 from HeLa and pc12 cell lysate: (1) HeLa lysate, (2) pc12 lysate, (3) supernatant after IP in Hela cells, (4) negative control, comprising beads and HeLa lysate, (5) IP in Hela cells, (6) IP in pc12 cells. Red cycled bands were subject to tryptic digest (C). MS analysis of these bands confirmed precipitation of GIGYF2 with the antiserum.

The endogenous protein present in control cells runs at 150 kD whereas the overexpressed cells show an additional higher band that was detected with the GIGYF2 antibody.

The antibody was also tested for immunoprecipitation (IP) of endogenous GIGYF2 from HeLa and pc12 cells. Figure 3.1 C shows the Coomassie gel of the immunoprecipitation. The first and second lanes represent HeLa and pc12 lysate, respectively, followed by the supernatant after IP in HeLa cells in lane 3. As negative control, beads were incubated with lysate without antibody resulting in no precipitate as shown in lane 4. The IP of GIGYF2 from HeLa and pc12 cells is shown in lane 5 and lane 6, respectively. In both IPs, a band at 150 kD was enriched, marked by red circles. MS analysis confirmed these bands to be GIGYF2. In summary, overexpression, knockdown and immunoprecipitation studies could confirm the specific recognition of endogenous and overexpressed GIGYF2 with anti-GIGYF2-GYF antibody serum.

3.1.2 **Localization and expression studies of GIGYF2**

The localization of GIGYF2 in human and rat cell lines was investigated by cell fractionation. HeLa and pc12 cells were separated into cytoplasmic and nuclear cell extracts. The purity of each fraction was tested with antibodies against proteins, characteristic for its exclusive nuclear or cytoplasmic localization. The lactate dehydrogenase A (LDH) served as cytoplasmic marker whereas the transcription factor SP1 (SP1) served as marker for the nuclear fraction.

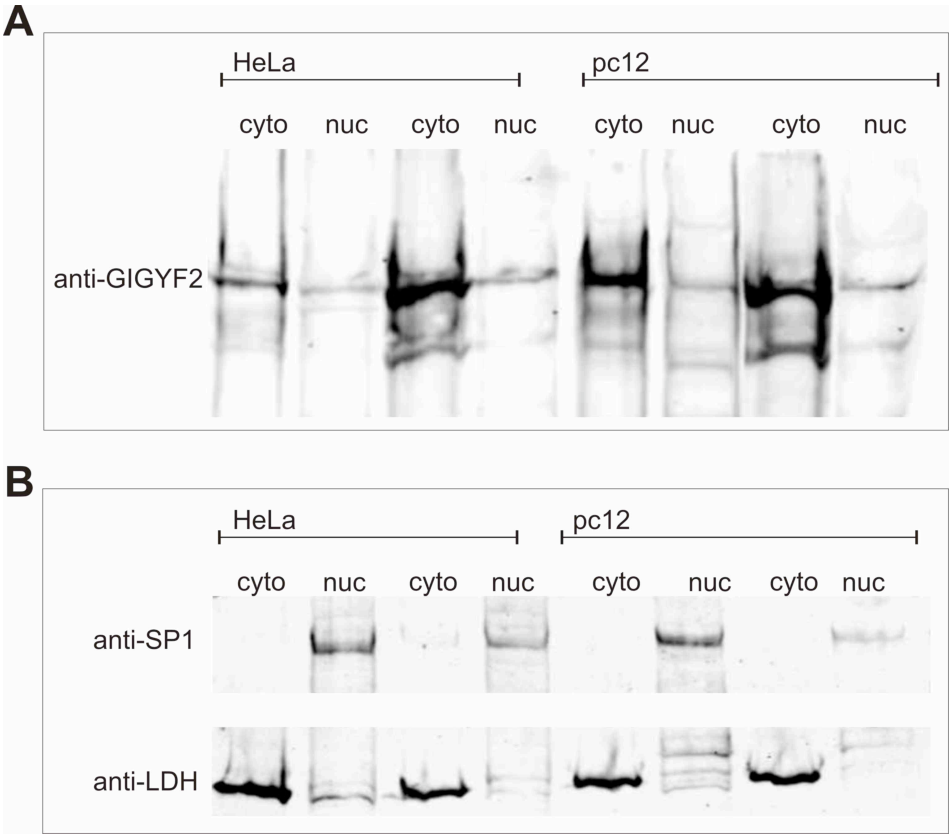

Figure 3.2. **GIGYF2 localizes to the cytoplasmic fraction of HeLa and pc12 cells**. Incubation of cytoplasmic and nuclear cell fractions with GIGYF2 reveals a stronger immunoreactive band and therefore the main localization of GIGYF2 to the cytoplasm (A). Successful separation into cytoplasmic (cyto) and nuclear (nuc) fraction is shown by the specific bands of the cytoplasmic marker LDH and the nuclear marker SP1 (B).

Figure 3.2.B illustrates successful separation of cytoplasmic and nuclear fractions from HeLa and pc12 cells. The cytoplasmic fractions show intense bands of the marker protein LDH that is not present in the nuclear fractions. The nuclear marker SP1 displays pronounced bands in the nucleus and no detectable bands in the cytoplasm. These fractions have been used to analyze the localization of GIGYF2 (Figure 3.2.A). GIGYF2 shows a distinct band in the cytoplasmic cell fraction whereas the immunoreactive band in the nucleus is much weaker, suggesting a cytoplasmic localization of GIGYF2 in these cell lines.

Next, proteins were extracted from 10 weeks old BL6 mouse organs to analyze the expression pattern within these organs (Figure 3.3). GIGYF2 was present in urinary system, liver, brain, spleen, lung, lymph node, heart, thymus and uterus. The analysis showed very low expression in the kidney. These data speak for a ubiquitous expression of GIGYF2 protein with slight variations in different organs such as the kidney.

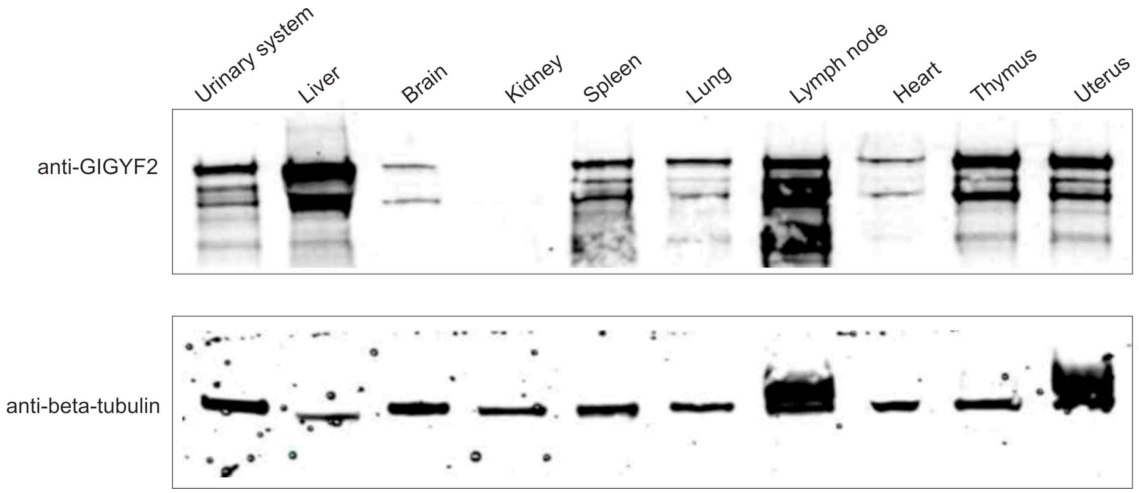

Figure 3.3. **Ubiquitous expression of GIGYF2 in mouse organs**. Immunoreactive bands against GIGYF2 were present in all lysates from mouse organs except kidney.

3.1.3 Screening for new interaction partners of GIGYF2

Recently, our group performed pull-down experiments with the GIGYF2-GYF domain as bait in combination with stable isotope labeling in cell culture (SILAC)-MS experiments to identify new interaction partners of GIGYF2 in human HeLa cells (see Method part). Since GIGYF2 is localized to the cytoplasm (Figure 3.2), pull-downs were performed with cytoplasmic extracts of HeLa cells that were either ^{13}C-arginine/^{13}C-lysine labeled or non-labeled. In pull-downs with non-labeled cells, a peptide, competing for the PRS-binding site, was added (see Figure 2.1). Several highly enriched interaction partners could be detected, which we grouped according to their cellular function. Figure 3.4 shows the potential interaction networks of GIGYF2.

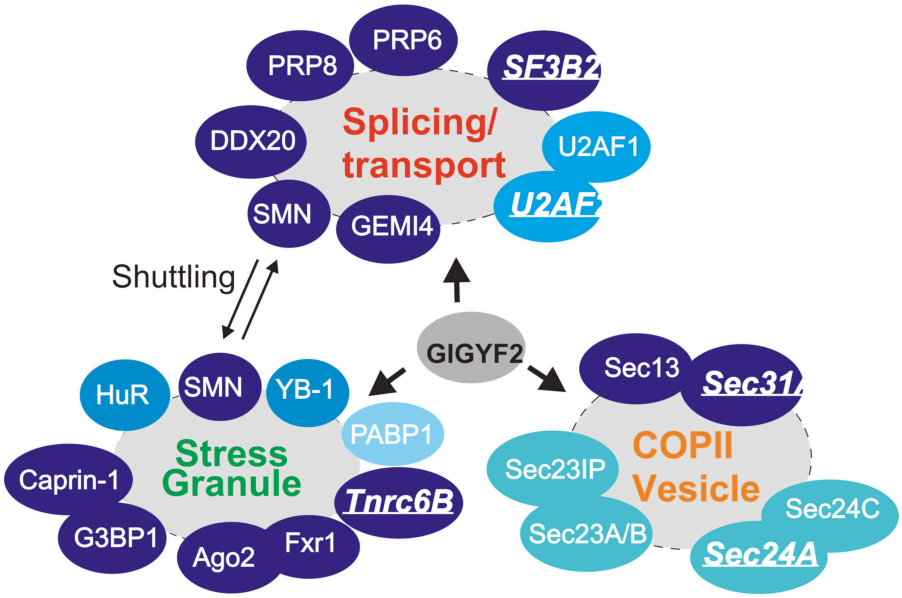

Figure 3.4. **Pull-down in combination with SILAC MS data suggest an involvement of GIGYF2 in stress granule formation and COPII vesicular transport.** Specific binding partners deriving from the pull-down MS analyses were assorted into different groups depending on the cellular function. Proteins containing the GYF consensus motif PPGϕ are depicted as bold italic underlined. Color grading is according to the enrichment factors. Overlapping circles and solid lines indicates direct interactions (adapted from [26]).

The highly enriched proteins derived via SILAC MS from pull-down experiments could be associated with three different functions, namely splicing and transport, stress granule and COPII vesicle formation. All four COPII coat components were identified. Both, Sec24 and 31 contain a Smy2-GYF consensus motif (bold italic underlined in Figure 3.4). Also, several proteins that serve as characteristic marker for cytoplasmic stress granules were found, such as SMN, Caprin-1, PABP-1 and TNR6B [113]. The latter one consists of a Smy2-GYF consensus motif. In subsequent studies, potential interactions found in these pull-downs were analyzed by fluorescence microscopy.

3.1.4 **Immunofluorescence co-localization studies**

Potential interactions of GIGYF2 from SILAC experiments were analyzed by immunofluoresence co-localization studies of endogenous and overexpressed proteins. Several fluorescence tags have been used for the overexpression studies, like enhanced yellow fluorescence protein (EYFP), enhanced cyan fluorescence protein (ECFP) and green fluorescence protein (GFP).

3.1.4.1 GIGYF2 and COPII mediated vesicular transport

COPII vesicle formation takes place at the endoplasmatic reticulum (ER) and they are transported to the Golgi Apparatus (Golgi) [121]. Live cell images in HeLa cells with overexpressed GIGYF2 and markers for ER or Golgi were performed. Figure 3.5 shows the localization of GIGYF2-ECFP (shown in red) and Golgi-EYFP (shown in green) and their overlay. Merging of both proteins is illustrated by the yellow color in C, confirming the localization of GIGYF2 to the Golgi in HeLa cells. In the ER (pictures D to F) ECFP-ER (shown in green) and GIGYF2-EYFP (shown in red) largely overlap, certifying the localization of GIGYF2 to the ER.

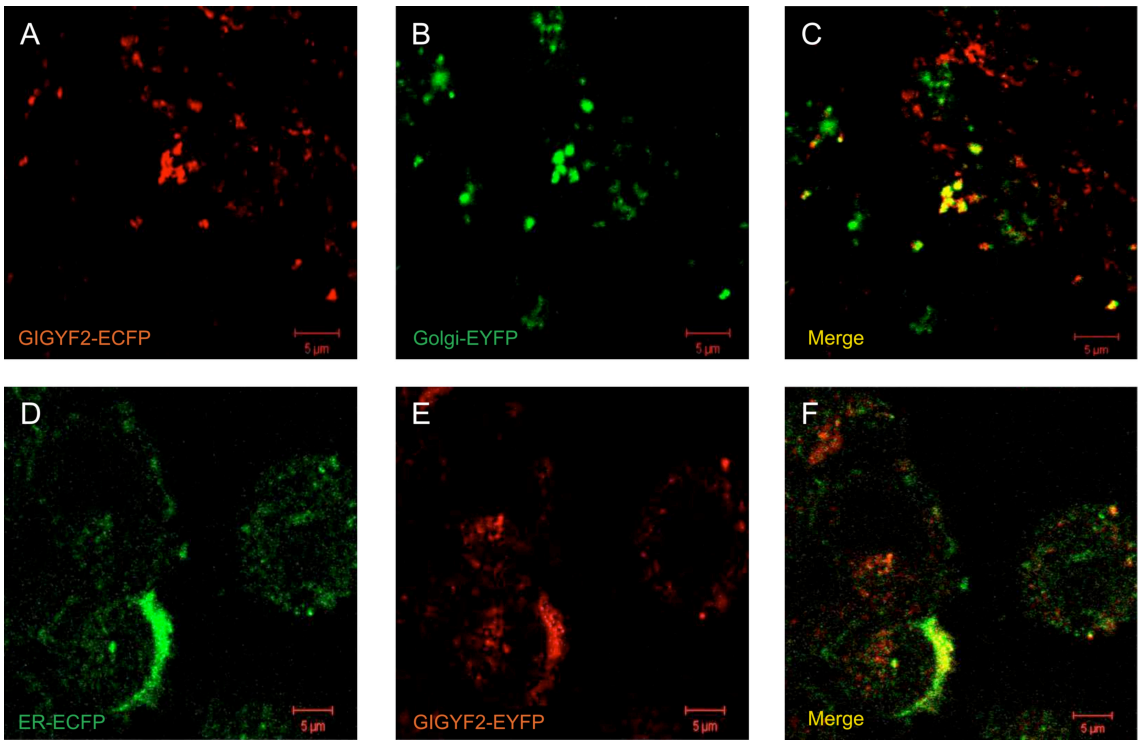

Figure 3.5. **GIGYF2 localizes to the Golgi and ER in HeLa cells.** Live cell images show localization of GIGYF2-ECFP (A) and EYFP (red) (D) to Golgi-EYFP (B) or ER-ECFP (green) (E), respectively. The merge shows large overlapping areas of GIGYF2 and the Golgi and ER marker (C and F, respectively) speaking for the localization of GIGYF2 to the Golgi and ER.

Next, co-localization of GIGYF2 and the COPII vesicle proteins Sec31 was analyzed. Therefore, HeLa cells were fixed and stained with antibodies against endogenous GIGYF2 and Sec31. Figure 3.6 shows the co-localization of both proteins in the cytoplasm of HeLa cells, mainly in punctuated patterns typical for ER and Golgi.

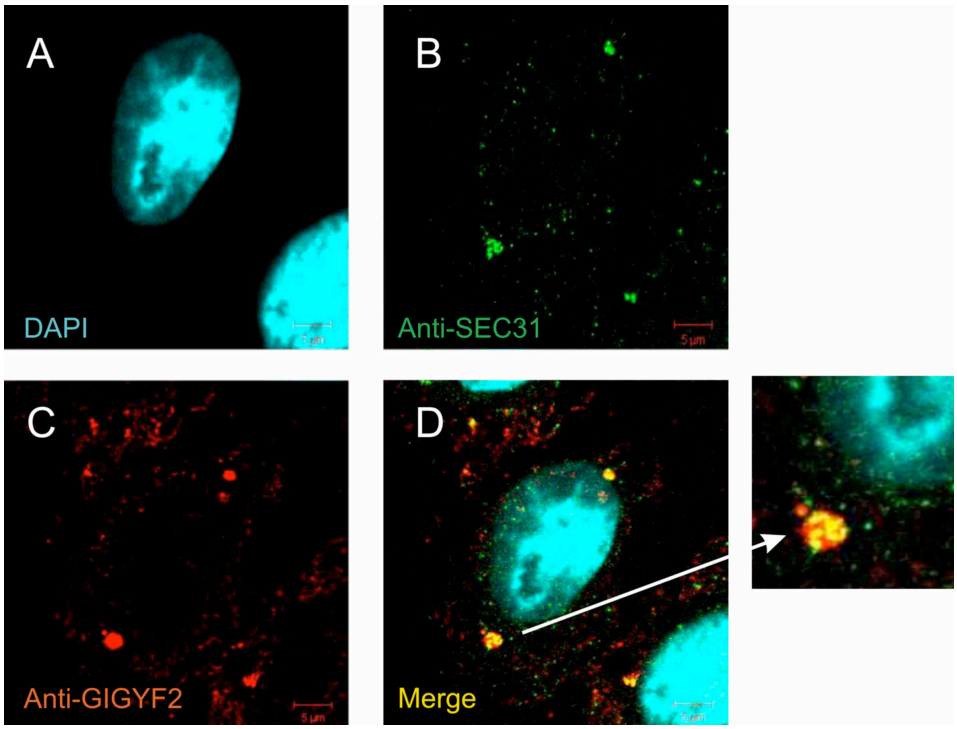

Figure 3.6. **The COPII vesicle component Sec31 co-localizes with GIGYF2 in HeLa cells.** In fixed HeLa cells, endogenous GIGYF2 (shown in red) merges with Sec31 (green), shown by the yellow color. The enlarged picture shows one area of localization.

3.1.4.2 GIGYF2 and the neurodegenerative disease protein Atrophin-1

Atrophin-1 was also found in the SILAC pull-down experiments with GIGYF2-GYF as bait. The protein contains a highly polymorphic polyglutamine region that leads to the neurodegenerative disease dentatorubral pallidoluysian atrophy when expanded to 49-75 repeats instead of the normal 7-23 [187]. Both forms comprise four GIGYF2 recognition motifs. Overexpressed GIGYF2-YFP (shown in red) and Atrophin-1-GFP (shown in green) largely overlap in the cytoplasm of HeLa cells (Figure 3.7) in regions close to the nucleus that could represent ER or Golgi.

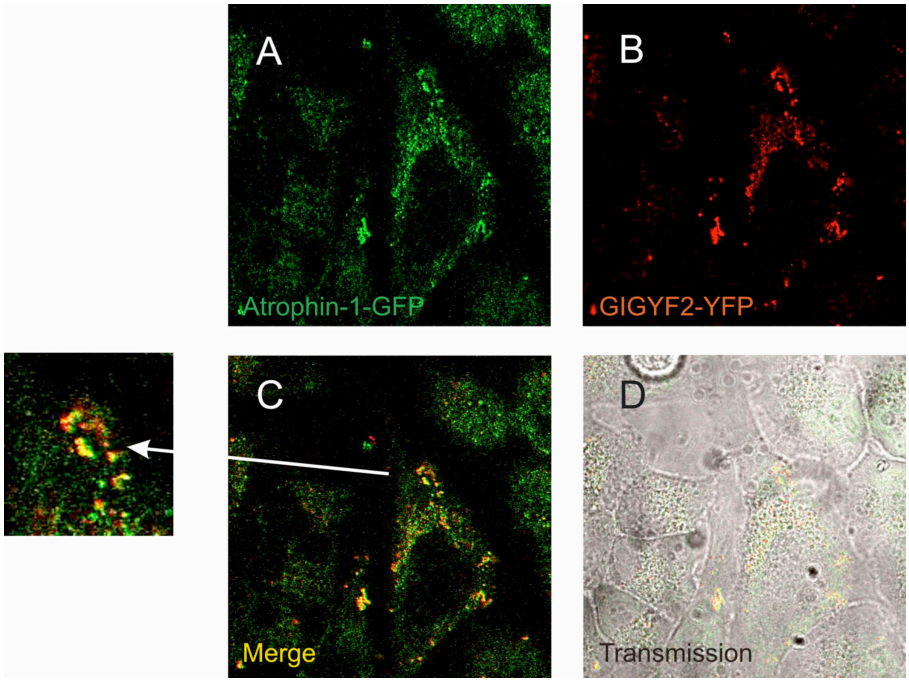

Figure 3.7. **Atrophin-1 co-localizes with GIGYF2 in HeLa cells.** Atrophin-GFP (shown in green) and GIGYF2-YFP (shown in red) co-localize in cytoplasm of HeLa cells.

3.1.4.3 GIGYF2 and stress granule formation

To examine whether or not GIGYF2 localizes to stress granules as speculated by the enrichment of stress granule markers in the SILAC pull-down experiments, stressed and non-stressed HeLa cells were stained against GIGYF2 and the stress granule marker TIA-1. Figure 3.8 shows that GIGYF2 and TIA-1 do not co-localize in resting HeLa cells.

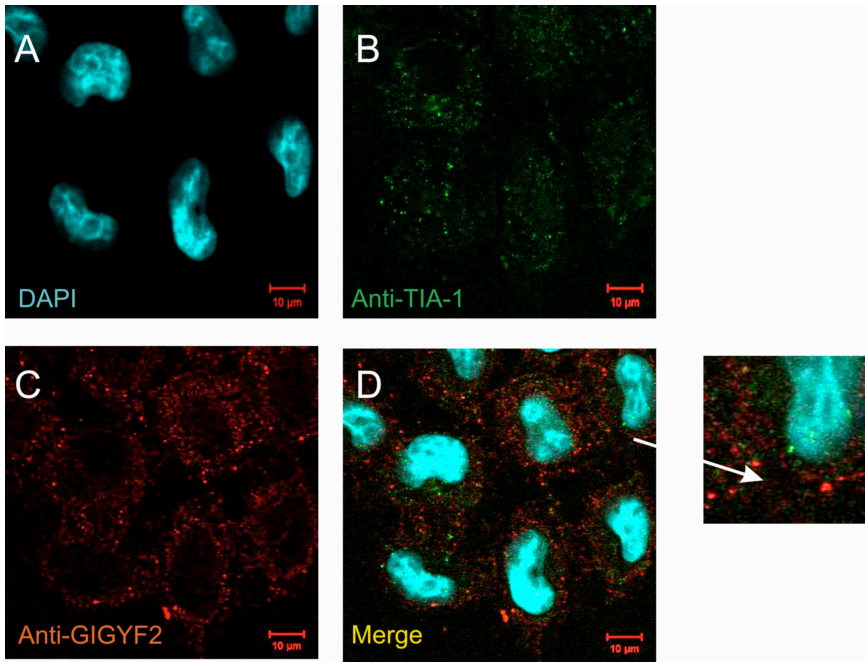

Figure 3.8. **No co-localization of GIGYF2 and TIA-1 in resting HeLa cells**. Fixed HeLa cells were stained against TIA-1 (green) and GIGYF2 (red). As shown in the merge and the enlarged view, both proteins localize to the cytoplasm but do not co-localize.

Upon treatment with arsenite, GIGYF2 and TIA-1 merge in granular formations in the cytoplasm (A-D in Figure 3.9) arguing that stress drives GIGYF2 into these granules.

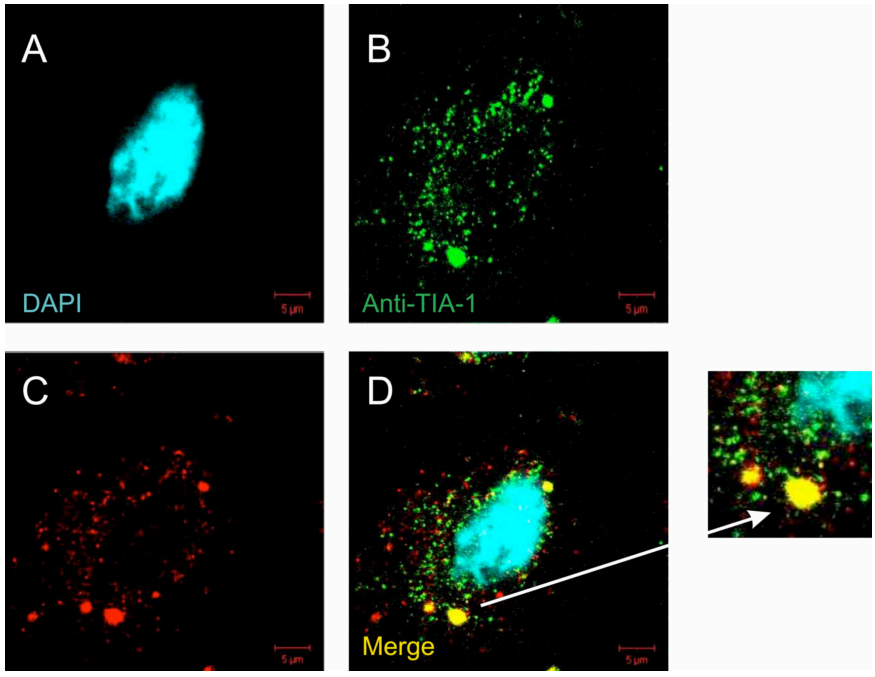

Figure 3.9 **Induction of stress drives GIGYF2 into cytoplasmic granules where it co-localizes with the stress granule marker TIA-1.** Treatment of HeLa cells with arsenite leads to the co-localization of GIGYF2 and TIA-1 cytoplasmic granules.

3.1.4.4 Analysis of GIGYF2 in neuronal cell lines

Lautier et al described GIGYF2 as a potential candidate gene for Parkinson's Disease (PD) [68], furthermore, GIGYF2-knockout mice showed a late onset neurodegenerative phenotype [86]. Therefore, we were curious if the localizations seen in human HeLa cells were also present in neuronal cell lines. Mouse neuroblastoma cells (Neuro2a) were transfected with GIGYF2 constructs and either ER-EYFP or endosome-YFP (another vesicular transporting system), respectively. As seen in Figure 3.10, GIGYF2 localizes to endosomes and the ER, as already seen in HeLa cells. From this we suggest that GIGYF2 also interacts with COPII vesicles in neuronal cells.

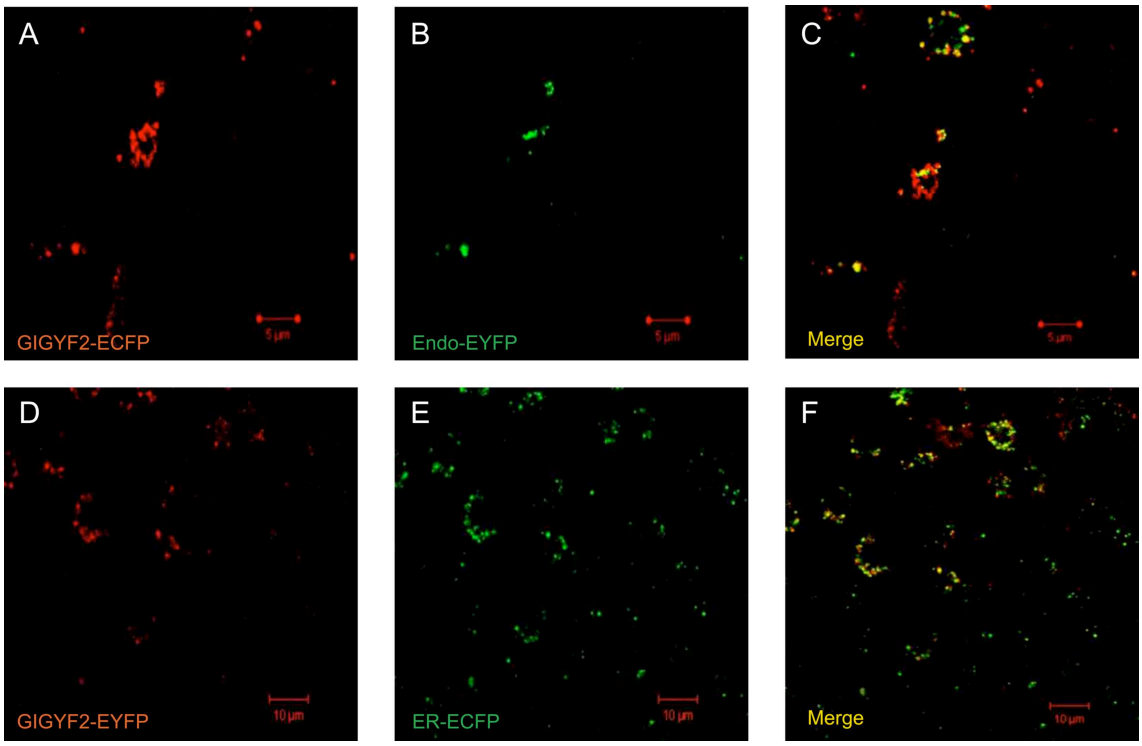

Figure 3.10 **GIGYF2 also localizes to endosomes and the ER of neuronal N2a cells**. GIGYF2-ECFP (red) and the endosomal marker (green) show large co-localization in Neuro2a cells (A-C). The same is true for GIGYF2-EYFP (red) and the ER marker ER-ECFP (green) (D-F). This stains show that GIGYF2 is also present in compartments of vesicular transport in neuronal cells.

Others found the PARKIN gene leucine-rich repeat kinase 2 (LRRK2) co-localizing with TIA-1 when over-expression in human SH-SY5Y cells [188].

Therefore, we used SH-SY5Y cells to analyze the recruitment of GIGYF2 into stress granules. First of all, the cellular distribution of GIGYF2 was analyzed in rat Neuro2a and SH-SY5Y cells. As seen in picture A to D in Figure 3.11, GIGYF2 localizes to the cytoplasm in both neuronal cell lines and can also be found in neurites of SH-SY5Y cells.

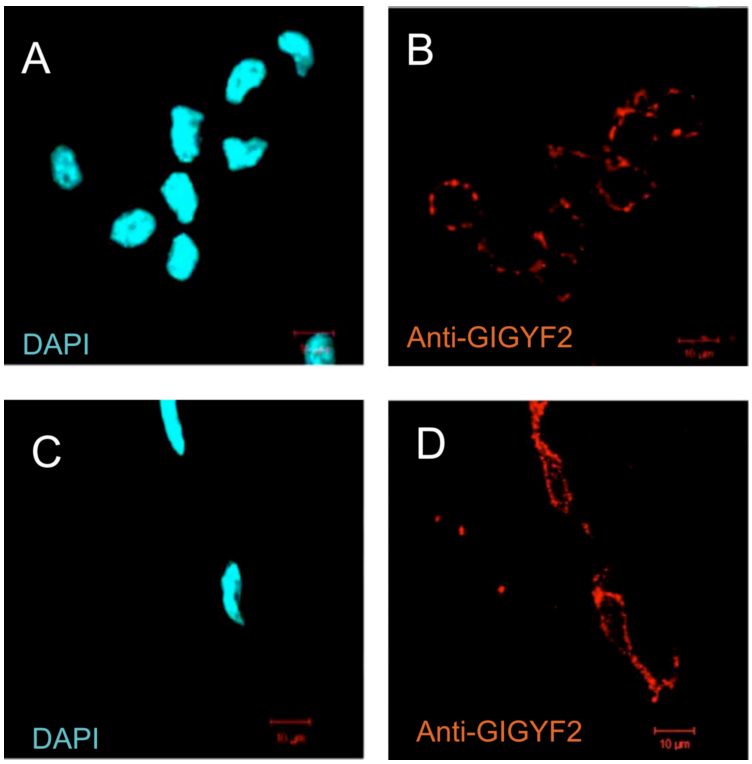

Figure 3.11. **GIGYF2 localizes to the cytoplasm of neuronal N2a and SH-SY5Y cell lines. In the latter ones, it is also present in neurites**. Stains of GIGYF2 in fixed rat Neuro2a cells shows the proteins in a punctual pattern in the cytoplasm (A-B). In human SH-SY5Y cells, GIGYF2 is distributed throughout the cytoplasm and neurites (C-D).

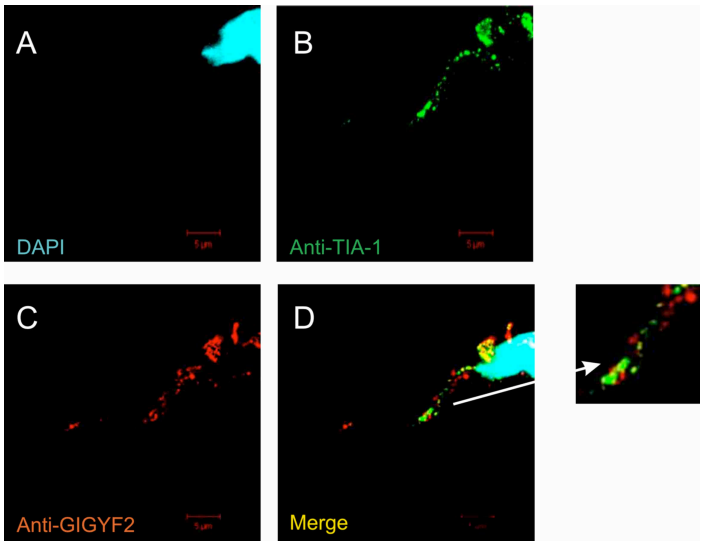

Figure 3.12. **GIGYF2 and TIA-1 only partly co-localize in resting SH-SY5Y cells.** In resting SH-SY5Y cells, GIGYF2 and the stress granules marker TIA-1 are distributed throughout the cell soma and neutrites in a punctional expression pattern with some localization in the cell soma.

Stains of GIGYF2 and TIA-1 in resting SH-SY5Y cells showed some overlap in the cell soma but no co-localization in neurites as shown in picture A to D in Figure 3.12. The administration of arsenite led to enhanced co-localize of both proteins in the cell soma and GIGYF2 and TIA-1 also co-localized in neurites (Figure 3.13).

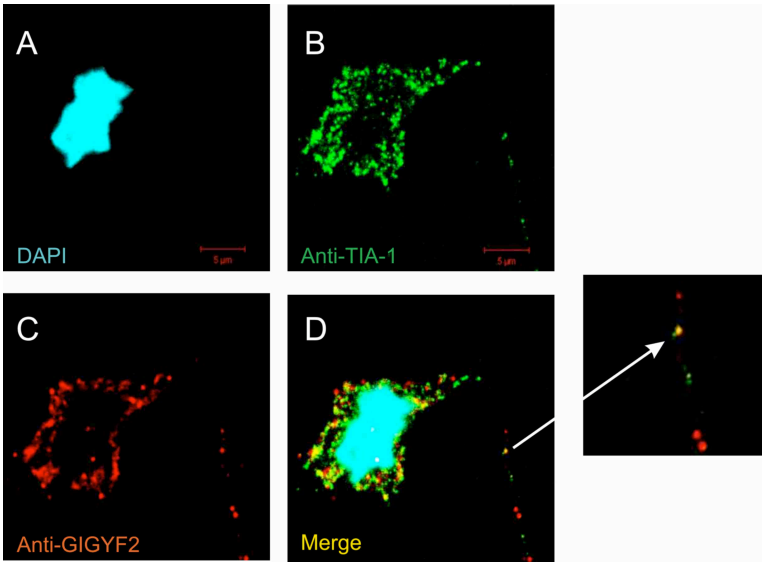

Figure 3.13 **Upon induction of stress, GIGYF2 and TIA-1 show enhanced co-localization in the soma and neurites of neuronal cell lines**. Stress induction leads to enhance co-localization of GIGYF2 and TIA-1 in the cell soma and neurites as marked in the enlarged picture.

Taken together, microscopic experiments suggest that GIGYF2 is involved in vesicular transport and, upon induction of stress, can be driven into stress granules in human HeLa and neuronal cell lines.

3.2 Functional characterization of CD2BP2 in mice

A potential role of CD2BP2 in the immune system [3] and splicing [58] is regarded by the current knowledge. These data are somewhat contradicting considering a plasma membrane associated role as binding partner of the CD2 receptor in T cells and a nuclear role in splicing. SILAC pull-down experiments identified splicing related interaction partners in HeLa cells [58] while the immune-related role is hard to address in cell lines [51]. Therefore, we performed analysis in mice to examine CD2BP2 expression and function in a multicellular system.

3.2.1 **Generation of a polyclonal antibody against CD2BP2**

Previous analyses of CD2BP2 have been performed with a polyclonal antibody kindly allocated by AG Lührmann in Göttingen, Germany. Limiting amounts of this antibody required the production of a new antibody.

Therefore, human his-tagged CD2BP2 construct (NM_006110.2) was expressed in Sf9 insect cells (performed by Sindy Blank in our group). Two different virus stocks were tested for overexpression of CD2BP2. Figure 3.14 A shows the Coomassie-stained SDS gel of the virus stocks (his-CD2BP2) in comparison with untransfected cells (control). A prominent band can be seen at 52 kD, marked with the black arrow. Western blot analysis of the virus-infected cells confirmed overexpression of CD2BP2 in both stocks as shown by the bands at 52 kD (Figure 3.14).

Cell lysates were purified via his-trap column and purity of the eluted fractions were analyzed in a Coomassie-gel (Figure 3.14 C). Fraction 4-11 showed the highest expression of his-CD2BP2 with the least amount of impurity and were therefore pooled, concentrated with 10 kD Vivaspin columns (Amicon) and further purified by gel filtration. The purified protein was used for immunization of rabbits (BioGenes GmBH, Berlin, Germany).

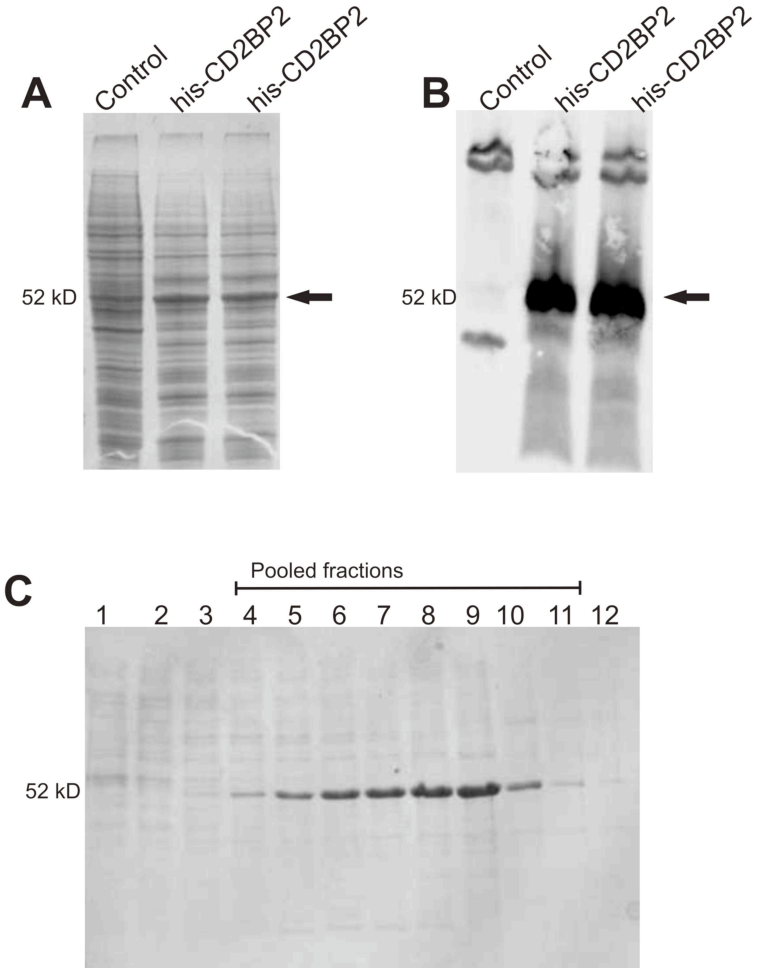

Figure 3.14 **Human his-tagged CD2BP2 protein was expressed in insect cells and purified**. The Coomassie-gel in A showes the expression of his-tagged CD2BP2 in insect cells. Two virus stocks (his-CD2BP2) are shown in comparison with untransfected control. Western blot of the virus stocks performed with anti-CD2BP2 from AG Lührmann confirmed overexpression of CD2BP2 (B). Eluate fractions 4-11 from his-trap purification showed the highest expression of CD2BP2 with the least amount of impurity and were therefore pooled and concentrated.

Serum of immunized rabbits showed specific bands of CD2BP2 in Western blot when compared to bands at the same height from the reference antibody (Figure 3.15). 30 μg of thymus lysate from BL6 mice were loaded per lane and incubated with reference antibody, antiserum from animal 81 and animal 82. A band at 52 kD was present in all lanes as marked with the black arrow in Figure 3.15.

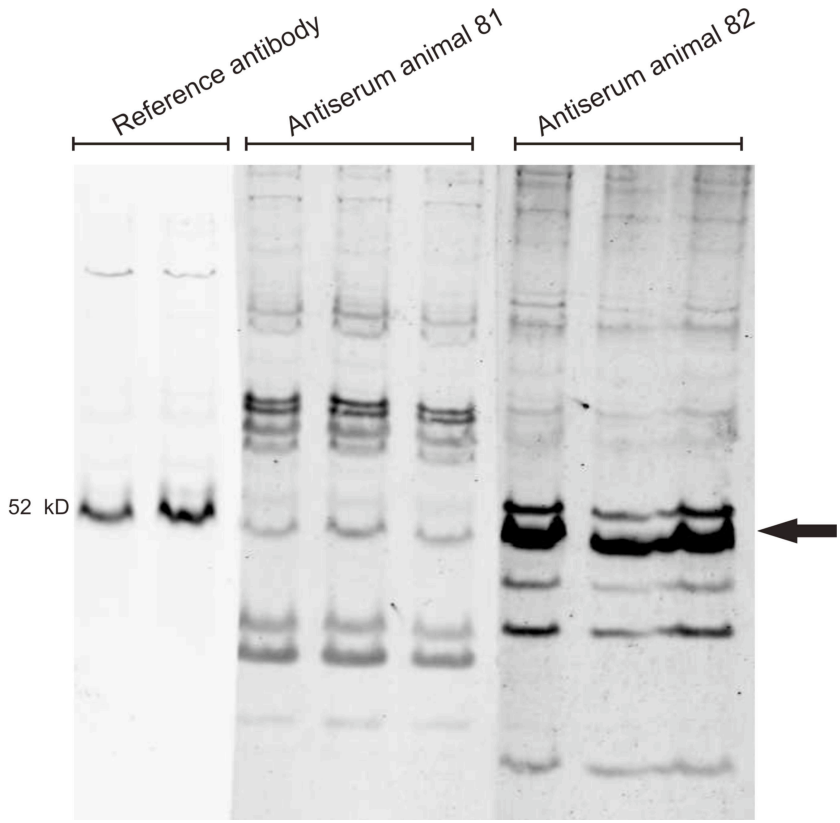

Figure 3.15 **Antibody serum from immunized rabbits shows pronounced bands at 52 KD in Western blots**. Thymus lysate was incubated with reference antibody (AG Lührmann), antiserum from animal 81 and from animal 82. Antiserum from both animals detected pronounced immunoreactive bands at the same height as the reference antibody, marked with the black arrow.

Antibody serum from animal 82 showed the highest amount of anti-CD2BP2 antibody titer and was therefore chosen for antibody purification (performed by the company BioGenes GmBH, Berlin, Germany). Here, his-CD2BP2 was coupled to a bromycan-activated sepharose column allowing the specific purification of anti-CD2BP2 polyclonal antibody.

The purified antibody was again tested for specificity in Western blot analysis. Figure 3.16 shows the gradual increase of antibody in subsequent immunization steps. In the pre-immune serum, only unspecific bands can be detected. After the first immunization, a faint band at the height of 52 kD can be detected but other bands at different heights show up as well. The unspecific band already present in the pre-immune serum becomes more pronounced.

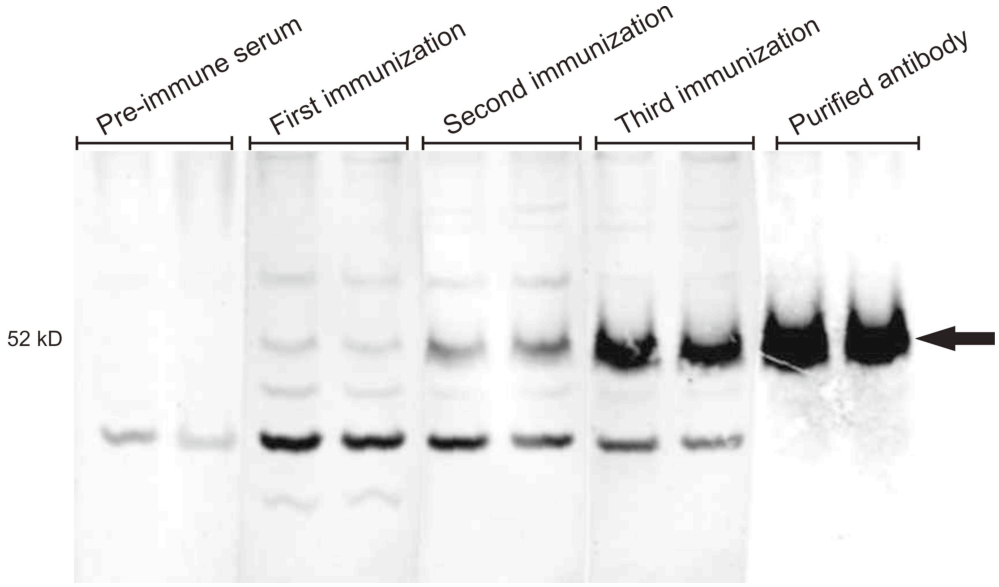

Figure 3.16. **Specific polyclonal anti-CD2BP2 antibody could be generated.** The Western blot shows the generation of the antibody. The pre-immune serum shows only unspecific bands. After three rounds of immunization, a band of 52 kD becomes more and more pronounced. Column purification with coupled his-tagged CD2BP2 leads specific anti-CD2BP2 antibody that recognizes one band at 52 kD in the Western Blot. 30 μg of BL6 thymus lysate was loaded per lane.

In the Western blot lanes incubated with antiserum after the second immunization, the potential band against CD2BP2 is more intense than the unspecific bands. The 3rd immunization produces a very strong immunoreactive band against CD2BP2 compared to the unspecific bands. After column purification, all unspecific bands including the one already present in pre-immune serum vanished, remaining one specific band against CD2BP2. This purified polyclonal rabbit anti-CD2BP2 antibody was used in the preceding studies.

3.2.2 **CD2BP2 RNA and protein levels in mice**

Different organs from male and female C57BL/6J mice at the age of 10 to 12 weeks were used for the extraction of either RNA or proteins.

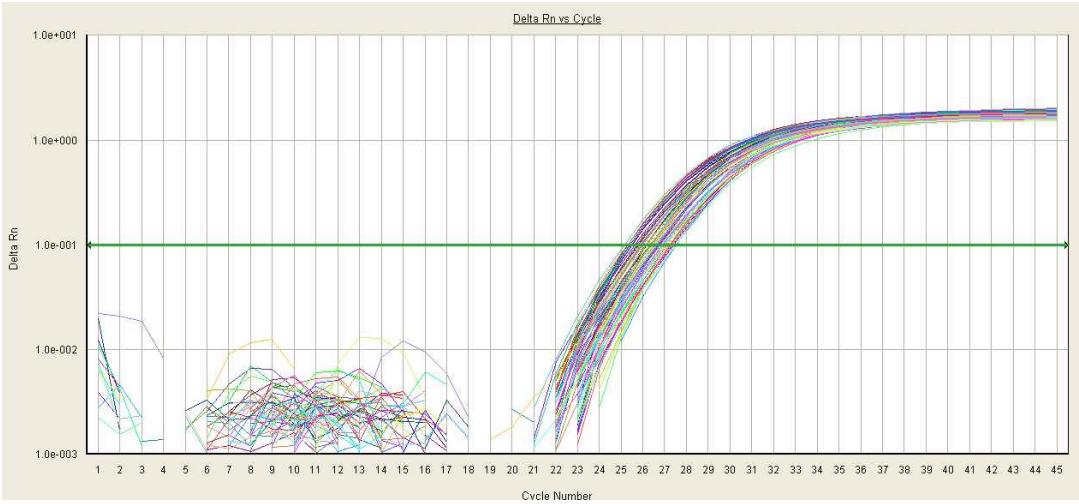

Figure 3.17 **TaqMan RT-PCR shows equal expression of CD2BP2 in mouse organs**. cDNA of CD2BP2 extracted from bladder, thymus, uterus, heart, oviduct, lymph node, testis, eye, lung, spleen, muscle, kidney, liver, brain, seminal vesicle and adrenal gland show up between cycle number 26 and 28.

Organs from three male and three female mice were used for RNA extraction. After reverse transcription of the RNA, the cDNA was measured with quantitative RT-PCR. As shown in the spectrum in Figure 3.17, all cDNA samples appear between cycle 26 and 28 at the exponential phase, where the threshold was set (shown as green line in Figure 3.17). No organ shows a significant different expression pattern by either showing up very early or late or by lacking the expression of CD2BP2 at all. Since no sex-specific differences of the RNA expression could be detected, all organs were combined and blotted against the reference gene 18S as shown in the upper graph in Figure 3.18. No major difference of RNA expression level could be detected. Therefore, it can be concluded that CD2BP2 is ubiquitous expressed in mouse organs on mRNA level.

The mRNA data should be compared to protein expression levels. Therefore, 20 µg of protein lysate from different mouse organs were separated by SDS-PAGE and analyzed with anti-CD2BP2 antibody. The ubiquitous expressed protein GAPDH was used as loading control. As shown in the Western blot in Figure 3.18, CD2BP2 is mainly expressed in thymus, lymph node, testis, lung and spleen whereas all other organs show no or a severely reduced protein expression levels. Six Western blots have been performed with the same results, namely differences in the expression of CD2BP2 protein levels in different organs.

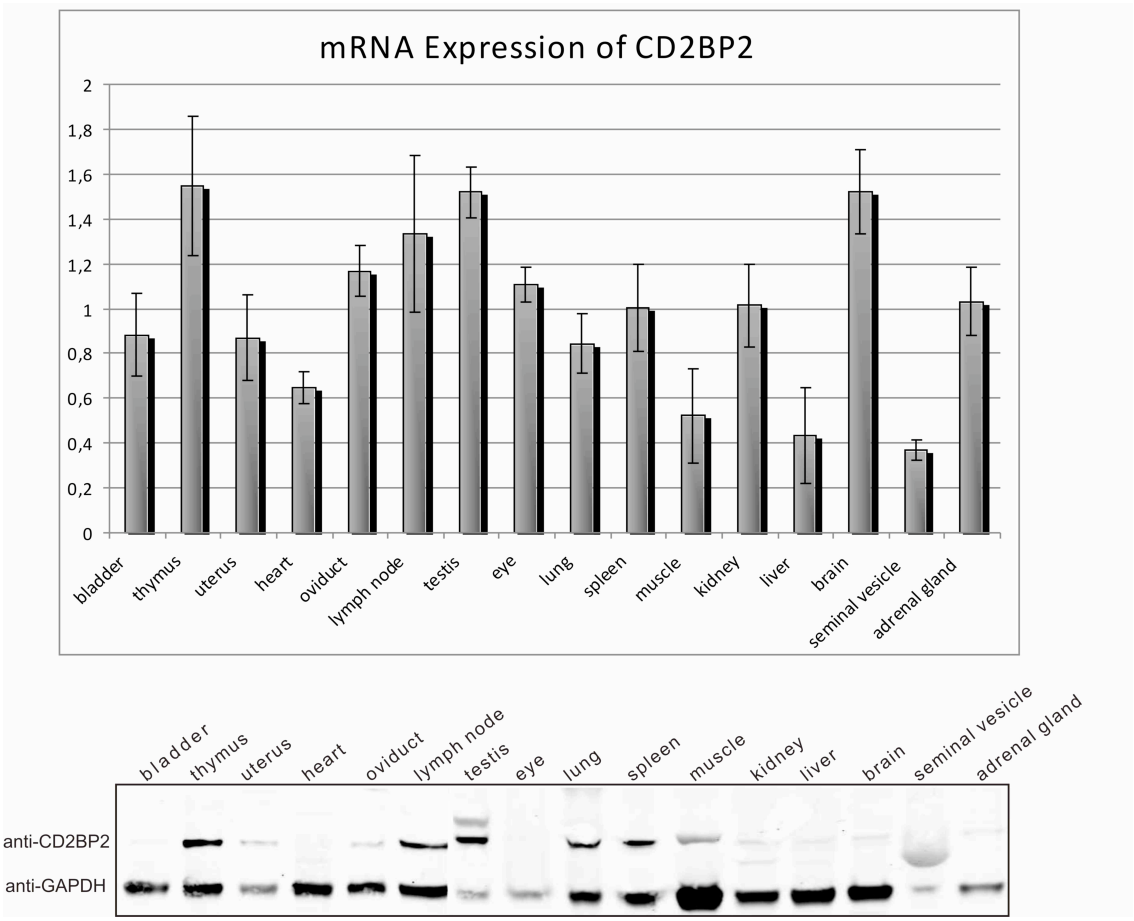

Figure 3.18 **Different expression patterns of CD2BP2 at mRNA versus protein level**. CD2BP2 is ubiquitously expressed on mRNA level in several mouse organs, as shown here after normalization with 18S (top panel). On protein level, Western blot of CD2BP2 reveals its expression in thymus, lymph node, testis, lung and spleen in non-perfused BL6 mice (bottom). Antibody against GAPDH was used as loading control.

Organ-specific comparison between RNA and protein levels suggested reduced expression of CD2BP2 protein in several organs. While, for example, the mRNA level of the brain shows a mean at 1.5 and the spleen of 1, relative to 18s rRNA, there is clearly a stronger expression of CD2BP2 protein in the spleen compared to the brain. These data suggest that the expression of CD2BP2 protein is regulated.

Thymus, spleen and lymph nodes are organs of the hematopoietic system. Here, the maturation of immune cells (bone marrow, thymus) takes place or the immune response is being formed (spleen, lymph node). Therefore, the expression of CD2BP2 in immune cells was analyzed in more detail.

3.2.3 **Fluorescence Activated Cell Sorting of immune cells**

Expression levels of CD2BP2 in mouse organs showed a major expression in primary and secondary mouse lymphoid organs (Figure 3.18). Fluorescence activated cell sorting (FACS) of immune cells was performed to address this question.

Sieving the cells through a 70 μM cell strainer isolated immune cells from thymus and spleen of 12 weeks old BL6 mice. After primary labeling with the respective antibodies, cells were sorted by FACS. Western blots of sorted populations were performed to analyze the cell specific expression of CD2BP2.

	CD4 T cells	**CD8 T cells**	**B cells**	**Macrophages**	**Dendritic cells**	**Myeloids**
First marker	TCR α/β	TCR α/β	B220	CD11b	MHCII	CD11b
2nd marker	CD3	CD3	CD19	F4/80	CD11c	No F/480
3rd marker	CD4	CD8	-	-	-	-

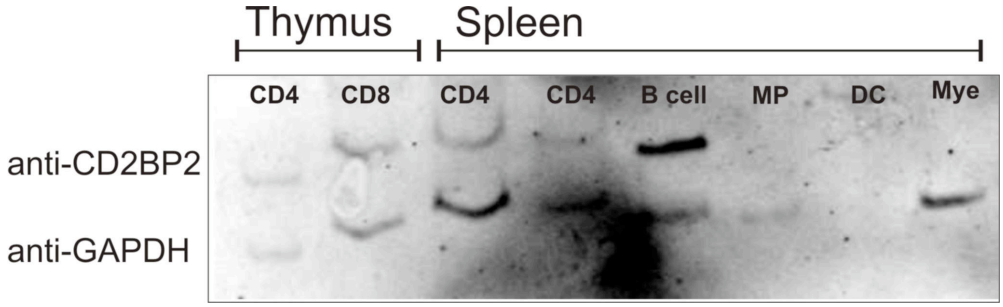

Figure 3.19. **CD2BP2 is expressed in CD4 and CD8 expressing T cells in thymus and spleen and in splenic B cells**. The top panel shows the staining procedure for the sorting of CD4 and CD8 expressing T cells, B cells, macrophages, dendritic cells and myeloid cells. The Western blot performed with the according cell lysates shows immunoreactive bands against CD2BP2 in $CD4^+$ and $CD8^+$ T and B cells while no bands can be seen in macrophages (MP), dendritic cells (DC) or Myeloid cells (Mye). GAPDH was used as loading control.

The different cells markers used are listed in the top panel of Figure 3.19. Staining with anti-CD4 and anti-CD3 antibody isolated $CD4^+$ T cells; $CD8^+$ cells could be isolated by anti-CD8 instead of anti-CD4 respectively. The B cell markers B220 and CD19 were used for the isolation of B cells. Macrophages were isolated by double staining with CD11b and F4/80 and dendritic cells with the antibody combination of anti-MHCII and CD11c. Cells expressing CD11b but no F4/80 were determined as myeloid cells. Western blots were performed with all sorted cells and stained against CD2BP2 and GAPDH as loading control. As shown in Figure 3.19, CD2BP2 is expressed in $CD4^+$ and $CD8^+$ T cells and B cells in the thymus and spleen. Western blot lanes of macrophages, dendritic cells and myeloid cells showed no immunoreactive band against CD2BP2, which can either be due to the limited number of cells or lack of CD2BP2 expression in these cells. The experiments started from pooled thymi and

spleens. Obviously, the amount was not sufficient for the analysis of minor cell populations such as macrophages or dendritic cells in mice raised under specific pathogen free (SPF) conditions.

3.2.4 **Intracellular staining of immune cells**

Western blot data from sorted immune cells showed the presence of CD2BP2 in $CD4^+$ and $CD8^+$ T and in B cells (Figure 3.19). Technical limitations hindered the analysis of minor cell populations, such as macrophages and dendritic cells. To overcome this and analyze the expression of CD2BP2 at different developmental stages, immune cells were fixed and directly stained with anti-CD2BP2 antibody.

3.2.4.1 Competition analysis for antibody specificity

The self-made purified polyclonal antibody against CD2BP2 was used for immune cell staining. Extracellular stains with CD2BP2 showed no shift of fluorescence. From this, it was concluded that CD2BP2 is only present within the cell. Preceding studies were performed with fixed, permeabilized cells. In all flow cytometric experiments performed, fluorochromes measured were compensated with compensation controls before the measurement of the samples.

To rule out unspecific binding of the polyclonal antibody in intracellular cell stains, a competition assay with purified his-tagged CD2BP2 was performed. Anti-CD2BP was incubated either with his-tagged CD2BP2 (Figure 3.20 A) or BSA (Figure 3.20 B) as negative control, and analyzed by flow cytometry. Spleen cells were gated on lymphocytes as illustrated in the density blot in Figure 3.20 A. Anti-CD2BP2 was detected with Fluoresceinisothiocyanat (FITC) coupled anti-rabbit antibody. Unstained cells showed no unspecific emission of FITC fluorescence as shown in the middle density blot of Figure 3.20 A, speaking for no background noise of FITC. The panel on the right in Figure 3.20 A shows the histogram of CD2BP2 absorption under different conditions. Unstained cells are shown in red. Cells, where anti-CD2BP2 was pre-incubated with his-CD2BP2 are shown in yellow. The anti-rabbit isotype control is shown in blue and the control stain against CD2BP2 in green. The green positive control shows a shift of the median fluorescence value (MFI value) in contrast to stains where the antibody was outcompeted by CD2BP2 protein or the anti-rabbit isotype control.

Cells incubated with BSA shift similar to the control stain as shown in Figure 3.20 B. BSA was unable to compete out anti-CD2BP2 antibody and therefore led to the same shift as the control stain (green). From this it was concluded that the polyclonal anti-rabbit CD2BP2 antibody binds CD2BP2 specifically and could be used for subsequent intracellular flow cytometric stains.

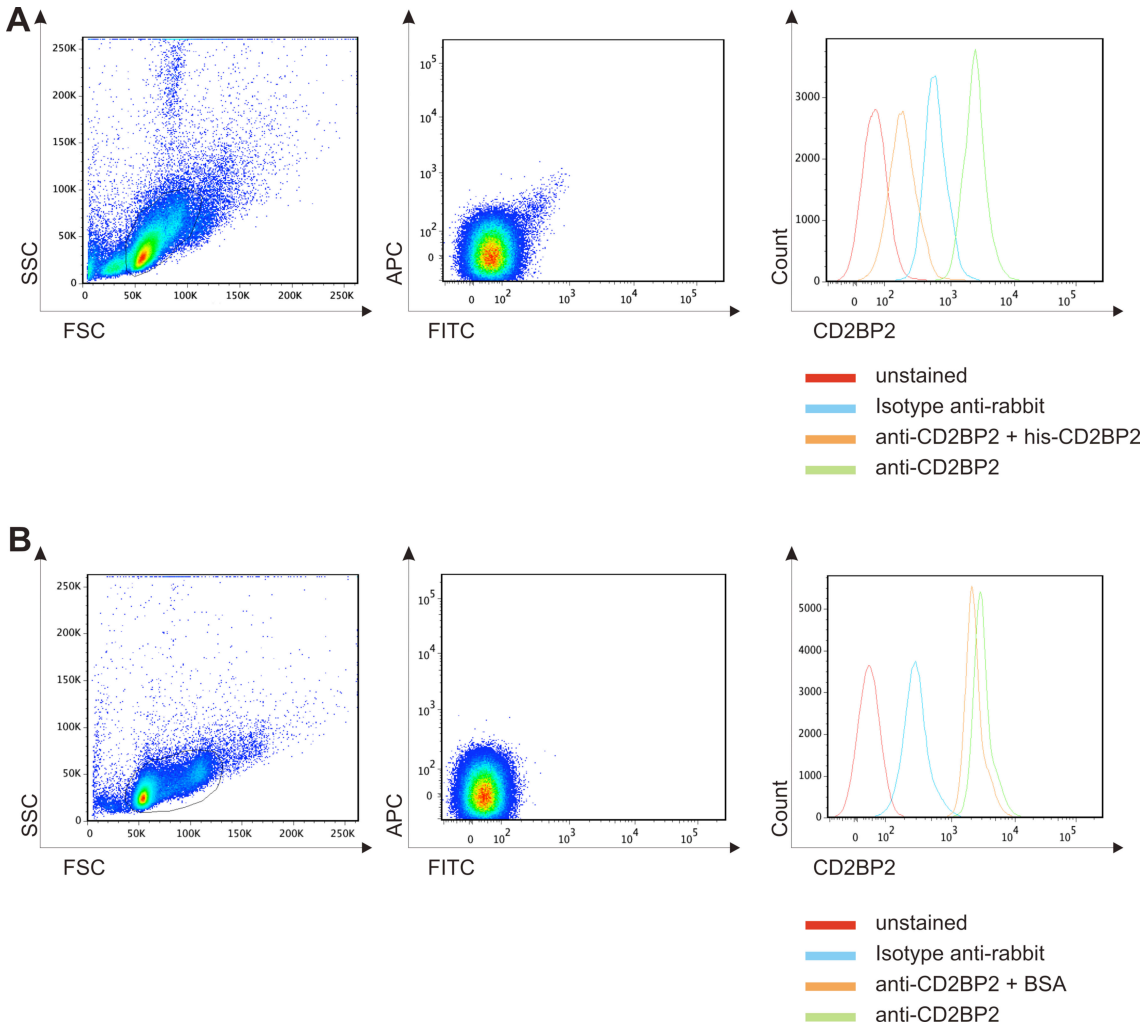

Figure 3.20. **Anti-CD2BP2 specifically binds to endogenous CD2BP2.** Spleen cells were gated on lymphocytes (left panel in A) and showed no unspecific fluorescence leakage (middle panel in A). Anti-CD2BP2 antibody was pre-incubated with his-tagged CD2BP2 before adding to the cells. This stain (orange in right panel in A) shows no shift in fluorescence in contrast to the stain with anti-CD2BP2 that was directly added to the cells (green in right panel). In the negative control, anti-CD2BP2 antibody was pre-incubated with BSA (Figure B). Here, the stain of the pre-incubated CD2BP2 antibody leads to the same shift (orange) as the control staining (green in right panel). Isotype control and unstained cells are shown in blue and red, respectively.

3.2.4.2 Titration experiments of anti-CD2BP2

The anti-CD2BP2 antibody was titrated to cells from lymph node, spleen and thymus to establish the best staining dilution for further experiments. Dilutions from 1:50 through 1:400 were chosen and compared with shifts of the anti-rabbit isotype control (Figure 3.21). All cells were gated on lymphocytes (not shown) and histograms of the fluorescence shifts were compared with shifts of the isotype control.

The histograms in Figure 3.21 show no shifts of the isotype controls in cells from the lymph node, spleenocytes or thymic cells (shown in green). Antibody dilutions from 1:400 to 1:200 (shown in red and blue, respectively) exhibit nearly identical shifts resulting in MFI values of about 1x 10^3. Dilutions of 1:100 (light green) and 1:50 (dark green) lead to the strongest fluorescence shifts.

From this experiment we chose the dilution of 1:100 since at this concentration the stain leads to pronounced shifts without consuming too much of the rabbit anti-CD2BP2. This antibody and an anti-goat CD2BP2 antibody generated against an N terminal peptide of the human CD2BP2 were used for all subsequent stains. The anti-goat antibody was compared with the anti-rabbit CD2BP2 and showed the same fluorescence shifts (not shown here).

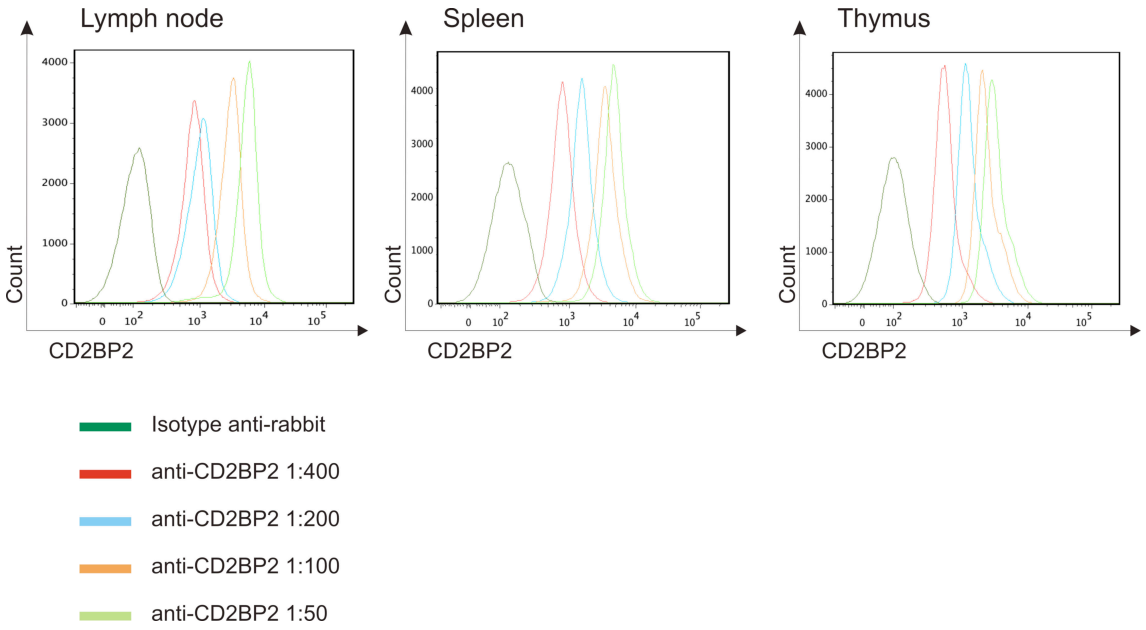

Figure 3.21. **Titration of anti-CD2BP2 showed the best staining result at a dilution of 1:100**. Lymph node, spleenocytes and thymic cells (C) were stained with anti-CD2BP2 in rising concentrations from 1:400 to 1:50. The fluorescence shift of each concentration was compared with the isotype control (shown in green). In all cells, the dilution 1:100 (shown in yellow) showed the best shift and was chosen for preceding experiments.

3.2.4.3 Expression of CD2BP2 in B and T cells

Western blot analysis of mouse organs showed an immune related expression of CD2BP2. Hence, cells from the bone marrow, thymus, lymph nodes and spleen from BL6 mice were analyzed for their cell specific expression of CD2BP2. Several male and female mice at different ages haven been tested but showed no significant differences. Therefore, the results from a 4 weeks old male BL6 mouse are exemplary shown here.

First, the expression of CD2BP2 was analyzed in lymphocytes. Bone marrow cells, extracted from femur and tibia, were stained against B cell markers B220 or CD19 and CD2BP2, respectively. B220, also called CD45R, is a member of the protein tyrosine phosphatase (PTP) family expressed on B cells (at all developmental stages from pro-B cells through mature B cells) and activated B cells. CD19, also known as B4 is expressed on pro-B to mature B cells but not on plasma cells. As shown in Figure 3.22, most of $B220^+$ and $CD19^+$ cells were also $CD2BP2^+$. In case of B220 cells, both, B220 high and B220 low cells also expressed CD2BP2. A large amount of cells in the bone marrow (about 70 %) were positive for CD2BP2 but not for the B cell markers. This is represented by the cell population that shows only a shift of CD2BP2 positive cells.

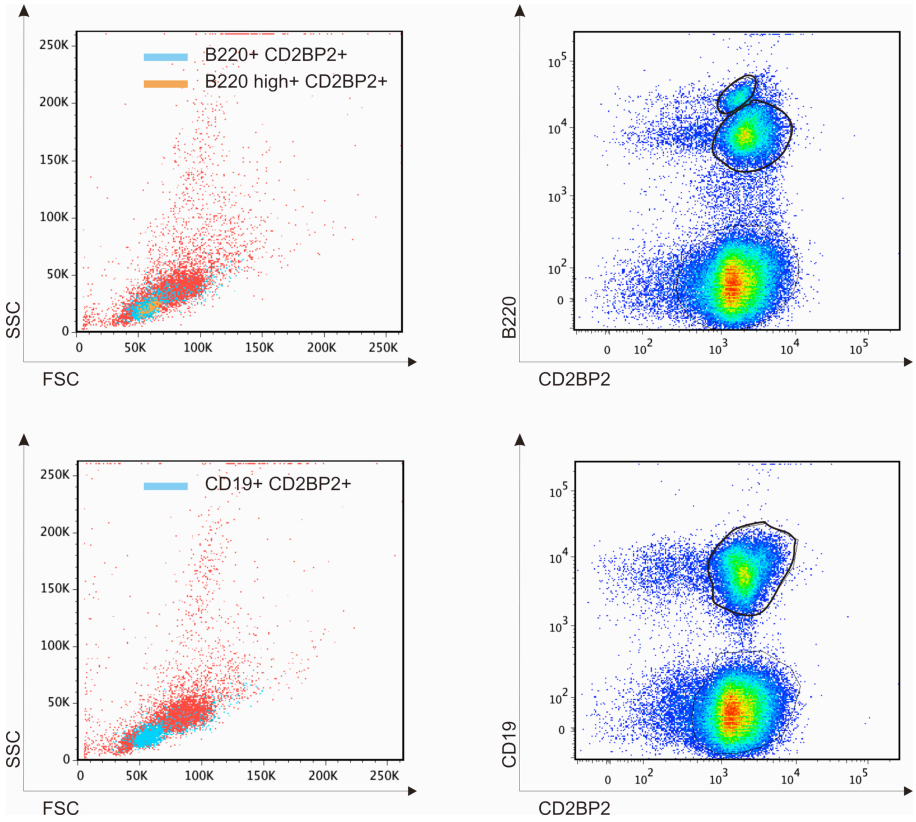

Figure 3.22**. CD2BP2 is expressed in $B220^+$ and $CD19^+$ bone marrow cells.** Bone marrow cells extracted from femur and tibia of BL6 mice were stained with the B cell markers B220 (top) and CD19 (bottom) and with CD2BP2. Most of the $CD19^+$ and $B220^+$ cells were also $CD2BP2^+$ whereas about 70% of $CD19^-$ and $B220^-$ cells did express CD2BP2. Backgating of the double positive cells showed their localization in the lymphocyte gate.

Backgating of B220^{+} CD2BP2^{+} or CD19^{+} CD2BP2^{+} cells showed the same localization of both stains in the forward and sideward scatter. In both cases, these double positive B cells showed almost no intracellular granularity or cell inclusions because they localized to the lower corner of the lymphocyte gate. B220 high^{+} CD2BP2^{+} cells were localized in the same area as B220 low cells so they showed no morphological differences.

T cell development takes place in the thymus. Mature T cells either express CD4 or CD8 on their surface. As shown in Figure 3.23, most of the CD4 and CD8 single positive cells also expressed CD2BP2. Because more than 80 % of all cells in the thymus expressed CD2BP2 that were also CD4^{+} and CD8^{+}, it is very likely that CD4^{+} CD8^{+} T cells express the protein as well. Backgating of CD4^{+} CD2BP2^{+} and CD8^{+} CD2BP2^{+} cells showed their localization at the upper end of the lymphocyte gate, speaking for the largest and most granular cells of the thymus.

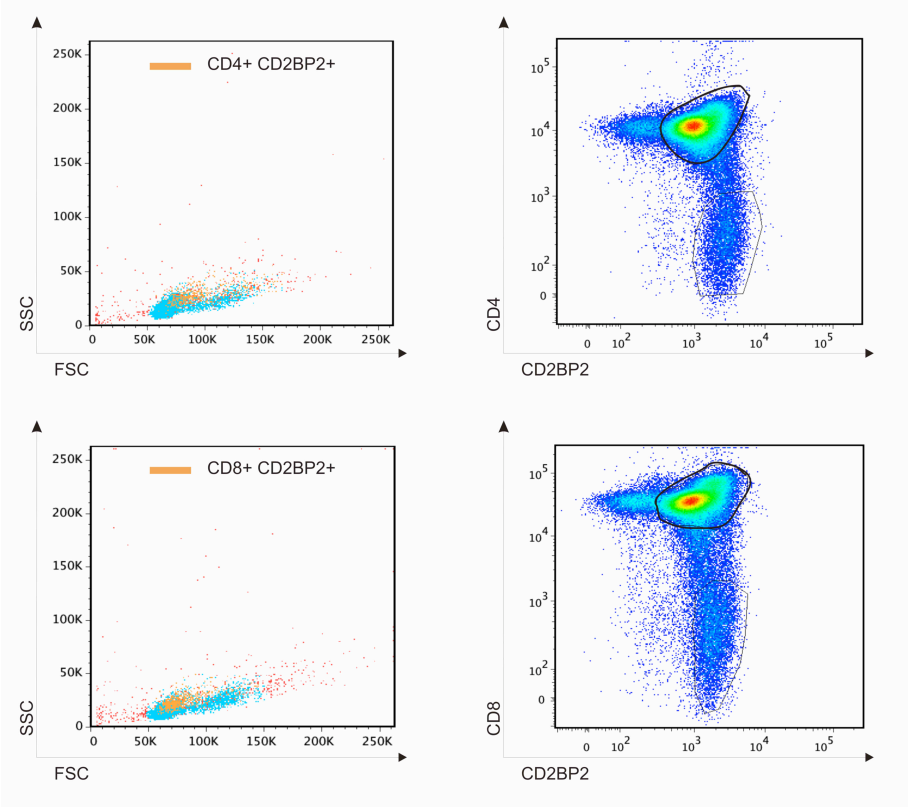

Figure 3.23. **CD4 and CD8 expressing thymic T cells also express CD2BP2.** Lymphocytes from thymus were stained with the T cell markers CD4 (top) and CD8 (bottom) and CD2BP2. Most of the CD4^{+} and CD8^{+} cells did also express CD2BP2. Backgating of the double positive cells shows both populations in the upper corner of the lymphocyte gate.

In lymph nodes, similar to bone marrow cells, most $CD19^+$ cells expressed CD2BP2 as shown in Figure 3.24. In contrast to the thymus, only about 40 % of all cells in the lymph node were $CD4^+$ $CD2BP2^+$ and about 5 % of $CD4^+$ T cells did not express CD2BP2.

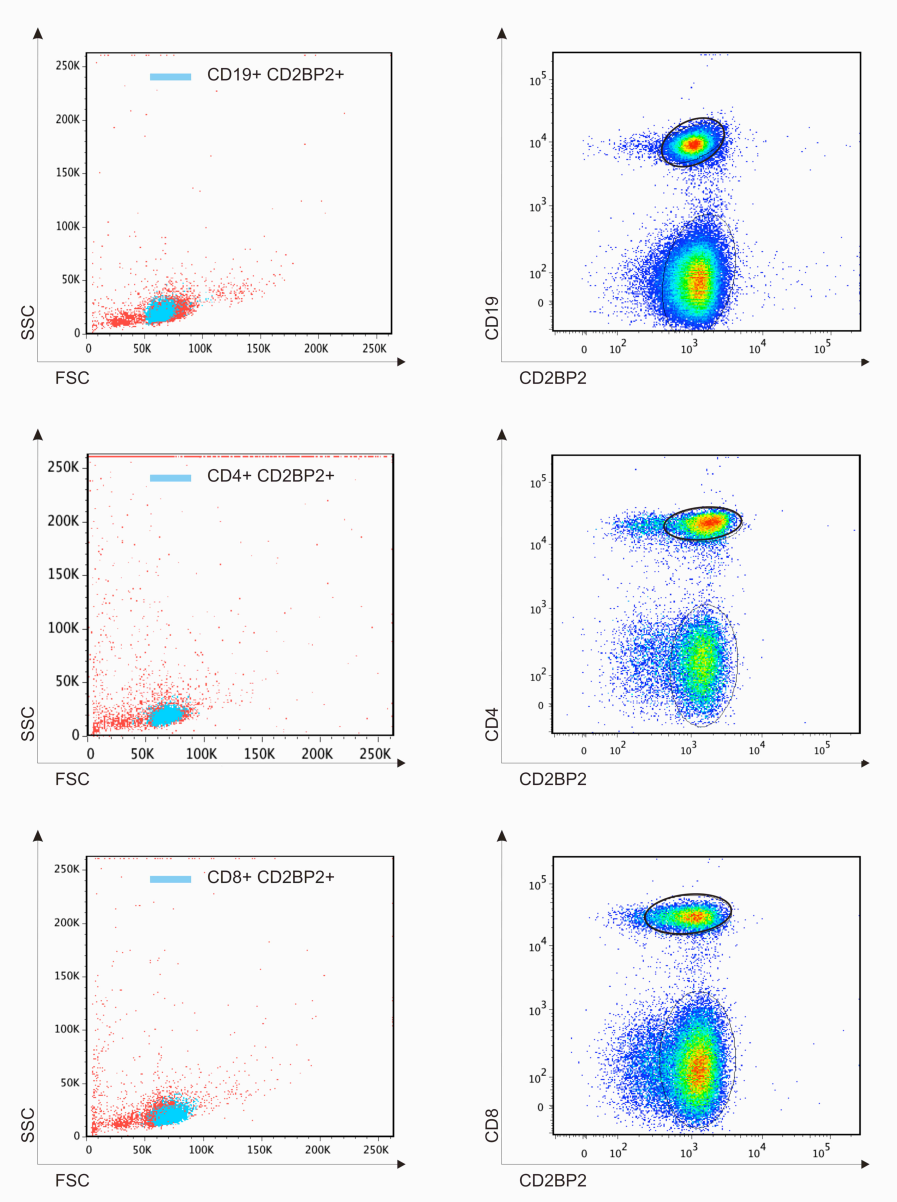

Figure 3.24. **CD2BP2 is expressed in $CD4^+$ and $CD8^+$ T cells and $CD19^+$ B cells in lymph nodes**. Most of the $CD19^+$ B cells did also express CD2BP2 (top). The same could be seen for CD4 (middle) and CD8 (bottom) expressing T cells. All double positive cells localized to the lymphocyte gate.

About 26 % of all cells in the lymph node were $CD8^+$; only 3 % of these cells were $CD2BP2^-$. Still the lymph nodes contained the highest amount of $CD2BP2^-$ cells of all cells analyzed. $CD19^+$ cells were localized in the same area of the gate as in bone marrow cells whereas $CD4^+$ and $CD8^+$ cells were detected in the lower corner of the lymphocyte gate, in contrast to their localization in the thymus. Obviously, other, more granular lymphocytes were present in the lymph nodes that were not expressed in the thymus.

In spleenocytes CD19$^+$ B cells were also CD2BP2$^+$. In contrast to lymph nodes, no population that was CD19$^+$ but CD2BP2$^-$ could be detected (Figure 3.25). Backgating of the CD19$^+$ CD2BP2$^+$ cells showed comparable localization as in bone marrow and lymph node cells. 20 % of all cells in the spleen were CD4$^+$ and all of them also expressed CD2BP2. The same was true for CD8$^+$ cells that showed an expression of about 7 % in the spleen. Both cells could be found in the same gating area as in lymph nodes.

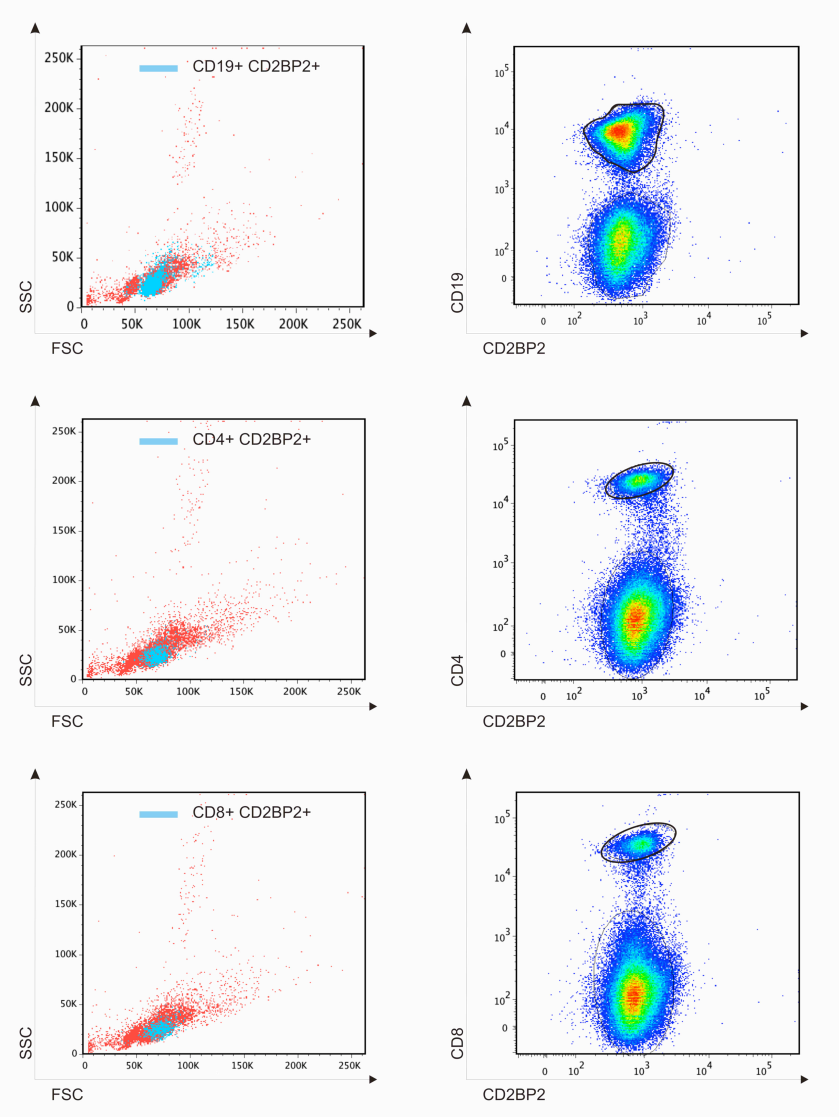

Figure 3.25. **Splenic B, CD4$^+$ and CD8$^+$ T cells express CD2BP2**. All spleenocytes that were CD19$^+$ also expressed CD2BP2 (top). The same can bee seen in the middle and bottom panel for CD4$^+$ and CD8$^+$ T cells, respectively. Backgating showed comparable localization to the gating areas in lymph nodes.

3.2.4.4 CD2BP2 expression in macrophages and natural killer cells

Next, macrophages and natural killer (NK) cells were analyzed for their expression of CD2BP2. Cells from the spleen were stained against the integrin α_M Mac1 and F4/80 for the detection of macrophages. $Mac1^+$ $F4/80^+$ cells could be detected at the lower end of the monocyte gate as shown in the upper left panel in Figure 3.26. As shown in the density plot in Figure 3.26, $Mac1^+$ $F4/80^+$ cells were positive for CD2BP2. By comparing MFI value of the isotype control and CD2BP2, the spectra differ in shifts by the power of ten.

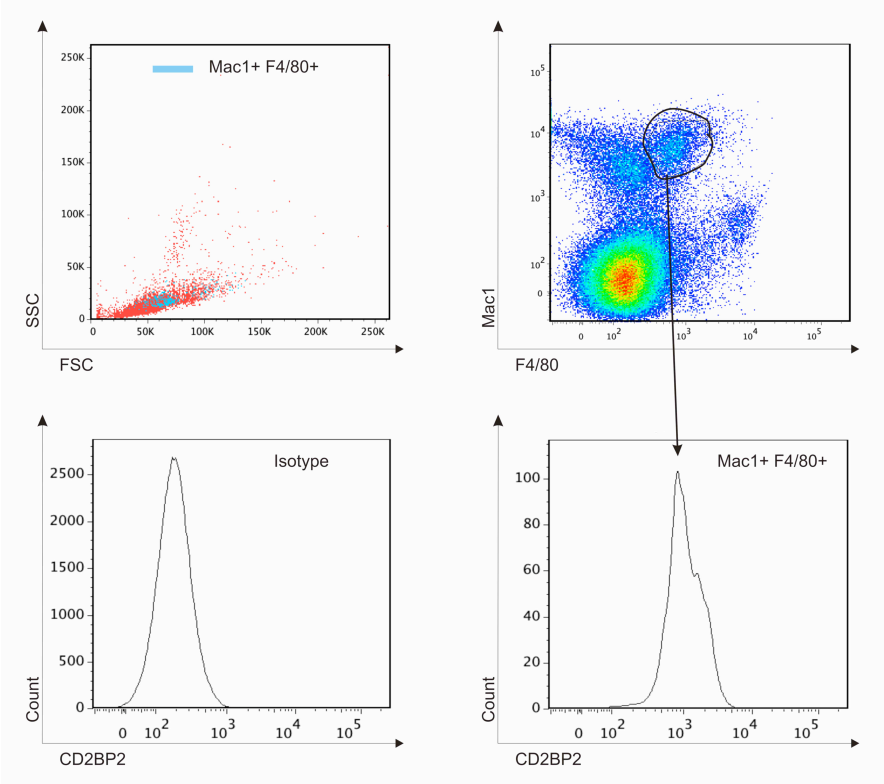

Figure 3.26. **Macrophages from BL6 splenic cells express CD2BP2.** Spleenocytes were stained with the macrophage markers Mac1 and F4/80. Backgating of $Mac1^+$ $F4/80^+$ cells showed their localization at the lower end of the monocyte gate. The histogram of these double positive cells showed a shift of $CD2BP2^+$ cells in comparison with the isotype control.

Splenic NK cells were detected by double staining with the NK cell markers CD11b and CD49. These double positive cells localized in an area between the lymphocyte and monocyte gate. The histogram of the $CD11b^+$ $CD49^+$ cells showed a shift for the expression of CD2BP2 in contrast to the isotype control (Figure 3.27).

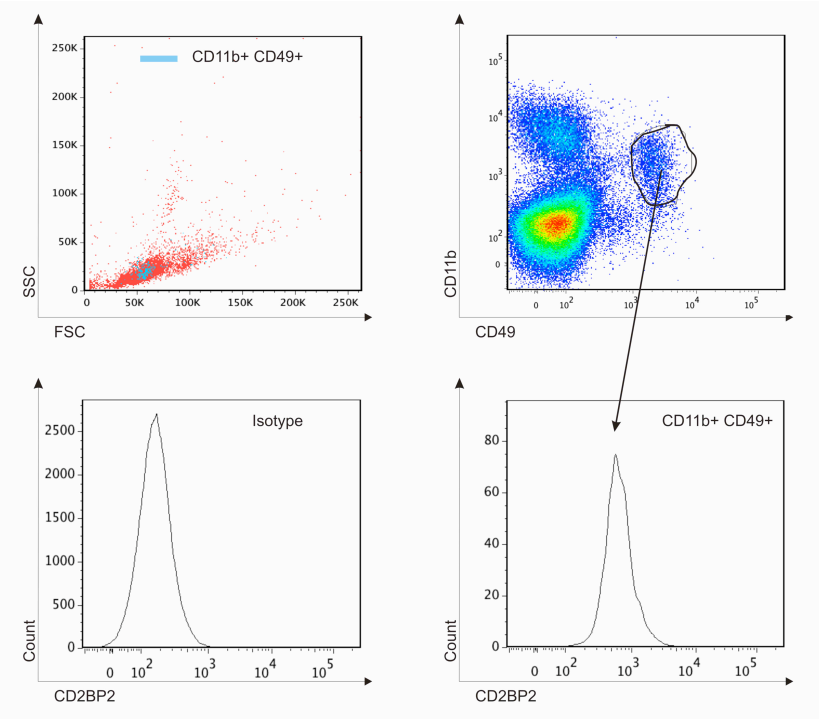

Figure 3.27. **Splenic NK cells express CD2BP2**. NK cells were detected with the markers CD11b and CD49. The histogram of $CD11b^+$ $CD49^+$ cells showed a shift of $CD2BP2^+$ cells in contrast to the isotype control.

3.2.4.5 CD2BP2 expression in the developing thymus

The analyses performed so far were restricted to matured immune cells, which showed high expression levels of CD2BP2. Single stains against CD4 and CD8 in the thymus speculated for an expression of CD2BP2 in double positive cells (Figure 3.23). Therefore, lymphocytes from up to 5 weeks old BL6 mice were double stained with CD4 and CD8. Single CD4 or CD8 expressing cells as well as $CD4^+$ $CD8^+$ and $CD4^-$ $CD8^-$ cells were probed for the presence of CD2BP2. The thymus of a 5 weeks old BL6 mouse is exemplary shown here. More than 80 % of the cells in the thymus were $CD4^+$ $CD8^+$, about 7 % $CD4^+$ $CD8^-$, 2 % $CD4^-$ $CD8^+$ and 2 % $CD4^-$ $CD8^-$. The four different subgroups were analyzed considering their expression of CD2BP2 in comparison with the isotype control (Figure 3.28).

$CD4^+$ $CD8^-$, $CD4^-$ $CD8^+$ and $CD4^+$ $CD8^+$ cells did all show a clear shift for CD2BP2 in the histogram when compared to the histogram of the isotype control. Still, one population of DN cells in the histogram of $CD4^-$ $CD8^-$ cells did not shift, speaking for no expression of CD2BP2 in this subpopulation. This peak contained developing T cells that did neither express CD4

nor CD8 and γδ T cells. Preceding studies in developing T cells were performed to further analyze this negative subpopulation.

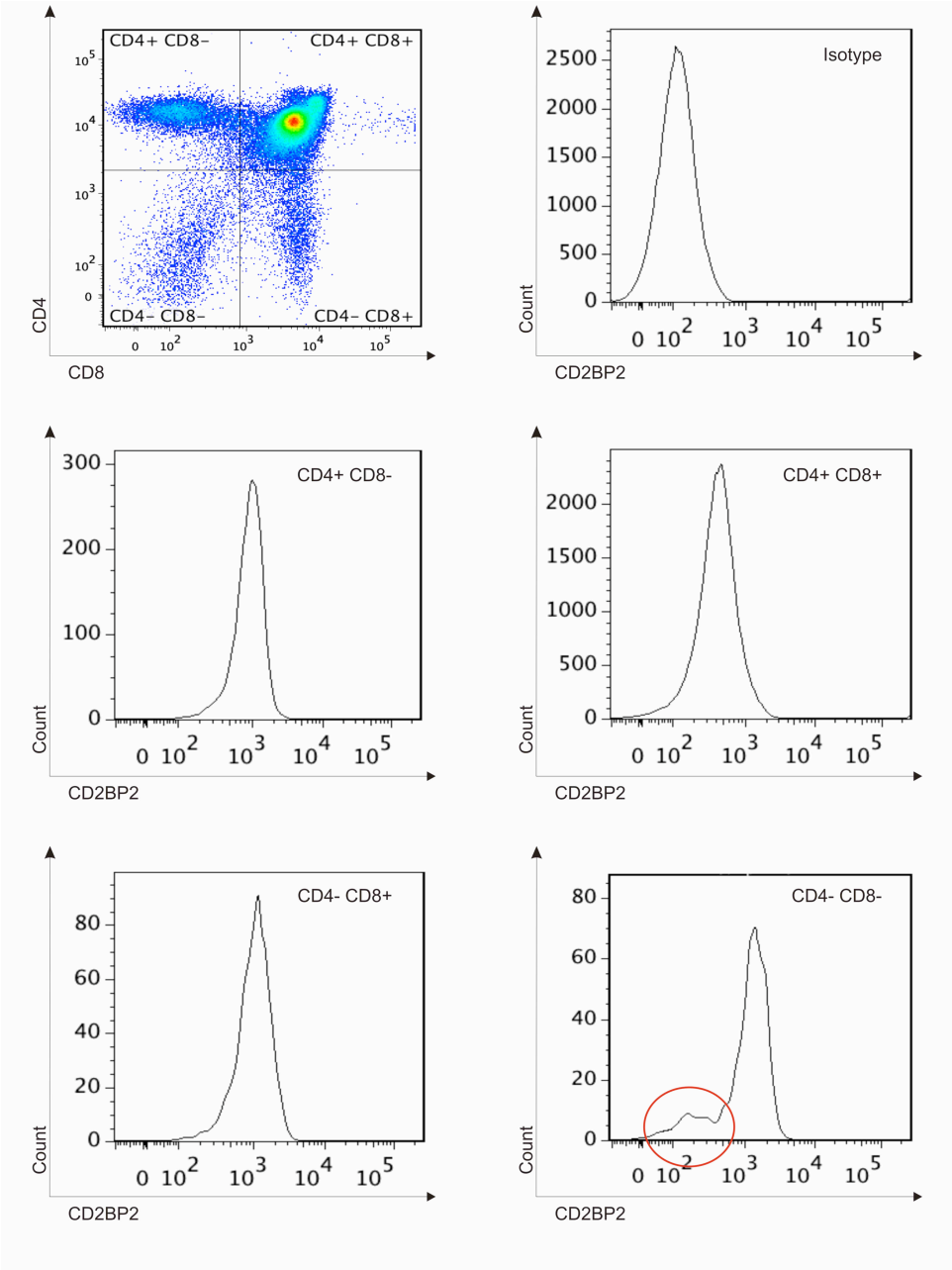

Figure 3.28. **The major population of single and double positive CD4 and CD8 T cells expressed CD2BP2**. Thymus from 5 weeks old BL6 mouse was double stained against CD4 and CD8. The histograms of the single and double positive as well as the double negative cells showed the expression of CD2BP2 in comparison with the isotype control. The histogram of $CD4^-$ $CD8^-$ cells showed one subpopulation that did not express CD2BP2, which is marker with a red cycle.

Early stages of T cell development were analyzed in $CD4^-$ $CD8^-$ cells. Therefore, cells from pooled thymuses of 5 weeks old BL6 mice where depleted of CD4 and CD8 expressing T cells with magnetic bead purification. Successful depletion was tested with CD4 and CD8 antibody and subsequently stained with the early T cell developmental marker CD44 and CD25. During T cell development, in the $CD4^-$ $CD8^-$ state, CD44 is upregulated first, leading to double negative state 1 (DN1) followed by the co-expression of CD44 and CD25 (DN2). Subsequently, CD44 is down regulated (DN3) followed by CD25 (DN4).

The four different DN stages are shown in Figure 3.29. Initially, efficient depletion of $CD4^+$ and $CD8^+$ cells were tested. As can be seen in the top left density blot, stains against CD4 and CD8 showed no shift in the spectrum. These cells could therefore be considered as $CD4^-$ $CD8^-$. Stains with CD44 and CD25 showed a distribution of the four DN stages with about 70 % of cells in DN stage1, 3 % in the DN2, 6 % in DN3 and 20 % in DN4. The four stages were analyzed for their expression of CD2BP2. As shown in Figure 3.29, histograms of DN stage 1-4 show shifts for the expression of CD2BP2 when compared to the isotype control. These results speak for the expression of CD2BP2 during early maturation of T cells in the thymus.

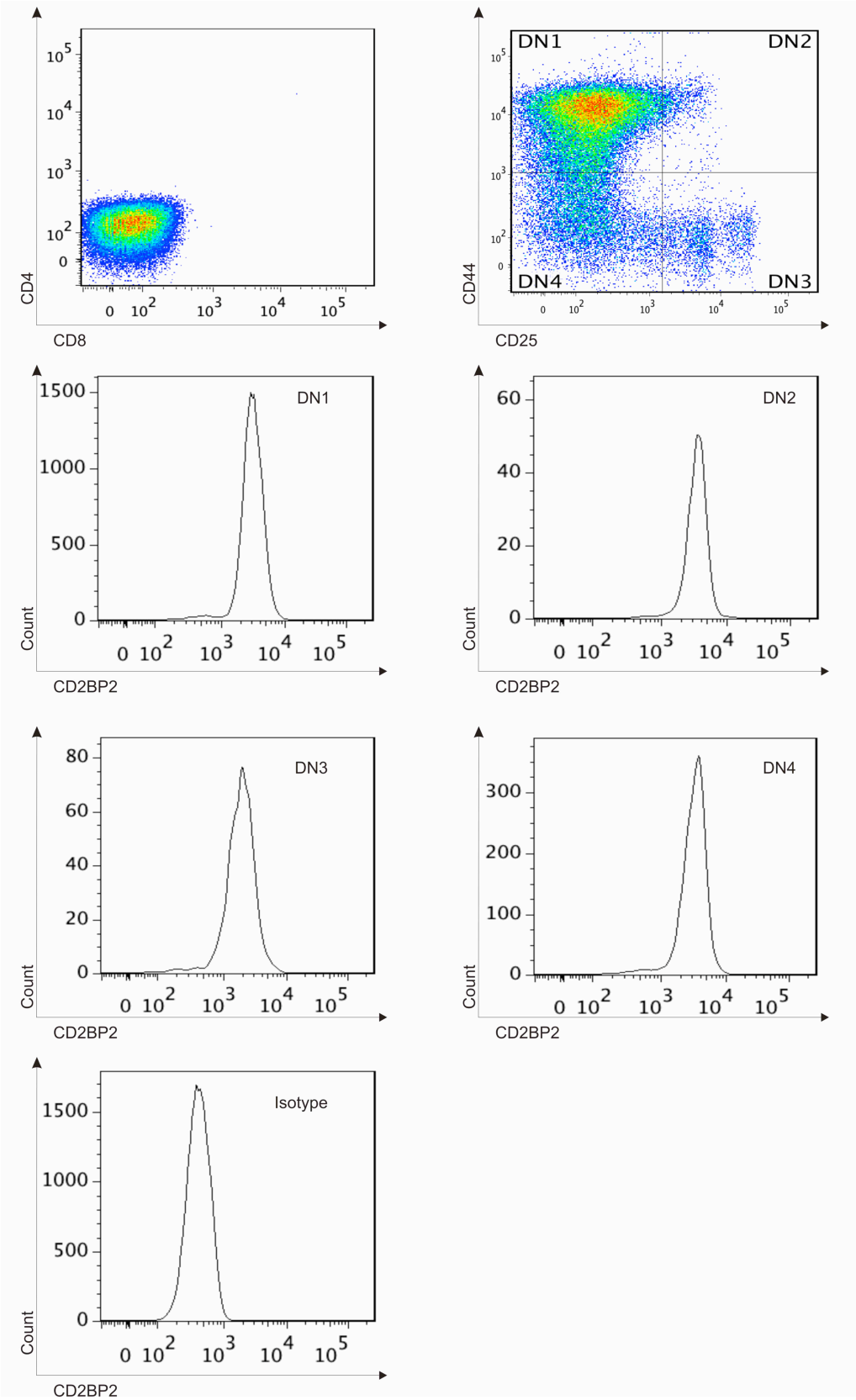

Figure 3.29. **CD2BP2 is expressed from DN stage 1 to 4 during T cell development**. Cells from the thymus were pooled and depleted of CD4 and CD8 positive T cells. Successful depletion can be seen in the top left panel, no CD4 or CD8 expressing cells could be detected. DN state 1 to 4 was separated by double staining against CD44 and CD25. In comparison with the isotype control, CD2BP2 was expressed in all four stages.

The percentage of CD2BP2 expressed in the different cell types is shown in Table 3.1. The table shows the amount of cells that express the cell specific marker and CD2BP2 with regard to the total amount of cells in the organ. CD4 and CD8 expressing T cells are expressed in high amounts in the thymus (up to 90 %) and also express CD2BP2. The least amount of cells present are NK cells and macrophages, that represent less than 5 % of splenic cells.

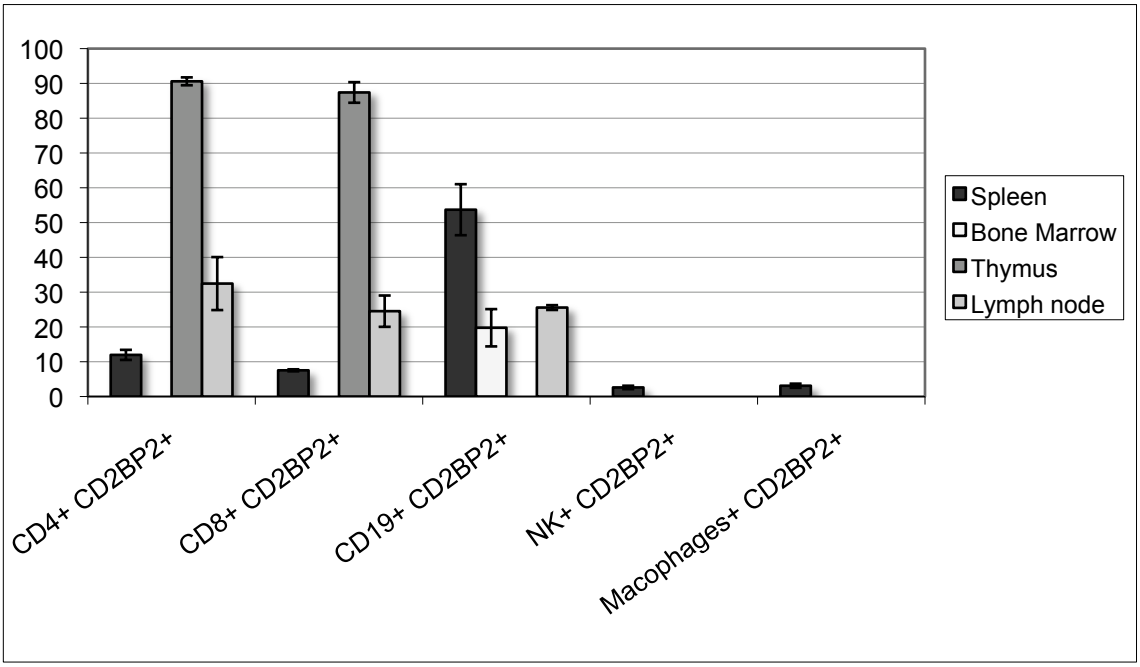

Table 3.1. **Summary of CD2BP2 expression levels in immune cells**. The table shows the amount of cells that are positive for the cell type specific marker and CD2BP2. The highest expressions with regard to the overall expression of the cells in these organs are CD4 and CD8 expressing T cells that also express CD2BP2. The least amounts are represented by Natural Killer (NK) cells and macrophages in the spleen.

In summary, CD2BP2 is expressed in mature $CD4^+$ and $CD8^+$ T cells in thymus, lymph node and spleen of BL6 mice and in B cells in the bone marrow, lymph node and spleen. Splenic macrophages and NK cells also express CD2BP2. In the bone marrow, B220 high and low cells express CD2BP2, suggesting its expression during development. The same could be seen for developing T cells in the thymus, where all double negative T cell stages were positive for CD2BP2 expression. The only negative population observed so far was present in $CD4^-$ $CD8^-$ T cells. This peak comprised DN T cells and γδ T cells. Further analysis of γδ T cells failed because of limited amount of cells available. Figure 3.30 summarizes the cell populations found so far expressing CD2BP2. The presence in common lymphoid precursors and small lymphocytes could not be addressed yet due to technical limitations.

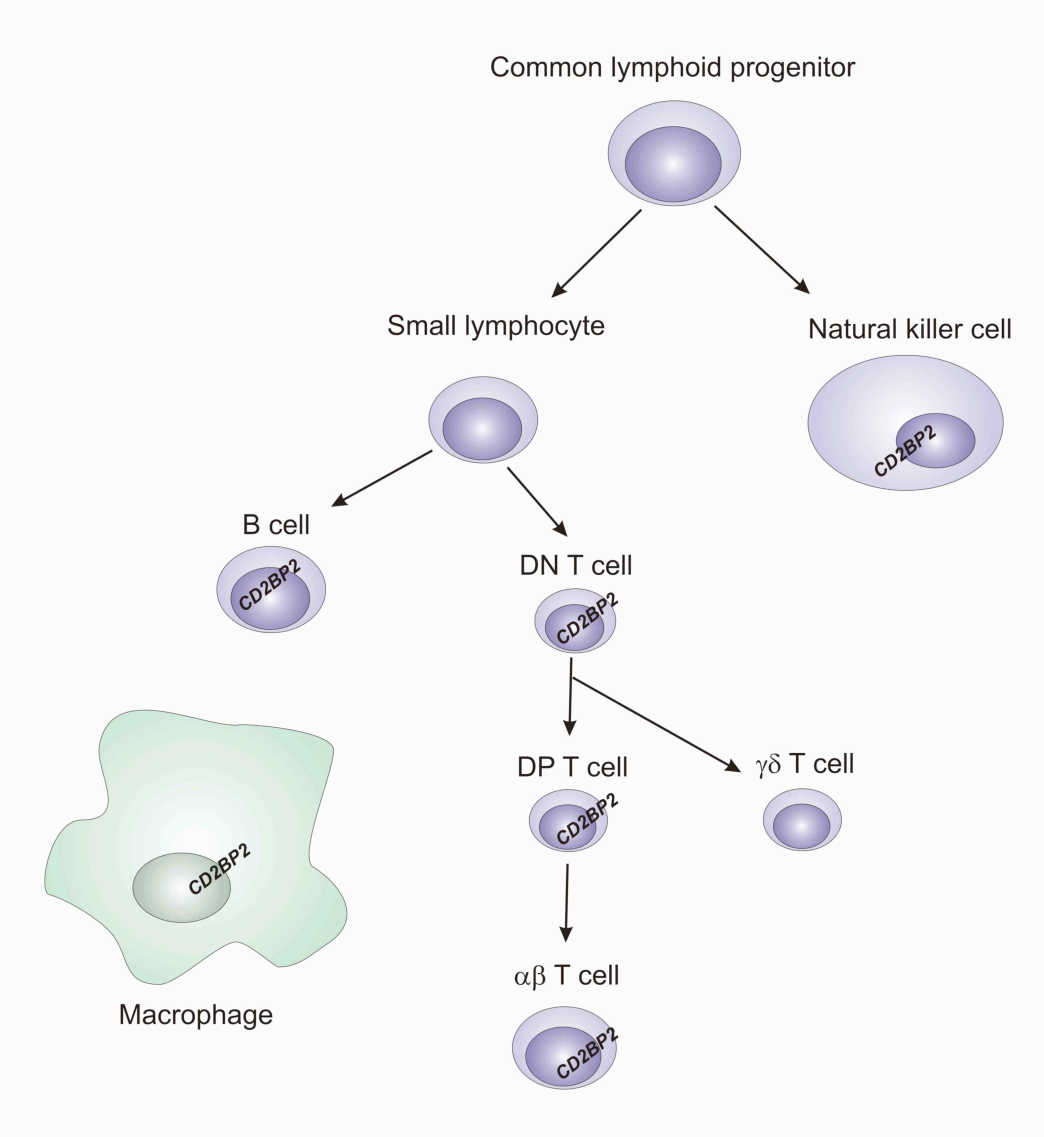

Figure 3.30. **CD2BP2 is expressed in major B and T cells, macrophages and NK cells**. The figure gives a summary of the expression analysis in this study. DN T cells, major T and B cells as well as NK cells and macrophages express CD2BP2. The expression of CD2BP2 in γδ T cells is questionable.

3.3 Conditional Gene Targeting of CD2BP2

So far, it was known that CD2BP2 belongs to the GYF-domain containing proteins that interact with PRS [2]. Several studies showed its involvement in the mRNA splicing cycle but a detailed understanding of the function is still missing [4, 58]. Even though the protein was first described as a binding partner of the CD2 adhesion molecule, its nuclear localization in human cell lines and knockdown studies question a role in CD2 signaling *in vivo* [51]. In mice, the mRNA of CD2BP2 is evenly expressed in several mouse organs whereas the protein is most abundant in hematopoietic organs. The mouse homolog of the human CD2BP2 features an alignment score of 90 percent. The GYF domain shows one AA substitution at position 384 where an aspartate in the human gene is substituted by a glutamate. The mouse protein has 342 AA, a molecular weight of 37 kD and similar phosphorylation sites at position 46, 49, 117 and 196 [15]. Targeted mouse mutations were performed to obtain a better understanding of the role of CD2BP2 *in vivo*.

3.3.1 The gene of CD2BP2

The gene of CD2BP2 in mouse is located on chromosome 7 in the F3 region in antisense direction as can be seen in Figure 3.31. The TBC1 domain family member 10B (Tbc1d10b), a gene with a suggested GTPase activator activity (pubmed) is located directly in front of CD2BP2.

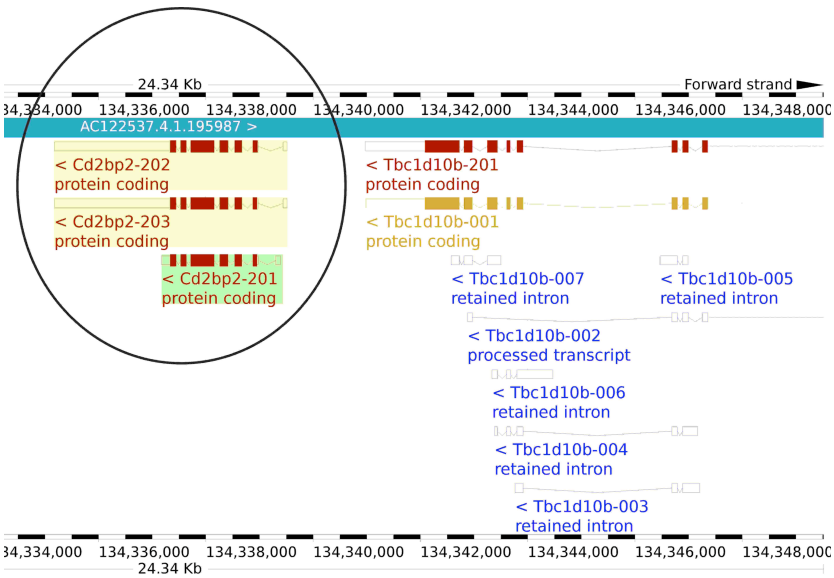

Figure 3.31. **Mouse CD2BP2 contains of 3 splicing variants**. CD2BP2 is localized on exon 7 directly following the gene Tbc1d10b. The three splice transcripts vary in different length of the untranslated part of 7th exon (adapted from [189].

On genomic level, CD2BP2 comprises 7 exons where the first one and large parts of the 7th are non-coding. CD2BP2 forms three splice variants that differ in the length of the 7th exon. Variant one and two have long 3'UTRs whereas in the third variant, the non-coding region of the 7th exon is largely reduced.

3.3.2 The targeting scheme

To create an inducible knockout system for CD2BP2, a targeting vector was designed in which loxP sites flox the first three exons including the start codon. Cre-induced deletion would lead to excision of the exons and thereby the induction of the knockout.

On the WT level, genomic CD2BP2 is localized between two EcoRI restriction sites in a distance of 12 kb as shown in Figure 3.32. For positive selection of ES cells, a neo cassette flanked by FRT-sites (shown in blue in Figure 3.32) was cloned in front of the first exon. The 5'loxP site (red) was cloned in front of the 5'FRT-site; the 3'loxP followed by an additional EcoRI restriction site was cloned behind the third exon. With this cloning strategy, Cre-expression also excises the FRT-flanked neo-cassette.

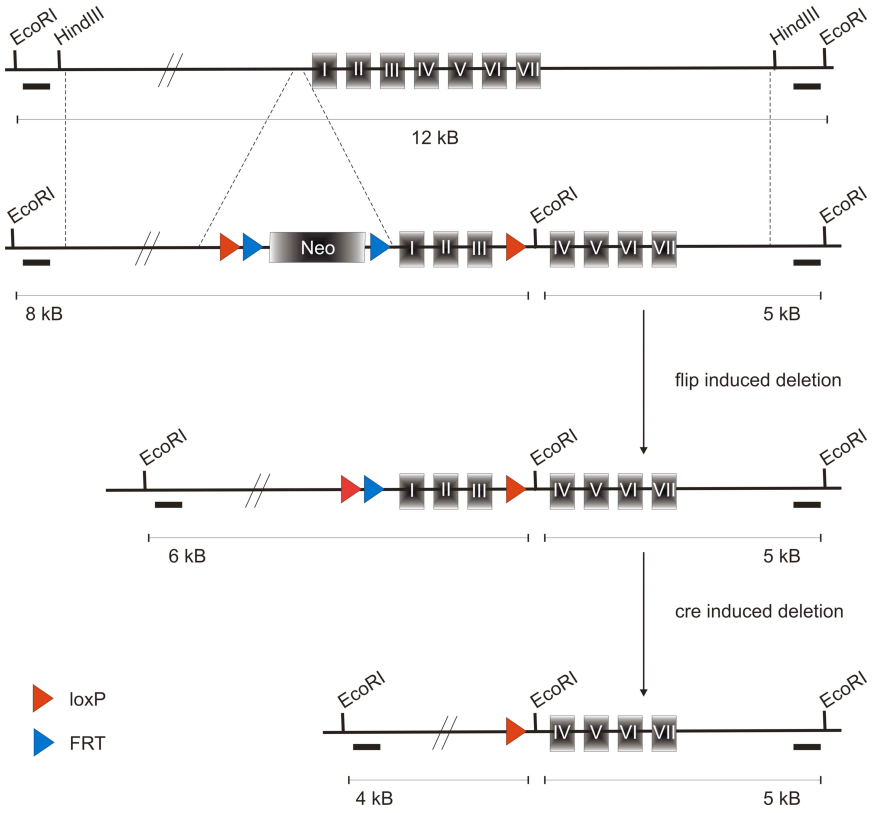

Figure 3.32 **Targeting scheme of CD2BP2**. The seven exons in the WT gene are flanked by endogenous EcoRI restriction sites with a distance of 12 kb. Homologous recombination of the targeting vector adds one additional EcoRI restriction sites leading to two fragments, 8 kb and 5kb, respectively. After flip-induced deletion, the 5'fragment is reduced to 6 kb, Recombination of loxP sites lead to a 4 kb fragment. loxP sites are shown in red, FRT sites in blue.

Upon homologous recombination of the targeting vector, which is marked by the dashed lines in Figure 3.32, EcoRI digestion will lead to two fragments because of the additional EcoRI restriction site. The 5'fragment has a size of 8 kb and the 3'fragment of 5 kb. These fragments can be probed in Southern blots with external 3' or 5'probes, that are illustrated as black bars in Figure 3.32.

Expression of the flip-recombinase will reduce the 5'targeting fragment upon excision of the neo cassette to a fragment of 6 kb. Cre-recombinase induced deletion will shorten this fragment to a size of 4 kb because of the deletions of exon one to three. The deletion of the first three exons is supposed to lead to truncated mRNA and no protein expression.

3.3.3 **Cloning of the targeting vector**

For the generation of the CD2BP2 targeting vector, a mouse genomic DNA bacteriophage P1 artificial chromosome (PAC) library RPCI-21 was used to screen for genomic DNA. Figure 3.33 gives an outline of the cloning strategy chosen to generate the CD2BP2 targeting vector. The first cloning steps were performed in the helper vector pZErO®-2. This vector contains of the lethal *E.coli* gene ccdB that is expressed if no insert disrupts the coding sequence [190] and inhibits thereby the growth of cells containing non-ligated DNA. Ligation assays with this vector reduce the background of cells containing the vector without insert. The 3'loxP site had to be cloned into the vector additionally. Since the handling of the 52 bp fragment was quite challenging, the cloning was performed with an extra cloning step into the pCR-Blunt TOPO vector. This step facilitated the handling of small-sized DNA fragments and allowed clean cuts with the restriction enzyme HpaI. In a final step, the 5' and 3'homologies were cut out of the pZERO vector and ligated into the final vector pPNT4. This chapter gives a detailed description of the cloning steps necessary for the generation of the CD2BP2 knockout vector.

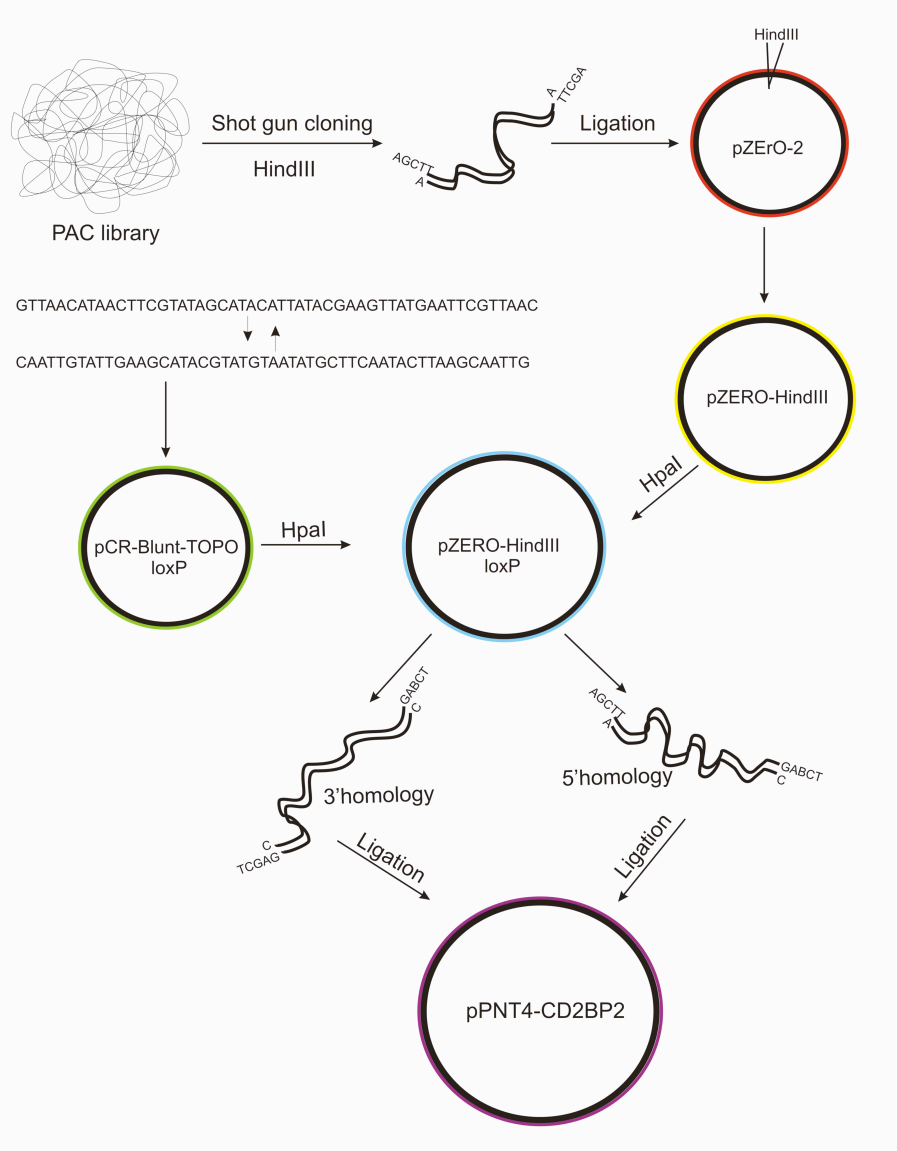

Figure 3.33. **Outline of the cloning strategy for the generation of the CD2BP2 targeting vector**. For the generation of the CD2BP2 targeting vector, murine ES cell clones from a PAC library was digested with HindIII via shot gun cloning. The 7.5 kb HindIII fragment was ligated into the helper vector pZERO-2. In parallel, the 3'loxP site was synthesized, annealed and cloned into the helper vector pCR-Blunt-TOPO. The loxP site was cut out with HpaI and ligated into pZERO-HindIII. The 5' and 3'Homologies were cut out of pZERO-HindIII-loxP and ligated into pPNT4.

3.3.3.1 Shot gun cloning of genomic CD2BP2

Genomic DNA of CD2BP2 and pZErO®-2 were digested with HindIII and transfected chemically into competent One Shot® Top10 bacteria. These bacteria are optimized for efficient expression of large DNA constructs. The 7.5 kb fragment flanked by endogenous HindIII restriction sites is shown in red in Figure 3.34. The start codon of the coding sequence of CD2BP2 is localized in the second exon. The gene of Tbc1d10b that lies directly in front of CD2BP2 on chromosome 7 is shown in green. Positive clones were detected via colony hybridization and confirmed with restriction digests (not shown here).

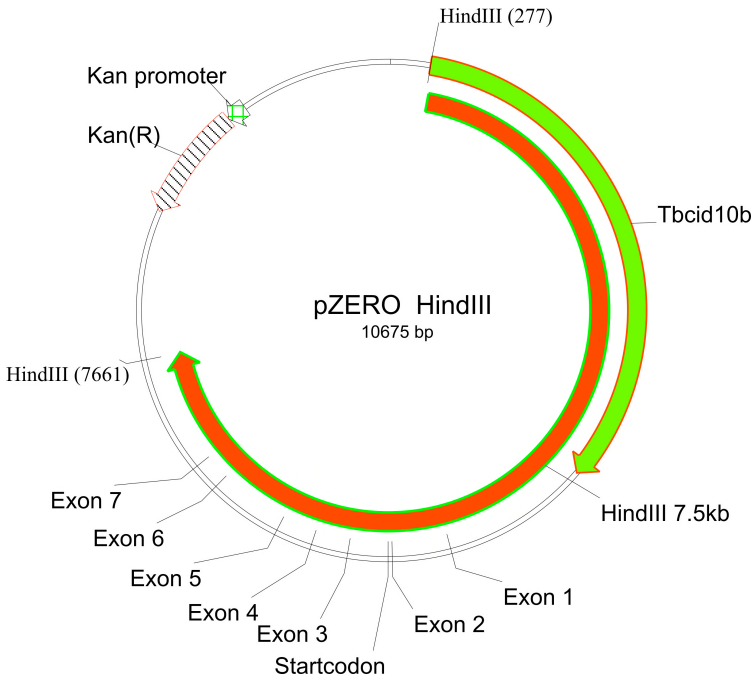

Figure 3.34. **Insertion of the HindIII fragments into pZErO®-2**. The HindIII fragment (shown in red) comprises the 5'homology and the 3'homology. The gene of Tbc1d10b that directly precedes CD2BP2 on chromosome 7 is shown in green.

3.3.3.2 Insertion of the 3'loxP site into pZERO HindIII

The final pPNT4 vector already contained the 5'loxP site. For cloning of the 3'loxP site, two DNA oligomers contain of the sequence of the loxP site (lilac in Figure 3.35) followed by an EcoRI site (shown in green), two HpaI sites (yellow) and additional thymine and adenines at both ends were synthesized. Cloning of the additional loxP site was more challenging than expected. Direct digest of the oligomere with HpaI after annealing failed because the additional thymine and adenines were not long enough for efficient restriction digest with HpaI. Therefore, both single strand constructs were annealed and ligated into pCR-BluntII-TOPO®, which allowed the efficient ligation of small blunt-end constructs.

```
5'TTTTTGTTAACATAACTTCGTATAGCATACATTATACGAAGTTATGAATTCGTTAACTTTTT'3
3'AAAAACAATTGTATTGAAGCATATCGTATGTAATATGCTTCAATACTTAAGCAATTGAAAAA'5
```

Figure 3.35. **LoxP oligomers with additional EcoRI restriction sites**. Two single DNA strands consist of a loxP site (shown in lilac), followed by an EcoRI restriction site (shown in green), two HpaI sites (yellow), thymidines and adenines were synthesized and annealed.

From here, the insert could be excised by digestion with HpaI. Successful excision of the loxP sites is shown in the agarose-gel in Figure 3.36. The loxP sites are marked with red cycles. The next challenge was the purification of these small oligomeres. Column purification was

not an option because of the small size. Purification succeeded with gel purification followed by DNA extraction with the QIAEXII Gel extraction Kit. Here, DNA is purified by a salt gradient allowing the purification of small DNA fragments.

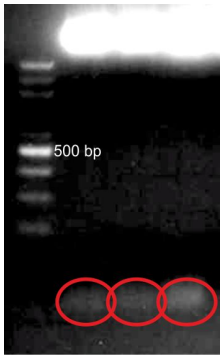

Figure 3.36. **Successful digestions of the loxP sites out of pCR-Blunt II-TOPO®.** The agarose gel shows the digested vector shining bright on the very top of the gel, the red cycles mark the loxP sites.

The loxP site was ligated blunt ended into the HpaI linearized pZERO HindIII vector leading to pZERO HindIII loxP (Figure 3.37). This vector consists of the 5'homology (3724 bp) and 3'homology (3661bp), both shown in light blue in Figure 3.37. The 3'homology contained all exons and the newly inserted 3'loxP site. The correct direction of the loxP site was analyzed by sequencing.

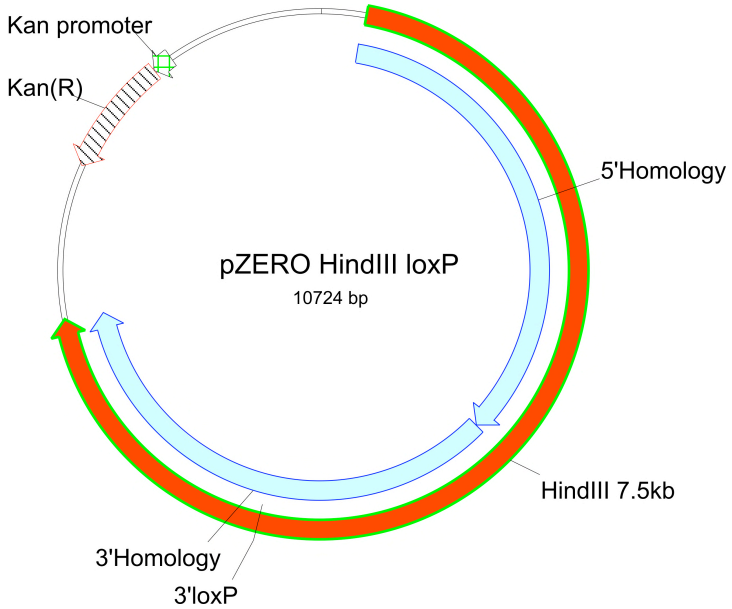

Figure 3.37**. pZERO HindIII loxP** consists of the 5' and 3' homologies and the newly inserted 3'loxP site.

3.3.3.3 Cloning of the final vector pPNT4

pZERO HindIII loxP was digested with SacI and HindIII to excise the 5'homology. This fragment (3723 bp) was cloned blunt-ended into the pPNT4 vector that was previously linearized with KpnI. The 3'homology with the inserted 3'loxP site was excised with SacI (3722 bp) and ligated blunt ended into the pPNT4-5'homology vector that was linearized with PmlI. The direction of the 3'homology was tested by PCR and sequencing.

The final vector comprised the 5'homology in green and the 3'homology in dark red shown in Figure 3.38. The vector already contained FRT-sites flanking the neo cassette and a Thymidine Kinase (both shown by red arrows) in its backbone that serve as positive and negative selection marker, respectively. The 5'loxP site was also part of the backbone. The insertion of the 3'homology integrated the 3'loxP site with additional EcoRI restriction site downstream of the third exon. Sequencing was performed at several steps during vector cloning. The sequence of the final vector is shown in the supplement. For the electroporation of pPNT4-CD2BP2 into ES cells, the vector was linearized with FseI, purified and resuspended with PBS under sterile conditions.

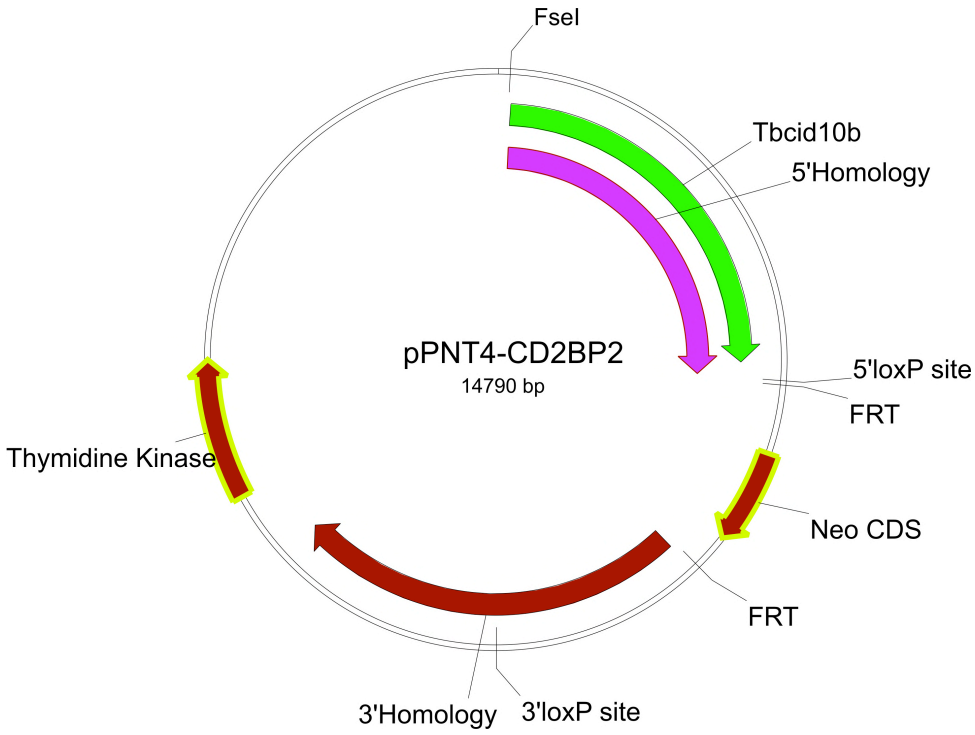

Figure 3.38. **Final pPNT4-CD2BP2 vector**. The final targeting vector comprises the 5' and 3' homologies (shown in lilac and dark red, respectively). The backbone of the vector already contains the neo cassette serving as positive control and the Thymidine Kinase as negative selection marker. The 5'loxP site is also already present in the backbone whereas the 3'loxP site was inserted with the 3'homology.

3.3.3.4 Successful recombination of the loxP sites

The functionality of the loxP sites was tested by transforming the vector into competent EL350 bacteria that express the Cre-recombinase upon induction with L-arabinose (see Method part). After DNA extraction, successful recombination of the loxP sites was analyzed by digesting the vector with EcoRI and AgeI.

Figure 3.39 shows the final pPNT4-CD2BP2 vector before and after recombination of loxP sites (A and B). The non-recombined vector comprises the loxP sites, the neo cassette and all seven exons. Upon loxP recombination, the neo cassette and the first three exons are excised. Digesting the vector with EcoRI and AgeI can monitor this. The digest of the non-recombined vector would lead to DNA fragments of 9364, 3372 and 2054 bp (not shown) whereas successful recombination leads to two fragments of 9170 and 2054 bp of size. Figure 3.39 C shows both fragments of the recombined vector and the undigested vector in its supercoiled and coiled form.

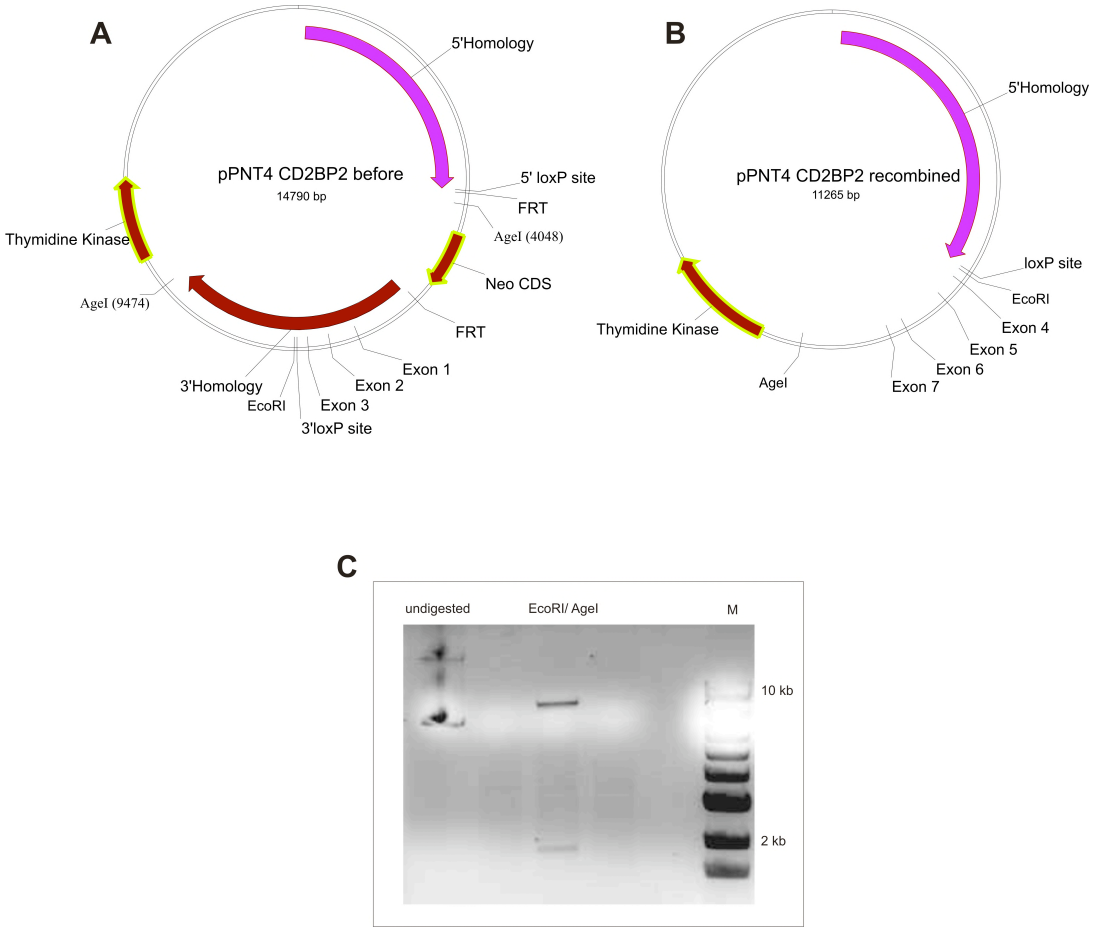

Figure 3.39. **Induction of Cre-recombinase leads to recombination of pPNT4-CD2BP2**. The vector pPNT4-CD2BP2 is shown before (A) and after (B) recombination of loxP sites. After recombination, exons 1 to 3 are excised. Successful recombination was confirmed by restriction digest with EcoRI and AgeI. The recombined vector led to fragments of 9170 and 2054 bp as shown in the agarose gel in C in comparison with the undigested vector. The non-recombined vector would lead to fragments of 9364, 3372 and 2054 bp (not shown here).

3.3.4 **Screening for positive ES cell clones**

As described in the Method part, R1/E and JM8.A3.N1 ES cells were electroporated with the linearized pPNT4-CD2BP2 vector. The ES cells were positively and negatively selected with G418 and Ganciclovir, respectively. Clones surviving the selection process were picked, expanded and genomic DNA was extracted. After digesting with EcoRI, the genomic DNA was separated on an agarose gel that was further used for Southern blotting.

One exemplary agarose gel after digestion of genomic DNA with EcoRI is shown in Figure 3.40. Clones A1 to B8 were separated on a 0.7 % agarose gel at 80 volts for 3.30 hours. The lanes of clone A1 and A8 were empty because the DNA was lost during DNA extraction. All other lanes show high amounts of genomic DNA, leading to the expected smear appearing with digested genomic DNA. The bands visible at 1 kb are called EcoRI islands that are typical for digestion of genomic DNA with EcoRI. They are caused by the assembly of unspecific DNA fragments.

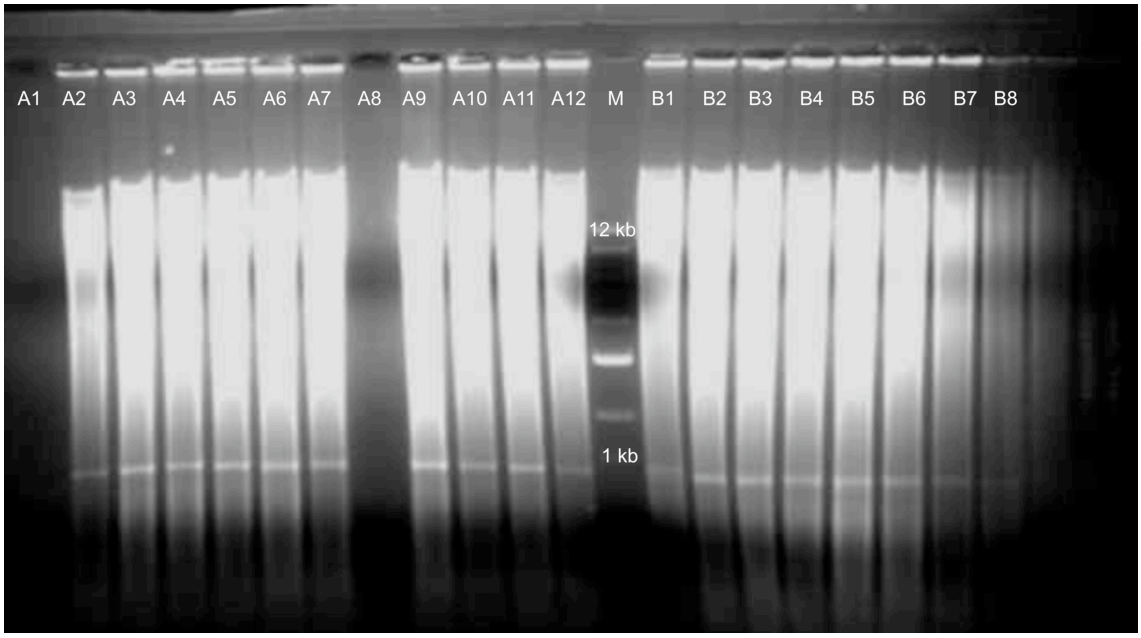

Figure 3.40. **Digestion of genomic DNA with EcoRI separated on agarose gel.** DNA from ES cell clones that were positively selected and expanded was separated on a 0.7 % agarose gel. In lane A1 and A8, the DNA extraction did not work. The bands at 1 kb represent EcoRI islands, that are typical after digest of genomic DNA with EcoRI.

One Southern blot screen with successfully integrated targeting vector is shown in Figure 3.41. The blot was incubated with the radioactive labeled 3'probe. WT DNA is represented with bands at the height of 12 kb whereas successfully recombined clones comprised one additional band at 5 kb. ES cell clones D12 and E2 show one WT band at 12 kb and one from the targeting vector at 5 kb. These clones are considered as positive clones and were further analyzed before injecting into eight-cell stage embryos.

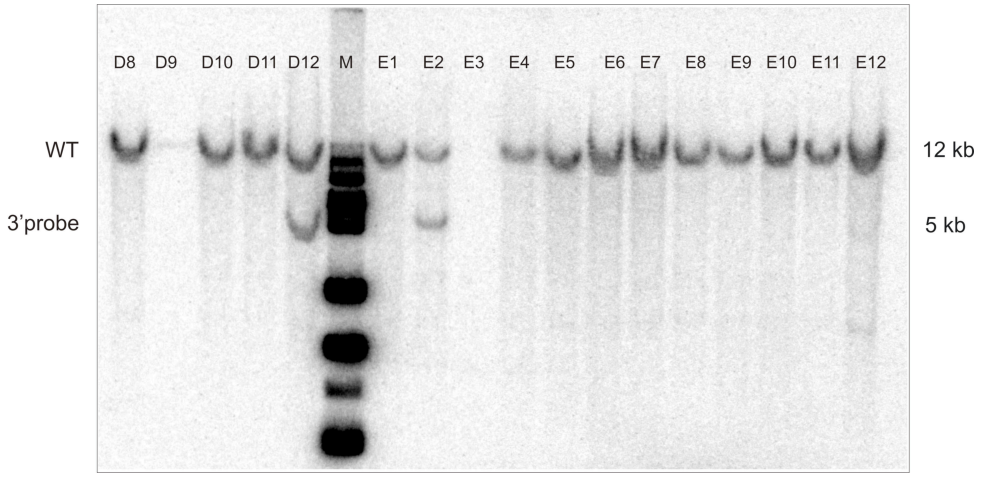

Figure 3.41. **Clone D12 and E2 showed successful homologous recombination of the targeting vector into R1/A cells.** This exemplary Southern blot was probed with a radioactive labeled 3'probe. While all clones showed the WT band at 12 kb, clones D12 and E2 integrated the targeting vector on one allele, leading to the second band of 5kb after incubation with the 3'probe.

Southern blot screening was also performed with JM8 cells. One Southern blot is shown in Figure 3.42. Here, clone A1 to C2 were incubated with the external 3'probe. The clones A5, A7 and B11 show two bands, the WT allele at 12 kb and the targeted allele at 5 kb representing the 3'homology region.

Figure 3.42. **Clone A5, A7 and B11 showed successful homologous recombination of the targeting vector into JM8 cells.** In this exemplary screen, the clones A5, A7 and B11 successfully integrated the targeting vector.

The clones A9, A10, B8, B10 and B12 exhibit an extra band larger than the 12 kb band in the Southern blot. Here, the complete integration of the targeting vector failed and only the 5'homology with neo cassette was integrated. Therefore, the additional EcoRI restriction side

downstream of the 3'loxP site is missing leading to a larger fragment after digestion with EcoRI.

For the screening of 129 ES cells, 672 clones were picked and analyzed by Southern blot. Table 3.2 shows the overall recombination efficiency of the 7 plates analyzed. One plate represents one 96 well plate. In plates 1 to 3, 7 positive clones could be detected while 14 cells could not be analyzed due to technical limitations. The plates 4 to 7 contained 46 positive clones. Plate 1 to 3 derived from one electroporation with an older Gene Pulser electroporator, whereas plates 4 to 7 have been electroporated under the same conditions on the newest Gene Pulser electroporator.

ES CELL CLONES	PLATE 1	PLATE 2	PLATE 3	PLATE 4	PLATE 5	PLATE 6	PLATE 7
Total number	96	96	96	96	96	96	96
Positive	4	1	2	13	12	10	11
Losses	6	5	3	5	3	14	16

Table 3.2 **In the second round of electroporation of 129 ES cells, the recombination efficiency rose by the power of ten**. 672 ES cell clones were picked and screened for positive hits. Positive refers to positive homologous recombination, losses to lost clones due to technical problems.

3.3.5 **Laser-assisted eight cell-stage injection of clones and germline breeding**

Clones from the R1/E and JM8 screenings were re-checked with 3'probes as shown in Figure 3.43. Two positive clones deriving from R1/E cells (+/ neo) are shown in comparison to a WT clone. Neo means the integration of the neo cassette into the genome. For JM8 cells, two positive clones with one WT clone are shown. The integrity of the loxP sites was confirmed by sequencing.

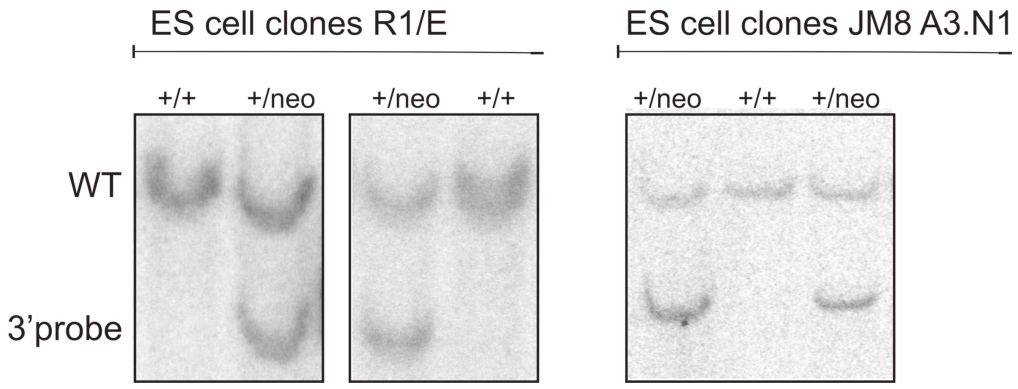

Figure 3.43. **Integration of the targeting vector could be confirmed in positive clones chosen for blastocyst injection.** ES cells from 129 R1/E and BL6 JM8A3.N1 were tested again for homologous recombination. Two clones from each background were chosen and probed with 3'probes and sequenced before injection into blastocysts.

The positive clones were laser-assisted injected into eight cell-stage embryos from BL6 mice. Six to eight ES cells were injected per morula (performed by Roland Naumann at the Max-Planck-Institute of Molecular Cell Biology and Genetics in Dresden, Germany).

The 129 ES cell-derived positive clones that were injected derived from the first electroporation (plate 1 to 3). Offspring from this electroporation showed high chimerism, which often correlates with good chances for germline transmission. The coat color of JM8 chimera was mainly black indicating a reduced implantation of ES cells into the morula. Therefore, the BL6 chimeras were not used for further germline breeding.

High chimeric mice deriving from the R1/E cells were bred with C57BL/6J, Flip and Cre-deleter mice. After 8 generations without successful germline transmission breeding was stopped.

Clone D12 (Figure 3.41) and B7 from plate 6 (second electroporation) were used for another injection into eight cell-stage embryos. Again, high chimeric mice were born that were bred with C57BL/6JOlaHsd mice. The first litter of that breeding led to 100 % germline transmission as can be seen by the agouti coat color deriving from 129 ES cell background shown in Figure 3.44. These mice are considered as founders, meaning they form a new strain.

Figure 3.44. **First litter of R1/E chimera gave 100 % germline transmission**. The offspring from the first litter all had agouti coat color, speaking for germline transmission of the targeting vector that was electroporated into 129 stem cells.

3.3.6 **Mouse Breeding**

Three breeding strains were set up with the founder mice. For backcrossing into pure BL6 background, fosters were bred with WT C57BL/6JOlaHsd. For the deletion of the neo cassette, founder mice were crossed with the deleter strain Flipo. These JM8.F6 ES cell derived mice were generated with a vector encoding for the CAGGs promoter driving a codon optimized Flp recombinase (Flpo) allowing high efficient recombination of FRT sites. [191] Breeding of the founder mice with PGK-Cre-deleter induced the knockout. In PGK-Cre mice, the Cre-recombinase is driven by the early acting PGK-1 promoter. The recombinase is already active in the early diploid phase of oogenesis. Since it is inherited under dominant maternal control, even offspring that does not inherit PGK-Cre recombines the targeted gene [181].

3.3.6.1 Genotyping with PCR

For genotyping of mouse offspring, PCRs were established that allowed efficient and unequivocal genotyping of genomic DNA. Germline transmission and breeding for homozygous neo/neo mice were screened with the PCRs shown in Figure 3.45. Here, the DNA still contains the entire targeting vector including the neo cassette. To detect the wildtype allele, a primer pair was chosen where the forward and reverse primer bind in front of the first exon leading to a fragment of 325 bp (shown in green in Figure 3.45).

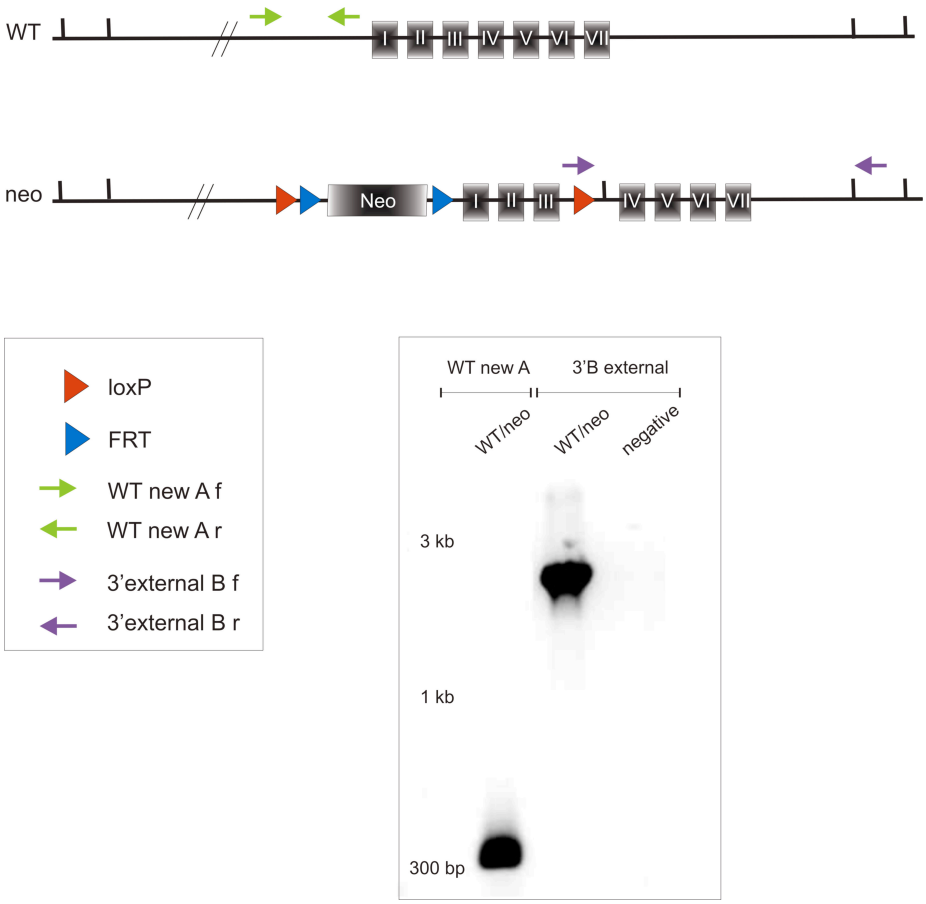

Figure 3.45. **Genotyping of neo/ WT or neo/ neo mice**. The WT primer pair detects a WT specific region in front of the first exon (presented by green errors). The forward primer of the primer pair 3'external B binds at the 3'loxP site, the reverse primer outside the homologous region (both shown in lilac) and thereby detect germline transmission or existence of the targeting vector. The agarose gel shows the genotyping of neo/WT mice resulting in a band of 325 bp for the WT PCR and of 2120 bp for the PCR with the primer pair 3'external B.

The forward primer can only bind the WT allele. In the targeting vector, the primer-binding site of the forward primer is disrupted by the insert. This primer pair was used for all genotypings where the presence of the WT allele was indication for heterozygous or homozygous mice. Germline transmission and neo targeting was detected with the primer pair 3'external B (lilac in Figure 3.45). Here, the forward primer binds at the 3'loxP site, the reverse primer outside the homologous region in the area where the external southern blot probes bind. This primer pair results in a fragment of 2120 bp and shows the integration of

the targeting vector at the correct chromosomal locus. The agarose gel in Figure 3.45 shows the result of the WT and 3'external B PCR when heterozygous WT/ neo mice were genotyped. In this case, a band at 325 bp and 2120 bp can be detected.

Flox-breeding means deletion of the neo cassette by mating of neo-mice with Flipo deleter resulting in a genotype, where the first three exons are floxed with loxP sites. Homozygous flox/ flox mice result from the crossing of two heterozygous flox/ WT mice.

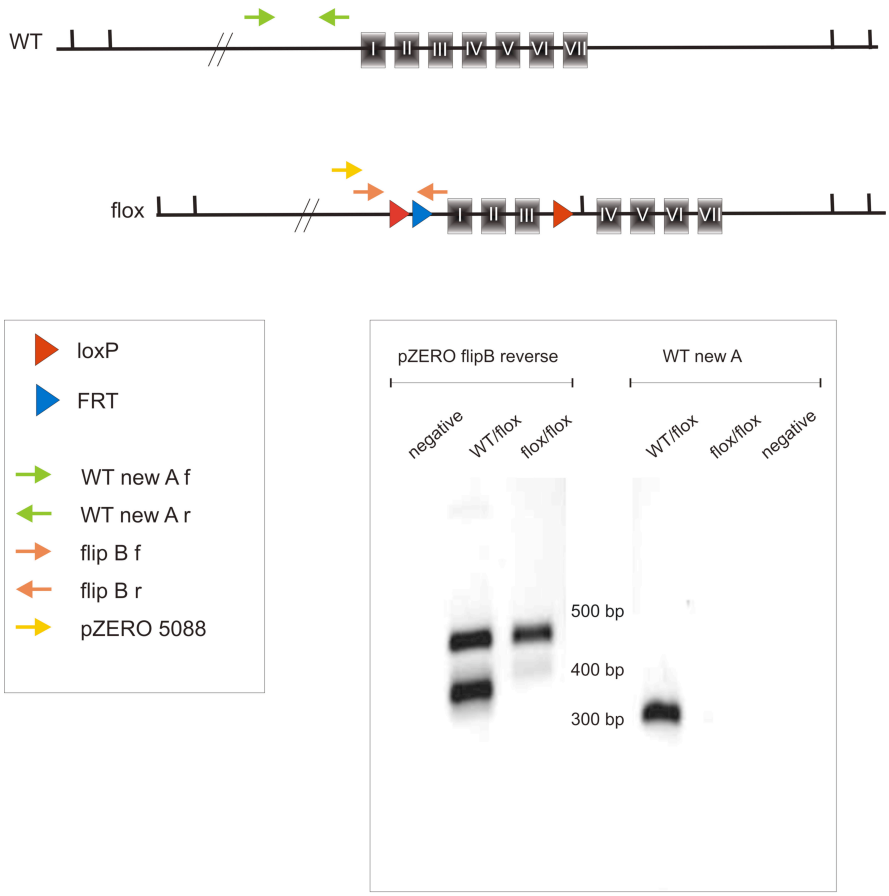

Figure 3.46. **Genotyping of flox/ WT or flox/ flox mice**. The WT allele is detected as described for the neo/ WT mice above. Two possible primer pair combinations detect the floxed, flipB (shown in orange) or pZERO 5088 (yellow) and flip B r (orange). In both cases, the forward primer binds upstream of the 5'loxP site, the reverse primer downstream of the residual FRT site. Genotyping of the heterozygous mouse resulted in a band at 265 bp for the WT allele and 332 bp for the floxed allele for the primer combination pZERO 5088 and flipB r. For the flox/ flox mouse, where the WT allele is missing, only a band at 332 bp can be seen in the agarose gel. The heterozygous flox/ WT DNA led to a band of 325 bp in the WT PCR.

This was again tested with the WT PCR primer pairs (green arrows in Figure 3.46). The deletion of the neo cassette was detected with two different primer combinations (yellow and orange in Figure 3.46). In both cases, the reverse primer flip B reverse binds behind the residual 5' FRT site, the forward primers, either pZERO 5088 or flip B forward, bind in front of the 5'loxP site. The flip B primer pair leads to a fragment of 2011 bp if the loxP site is not excised, of 265 bp in the WT and of 332 bp in the floxed situation. The binding of the pZERO 5088 as forward primer and flip B reverse lead to fragments of 2148 bp for neo-mice, 378 bp

for WT mice and 446 bp for floxed mice. The agarose gel in Figure 3.46 shows the genotyping of a WT/ flox and a flox/ flox mouse with the WT primer pair and the pZERO 5088 flip + B reverse. In case of the heterozygous floxed mouse, the pZERO 5088 + flip B PCR leads to a fragment of 378 bp, representing the WT allele and of 446 bp for the floxed allele. The genotyping of homozygous flox/ flox mouse shows a band of the floxed allele at 446 bp. The WT PCR lead to a DNA fragment of 325 bp for the flox/WT mouse while the primer can not bind in case of the flox/ flox mouse.

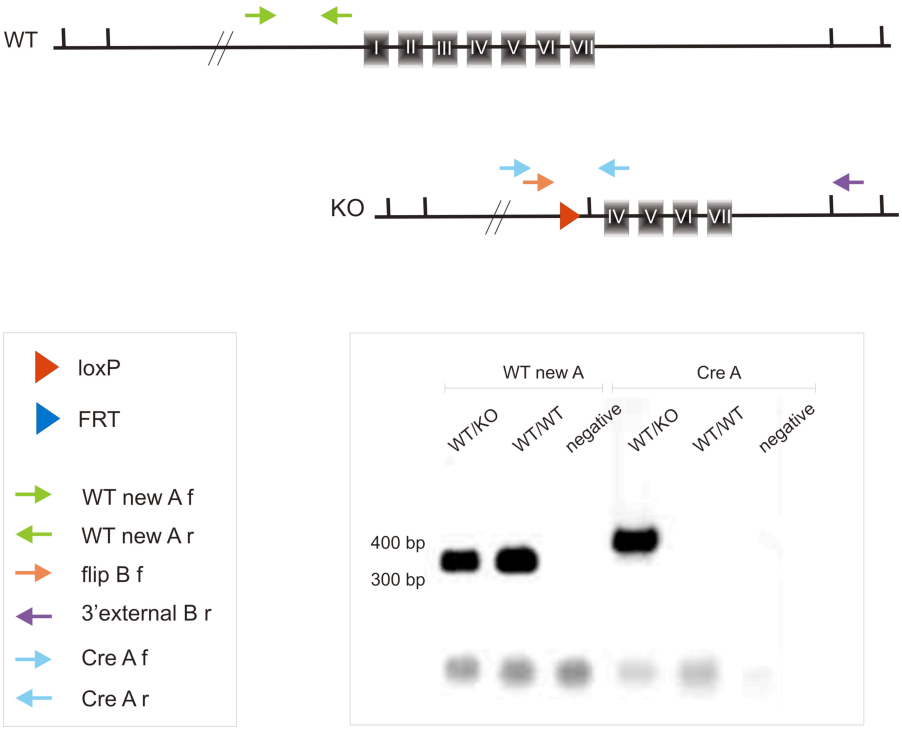

Figure 3.47. **Genotyping of KO/ WT or KO/ KO mice.** One internal and one external primer pair can detect the knockout. The internal pair, Cre A, flanked the residual loxP and EcoRI restriction site (light blue), the forward primer for the external PCR binds in front of the loxP site (flip B f), the reverse primer (3'external B r) behind the 3'homology. The genotyping PCR Cre A leads to a knockout fragment of 423 bp as shown in the agarose gel, the WT PCRs results in a band of 325 bp.

Induction of the KO by breeding of founder mice with PGK-Cre deleter leads to the excision of the first three exons. The detection of the WT allele was again performed with the WT primer pair (green in Figure 3.47). The KO allele was either analyzed with an internal primer pair, Cre A (shown in light blue), where the forward primer binds in front of the residual loxP site and the reverse primer behind the additional induced EcoRI restriction site. In the WT situation, this would lead to a fragment of 2138 bp, 3949 bp for the neo and 2232 bp for the floxed allele. The KO leads to a band of 423 bp. The external primer binding pair comprising flip B forward (shown in orange) and 3'external B reverse (shown in lilac) would result in 3862 bp for WT, 5672 bp for neo and 3974 bp for flowed mice. The KO can be detected with a band of 2146 bp. The agarose gel in Figure 3.47 shows the genotyping PCR performed with the Cre A primer pair and the WT PCR. Heterozygous KO mice exhibited a band at 423 bp

for the KO and at 325 bp for the WT allele. In case of the WT mouse, only a band of the WT primer pair at 325 bp can be detected.

3.3.6.2 Genotyping via Southern blot

The genotypes of the first heterozygous KO mice were also confirmed by Southern blots. Because the Southern blot probes bind outside of the homologous region, bands of the right size in the blot would confirm successful integration of the targeting vector at the correct chromosomal locus. Extraction of DNA from mouse-tails led to very small and impure amounts of DNA. Therefore, small pieces of ear from ear clipping where used for the generation of murine adult fibroblasts (MAFs) from which high amounts of pure DNA could be generated

Figure 3.48 shows the Southern blot of MAFs generated from three WT mice and one heterozygous KO mouse that were incubated with 3' and 5'external probes.

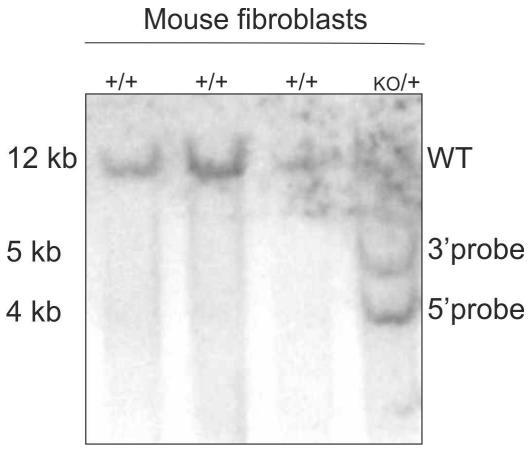

Figure 3.48. **Southern blot of MAFs confirmed successful induction of the KO.** Fibroblasts were generated from heterozygous WT/KO mice and used for Southern blotting. Incubation with the 3' and 5'probes resulted in the WT band at 12 kb. The 3'probe detected the KO allele at 5 kb, the 5'probe at 4 kb.

The WT allele is represented by a band of 12 kb, present in all animals. In case of the KO, the 3'probe bound at 5 kb. As can be seen in the cloning strategy, the 3'probe always detects a fragment of 5 kb, independent of neo, floxed or KO mice. Recombination of the loxP sites takes place in the 5'homology region (Figure 3.32). Therefore, the 5'probe binds fragments of different sizes, depending on the genotype. In case of neo mice, a DNA fragments of 8 kb, at 6 kb in floxed mice and at 4 kb in the KO situation can be detected, as shown here (Figure 3.48).

3.3.6.3 Results from the mouse breeding

As described above, the founder mice were bred to result three different breeding strains. Neo/ WT and flox/ WT mice were mated with each other to receive homozygous mice and were also backcrossed into pure C57BL/6JOlaHsd background. PKG-Cre deleter mice were used to induce the knockout. Heterozygous KO mice were healthy and showed a normal phenotype with healthy looking coat and eyes. The protein expression of CD2BP2 was not altered when compared to WT littermates as can be seen in Figure 3.49. Here, a Western blot is shown deriving from cell lysates of thymus, spleen, bone marrow and lymph nodes from 5 weeks old WT/ KO and WT mice. The immunoreactive band against CD2BP2 shows the same intensity in heterozygous KO mouse when compared to WT littermate controls.

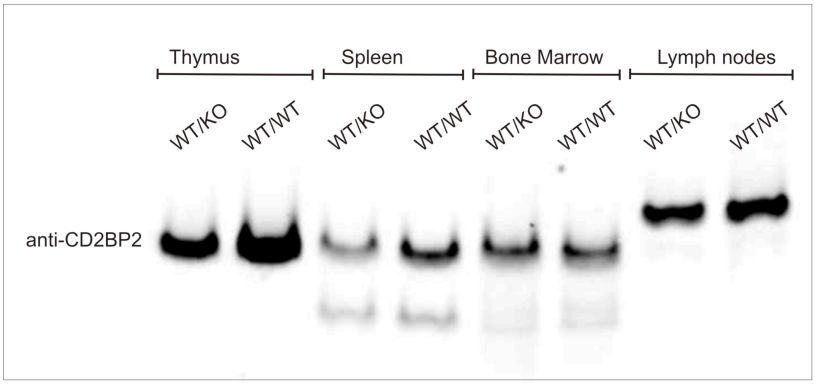

Figure 3.49. **Protein levels of heterozygous CD2BP2 KO mice is comparable to WT mice**. Same amount of cell lysate from thymus, spleen bone marrow and lymph nodes of WT and WT/ KO mice were tested in Western blot for protein expression level of CD2BP2. The expression of CD2BP2 is not altered in WT/ KO mice compared to WT littermates.

Heterozygous KO mice were crossed with each other to receive CD2BP2 null mice. So far, 23 breedings have been analyzed by genotyping PCR but no homozygous KO could be detected. The litters of nine breeding pairs were genotyped, resulting in 54 WT, 91 heterozygous but no homozygous offspring as shown in Table 3.3. The table shows the dates of birth of the offspring and the number of the father (male) and mother (female). In case of one to two breedings, two mothers are listed. The breeding with the buck number 5951 and the females 5953 and 5952 gave birth to 9 litters, which represented at least four generations from one female. No homozygous KO was born from this mating. To find the reason for no homozygous KO mouse alive, the offspring was monitored during embryonic development. Therefore, time matings were set up.

Date of Birth	**male**	**female**	**WT**	**WT/ KO**	**KO/KO**
20110312	5951	5953/ 5952	1	1	0
20110316	5951	5953/ 5952	2	2	0

20110402	5951	5953/ 5952	2	3	0
20110405	5951	5953/ 5952	3	3	0
20110520	5951	5953/ 5952	4	5	0
20110610	1284	1294	2	5	0
20110627	1333	1297	3	4	0
20110709	1284	1294	3	4	0
20110703	1334	1328	3	4	0
20110630	5951	5953/ 5952	0	4	0
20110707	5951	5953/ 5952	2	4	0
20110707	1334	1328	3	4	0
20110714	1285	1288/ 1282	5	3	0
20110723	1285	1288/ 1282	1	4	0
20110724	1333	1297	2	6	0
20110802	1428	1403	0	3	0
20110803	1389	1386/ 1384	4	5	0
20110803	1335	1340/ 1339	2	6	0
20110812	5951	5953/5952	0	3	0
20110905	1577	1297	5	3	0
20110922	5951	5953/5952	3	5	0
20110914	1428	1283	3	4	0
20110928	1577	1297	1	6	0
Total number of mice			**54**	**91**	**0**

Table 3.3. **23 heterozygous KO breedings led to 54 WT and 91 WT/ KO offspring but no homozygous KO mouse**. The left column represents the date of birth of the offspring, followed by the record number of the father and mother. In case of one to two breeding, the numbers of both potential mothers are shown.

3.3.6.4 Timed mating of heterozygous KO mice

In timed matings, the morning after positive vaginal plug is counted as embryonic day (E) 0.5. Several pregnant mice starting from E16.5 were analyzed considering the health status of their offspring. Each mouse carried healthy and dead embryos. One exemplary mouse at E11.5 is shown in Figure 3.50. Nine embryos could be detected in the uterus of the mouse. Six of them were nicely developed whereas three were hemorrhagic and resorbed (as shown by the arrows in Figure 3.50. A). Healthy embryos were supplied with several blood vessels coming from the mother in contrast to the resorbed ones, where only thin vessels were remaining. All

embryos were genotyped by PCR as shown by the agarose gel in Figure 3.50 B. The healthy offspring were either heterozygous (3) or WT (3) while all resorbed embryos were genotyped as KO. Embryos analyzed at E10.5 showed growth retardation but were not hemorrhagic yet. These data speak for embryonic lethality of CD2BP2 null mice between before E10.5.

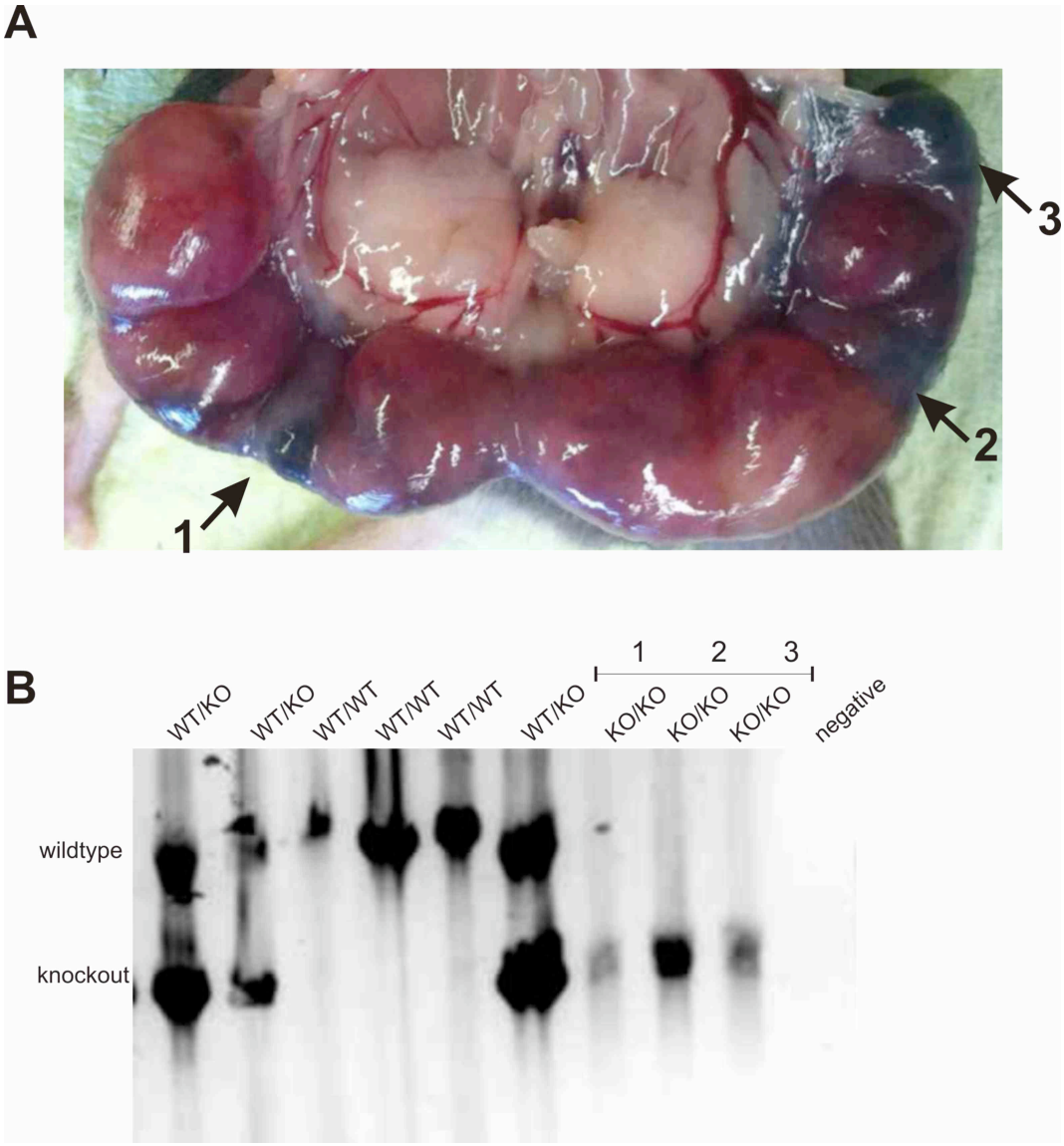

Figure 3.50. **KO of CD2BP2 leads to embryonic lethality**. Nine embryos were present in the mouse; three of them were hemorrhagic and resorbed (marked with arrows in A). The genotyping PCR in B shows that the genotype of the healthy offspring was either WT or WT/ KO while the resorbed embryos showed only the knockout band.

4 Discussion

This study investigates the two GYF-domain containing proteins CD2BP2 and GIGYF2. While the function of the Smy2-type GYF-domain containing protein GIGYF2 was largely unknown at the beginning of this study, this work revealed potential involvement of the protein in SGs and COPII vesicles in human and mouse cells. CD2BP2 is involved in immune system and splicing. Here, a more detailed analysis of its immune-related function was performed. Also, the generation of CD2BP2 null mutants was supposed to address the questions of whether mice can live without CD2BP2. Timed matings of heterozygous KO mice showed embryonic lethality of CD2BP2$^{-/-}$ mice before embryonic day 10.5.

GYF-domains are small adaptor domains that interact with proline-rich sequences of other proteins present in most eukaryotic species. Two subfamilies of GYF-domain proteins can be distinguished. The Smy2-type family has an aspartate at position 22 of the GYF domain, whereas the CD2BP2-type subfamily consists of a tryptophan at this position. Also, the loop between the β1 and β2 sheet of the GYF-domain is shorter in the Smy2-type than in the CD2BP2-type subfamily. The CD2BP2-type subfamily preferentially binds to the consensus sequence PPGW but also recognizes positively charged residues flanking the PPG core (x x PPG x (R/K)) [6, 22]. The Smy2-type family prefers ligands with the consensus motif PPGΦ (Φ any hydrophobic AA except for tryptophan). Several motifs in close proximity (maximum of 40 AA) compensate for low binding by avidity. [22, 26].

4.1 Potential Functions of GIGYF2

The Smy2-type protein GIGYF2 was found in a genome wide search for novel GYF-domain containing proteins. The relaxed consensus motif (PPG (AEFHILMSTWY)) deriving from phage-display experiments was identified in the genome of GIGYF2. In subsequent screens with GIGYF2 as bait potential interaction partners were found. Deduced from functions of the interaction partners, a potential role of GIGYF2 in mRNA splicing in the nucleus was speculated [6].

4.1.1 GIGYF2 localization in cell lines and mouse organs

Cell separation analyses performed in this study showed GIGYF2 in the cytoplasm of human HeLa cells and rat pc12 cells (Figure 3.2), contradicting the previous assumption of a nuclear localization of GIGYF2. These experiments were made possible by the generation of a polyclonal antibody against the GYF-domain of GIGYF2. The antibody is, to my knowledge, the first antibody generated against GIGYF2 working in Western blot and immunofluorescence analyses. The specificity of the antibody was confirmed by Western blot analyses in combination with overexpression and knockdown studies. Also, the antibody

precipitated endogenous GIGYF2 from cell lysate (Figure 3.1), which was confirmed by mass spectrometry, thereby showing the specificity of anti-GIGYF2.

To get an impression of the distribution of GIGYF2 in living organisms, mouse organs were analyzed with respect to their expression of GIGYF2. Western blots of the urinary system, liver, brain, kidney, spleen, lung, lymph node, heart, thymus and uterus of BL6 mice showed the presence of GIGYF2 in all organs with lowest expression level in kidney (Figure 3.3). The ubiquitous expression in mouse organs speaks for a general function of GIGYF2 in adult mice. Further analyses should address the upregulation of GIGYF2 during embryogenesis to delineate for which developmental state the protein is of importance.

4.1.2 **Potential interaction partners of GIGYF2**

Pull-down studies in combination with SILAC-MS with the GYF-domain of GIGYF2 were performed to screen for new interaction partners. The pull-down experiments were performed either in the presence (non-labeled lysate) or absence (^{13}C-arginine/^{13}C lysine labeled lysate) of competitive peptides competing for the PRS-binding site (see Method part). These two modes allowed the identification of binding partners that specifically bind the PRD of GIGYF2. Proteins with high enrichment factors were chosen for subsequent functional analyses (Figure 3.4).

4.1.2.1 GIGYF2 and COPII vesicular transport

COPII vesicles are small membrane vesicles that allow the transport of cargo proteins to their specific destination. The folding of newly synthesized proteins takes place in the ER, which is the starting point of the secretory pathway. From here, COPII vesicles transport proteins to the Golgi and other donor organelles [121]. The complex contains of five core components, Sar1p [122] and the two subcomplexes Sec23/ Sec24 and Sec13/ Sec31 [123] but other protein beside the core components are necessary for correct COPII transport *in vivo*. The core components of COPII-vesicles, Sec24, Sec31 Sec 13 and Sec24 were highly enriched in pull-downs performed with cyoplasmic HeLa lysate. Sec24 and Sec31 contain two and one Smy2 type-binding motif, respectively, whereas Sec13 and Sec23 lack of any consensus motif [26]. Therefore, we conclude a direct binding of GIGYF2 to Sec24 and 31 and an indirect recruitment of their interaction partners Sec23 and 13 (Figure 3.4). These assumptions were further analyzed in immunofluorescence studies with endogenous or overexpressed proteins.

Live cell images performed in HeLa cells showed the localization of overexpressed GIGYF2 to ER and Golgi. Moreover, endogenous GIGYF2 and the COPII component Sec31 co-localized in the cytoplasm of fixed HeLa cells, supporting the potential interaction of GIGYF2 with COPII vesicles members and an involvement of GIGYF2 in the COPII mediated vesicular transport.

The yeast ortholog of GIGYF2, Smy2 was found as genetically high copy suppressor of mutations in the multivalent cargo adaptor protein Sec24p. Sec24-20 mutations lead to blockage of ER to Golgi transport, caused by defects in COPII vesicle formation. Smy2 could be detected on the membrane of the ER [133, 134]. Pull-down experiments with Smy2 did not enrich any COPII-proteins, questioning the function of the Smy2 protein in vesicular transport [26]. Smy2 and GIGYF2 share no common features except the Smy2-type GYF domain. It is therefore likely that the two proteins are involved in different cytoplasmic functions and the GYF domain of GIGYF2 seems to be important for the interaction with COPII proteins. This assumption is strengthened by the direct interaction of GIGYF2 with Sec13, Sec23. Still, it is not clear whether GIGYF2 is involved in the formation of the complex or if it rather is important for the stable transport of folded proteins. This needs to be addressed in future studies.

4.1.2.2 GIGYF2 and stress granule formation

Previous studies showed the co-localization of the yeast protein Smy2 with the P-body marker DCP2 [87]. Further P-body markers such as XRN1 and CCR4 could be detected in Smy2 pull-down experiments, speaking for a function of Smy2 in these cytoplasmic granules [26]. GIGYF2-GYF as bait did not co-precipitate any members of the P-body family but several proteins that serve as stress granule (SG) markers. TNR6B, PABP-1, SMN and FXR1 were all found as highly enriched proteins and are well-known members of SGs. SGs are cytoplasmic foci that form upon stress in contrast to P-bodies that are more constitutively present within the cell. Both granules exchange and share common proteins. However, P-bodies contain deadenylated mRNA and proteins involved in the deadenylation process whereas SGs consist of polyadenylated transcripts and translation initiation factors [113]. Immunofluorescence studies could show that GIGYF2 and the SG marker TIA-1 co-localize in HeLa cells upon treatment with arsenite (Figure 3.9). These data support the idea of an involvement of GIGYF2 in SG formation in human HeLa cells.

4.1.2.3 GIGYF2 in the neuronal system

The data published by Ash et al in 2010 have been restricted to human cervix carcinoma cells [26]. Results from other studies linked GIGYF2 to a function in neuronal cells. The role of GIGYF2 as candidate gene of PDs remains much in question; still, GIGYF2 knockout mice show a late onset neurodegenerative phenotype [86]. Atrophin-1, SMN and FXR-1, proteins that were highly enriched in the GIGYF2 pull-downs, are also involved in neurodegenerative diseases. Pathological expansion of polyglutamine (polyQ) repeats in Atrophin-1 lead to the neurodegenerative disease Dentatorubral-pallidoluysian atrophy (DRPLA) [192]. Also, FXR-1 form mutants with pathological expansion of CAG or CGG repeats leading to triple repeat

disorders [193]. SMN is the gene causing Spinal Muscular Atrophy (SMA), an autosomal recessive degenerative disease [194]. Therefore, the analyses performed in HeLa cells previously were repeated in neuronal cell lines. As shown in Figure 3.10, GIGYF2 also localizes to the Golgi and endosome, another compartment involved in vesicular transport, in mouse Neuro2a cells. So the involvement of GIGYF2 in COPII transport is also likely in neuronal cells. Cells from the human neuronal cell line SH-SY5Y were analyzed considering the co-localization of GIGYF2 and TIA-1 upon treatment with arsenite. Figure 3.13 shows the stress induced merge of GIGYF2 and TIA-1 in the soma and neurites of SH-SY5Y cells. These data show for the first time the presence of GIGYF2 in neurites and its co-localization with the SG marker TIA-1 in these cells.

The transport of mRNA to local compartments within cells serves as a mechanism to induce and maintain cell polarity. Also, local and temporal control of protein expression allows rapid responses to physiological changes within the cell. Ribonucleoprotein (RNP) complexes are known as functional units in primary neurons that form in the cell soma and are transported motor- protein dependent to destinations like synapses or growth cones. The composition of these RNPs is a mixture of mRNAs and two different kinds of proteins. The one class of proteins is necessary for RNP transport; the second class is involved in temporal translational repression of mRNA. SMN and FXR-1 have been described as proteins involved in mRNA transport and local translation of mRNA [195]. SMN is present in RNPs that transport β-actin mRNA from motor neuron soma to growth cones. Low levels of SMN lead to low levels of local β-actin mRNA expression [196]. FXR-1 is involved in activity-regulated localization and translation of mRNA in dendrites and synapses [197]. Several kinds of RNP granules involved in these transport and regulation mechanisms seem to exist but a detailed understanding of their unique characteristics is still missing.

SGs are also present in primary neuronal cells. Treatment of rat spinal cord neurons with arsenite induced SG formation in soma and neurites. The induction of stress led to the accumulation of mRNA in SGs that was evenly distributed throughout the cell before treatment [198], proving the active transport of mRNA upon cellular changes. SMN, FXR-1 and several other SG proteins could also be found in such SGs in neuronal cells [195]. These data raise the question of whether SGs could serve as temporal or local storage compartments of mRNA that form upon changes of the cellular state and thereby prevent unintentional protein translation.

The presence of GIGYF2 in TIA-1 containing cytoplasmic granules in SH-SY5Y cells speaks for the localization of GIGYF2 to SGs in neuronal cells.

Interactions of GIGYF2 with proteins involved in vesicle transport, mRNA binding and proteins present in cytoplasmic granules make a role of GIGYF2 in mRNA transport or regulation likely. Direct mRNA binding could not be shown yet but needs to be addressed in future studies. A role of GIGYF2 in RNP complexes in neurons, together with SMN, FXR-1, could be envisioned. Mutations in these transport mechanisms could result in

neurodegenerative disease similar to the ones already described for Atrophin-1, SMN and FXR-1.

Also of interest is the assembly of these RNP complexes. The GYF-domain is the best-characterized domain of GIGIYF2 but whether it is involved in potential mRNA recruitment or mediates the interaction with other proteins is unclear. The polyQ repeats of the translational repressor protein Pumilio 2 can induce SG formation in neuronal cells [199]. Beside GIGYF2, the SG components TIA-1, FXR-1 and Atrophin-1 also contain polyQ repeats. It is therefore likely that the glumatine repeats rather than the GYF-domain mediate interactions of GIGYF2 with other components of cytoplasmic RNP granules.

The Smith lab created a GIGYF2 knockout mouse from a gene trap vector. Analysis of these mice showed that lack of feeding led to death of GIGYF2 null mice within the first couple days after birth. Heterozygous mice showed a mild late onset motor neuron degenerative phenotype [86]. This phenotype lacks any linkage to PDs and makes the involvement of GIGYF2 in these diseases very unlikely. Motor neuron diseases have also been described in SMN mouse models. It would be therefore rather likely that the GIGYF2 gene is involved in other neurodegenerative diseases that lead to motor neuron degeneration or phenotypical changes as seen in patients with triple repeat disorders. Drawing such a link at this state of knowledge seems quite speculative but is meant to push the focus away from the involvement of GIGYF2 in PDs.

Together, this study could show the interaction of GIGYF2 with proteins involved in COPII complex formation and SG formation. With this data, a potential role of GIGYF2 in the transport and regulation of RNP complexes in neuronal cells is suggested. Future studies need to address the question of whether GIGYF2 plays a role in temporal repression of mRNA or in assembly of these RNP complexes. The disease-related role of GIGYF2 remains unresolved. Deletions of the protein seem to be rather related to motor neuron dysfunctions than abnormalities in the substantia nigra leading to PDs.

4.2 Characterization of CD2BP2

CD2BP2, the first GYF-domain containing protein discovered was found in a screen of an activated T cell library, interacting with the cytoplasmic tail of the CD2 adhesion molecule [3]. Further analyses showed a nuclear localization of the protein in human HeLa cells and a role in mRNA splicing [4, 58]. CD2BP2 could be detected in the U5 snRNP at early stages of splicing assembly but not at later stages of the cycle, when the catalytic excision of introns takes place.

In this study, the focus was on the involvement of CD2BP2 in the immune system. Because cell lines provide limited insights into the communication between immune cells, experiments were shifted to the mouse model.

4.2.1 **Generation of anti-CD2BP2 antibody**

A detailed analysis of CD2BP2 required sufficient amounts of antibodies. Therefore, new anti-CD2BP2 needed to be generated. Expression of human CD2BP2 in *E. Coli* led to instable protein so the expression was performed in eukaryotic Sf9 insect cells. Two animals where immunized with his-tagged CD2BP2. The Western blot in Figure 3.16 summarizes the immunization. Western blot analyses showed that the pre-immune serum detected a pronounced immunoreactive band at 30 kD. Since the pre-immune serum was extracted before immunization with CD2BP2 protein, this band derives very likely from another protein and is therefore unspecific. Housing of the rabbits under non-specific pathogen free conditions likely explains this contamination. After the first immunization (boost), the unspecific band became more enhanced, probably because of the overall induction of the immune system. This might also explain why increasing numbers of immunization led to new unspecific bands. Additional immunoreactions with his-tagged CD2BP2 led to an enhancing immuoreactive band at the height of 52 kD, very likely representing CD2BP2. Serum of the third immunization mostly detected this band at 52 kD but the unspecific band from the immune serum was still present. Therefore, the antiserum was purified with his-tagged CD2BP2 protein. This purification not only removed unspecific antibodies from the serum but also generated a polyclonal antibody that specifically recognizes CD2BP2. Successful purification can be seen in the last lane in Figure 3.16. The antibody exclusively detects CD2BP2.

4.2.2 **Different expression of CD2BP2 on mRNA versus protein level**

Expression levels of CD2BP2 on mRNA and protein were examined to get a fist indication of a possible organ related function of CD2BP2 in adult mice. The analysis of adult (10 weeks of age) BL6 mice showed ubiquitous expression of CD2BP2 on mRNA level with no sex-specific differences. All mRNAs ranged between cycle 26 and 28. At the protein level, the expression was restricted to hematopoietic cells, thymus, lymph nodes and spleen, the reproduction system, and the lung (Figure 3.18). Comparing the expression of CD2BP2 on mRNA and protein level showed differences in the expression pattern. The ubiquitous expression of CD2BP2 mRNA did not correspond to the mainly immune organ-restricted expression of the protein. We focused on comparing organ-to-organ differences on mRNA versus protein level. For example, the mRNA expression of CD2BP2 was higher in brain than in spleen but on the protein level, the expression was inverted with high expression in spleen and very low expression in brain (Figure 3.18). These results speak for post-transcriptional regulations of CD2BP2 in mouse organs. Two of the three splicing variants of CD2BP2 have long 3'UTRs (Figure 3.31). It is very likely that this region is the acting point for regulatory mechanisms. Several seed regions for miRNA-mediated regulation could be detected but

more detailed studies are necessary to understand the mechanism by which the regulation takes place.

The study was performed in non-perfused animals. Because of an immune-related function of CD2BP2 we expect it to be expressed in blood cells. Therefore, it is likely that CD2BP2 expression of some organs shown in the Western blot derive from contaminating blood and not the organ itself. This scenario is quite likely in the lung. Future experiments should be performed with perfused animals to circumvent this background noise.

4.2.3 **Widespread expression of CD2BP2 in murine immune cells**

4.2.3.1 CD2BP2 expression studies in sorted immune cells

In preceding studies, immune cells were analyzed considering their expression of CD2BP2. For a first impression, cells from thymus, spleen and lymph node of BL6 mice were sorted with antibodies against lymphoid and other immune cells. Western blots performed with lysates from the sorted cells were analyzed upon expression of CD2BP2. It could be shown that CD2BP2 is expressed in CD4 and CD8 expressing T cells in thymus and spleen and in splenic B cells. Macrophages, dendritic cells and other myeloid cells showed no immunoreactive band against CD2BP2 (Figure 3.19). This can either be due to a lack of expression of CD2BP2 in these cells or the amount of cell lysate loaded was below the detection limit of Western blot analyses. Since intracellular stains showed the presence of CD2BP2 in dendritic cells and macrophages (see next paragraph), the limitations of FACS sorting followed by Western blot analyses can be seen here. The concentration of T and B cells in thymus and spleen is much higher than for dendritic cells and macrophages in healthy animals. Several animals have been pooled and enough dendritic cells were counted in the cytometer but the final volume of the sorted cells was too high for direct cell lysis. Therefore, the cells had to be concentrated by several centrifugation steps. Here, too many cells were lost so that the final protein concentration was below the detection limit for Western blot analyses. Efficient analyses of the expression level of CD2BP2 in these cells was therefore only possible with intracellular stains of fixed cells, which was performed next.

4.2.3.2 Characterization of the polyclonal anti-CD2BP2 antibody

In first experiments with fixed cells, CD2BP2 was stained extracellular. Since no extracellular expression of CD2BP2 could be measured, all subsequent expression analyses were performed in permeabilized cells. Intracellular stains of immune cells allowed the analysis of CD2BP2 expression in minor cell populations, during different developmental stages and the detection of cells that did not express CD2BP2. Specific intracellular binding of the polyclonal anti-CD2BP2 antibody was demonstrated by competition experiment. His-tagged CD2BP2 protein but not the negative control BSA could capture anti-CD2BP2 antibody and

thereby prevent its binding to immune cells (Figure 3.20). Since the antibody was purified with his-tagged CD2BP2, a specific binding was expected. What cannot be ruled out though is unspecific binding of the antibody to proteins with similar binding epitopes. Such an unlikely scenario can not easily be ruled out. The best negative control would be CD2BP2 expressing immune cells that are depleted of CD2BP2, as it would be the case in $CD2BP2^{-/-}$ mice. Since such cells do not exist yet, this experiment is the best approach to show the specificity of the polyclonal rabbit anti-CD2BP2 antibody.

Titration experiments in cells from lymph node, spleen and thymus were performed to determine the optimal staining concentration of the antibody. In all cells, a dilution of 1:100 showed a clear shift in the histogram in contrast to the anti-rabbit isotype control. Therefore, this concentration was applied in subsequent experiments.

4.2.3.3 Expression of CD2BP2 in intracellular flow experiments

Intracellular flow cytometric experiments showed the presence of CD2BP2 in $B220^+$ and $CD19^+$ cells in bone marrow, spleen and lymph nodes. $CD4^+$ and $CD8^+$ T cells in thymus, spleen and lymph nodes also expressed CD2BP2. Macrophages and NK cells isolated from the spleen showed the expression of CD2BP2 in contrast to the isotype control. Subsequent studies in developing T cells were performed to see at which stage CD2BP2 is upregulated. CD2BP2 was present in all CD4/ CD8 single and double positive states and the majority of cells in the $CD4^-$ $CD8^-$ state expressed CD2BP2. Only a small population here was negative for CD2BP2. In $CD4^-$ $CD8^-$ cells, CD2BP2 was present from double negative state 1 to 4. The summary of all these expressions is shown in Figure 3.30.

We tried to analyze the population of $CD2BP2^-$ cells in the DN staining shown in Figure 3.28. In addition to $CD4^-$ $CD8^-$ cells, γδ T cells were very likely present in this population. Since $CD44^+$ $CD25^+$ cells were positive for CD2BP2, γδ T cells were the only other cells that could be represented by the negative peak. We tried to confirm this assumption by extracting γδ T cells with a kit optimized for this extraction. Unfortunately, the cells extracted were not sufficient for further Western blot or flow cytometric analyses. Aβ versus γδ T cell commitment takes place during DN stages 1-4 of T cell development [200]. If the negative peak represents γδ T cells, then down regulation of CD2BP2 takes place in differentiated γδ T cells and not during T cell development. If the technical limitations avoiding the analysis of γδ T cells so far could be circumvented in future experiment, it would be very interesting too see if these cells downregulate CD2BP2 and why only this cell population does not require CD2BP2.

The data obtained from flow cytomteric analyses argue for a ubiquitous expression of CD2BP2 in mature lymphocytes and monocytes. Since the protein is down regulated in most of the other organs in adult mice, the function of CD2BP2 seems to be restricted to the immune system. The ubiquitous expression here points out its relevance in these cells. The

presence of CD2BP2 during early T cell development speaks for a functional relevance of the protein during T cell maturation.

CD2BP2 was first discovered as intracellular binding partner of the cytoplasmic domain of the CD2 adhesion molecule. CD2 is upregulated in the late DN stage of T cell development [1]. Since CD2BP2 is already present in the DN1 stage, the protein seems to fulfill a CD2 receptor independent function at least in the earliest stage of T cell development in mice. To analyze the presence of CD2BP2 in developing B cells or earlier stages of hematopoiesis would be of interest as well but is technically challenging. Staining and permeabilization of these cells is not possible. Deletion of CD2BP2 in these cells could circumvent the technical limitations and help to see if that influences the maturation of B and T cells.

The restricted expression of CD2BP2 at the protein level to mostly immune-related organs seems to contradict the function of CD2BP2 in ubiquitous mRNA splicing. Also, immunofluorescence stains in human HeLa cells showed a nuclear localization of the protein while the CD2 binding is expected to take place at the inner side of the plasma membrane [51].

While CD2BP2 might not play a constitutive role in mRNA splicing it might have gained a specialized function in organ-specific or alternative splicing. Various cells in the immune system use alternative splicing to adapt to an ongoing immune response. The B cell specific class switch from IgM to any other immunoglobulin is dependent on alternative splicing [201]. Also, recent studies showed that IL-23, expressed from dendritic cells to induce Th17 cells, consists of several splice variants [202]. A potential involvement of CD2BP2 in these immune-specific alternative splicing events could explain its restricted expression in immune cells and need to be addressed in future studies.

Human and mouse CD2BP2 contains several known serine phosphorylation sites [203-206]. One likely scenario would be that the stimulation of cells lead to post-translational modifications of CD2BP2 and induces changes in its cellular localization. This has been described for other proteins before. Beta-catenin transfers from the cytoplasm into the nucleus upon serine phosphorylation [207]. Stability of β-catenin is dependent on N-terminal phosphorylation. CD2BP2 cannot be functionally expressed in *E. Coli* cells but in eukaryotic insect cells that allow post-translational modifications to occur. A similar scenario as for β-catenin could be envisioned for CD2BP2. Unpublished analyses confirmed serine phosphorylations in insect cells expressing his-tagged versions of CD2BP2. The dual specificity kinase PRP4 was found to phosphorylate 102K in the nucleus of HeLa cells. It is well conceivable that this kinase does not only phosphorylate 102K but also its direct interaction partner CD2BP2. If such phosphorylations would induce a change in localization or rather control splicing-related functions of CD2BP2 needs to be analyzed further.

So far, analyses of the expression pattern of CD2BP2 have been restricted to born mice. It may well be that the protein has important functions in other organs during embryonic

development but is down regulated after fulfillment of the maturation dependent purpose. In adult mice, the function seems to be restricted to the immune system; since CD2BP2 is not present in other organs at the protein level. Since mRNA is present in all organs analyzed, it is likely that protein translation is down regulated at some point during development and could potentially be up-regulated again in certain tissues.

4.2.4 **CD2BP2 mouse model**

Localization and expression studies performed in cell lines and mouse organs showed non-uniform patterning of CD2BP2. Studies in HeLa cells suggested that the protein is involved in the splicing cycle that takes place in the nucleus of all cells. Expression studies found CD2BP2 almost exclusively in hematopoietic organs of adult mice. A detailed characterization revealed a very early upregulation of CD2BP2 during T cell development and a ubiquitous expression in macrophages, NK cells and developing and mature lymphocytes. We were wondering of whether mice would survive without CD2BP2. This question was addressed with the generation of a conditional CD2BP2 KO mouse. We decided for a conditional KO system with respect to long-term analyses in organ-specific and temporal knockouts that would consider the functional properties of CD2BP2 in splicing and the immune system in more detail.

4.2.4.1 Cloning of the CD2BP2 targeting vector

A cloning strategy of the targeting vector was selected in which a neo-cassette, serving as positive selection marker, was cloned in front of the first exon. One loxP site was positioned upstream of the selection marker, the second one including an additional EcoRI restriction site behind the third exon (Figure 3.32). Cre-expression would induce the deletion of the first three exons including the start codon. We were aware of the potential drawback of this targeting strategy, in that additional start codons could lead to truncated but partially active protein, the sparseness of endogenous restriction sites excluded any other cloning strategy. Also, it was known that full length CD2BP2 is very unstable itself *in vitro* so it was speculated that truncated forms would not be functional either. All of the three known splicing variants of CD2BP2 would be affected by deletions of the first three exons since they differ in the length of the 3'UTR (Figure 3.31).

Several cloning steps and helper vectors were necessary to clone the final CD2BP2 knockout vector. In particular, the introduction of the 3'loxP site was challenging and several approaches failed until the cloning succeeded. At the end, an additional cloning step via a helper vector found to be necessary. The loxP oligomer was ligated blunt-ended into this vector. From here, the HpaI restriction sites that were added at both ends of loxP site could be easily approached by restriction enzymes resulting in clean blunt ends. The cloning of the 5'

and 3'homology was also performed in a helper vector. In the final cloning step, both homologies were cloned into the vector pPNT4 that already contained the neo- and TK cassette and the 5'loxP site in its backbone (Figure 3.38).

The functionality of loxP sites is essential for successful recombination at both sides. Several factors can minimize excision efficiency such as the distance between loxP sites and the probability of DNA secondary structure formation. The functionality of the two loxP sites of the CD2BP2-pPNT4 vector were tested by its expression in bacterial cells that inducibly produce the Cre-recombinase. As shown in Figure 3.39, the loxP sites of CD2BP2-pPNT4 successfully recombined *in vitro*. This experiment proved the efficient recombination of loxP sites but could not exclude that an odd chromosomal locus of the floxed gene precludes gene excision.

4.2.4.2 Murine Stem Cell Analyses

The final CD2BP2-pPNT4 vector was linearized and electroporated into 129 and BL6 derived ES cells. This step is very critical for the success of targeted mouse mutations. Mishandling of ES cells or technical mistakes during the electroporation process can impede germline transmission of the targeted gene. Morphological abnormalities of ES cells do not correlate with the likeliness of germline transmission. Because several months can pass between electroporation and germline transmission, failure at this step may cost a lot of time.

Electroporation into ES cells of two different mouse strains was performed to benefit from both systems. 129-derived ES cells are known for their robustness and exhibit good germline transmission rates but 129 mice are poor breeders and show abnormal phenotypes (see introduction). Therefore, time consuming backcrossing into pure BL6 strains is necessary. Most of the BL6 ES cell lines electroporated so far showed low or no germline transmission. Generation of BL6 founder mice would save time and experiments with pure BL6 founder strains could be started immediately.

Southern blots were performed to screen for positive clones, meaning successful recombination of the targeting vector into the genome. As shown in the blot in Figure 3.41, the targeting vector was homologously recombined on one allele in the clones D12 and E12. The 3'external band therefore detected one additional band at 5 kb. This smaller fragment results from restriction digest with EcoRI, which leads to two instead of one gene fragment for the targeted gene because of the additional EcoRI restriction site downstream of the 3'loxP site. Since the 3'probe lies outside of the area of homologous recombination, the Southern blot confirmed the incorporation of the targeting vector at the correct chromosomal locus.

Positive recombination was also detected in the JM8 cell screens for clone A5, A7 and B11 (Figure 3.42). An additional, larger band could be seen in Clone A9, A10, B8, B10 and B12 in Figure 3.42. Here, it may well be that the 3'loxP site with additional EcoRI restriction site

did not integrate into the genome, so only the 5'part of the vector with neo-cassette was recombined, leading to a larger fragment.

Two rounds of electroporations have been performed for 129-derived ES cells. The only difference was the electroporation setup, as the first round was performed in an older version of the electroporation apparatus than the second. BL6 cells were electroporated with the new machine (eppendorf Gene Pulser # 165-2661). Homologous recombination rates were evaluated for 129-derived ES cells. The event of homologous recombination depends on the size of the recombination sites. The CD2BP2 targeting construct comprises a 5'homology region of 3724 bp and a 3'homology site of 3661 bp. Because of the large size good recombination rates were expected. As shown in Table 3.2, the efficiency of the first electroporation accounted for 1 positive clone out of 50 whereas in the second round, the success rate was one out of ten. Often, electroporation lead to one positive clone in 1000 so these rates were considered to be excellent. The electroporations were performed with a time lapse of four weeks. The exact same conditions of the ES cells can therefore not be guaranteed but major differences are very unlikely. Technical differences between the electroporation apparatuses might rather account for the different recombination efficiencies. Two positive clones from the first electroporation were injected into eight-cell stage embryos. Even though these clones derived high chimeric mice, no germline transmission was achieved. It is very likely that this derives from alterations in the karyotype, which has not been analyzed previously.

Mice deriving from JM8 implanted ES cells showed very low chimerism indicated by a mainly black coat color. This means that only few of the chimeric cells derive from the targeted gene. In this case, it is very unlikely that the targeted cells form germ cells and the probability of germline transmission is extremely low. Generation of founders was therefore unlikely and no further matings were set up with JM8 chimera. The efficiency of germline transmission of this newly generated JM8 cell strain has only been tested once before with ES cells that were not electroprated but injected directly without previous treatment. Obviously, the cells could not cope with the electroporation process and therefore failed in the process of germline transmission.

Two clones from the second 129-derived ES cell electroporation were injected into eight-cell stage embryos. The first litter resulted in 100 % germline transmission as can be seen by the agouti coat color of the offspring in Figure 3.44. Offspring without cells from the targeting vector would be of black coat color in line with the black coat color of the foster mother. This excellent germline transmission efficiency is due to an improved injection process. Conventional injections of ES cells are performed in the blastocyst state, at day 3.5 during embryonic development. By injecting ES cells at day 2.5, the eight-cell morula state, the targeted ES cells that already committed to the epiblast lineage are preferentially implanted [208]. With this method, germline transmission can be improved enormously.

4.2.4.3 Mouse breeding and genotyping

Three breeding strains were set up with the founder mice. In breedings with neo mice, the targeting vector with neo cassette was propagated. Flip-induced deletions resulted in floxed mice. Here, the neo cassette was excised and the first three exons were floxed by loxP sites. Breeding germline-transmitted offspring with PGK-Cre deleter induced the KO. As seen before, offspring that propagated the PGK-Cre gene heterozygously could induce the recombination on both alleles. In contrast to that, flip-deleter breedings resulted in either floxed or neo mice, depending on the allelic distribution of the flip gene.

For the genotyping of mouse-tails, a screening system via PCR was established. For each strain, a combination of PCRs was performed which allowed the unambiguous determination of the according genotype. Primer pairs with one primer binding outside the region of homologous recombination, the other in a vector-specific gene segment allowed ascertainment of correct chromosomal insertion of the targeting vector (for example 3'external B in Figure 3.45). PCRs that exclusively bound inside the targeted region were mainly used for high throughput screenings of offspring from parents where the correct chromosomal locus was confirmed before (for example flip B in Figure 3.46). The first $CD2BP2^{+/-}$ mice were additionally confirmed with Southern blots. DNA extracted from mouse-tails was not pure enough to result in good Southern blots. The 5'probe, which detects the KO band, turned out to be a weak binder, which makes the detection of the KO more difficult. Therefore, pieces from ear clips were used to generate MAFs from which DNA was extracted and used for Southern blot analyses. Since clipping was performed for animal tagging anyway, mice were not exposed to additional stress for the generation of MAFs. Figure 3.48 shows the Southern blot of MAFs deriving from $CD2BP2^{+/-}$ mouse incubated with the 3' and 5'probes. As expected from the cloning scheme, the 3'probe binds at 5 kb, reflective to exon four to seven, representing the 3'homology. LoxP induced deletion of exon one to three leads to the reduction of the 5'homology region to 4 kb. Due to a strong background signal, the WT band is hardly visible at 12 kb but was detected in PCRs experiments before. In summary, this Southern blot analyses show successful induction of the knockout with the targeting vector of CD2BP2.

$CD2BP2^{+/-}$ mice were healthy and showed a normal phenotype. This was expected since the expression of CD2BP2 on protein level was comparable to WT mice (Figure 3.49). The deletion of one allele was compensated by the other. No changes in protein expression levels between $CD2BP2^{+/-}$ and WT mice speak for a recessive inheritance of CD2BP2.

Heterozygous mice from each strain were bred with each other to receive $CD2BP2^{-/-}$ mice. This succeeded for neo and floxed strains. The gene Tbc1d10b lies directly upstream of CD2BP2 on chromosome 7 in the mouse genome and is part of the 5'homology region. Breeding of homozygous neo and floxed mice resulted in healthy animals. Therefore, it was expected that Tbc1d10b is not affected by the targeting vector. Western blots performed with flox/ flox mice showed equal expression of Tbc1d10b when compared to WT littermates,

which confirmed that the gene locus was intact. Even though the DNA of the targeting vector is localized to introns, it is hard to predict if any regulatory region for CD2BP2 expression could be affected by the insertion of additional DNA. The homozygous neo and floxed mice could show that the DNA deriving from the targeting vector does not influence CD2BP2 protein expression.

4.2.4.4 Embryonic lethality of CD2BP2 null mice

For the generation of CD2BP2 null mice, matings with CD2BP2$^{+/-}$ mice were initiated. Up so far, 23 matings from 9 different breeding pairs have been analyzed leading to 54 WT mice, 91 WT/ KO mice and no KO/ KO mouse (Table 3.3). These studies indicated that homozygous CD2BP2 KO mice die during embryonic development. To confirm this assumption, timed matings were set up and the genotype of the embryos was analyzed at different embryonic stages. Starting from E16.5, embryos were examined with regard to their phenotype and genotype. Until E11.5, dead embryos were present in all mice analyzed. One exemplary uterus of a female mouse at E11.5 is shown in Figure 3.50. Three resorbed and hemorrhagic embryos can bee seen. Genotyping by PCR resulted in WT or WT/ KO for the healthy embryos whereas the dead embryos were KO/ KO. These data show for the first time that mice lacking CD2BP2 are embryonic lethal. Embryos at E10.5 show growth retardation but are not hemorrhagic yet. Therefore, we speculate embryonic lethality to take place previous to E10.5. With this result, the primary question of this study, considering the survival of mice without CD2BP2 can be answered with a clear no.

Knockout studies from other genes leading to embryonic lethality at E10.5 resulted in impaired heart development and depletions of the hematopoietic precursor pool [209]. Also, defects at early stages of vascular development in the embryo and yolk sac could be observed [210]. Experiments in developing embryos will help to determine the deficits leading to embryonic lethality of CD2BP2 null mice.

During the course of evolution CD2BP2 has gained several functions that are essential for mice. Primitive eukaryotes such as yeast perform splicing only for a minority of genes and have no immune system. Deletion studies in *S. cerevisiae* showed growth inhibition of U5-15K null strains but CD2BP2 deletion strains are viable [56]. Obviously, *S. cerevisiae* can compensate the splicing-related function of CD2BP2.

Recent studies from the Luehrmann group showed that the dual specific Cdk like serine/ threonin kinase Prp4 is essential for the stable formation of the mRNA splicing complex B [54]. In contrast to *S. pombe, S. cerevisiae* does not express PRP4 kinase. It would be of interest to see if *S. pombe* is more susceptible to deletion of CD2BP2. If so, post-translational modifications such as phosphorylation might be essential for the functionality of CD2BP2 in splicing that cannot be studied in *S. cerevisiae,* where the kinase is missing. There are no KO mice existing for any direct interaction partner of CD2BP2 in splicing, neither for U5-15K,

U5-102K nor NpwBP. Therefore, it is difficult to estimate phenotypical changes caused by null mutants of splicing-related interaction partners.

In contrast to CD2BP2, CD2 KO mice are healthy and can raise an effective immune response [49]. As we could show in this study, the expression of CD2BP2 in the immune system goes beyond that of CD2. Hence, CD2 null mutants provide only limited information considering the influence of CD2BP2 on immune cells. Organ-specific deletions of CD2BP2 in the immune system of mice should help to narrow down its function here.

From what we know by now, CD2BP2 seems to have gained several functions within the cell that might alter during pre-and postnatal mouse development. From yeast studies, it is assumed that the splicing-related function is not essential in yeast and can be compensated by other proteins. This needs to be confirmed in different yeast strains. In adult mice, CD2BP2 seems to act mainly in the immune system. If the immune-related function of CD2BP2 is essential or the role in splicing is restricted to the immune system needs to be addressed in future studies.

5 Outlook

5.1 Future Studies of GIGYF2

This study strongly indicates a role of GIGYF2 in vesicular transport and assembly of RNP granules in different cell systems. Future studies should focus on its role in the neuronal cell system. If binding of GIGYF2 to mRNA could be shown, this would support a regulatory function of GIGYF2 in cytoplasmic granules. Here, it would be of interest to see if a general interaction with mRNA takes place or if GIGYF2 would also interact with specific mRNAs that fulfill important functions at certain cellular compartments, such as the growth cone of neuronal cells. Since the protein is present in neurites of SH-SY5Y cells, specific dendritical and axonal markers such as MAP2 and neurofilament, respectively, would further specify its localization in neuronal outgrowths. Potential transport mechanism could be addressed with live cell imaging using overexpressd GIGYF2. Stress induced changes could influence the localization of cytoplasmic complexes that contain GIGYF2.

A more detailed analysis of the function of GIGYF2 in mouse could be addressed by conditional KO mice. Brain or motor neuron specific deletions of GIGYF2 would help to understand its involvement in neurodegenerative diseases. Also, since a neurodegenerative-like phenotype was observed before, the rat could serve as even better model to analyses these pathologies in more detail because their cognition, memory and behavior is much closer to human than the mouse [211]. Since GIGYF2 KO mice are not embryonic lethal, targeted mutations with zinc finger nucleases would be the technique of choice.

On the long term, if linkage to other neurodegenerative diseases could be drawn and mechanisms are understood, therapeutic screening for interaction inhibitors could be taken into account. One likely scenario would be screenings for small molecules that inhibit potential interactions of the polyQ repeat of GIGYF2.

5.2 Future Studies to analyze the immune function of CD2BP2

While the primary question of this study considering the survival of CD2BP2 null mice could be answered, the generation of a conditional CD2BP2 knockout system opens the field for countless new experiments. Still, there are some questions that can be addressed straight away.

The differences of mRNA versus protein expression level in mouse organs should be addressed by screening for protein expression regulators. It is conceivable that CD2BP2 is regulated by miRNA that bind to the long 3'UTR of the protein and thereby modulate protein translation. Since the three splice variants of CD2BP2 differ in the length of the 3'UTR, miRNA-mediated regulation might have diverse impacts. Luciferase assays could help to identify the according miRNA.

5.3 Future studies to analyze embryonic lethality of CD2BP2

To get a better hold on the expression of CD2BP2 during embryonic development, whole mount *in situ* hybridization should be performed. The expression pattern of WT and KO mice could help to find the organ specific defects of the KO mice leading to lethality. Histological analyses of mice before E10.5 will help to dissect organ-related alterations. The vascular network of embryos during this developmental stage can be visualized by stains with the platelet endothelial cell adhesion molecules-1 (PECAM-1).

In immortalized murine embryonic fibroblasts (MEF) cell lines of CD2BP2 null mice, the consequences of CD2BP2 deletions can be analyzed on cellular level. Moreover, MEF cells will help to find molecular mechanisms in which CD2BP2 is involved. These MEFs can be generated by producing KO/ flox embryos that become virally transfected with Cre-recombinase, thereby inducing the KO of the floxed allele. If these cell lines are viable, they will serve as great tool for a better molecular understanding of CD2BP2.

The role of CD2BP2 in adult mice should be addressed by inducible or organ specific Cre-expression. MX-Cre mice that inducible delete the gene at any stage of development will show which organs are effected by the KO in adult mice. In organ-specific deletions, potential function of CD2BP2 can be addressed in more detail. Null mice of the CD2-associated protein (CD2AP) develop a congenital nephrotic syndrome after 6 to 7 weeks of age [212]. Since the protein is important for stabilizing the contact between T cell and APC, the kidney specific phenotype came as surprise. Organ-specific KO of CD2BP2 in podocytes, the place of action for CD2AP in kidney, will reveal a kidney-related function of CD2BP2.

Special focus should be on backcrossing of CD2BP2 targeted mice into pure strains. Pure BL6J and N background will probably show little differences. Analyses in pure BL6 and Balb/c strains could have an impact on the time point of lethality and phenotype and should therefore be considered as future steps. Also, a pure background will be of great importance for analyses of the immune system. Organ specific deletions of CD2BP2 in T, B and dendritic cells will allow a more detailed analysis of the importance of the protein in these cells. Viral and bacterial infection assays performed in these cell-specific deleted mice should reveal if CD2BP2 is mostly important in the overall integrity of the immune system or plays a role during combating of invaders.

Overall, there seem no limitations for subsequent studies with the conditional CD2BP2 KO mice. Double and triple KO mice with interaction partners can be of interest or matings with mice carrying reporter genes that allow an easier evaluation of phenotypical alterations.

Novel techniques such as Zinc finger nucleases and homologues recombination of rat ES cells no longer restrict gene mutations to mice but also allow targeted mutations in rat.

References

1. Janeway CA, Travers, P, Walport, M, Shlomchik, M (2002) *Immunbiologie*. Spektrum.

2. Freund C, Dotsch V, Nishizawa K, Reinherz EL & Wagner G (1999) The GYF domain is a novel structural fold that is involved in lymphoid signaling through proline-rich sequences. *Nature structural biology* **6**, 656-660, doi: 10.1038/10712.

3. Nishizawa K, Freund C, Li J, Wagner G & Reinherz EL (1998) Identification of a proline-binding motif regulating CD2-triggered T lymphocyte activation. *Proc Natl Acad Sci U S A* **95**, 14897-14902.

4. Laggerbauer B, Liu S, Makarov E, Vornlocher HP, Makarova O, Ingelfinger D, Achsel T & Luhrmann R (2005) The human U5 snRNP 52K protein (CD2BP2) interacts with U5-102K (hPrp6), a U4/U6.U5 tri-snRNP bridging protein, but dissociates upon tri-snRNP formation. *RNA* **11**, 598-608, doi: 11/5/598 [pii]

10.1261/rna.2300805.

5. Ehmke H (2003) Mouse gene targeting in cardiovascular physiology. *American journal of physiology Regulatory, integrative and comparative physiology* **284**, R28-30, doi: 10.1152/ajpregu.00531.2002.

6. Kofler M, Motzny K, Beyermann M & Freund C (2005) Novel interaction partners of the CD2BP2-GYF domain. *J Biol Chem* **280**, 33397-33402, doi: M503989200 [pii]

10.1074/jbc.M503989200.

7. Mayer BJ, Hamaguchi M & Hanafusa H (1988) A novel viral oncogene with structural similarity to phospholipase C. *Nature* **332**, 272-275, doi: 10.1038/332272a0.

8. Varmus H, Hirai H, Morgan D, Kaplan J & Bishop JM (1989) Function, location, and regulation of the src protein-tyrosine kinase. *Princess Takamatsu symposia* **20**, 63-70.

9. Bork P & Sudol M (1994) The WW domain: a signalling site in dystrophin? *Trends in biochemical sciences* **19**, 531-533.

10. Sudol M, Chen HI, Bougeret C, Einbond A & Bork P (1995) Characterization of a novel protein-binding module--the WW domain. *FEBS letters* **369**, 67-71.

11. Niebuhr K, Ebel F, Frank R, Reinhard M, Domann E, Carl UD, Walter U, Gertler FB, Wehland J & Chakraborty T (1997) A novel proline-rich motif present in ActA of Listeria monocytogenes and cytoskeletal proteins is the ligand for the EVH1 domain, a protein module present in the Ena/VASP family. *The EMBO journal* **16**, 5433-5444, doi: 10.1093/emboj/16.17.5433.

12. Zarrinpar A, Bhattacharyya RP & Lim WA (2003) The structure and function of proline recognition domains. *Science's STKE : signal transduction knowledge environment* **2003**, RE8, doi: 10.1126/stke.2003.179.re8.

13. Pornillos O, Alam SL, Rich RL, Myszka DG, Davis DR & Sundquist WI (2002) Structure and functional interactions of the Tsg101 UEV domain. *The EMBO journal* **21**, 2397-2406, doi: 10.1093/emboj/21.10.2397.

14. Carlsson L, Nystrom LE, Sundkvist I, Markey F & Lindberg U (1977) Actin polymerizability is influenced by profilin, a low molecular weight protein in non-muscle cells. *Journal of molecular biology* **115**, 465-483.

15. (2011) Ongoing and future developments at the Universal Protein Resource. *Nucleic Acids Res* **39**, D214-219, doi: 10.1093/nar/gkq1020.

16. Cicchetti P, Mayer BJ, Thiel G & Baltimore D (1992) Identification of a protein that binds to the SH3 region of Abl and is similar to Bcr and GAP-rho. *Science* **257**, 803-806.

17. Egan SE, Giddings BW, Brooks MW, Buday L, Sizeland AM & Weinberg RA (1993) Association of Sos Ras exchange protein with Grb2 is implicated in tyrosine kinase signal transduction and transformation. *Nature* **363**, 45-51, doi: 10.1038/363045a0.

18. Gout I, Dhand R, Hiles ID, Fry MJ, Panayotou G, Das P, Truong O, Totty NF, Hsuan J, Booker GW, et al. (1993) The GTPase dynamin binds to and is activated by a subset of SH3 domains. *Cell* **75**, 25-36.

19. Catling AD, Schaeffer HJ, Reuter CW, Reddy GR & Weber MJ (1995) A proline-rich sequence unique to MEK1 and MEK2 is required for raf binding and regulates MEK function. *Molecular and cellular biology* **15**, 5214-5225.

20. Kay BK, Williamson MP & Sudol M (2000) The importance of being proline: the interaction of proline-rich motifs in signaling proteins with their cognate domains. *The FASEB journal : official publication of the Federation of American Societies for Experimental Biology* **14**, 231-241.

21. Musacchio A, Wilmanns M & Saraste M (1994) Structure and function of the SH3 domain. *Progress in biophysics and molecular biology* **61**, 283-297.

22. Kofler M, Motzny K & Freund C (2005) GYF domain proteomics reveals interaction sites in known and novel target proteins. *Molecular & cellular proteomics : MCP* **4**, 1797-1811, doi: 10.1074/mcp.M500129-MCP200.

23. Kofler MM & Freund C (2006) The GYF domain. *The FEBS journal* **273**, 245-256, doi: 10.1111/j.1742-4658.2005.05078.x.

24. Pahlke D, Freund C, Leitner D & Labudde D (2005) Statistically significant dependence of the Xaa-Pro peptide bond conformation on secondary structure and amino acid sequence. *BMC structural biology* **5**, 8, doi: 10.1186/1472-6807-5-8.

25. Kofler M, Heuer K, Zech T & Freund C (2004) Recognition sequences for the GYF domain reveal a possible spliceosomal function of CD2BP2. *J Biol Chem* **279**, 28292-28297, doi: 10.1074/jbc.M402008200

M402008200 [pii].

26. Ash MR, Faelber K, Kosslick D, Albert GI, Roske Y, Kofler M, Schuemann M, Krause E & Freund C (2010) Conserved beta-hairpin recognition by the GYF domains of Smy2 and GIGYF2 in mRNA surveillance and vesicular transport complexes. *Structure* **18**, 944-954, doi: 10.1016/j.str.2010.04.020.

27. Freund C, Kuhne R, Yang H, Park S, Reinherz EL & Wagner G (2002) Dynamic interaction of CD2 with the GYF and the SH3 domain of compartmentalized effector molecules. *The EMBO journal* **21**, 5985-5995.

28. Abbas AK LA, Pillai S (2007) *Cellular and Molecular Immunology*. 6th Edition edn.

29. McHeyzer-Williams MG (2003) B cells as effectors. *Curr Opin Immunol* **15**, 354-361.

30. Godfrey DI, Kennedy J, Suda T & Zlotnik A (1993) A developmental pathway involving four phenotypically and functionally distinct subsets of CD3-CD4-CD8- triple-negative adult mouse thymocytes defined by CD44 and CD25 expression. *J Immunol* **150**, 4244-4252.

31. Carlyle JR & Zuniga-Pflucker JC (1998) Requirement for the thymus in alphabeta T lymphocyte lineage commitment. *Immunity* **9**, 187-197.

32. Capone M, Hockett RD, Jr. & Zlotnik A (1998) Kinetics of T cell receptor beta, gamma, and delta rearrangements during adult thymic development: T cell receptor rearrangements are present in CD44(+)CD25(+) Pro-T thymocytes. *Proc Natl Acad Sci U S A* **95**, 12522-12527.

33. Kondo M, Weissman IL & Akashi K (1997) Identification of clonogenic common lymphoid progenitors in mouse bone marrow. *Cell* **91**, 661-672.

34. Robey E (1999) Regulation of T cell fate by Notch. *Annual review of immunology* **17**, 283-295, doi: 10.1146/annurev.immunol.17.1.283.

35. Bierer BE & Hahn WC (1993) T cell adhesion, avidity regulation and signaling: a molecular analysis of CD2. *Seminars in immunology* **5**, 249-261, doi: 10.1006/smim.1993.1029.

36. Punnonen J & de Vries JE (1993) Characterization of a novel CD2+ human thymic B cell subset. *J Immunol* **151**, 100-110.

37. Tangye SG, Phillips JH & Lanier LL (2000) The CD2-subset of the Ig superfamily of cell surface molecules: receptor-ligand pairs expressed by NK cells and other immune cells. *Seminars in immunology* **12**, 149-157, doi: 10.1006/smim.2000.0217.

38. Kishimoto T KH, von demBorne AEG, Goyert SM, Mason DY, Miyasaka M, Moretta L, Okumura K, Shaw S, Ž .Springer TA, Sugamura K, Zola H (1997) *Leucocyte typing VI*. Garland Publishing Inc, New York.

39. Kato K, Koyanagi M, Okada H, Takanashi T, Wong YW, Williams AF, Okumura K & Yagita H (1992) CD48 is a counter-receptor for mouse CD2 and is involved in T cell activation. *The Journal of experimental medicine* **176**, 1241-1249.

40. Thorley-Lawson DA, Schooley RT, Bhan AK & Nadler LM (1982) Epstein-Barr virus superinduces a new human B cell differentiation antigen (B-LAST 1) expressed on transformed lymphoblasts. *Cell* **30**, 415-425.

41. Yokoyama S, Staunton D, Fisher R, Amiot M, Fortin JJ & Thorley-Lawson DA (1991) Expression of the Blast-1 activation/adhesion molecule and its identification as CD48. *J Immunol* **146**, 2192-2200.

42. Chang HC, Moingeon P, Lopez P, Krasnow H, Stebbins C & Reinherz EL (1989) Dissection of the human CD2 intracellular domain. Identification of a segment required for signal transduction and interleukin 2 production. *The Journal of experimental medicine* **169**, 2073-2083.

43. Hahn WC & Bierer BE (1993) Separable portions of the CD2 cytoplasmic domain involved in signaling and ligand avidity regulation. *The Journal of experimental medicine* **178**, 1831-1836.

44. Holter W, Schwarz M, Cerwenka A & Knapp W (1996) The role of CD2 as a regulator of human T-cell cytokine production. *Immunological reviews* **153**, 107-122.

45. Koyasu S, Lawton T, Novick D, Recny MA, Siliciano RF, Wallner BP & Reinherz EL (1990) Role of interaction of CD2 molecules with lymphocyte function-associated antigen 3 in T-cell recognition of nominal antigen. *Proc Natl Acad Sci U S A* **87**, 2603-2607.

46. Springer TA (1990) Adhesion receptors of the immune system. *Nature* **346**, 425-434, doi: 10.1038/346425a0.

47. Gollob JA, Li J, Reinherz EL & Ritz J (1995) CD2 regulates responsiveness of activated T cells to interleukin 12. *The Journal of experimental medicine* **182**, 721-731.

48. Eibert SM, Lee KH, Pipkorn R, Sester U, Wabnitz GH, Giese T, Meuer SC & Samstag Y (2004) Cofilin peptide homologs interfere with immunological synapse formation and T cell activation. *Proc Natl Acad Sci U S A* **101**, 1957-1962, doi: 10.1073/pnas.0308282100.

49. Killeen N, Stuart SG & Littman DR (1992) Development and function of T cells in mice with a disrupted CD2 gene. *The EMBO journal* **11**, 4329-4336.

50. Gonzalez-Cabrero J, Wise CJ, Latchman Y, Freeman GJ, Sharpe AH & Reiser H (1999) CD48-deficient mice have a pronounced defect in CD4(+) T cell activation. *Proc Natl Acad Sci U S A* **96**, 1019-1023.

51. Heinze M, Kofler M & Freund C (2007) Investigating the functional role of CD2BP2 in T cells. *Int Immunol* **19**, 1313-1318, doi: dxm100 [pii]

10.1093/intimm/dxm100.

52. Will CL & Luhrmann R (2001) Spliceosomal UsnRNP biogenesis, structure and function. *Current opinion in cell biology* **13**, 290-301.

53. Behrens SE & Luhrmann R (1991) Immunoaffinity purification of a [U4/U6.U5] tri-snRNP from human cells. *Genes Dev* **5**, 1439-1452.

54. Lutzelberger M, Bottner CA, Schwelnus W, Zock-Emmenthal S, Razanau A & Kaufer NF (2010) The N-terminus of Prp1 (Prp6/U5-102 K) is essential for spliceosome activation in vivo. *Nucleic Acids Res* **38**, 1610-1622, doi: 10.1093/nar/gkp1155.

55. Schneider M, Hsiao HH, Will CL, Giet R, Urlaub H & Luhrmann R (2010) Human PRP4 kinase is required for stable tri-snRNP association during spliceosomal B complex formation. *Nature structural & molecular biology* **17**, 216-221, doi: 10.1038/nsmb.1718.

56. Stevens SW, Barta I, Ge HY, Moore RE, Young MK, Lee TD & Abelson J (2001) Biochemical and genetic analyses of the U5, U6, and U4/U6 x U5 small nuclear ribonucleoproteins from Saccharomyces cerevisiae. *RNA* **7**, 1543-1553.

57. Zhang Y, Lindblom T, Chang A, Sudol M, Sluder AE & Golemis EA (2000) Evidence that dim1 associates with proteins involved in pre-mRNA splicing, and delineation of residues essential for dim1 interactions with hnRNP F and Npw38/PQBP-1. *Gene* **257**, 33-43.

58. Kofler M, Schuemann M, Merz C, Kosslick D, Schlundt A, Tannert A, Schaefer M, Luhrmann R, Krause E & Freund C (2009) Proline-rich sequence recognition: I. Marking GYF and WW domain assembly sites in early spliceosomal complexes. *Molecular & cellular proteomics : MCP* **8**, 2461-2473, doi: 10.1074/mcp.M900191-MCP200.

59. Takahashi M, Mizuguchi M, Shinoda H, Aizawa T, Demura M, Okazawa H & Kawano K (2010) Polyglutamine tract-binding protein-1 binds to U5-15kD via a continuous 23-residue segment of the C-terminal domain. *Biochimica et biophysica acta* **1804**, 1500-1507, doi: 10.1016/j.bbapap.2010.03.007.

60. Okazawa H, Rich T, Chang A, Lin X, Waragai M, Kajikawa M, Enokido Y, Komuro A, Kato S, Shibata M, et al. (2002) Interaction between mutant ataxin-1 and PQBP-1 affects transcription and cell death. *Neuron* **34**, 701-713.

61. Llorian M, Beullens M, Andres I, Ortiz JM & Bollen M (2004) SIPP1, a novel pre-mRNA splicing factor and interactor of protein phosphatase-1. *The Biochemical journal* **378**, 229-238, doi: 10.1042/BJ20030950.

62. Giovannone B, Lee E, Laviola L, Giorgino F, Cleveland KA & Smith RJ (2003) Two novel proteins that are linked to insulin-like growth factor (IGF-I) receptors by the Grb10 adapter and modulate IGF-I signaling. *J Biol Chem* **278**, 31564-31573, doi: 10.1074/jbc.M211572200.

63. Liu F & Roth RA (1995) Grb-IR: a SH2-domain-containing protein that binds to the insulin receptor and inhibits its function. *Proc Natl Acad Sci U S A* **92**, 10287-10291.

64. O'Neill TJ, Rose DW, Pillay TS, Hotta K, Olefsky JM & Gustafson TA (1996) Interaction of a GRB-IR splice variant (a human GRB10 homolog) with the insulin and insulin-like growth factor I receptors. Evidence for a role in mitogenic signaling. *J Biol Chem* **271**, 22506-22513.

65. Wojcik J, Girault JA, Labesse G, Chomilier J, Mornon JP & Callebaut I (1999) Sequence analysis identifies a ras-associating (RA)-like domain in the N-termini of band 4.1/JEF domains and in the Grb7/10/14 adapter family. *Biochem Biophys Res Commun* **259**, 113-120, doi: 10.1006/bbrc.1999.0727.

66. Langlais P, Dong LQ, Hu D & Liu F (2000) Identification of Grb10 as a direct substrate for members of the Src tyrosine kinase family. *Oncogene* **19**, 2895-2903, doi: 10.1038/sj.onc.1203616.

67. Ooi J, Yajnik V, Immanuel D, Gordon M, Moskow JJ, Buchberg AM & Margolis B (1995) The cloning of Grb10 reveals a new family of SH2 domain proteins. *Oncogene* **10**, 1621-1630.

68. Lautier C, Goldwurm S, Durr A, Giovannone B, Tsiaras WG, Pezzoli G, Brice A & Smith RJ (2008) Mutations in the GIGYF2 (TNRC15) gene at the PARK11 locus in familial Parkinson disease. *Am J Hum Genet* **82**, 822-833, doi: 10.1016/j.ajhg.2008.01.015.

69. Pankratz N, Nichols WC, Uniacke SK, Halter C, Murrell J, Rudolph A, Shults CW, Conneally PM & Foroud T (2003) Genome-wide linkage analysis and evidence of gene-by-gene interactions in a sample of 362 multiplex Parkinson disease families. *Hum Mol Genet* **12**, 2599-2608, doi: 10.1093/hmg/ddg270.

70. Pankratz N, Nichols WC, Uniacke SK, Halter C, Rudolph A, Shults C, Conneally PM & Foroud T (2002) Genome screen to identify susceptibility genes for Parkinson disease in a sample without parkin mutations. *Am J Hum Genet* **71**, 124-135, doi: 10.1086/341282.

71. Pankratz N, Nichols WC, Uniacke SK, Halter C, Rudolph A, Shults C, Conneally PM & Foroud T (2003) Significant linkage of Parkinson disease to chromosome 2q36-37. *Am J Hum Genet* **72**, 1053-1057, doi: 10.1086/374383.

72. Bras J, Simon-Sanchez J, Federoff M, Morgadinho A, Januario C, Ribeiro M, Cunha L, Oliveira C & Singleton AB (2009) Lack of replication of association between GIGYF2 variants and Parkinson disease. *Hum Mol Genet* **18**, 341-346, doi: 10.1093/hmg/ddn340.

73. Sutherland GT, Siebert GA, Newman JR, Silburn PA, Boyle RS, O'Sullivan JD & Mellick GD (2009) Haplotype analysis of the PARK 11 gene, GIGYF2, in sporadic Parkinson's disease. *Mov Disord* **24**, 449-452, doi: 10.1002/mds.22427.

74. Vilarino-Guell C, Ross OA, Soto AI, Farrer MJ, Haugarvoll K, Aasly JO, Uitti RJ & Wszolek ZK (2009) Reported mutations in GIGYF2 are not a common cause of Parkinson's disease. *Mov Disord* **24**, 619-620, doi: 10.1002/mds.22451.

75. Zimprich A, Schulte C, Reinthaler E, Haubenberger D, Balzar J, Lichtner P, El Tawil S, Edris S, Foki T, Pirker W, et al. (2009) PARK11 gene (GIGYF2) variants Asn56Ser and Asn457Thr are not pathogenic for Parkinson's disease. *Parkinsonism Relat Disord* **15**, 532-534, doi: 10.1016/j.parkreldis.2009.01.005.

76. Nichols WC, Kissell DK, Pankratz N, Pauciulo MW, Elsaesser VE, Clark KA, Halter CA, Rudolph A, Wojcieszek J, Pfeiffer RF, et al. (2009) Variation in GIGYF2 is not associated with Parkinson disease. *Neurology* **72**, 1886-1892, doi: 10.1212/01.wnl.0000346517.98982.1b.

77. Meeus B, Nuytemans K, Crosiers D, Engelborghs S, Pals P, Pickut B, Peeters K, Mattheijssens M, Corsmit E, Cras P, et al. (2011) GIGYF2 has no major role in Parkinson genetic etiology in a Belgian population. *Neurobiol Aging* **32**, 308-312, doi: 10.1016/j.neurobiolaging.2009.02.016.

78. Guo Y, Jankovic J, Zhu S, Le W, Song Z, Xie W, Liao D, Yang H & Deng H (2009) GIGYF2 Asn56Ser and Asn457Thr mutations in Parkinson disease patients. *Neurosci Lett* **454**, 209-211, doi: 10.1016/j.neulet.2009.03.039.

79. Tan EK, Lin CH, Tai CH, Tan LC, Chen ML, Li R, Lim HQ, Pavanni R, Yuen Y, Prakash KM, et al. (2009) Non-synonymous GIGYF2 variants in Parkinson's disease from two Asian populations. *Hum Genet* **126**, 425-430, doi: 10.1007/s00439-009-0678-x.

80. Di Fonzo A, Fabrizio E, Thomas A, Fincati E, Marconi R, Tinazzi M, Breedveld GJ, Simons EJ, Chien HF, Ferreira JJ, et al. (2009) GIGYF2 mutations are not a frequent cause of familial Parkinson's disease. *Parkinsonism Relat Disord* **15**, 703-705, doi: 10.1016/j.parkreldis.2009.05.001.

81. Bonetti M, Ferraris A, Petracca M, Bentivoglio AR, Dallapiccola B & Valente EM (2009) GIGYF2 variants are not associated with Parkinson's disease in Italy. *Mov Disord* **24**, 1867-1868; author reply 1868-1869, doi: 10.1002/mds.22640.

82. Zhang Y, Zheng L, Zhang T, Wang Y, Xiao Q, Fei QZ, Cui PJ, Cao L & Chen SD (2009) GIGYF2 Asn56Ser mutation is rare in Chinese Parkinson's disease patients. *Neurosci Lett* **463**, 172-175, doi: 10.1016/j.neulet.2009.07.067.

83. Samaranch L, Lorenzo E, Pastor MA, Riverol M, Luquin MR, Rodriguez-Oroz MC, Obeso JA & Pastor P (2010) Analysis of the GIGYF2 gene in familial and sporadic Parkinson disease in the Spanish population. *Eur J Neurol* **17**, 321-325, doi: 10.1111/j.1468-1331.2009.02812.x.

84. Tan EK & Schapira AH (2010) Summary of GIGYF2 studies in Parkinson's disease: the burden of proof. *Eur J Neurol* **17**, 175-176, doi: 10.1111/j.1468-1331.2009.02834.x.

85. Lesage S, Condroyer C, Lohman E, Troiano A, Tison F, Viallet F, Damier P, Tranchant C, Vidhaillet M, Ouvrard-Hernandez AM, et al. (2010) Follow-up study of the GIGYF2 gene in French families with Parkinson's disease. *Neurobiol Aging* **31**, 1069-1071; discussion 1072-1064, doi: 10.1016/j.neurobiolaging.2009.06.008.

86. Giovannone B, Tsiaras WG, de la Monte S, Klysik J, Lautier C, Karashchuk G, Goldwurm S & Smith RJ (2009) GIGYF2 gene disruption in mice results in neurodegeneration and altered insulin-like growth factor signaling. *Hum Mol Genet* **18**, 4629-4639, doi: 10.1093/hmg/ddp430.

87. Georgiev A, Sjostrom M & Wieslander A (2007) Binding specificities of the GYF domains from two Saccharomyces cerevisiae paralogs. *Protein Eng Des Sel* **20**, 443-452, doi: 10.1093/protein/gzm041.

88. Dunckley T, Tucker M & Parker R (2001) Two related proteins, Edc1p and Edc2p, stimulate mRNA decapping in Saccharomyces cerevisiae. *Genetics* **157**, 27-37.

89. Sheth U & Parker R (2003) Decapping and decay of messenger RNA occur in cytoplasmic processing bodies. *Science* **300**, 805-808, doi: 10.1126/science.1082320.

90. Thomas MG, Loschi M, Desbats MA & Boccaccio GL (2011) RNA granules: the good, the bad and the ugly. *Cell Signal* **23**, 324-334, doi: 10.1016/j.cellsig.2010.08.011.

91. Brengues M, Teixeira D & Parker R (2005) Movement of eukaryotic mRNAs between polysomes and cytoplasmic processing bodies. *Science* **310**, 486-489, doi: 10.1126/science.1115791.

92. Loschi M, Leishman CC, Berardone N & Boccaccio GL (2009) Dynein and kinesin regulate stress-granule and P-body dynamics. *J Cell Sci* **122**, 3973-3982, doi: 10.1242/jcs.051383.

93. Coller J & Parker R (2004) Eukaryotic mRNA decapping. *Annu Rev Biochem* **73**, 861-890, doi: 10.1146/annurev.biochem.73.011303.074032.

94. Sen GL & Blau HM (2005) Argonaute 2/RISC resides in sites of mammalian mRNA decay known as cytoplasmic bodies. *Nat Cell Biol* **7**, 633-636, doi: 10.1038/ncb1265.

95. McManus MT & Sharp PA (2002) Gene silencing in mammals by small interfering RNAs. *Nat Rev Genet* **3**, 737-747, doi: 10.1038/nrg908.

96. Meister G & Tuschl T (2004) Mechanisms of gene silencing by double-stranded RNA. *Nature* **431**, 343-349, doi: 10.1038/nature02873.

97. Fire A, Xu S, Montgomery MK, Kostas SA, Driver SE & Mello CC (1998) Potent and specific genetic interference by double-stranded RNA in Caenorhabditis elegans. *Nature* **391**, 806-811, doi: 10.1038/35888.

98. Behm-Ansmant I, Rehwinkel J, Doerks T, Stark A, Bork P & Izaurralde E (2006) mRNA degradation by miRNAs and GW182 requires both CCR4:NOT deadenylase and DCP1:DCP2 decapping complexes. *Genes Dev* **20**, 1885-1898, doi: 10.1101/gad.1424106.

99. Tourriere H, Chebli K, Zekri L, Courselaud B, Blanchard JM, Bertrand E & Tazi J (2003) The RasGAP-associated endoribonuclease G3BP assembles stress granules. *J Cell Biol* **160**, 823-831, doi: 10.1083/jcb.200212128.

100. Bhattacharyya SN, Habermacher R, Martine U, Closs EI & Filipowicz W (2006) Relief of microRNA-mediated translational repression in human cells subjected to stress. *Cell* **125**, 1111-1124, doi: 10.1016/j.cell.2006.04.031.

101. Kedersha NL, Gupta M, Li W, Miller I & Anderson P (1999) RNA-binding proteins TIA-1 and TIAR link the phosphorylation of eIF-2 alpha to the assembly of mammalian stress granules. *J Cell Biol* **147**, 1431-1442.

102. Dang Y, Kedersha N, Low WK, Romo D, Gorospe M, Kaufman R, Anderson P & Liu JO (2006) Eukaryotic initiation factor 2alpha-independent pathway of stress granule induction by the natural product pateamine A. *J Biol Chem* **281**, 32870-32878, doi: 10.1074/jbc.M606149200.

103. Mokas S, Mills JR, Garreau C, Fournier MJ, Robert F, Arya P, Kaufman RJ, Pelletier J & Mazroui R (2009) Uncoupling stress granule assembly and translation initiation inhibition. *Mol Biol Cell* **20**, 2673-2683, doi: 10.1091/mbc.E08-10-1061.

104. Mazroui R, Huot ME, Tremblay S, Filion C, Labelle Y & Khandjian EW (2002) Trapping of messenger RNA by Fragile X Mental Retardation protein into cytoplasmic granules induces translation repression. *Hum Mol Genet* **11**, 3007-3017.

105. Kedersha N, Stoecklin G, Ayodele M, Yacono P, Lykke-Andersen J, Fritzler MJ, Scheuner D, Kaufman RJ, Golan DE & Anderson P (2005) Stress granules and processing bodies are dynamically linked sites of mRNP remodeling. *J Cell Biol* **169**, 871-884, doi: 10.1083/jcb.200502088.

106. Wilczynska A, Aigueperse C, Kress M, Dautry F & Weil D (2005) The translational regulator CPEB1 provides a link between dcp1 bodies and stress granules. *J Cell Sci* **118**, 981-992, doi: 10.1242/jcs.01692.

107. De Leeuw F, Zhang T, Wauquier C, Huez G, Kruys V & Gueydan C (2007) The cold-inducible RNA-binding protein migrates from the nucleus to cytoplasmic stress granules by a methylation-dependent mechanism and acts as a translational repressor. *Exp Cell Res* **313**, 4130-4144, doi: 10.1016/j.yexcr.2007.09.017.

108. Kedersha N, Cho MR, Li W, Yacono PW, Chen S, Gilks N, Golan DE & Anderson P (2000) Dynamic shuttling of TIA-1 accompanies the recruitment of mRNA to mammalian stress granules. *J Cell Biol* **151**, 1257-1268.

109. Buchan JR, Muhlrad D & Parker R (2008) P bodies promote stress granule assembly in Saccharomyces cerevisiae. *J Cell Biol* **183**, 441-455, doi: 10.1083/jcb.200807043.

110. Kedersha N, Chen S, Gilks N, Li W, Miller IJ, Stahl J & Anderson P (2002) Evidence that ternary complex (eIF2-GTP-tRNA(i)(Met))-deficient preinitiation complexes are core constituents of mammalian stress granules. *Mol Biol Cell* **13**, 195-210, doi: 10.1091/mbc.01-05-0221.

111. Kimball SR, Horetsky RL, Ron D, Jefferson LS & Harding HP (2003) Mammalian stress granules represent sites of accumulation of stalled translation initiation complexes. *Am J Physiol Cell Physiol* **284**, C273-284, doi: 10.1152/ajpcell.00314.2002.

112. Mazroui R, Sukarieh R, Bordeleau ME, Kaufman RJ, Northcote P, Tanaka J, Gallouzi I & Pelletier J (2006) Inhibition of ribosome recruitment induces stress granule formation independently of eukaryotic initiation factor 2alpha phosphorylation. *Mol Biol Cell* **17**, 4212-4219, doi: 10.1091/mbc.E06-04-0318.

113. Anderson P & Kedersha N (2006) RNA granules. *J Cell Biol* **172**, 803-808, doi: 10.1083/jcb.200512082.

114. Buchan JR & Parker R (2009) Eukaryotic stress granules: the ins and outs of translation. *Mol Cell* **36**, 932-941, doi: 10.1016/j.molcel.2009.11.020.

115. DeGracia DJ, Rudolph J, Roberts GG, Rafols JA & Wang J (2007) Convergence of stress granules and protein aggregates in hippocampal cornu ammonis 1 at later reperfusion following global brain ischemia. *Neuroscience* **146**, 562-572, doi: 10.1016/j.neuroscience.2007.01.050.

116. Kayali F, Montie HL, Rafols JA & DeGracia DJ (2005) Prolonged translation arrest in reperfused hippocampal cornu Ammonis 1 is mediated by stress granules. *Neuroscience* **134**, 1223-1245, doi: 10.1016/j.neuroscience.2005.05.047.

117. Nakano S, Shinde A, Ito H & Kusaka H (2005) Messenger RNA degradation may be inhibited in sporadic inclusion body myositis. *Neurology* **65**, 420-425, doi: 10.1212/01.wnl.0000171341.76482.15.

118. McEwen E, Kedersha N, Song B, Scheuner D, Gilks N, Han A, Chen JJ, Anderson P & Kaufman RJ (2005) Heme-regulated inhibitor kinase-mediated phosphorylation of eukaryotic translation initiation factor 2 inhibits translation, induces stress granule formation, and mediates survival upon arsenite exposure. *J Biol Chem* **280**, 16925-16933, doi: 10.1074/jbc.M412882200.

119. Kedersha N & Anderson P (2009) Regulation of translation by stress granules and processing bodies. *Prog Mol Biol Transl Sci* **90**, 155-185, doi: 10.1016/S1877-1173(09)90004-7.

120. Thomas MG, Martinez Tosar LJ, Desbats MA, Leishman CC & Boccaccio GL (2009) Mammalian Staufen 1 is recruited to stress granules and impairs their assembly. *J Cell Sci* **122**, 563-573, doi: 10.1242/jcs.038208.

121. Schekman R & Orci L (1996) Coat proteins and vesicle budding. *Science* **271**, 1526-1533.

122. Nakano A & Muramatsu M (1989) A novel GTP-binding protein, Sar1p, is involved in transport from the endoplasmic reticulum to the Golgi apparatus. *J Cell Biol* **109**, 2677-2691.

123. Barlowe C, Orci L, Yeung T, Hosobuchi M, Hamamoto S, Salama N, Rexach MF, Ravazzola M, Amherdt M & Schekman R (1994) COPII: a membrane coat formed by Sec proteins that drive vesicle budding from the endoplasmic reticulum. *Cell* **77**, 895-907.

124. Lee MC, Orci L, Hamamoto S, Futai E, Ravazzola M & Schekman R (2005) Sar1p N-terminal helix initiates membrane curvature and completes the fission of a COPII vesicle. *Cell* **122**, 605-617, doi: 10.1016/j.cell.2005.07.025.

125. Nakano A, Brada D & Schekman R (1988) A membrane glycoprotein, Sec12p, required for protein transport from the endoplasmic reticulum to the Golgi apparatus in yeast. *J Cell Biol* **107**, 851-863.

126. Barlowe C & Schekman R (1993) SEC12 encodes a guanine-nucleotide-exchange factor essential for transport vesicle budding from the ER. *Nature* **365**, 347-349, doi: 10.1038/365347a0.

127. Bonifacino JS & Glick BS (2004) The mechanisms of vesicle budding and fusion. *Cell* **116**, 153-166.

128. Matsuoka K, Orci L, Amherdt M, Bednarek SY, Hamamoto S, Schekman R & Yeung T (1998) COPII-coated vesicle formation reconstituted with purified coat proteins and chemically defined liposomes. *Cell* **93**, 263-275.

129. Sato K & Nakano A (2004) Reconstitution of coat protein complex II (COPII) vesicle formation from cargo-reconstituted proteoliposomes reveals the potential role of GTP hydrolysis by Sar1p in protein sorting. *J Biol Chem* **279**, 1330-1335, doi: 10.1074/jbc.C300457200.

130. Gimeno RE, Espenshade P & Kaiser CA (1995) SED4 encodes a yeast endoplasmic reticulum protein that binds Sec16p and participates in vesicle formation. *J Cell Biol* **131**, 325-338.

131. Heidtman M, Chen CZ, Collins RN & Barlowe C (2003) A role for Yip1p in COPII vesicle biogenesis. *J Cell Biol* **163**, 57-69, doi: 10.1083/jcb.200306118.

132. Heidtman M, Chen CZ, Collins RN & Barlowe C (2005) Yos1p is a novel subunit of the Yip1p-Yif1p complex and is required for transport between the endoplasmic reticulum and the Golgi complex. *Mol Biol Cell* **16**, 1673-1683, doi: 10.1091/mbc.E04-10-0873.

133. Higashio H, Kimata Y, Kiriyama T, Hirata A & Kohno K (2000) Sfb2p, a yeast protein related to Sec24p, can function as a constituent of COPII coats required for vesicle budding from the endoplasmic reticulum. *J Biol Chem* **275**, 17900-17908, doi: 10.1074/jbc.M000751200.

134. Buchanan R, Kaufman A, Kung-Tran L & Miller EA (2010) Genetic analysis of yeast Sec24p mutants suggests cargo binding is not co-operative during ER export. *Traffic* **11**, 1034-1043, doi: 10.1111/j.1600-0854.2010.01080.x.

135. Higashio H, Sato K & Nakano A (2008) Smy2p participates in COPII vesicle formation through the interaction with Sec23p/Sec24p subcomplex. *Traffic* **9**, 79-93, doi: 10.1111/j.1600-0854.2007.00668.x.

136. Jaenisch R & Mintz B (1974) Simian virus 40 DNA sequences in DNA of healthy adult mice derived from preimplantation blastocysts injected with viral DNA. *Proc Natl Acad Sci U S A* **71**, 1250-1254.

137. Capecchi MR (1980) High efficiency transformation by direct microinjection of DNA into cultured mammalian cells. *Cell* **22**, 479-488.

138. Martinell J, Whitney JB, 3rd, Popp RA, Russell LB & Anderson WF (1981) Three mouse models of human thalassemia. *Proc Natl Acad Sci U S A* **78**, 5056-5060.

139. Brinster RL, Chen HY, Trumbauer M, Senear AW, Warren R & Palmiter RD (1981) Somatic expression of herpes thymidine kinase in mice following injection of a fusion gene into eggs. *Cell* **27**, 223-231.

140. Costantini F & Lacy E (1981) Introduction of a rabbit beta-globin gene into the mouse germ line. *Nature* **294**, 92-94.

141. Gordon JW & Ruddle FH (1981) Integration and stable germ line transmission of genes injected into mouse pronuclei. *Science* **214**, 1244-1246.

142. Harbers K, Jahner D & Jaenisch R (1981) Microinjection of cloned retroviral genomes into mouse zygotes: integration and expression in the animal. *Nature* **293**, 540-542.

143. Wagner EF, Stewart TA & Mintz B (1981) The human beta-globin gene and a functional viral thymidine kinase gene in developing mice. *Proc Natl Acad Sci U S A* **78**, 5016-5020.

144. Jankowsky JL, Savonenko A, Schilling G, Wang J, Xu G & Borchelt DR (2002) Transgenic mouse models of neurodegenerative disease: opportunities for therapeutic development. *Current neurology and neuroscience reports* **2**, 457-464.

145. Evans MJ & Kaufman MH (1981) Establishment in culture of pluripotential cells from mouse embryos. *Nature* **292**, 154-156.

146. Bradley A, Evans M, Kaufman MH & Robertson E (1984) Formation of germ-line chimaeras from embryo-derived teratocarcinoma cell lines. *Nature* **309**, 255-256.

147. Thomas KR, Folger KR & Capecchi MR (1986) High frequency targeting of genes to specific sites in the mammalian genome. *Cell* **44**, 419-428.

148. Smithies O, Gregg RG, Boggs SS, Koralewski MA & Kucherlapati RS (1985) Insertion of DNA sequences into the human chromosomal beta-globin locus by homologous recombination. *Nature* **317**, 230-234.

149. Doetschman T, Gregg RG, Maeda N, Hooper ML, Melton DW, Thompson S & Smithies O (1987) Targetted correction of a mutant HPRT gene in mouse embryonic stem cells. *Nature* **330**, 576-578, doi: 10.1038/330576a0.

150. Thomas KR & Capecchi MR (1987) Site-directed mutagenesis by gene targeting in mouse embryo-derived stem cells. *Cell* **51**, 503-512.

151. Mansour SL, Thomas KR & Capecchi MR (1988) Disruption of the proto-oncogene int-2 in mouse embryo-derived stem cells: a general strategy for targeting mutations to non-selectable genes. *Nature* **336**, 348-352, doi: 10.1038/336348a0.

152. Thompson S, Clarke AR, Pow AM, Hooper ML & Melton DW (1989) Germ line transmission and expression of a corrected HPRT gene produced by gene targeting in embryonic stem cells. *Cell* **56**, 313-321.

153. Koller BH, Hagemann LJ, Doetschman T, Hagaman JR, Huang S, Williams PJ, First NL, Maeda N & Smithies O (1989) Germ-line transmission of a planned alteration made in a hypoxanthine phosphoribosyltransferase gene by homologous recombination in embryonic stem cells. *Proc Natl Acad Sci U S A* **86**, 8927-8931.

154. Zijlstra M, Li E, Sajjadi F, Subramani S & Jaenisch R (1989) Germ-line transmission of a disrupted beta 2-microglobulin gene produced by homologous recombination in embryonic stem cells. *Nature* **342**, 435-438, doi: 10.1038/342435a0.

155. Thomas KR & Capecchi MR (1990) Targeted disruption of the murine int-1 proto-oncogene resulting in severe abnormalities in midbrain and cerebellar development. *Nature* **346**, 847-850, doi: 10.1038/346847a0.

156. Skarnes WC, Rosen B, West AP, Koutsourakis M, Bushell W, Iyer V, Mujica AO, Thomas M, Harrow J, Cox T, et al. (2011) A conditional knockout resource for the genome-wide study of mouse gene function. *Nature* **474**, 337-342, doi: 10.1038/nature10163.

157. Lerner A, D'Adamio L, Diener AC, Clayton LK & Reinherz EL (1993) CD3 zeta/eta/theta locus is colinear with and transcribed antisense to the gene encoding the transcription factor Oct-1. *J Immunol* **151**, 3152-3162.

158. Ohno H, Goto S, Taki S, Shirasawa T, Nakano H, Miyatake S, Aoe T, Ishida Y, Maeda H, Shirai T, et al. (1994) Targeted disruption of the CD3 eta locus causes high lethality in mice: modulation of Oct-1 transcription on the opposite strand. *The EMBO journal* **13**, 1157-1165.

159. Branda CS & Dymecki SM (2004) Talking about a revolution: The impact of site-specific recombinases on genetic analyses in mice. *Developmental cell* **6**, 7-28.

160. Hoess RH, Ziese M & Sternberg N (1982) P1 site-specific recombination: nucleotide sequence of the recombining sites. *Proc Natl Acad Sci U S A* **79**, 3398-3402.

161. McLeod M, Craft S & Broach JR (1986) Identification of the crossover site during FLP-mediated recombination in the Saccharomyces cerevisiae plasmid 2 microns circle. *Molecular and cellular biology* **6**, 3357-3367.

162. Sadowski PD (1995) The Flp recombinase of the 2-microns plasmid of Saccharomyces cerevisiae. *Progress in nucleic acid research and molecular biology* **51**, 53-91.

163. Hoess R, Wierzbicki A & Abremski K (1985) Formation of small circular DNA molecules via an in vitro site-specific recombination system. *Gene* **40**, 325-329.

164. Amin A, Roca H, Luetke K & Sadowski PD (1991) Synapsis, strand scission, and strand exchange induced by the FLP recombinase: analysis with half-FRT sites. *Molecular and cellular biology* **11**, 4497-4508.

165. Hoess RH, Wierzbicki A & Abremski K (1986) The role of the loxP spacer region in P1 site-specific recombination. *Nucleic Acids Res* **14**, 2287-2300.

166. Gu H, Marth JD, Orban PC, Mossmann H & Rajewsky K (1994) Deletion of a DNA polymerase beta gene segment in T cells using cell type-specific gene targeting. *Science* **265**, 103-106.

167. Kuhn R, Schwenk F, Aguet M & Rajewsky K (1995) Inducible gene targeting in mice. *Science* **269**, 1427-1429.

168. Crawley JN, Belknap JK, Collins A, Crabbe JC, Frankel W, Henderson N, Hitzemann RJ, Maxson SC, Miner LL, Silva AJ, et al. (1997) Behavioral phenotypes of inbred mouse strains: implications and recommendations for molecular studies. *Psychopharmacology* **132**, 107-124.

169. Wahlsten D, Ozaki HS & Livy D (1992) Deficient corpus callosum in hybrids between ddN and three other abnormal mouse strains. *Neuroscience letters* **136**, 99-101.

170. McVicar DW, Winkler-Pickett R, Taylor LS, Makrigiannis A, Bennett M, Anderson SK & Ortaldo JR (2002) Aberrant DAP12 signaling in the 129 strain of mice: implications for the analysis of gene-targeted mice. *Journal of immunology* **169**, 1721-1728.

171. Pettitt SJ, Liang Q, Rairdan XY, Moran JL, Prosser HM, Beier DR, Lloyd KC, Bradley A & Skarnes WC (2009) Agouti C57BL/6N embryonic stem cells for mouse genetic resources. *Nature methods* **6**, 493-495, doi: 10.1038/nmeth.1342.

172. Green MC, Grueneberg H, Hertwig P, Heston WE, Lyon MF, Medvedev NN, Snell GD & Staats J (1963) A Revision of the Standardized Genetic Nomenclature for Mice. *The Journal of heredity* **54**, 159-162.

173. Seong E, Saunders TL, Stewart CL & Burmeister M (2004) To knockout in 129 or in C57BL/6: that is the question. *Trends in genetics : TIG* **20**, 59-62.

174. Roth DM, Swaney JS, Dalton ND, Gilpin EA & Ross J, Jr. (2002) Impact of anesthesia on cardiac function during echocardiography in mice. *American journal of physiology Heart and circulatory physiology* **282**, H2134-2140, doi: 10.1152/ajpheart.00845.2001.

175. Mekada K, Abe K, Murakami A, Nakamura S, Nakata H, Moriwaki K, Obata Y & Yoshiki A (2009) Genetic differences among C57BL/6 substrains. *Experimental animals / Japanese Association for Laboratory Animal Science* **58**, 141-149.

176. Markel P, Shu P, Ebeling C, Carlson GA, Nagle DL, Smutko JS & Moore KJ (1997) Theoretical and empirical issues for marker-assisted breeding of congenic mouse strains. *Nat Genet* **17**, 280-284, doi: 10.1038/ng1197-280.

177. Laboritory" TJ (2011) B6(Cg)-Tyrc-2J/J-PRX-B6-albino #1 mES cells. In.

178. Skaletsky SRaHJ (2000) *Methods in Molecular Biology*. Humana Press Inc., Totowa, NJ.

179. Osoegawa K, Tateno M, Woon PY, Frengen E, Mammoser AG, Catanese JJ, Hayashizaki Y & de Jong PJ (2000) Bacterial artificial chromosome libraries for mouse sequencing and functional analysis. *Genome research* **10**, 116-128.

180. Taniwaki T, Haruna K, Nakamura H, Sekimoto T, Oike Y, Imaizumi T, Saito F, Muta M, Soejima Y, Utoh A, et al. (2005) Characterization of an exchangeable gene trap using pU-17 carrying a stop codon-beta geo cassette. *Development, growth & differentiation* **47**, 163-172, doi: 10.1111/j.1440-169X.2005.00792.x.

181. Lallemand Y, Luria V, Haffner-Krausz R & Lonai P (1998) Maternally expressed PGK-Cre transgene as a tool for early and uniform activation of the Cre site-specific recombinase. *Transgenic Res* **7**, 105-112.

182. Klenow H & Henningsen I (1970) Selective elimination of the exonuclease activity of the deoxyribonucleic acid polymerase from Escherichia coli B by limited proteolysis. *Proc Natl Acad Sci U S A* **65**, 168-175.

183. Southern EM (1975) Detection of specific sequences among DNA fragments separated by gel electrophoresis. *Journal of molecular biology* **98**, 503-517.

184. Holland PM, Abramson RD, Watson R & Gelfand DH (1991) Detection of specific polymerase chain reaction product by utilizing the 5'----3' exonuclease activity of Thermus aquaticus DNA polymerase. *Proc Natl Acad Sci U S A* **88**, 7276-7280.

185. Bradford MM (1976) A rapid and sensitive method for the quantitation of microgram quantities of protein utilizing the principle of protein-dye binding. *Analytical biochemistry* **72**, 248-254.

186. Liu P, Jenkins NA & Copeland NG (2003) A highly efficient recombineering-based method for generating conditional knockout mutations. *Genome research* **13**, 476-484, doi: 10.1101/gr.749203.

187. Nagafuchi S, Yanagisawa H, Ohsaki E, Shirayama T, Tadokoro K, Inoue T & Yamada M (1994) Structure and expression of the gene responsible for the triplet repeat disorder, dentatorubral and pallidoluysian atrophy (DRPLA). *Nat Genet* **8**, 177-182, doi: 10.1038/ng1094-177.

188. D. CHAN GCS, J. MEI, B. WOLOZIN (2010) LRRK2 associates with RNA stress granules and regulates protein translation In *Neuroscience 2010*, San Diego.

189. Flicek P, Amode MR, Barrell D, Beal K, Brent S, Chen Y, Clapham P, Coates G, Fairley S, Fitzgerald S, et al. (2011) Ensembl 2011. *Nucleic Acids Res* **39**, D800-806, doi: 10.1093/nar/gkq1064.

190. Bernard P, Gabant P, Bahassi EM & Couturier M (1994) Positive-selection vectors using the F plasmid ccdB killer gene. *Gene* **148**, 71-74.

191. Kranz A, Fu J, Duerschke K, Weidlich S, Naumann R, Stewart AF & Anastassiadis K (2010) An improved Flp deleter mouse in C57Bl/6 based on Flpo recombinase. *Genesis* **48**, 512-520, doi: 10.1002/dvg.20641.

192. Suzuki Y & Yazawa I (2011) Pathological accumulation of atrophin-1 in dentatorubralpallidoluysian atrophy. *Int J Clin Exp Pathol* **4**, 378-384.

193. Pieretti M, Zhang FP, Fu YH, Warren ST, Oostra BA, Caskey CT & Nelson DL (1991) Absence of expression of the FMR-1 gene in fragile X syndrome. *Cell* **66**, 817-822.

194. Lefebvre S, Burglen L, Reboullet S, Clermont O, Burlet P, Viollet L, Benichou B, Cruaud C, Millasseau P, Zeviani M, et al. (1995) Identification and characterization of a spinal muscular atrophy-determining gene. *Cell* **80**, 155-165.

195. Kiebler MA & Bassell GJ (2006) Neuronal RNA granules: movers and makers. *Neuron* **51**, 685-690, doi: 10.1016/j.neuron.2006.08.021.

196. Torres-Benito L, Ruiz R & Tabares L (2011) Synaptic defects in SMA animal models. *Dev Neurobiol*, doi: 10.1002/dneu.20912.

197. Antar LN, Afroz R, Dictenberg JB, Carroll RC & Bassell GJ (2004) Metabotropic glutamate receptor activation regulates fragile x mental retardation protein and FMR1 mRNA localization differentially in dendrites and at synapses. *J Neurosci* **24**, 2648-2655, doi: 10.1523/JNEUROSCI.0099-04.2004.

198. Tsai NP, Tsui YC & Wei LN (2009) Dynein motor contributes to stress granule dynamics in primary neurons. *Neuroscience* **159**, 647-656, doi: 10.1016/j.neuroscience.2008.12.053.

199. Vessey JP, Vaccani A, Xie Y, Dahm R, Karra D, Kiebler MA & Macchi P (2006) Dendritic localization of the translational repressor Pumilio 2 and its contribution to dendritic stress granules. *J Neurosci* **26**, 6496-6508, doi: 10.1523/JNEUROSCI.0649-06.2006.

200. Berg LJ & Kang J (2001) Molecular determinants of TCR expression and selection. *Curr Opin Immunol* **13**, 232-241.

201. Wang CL & Wabl M (2004) DNA acrobats of the Ig class switch. *J Immunol* **172**, 5815-5821.

202. Waibler Z, Kalinke U, Will J, Juan MH, Pfeilschifter JM & Radeke HH (2007) TLR-ligand stimulated interleukin-23 subunit expression and assembly is regulated differentially in murine plasmacytoid and myeloid dendritic cells. *Mol Immunol* **44**, 1483-1489, doi: 10.1016/j.molimm.2006.09.001.

203. Wang B, Malik R, Nigg EA & Korner R (2008) Evaluation of the low-specificity protease elastase for large-scale phosphoproteome analysis. *Anal Chem* **80**, 9526-9533, doi: 10.1021/ac801708p.

204. Wise A & Gilburt DJ (1982) Phytate hydrolysis by germfree and conventional rats. *Appl Environ Microbiol* **43**, 753-756.

205. Dephoure N, Zhou C, Villen J, Beausoleil SA, Bakalarski CE, Elledge SJ & Gygi SP (2008) A quantitative atlas of mitotic phosphorylation. *Proc Natl Acad Sci U S A* **105**, 10762-10767, doi: 10.1073/pnas.0805139105.

206. Gauci S, Helbig AO, Slijper M, Krijgsveld J, Heck AJ & Mohammed S (2009) Lys-N and trypsin cover complementary parts of the phosphoproteome in a refined SCX-based approach. *Anal Chem* **81**, 4493-4501, doi: 10.1021/ac9004309.

207. Wu X, Tu X, Joeng KS, Hilton MJ, Williams DA & Long F (2008) Rac1 activation controls nuclear localization of beta-catenin during canonical Wnt signaling. *Cell* **133**, 340-353, doi: 10.1016/j.cell.2008.01.052.

208. Poueymirou WT, Auerbach W, Frendewey D, Hickey JF, Escaravage JM, Esau L, Dore AT, Stevens S, Adams NC, Dominguez MG, et al. (2007) F0 generation mice fully derived from gene-targeted embryonic stem cells allowing immediate phenotypic analyses. *Nat Biotechnol* **25**, 91-99, doi: 10.1038/nbt1263.

209. Varfolomeev EE, Schuchmann M, Luria V, Chiannilkulchai N, Beckmann JS, Mett IL, Rebrikov D, Brodianski VM, Kemper OC, Kollet O, et al. (1998) Targeted disruption of the mouse Caspase 8 gene ablates cell death induction by the TNF receptors, Fas/Apo1, and DR3 and is lethal prenatally. *Immunity* **9**, 267-276.

210. Xue Y, Gao X, Lindsell CE, Norton CR, Chang B, Hicks C, Gendron-Maguire M, Rand EB, Weinmaster G & Gridley T (1999) Embryonic lethality and vascular defects in mice lacking the Notch ligand Jagged1. *Hum Mol Genet* **8**, 723-730.

211. Dolgin E (2010) The knockout rat pack. *Nat Med* **16**, 254-257, doi: 10.1038/nm0310-254.

212. Shih NY, Li J, Karpitskii V, Nguyen A, Dustin ML, Kanagawa O, Miner JH & Shaw AS (1999) Congenital nephrotic syndrome in mice lacking CD2-associated protein. *Science* **286**, 312-315.

Supplement

Abbreviations

Abbreviation	Name
3'UTR	3'untranslated region
AA	Amino acids
ACN	Acetonitril
Ago	Argonaut2
AMBA	Acrylamid/N,N'-methylen-bis-acrylamid
Amp	Ampicillin
APC	Antigen presenting cells
BCR	B cell receptor
bHLH	Basic helix-loop-helix
BL6	C57BL/6
BM	Bone marrow
BPS	Branch point sequence
BSA	Bovine serum albumin
C. elegans	Caenorhabditis elegans
CD	Cluster of differentiation
CD2BP2	CD2 binding protein 2
CHO	Chinese hamster ovary
CLP	Common lymphoid progenitor
CNS	Central nervous system
COPII	Coat protein complex II
CTD	Carboxyl-terminal domain

DC	Dendritic cells
DN	Double negative
DNA	Deoxyribonucleic acid
DP	Double positive stage
DRPLA	Dentatorubral-pallidoluysian atrophy
E	Embryonic day
ECFP	Enhanced cyan fluorescence protein
eIF4E	Elongation initiation factor 4 E
ER	Endoplasmatic Reticulum
ES cells	Embryonic stem cells
ETP	Early T lineage progenitors
EVH1	Enabled/WASP homology
EYFP	Enhanced yellow fluorescence protein
FACS	Fluorescence activated cell sorting
fam	6-carboxyfluorescein
FCS	Fetal calf serum
FITC	Fluoresceinisothiocyanat
FRT	Flip recombinase recognition target
FSC	Forward scatter
GEF	Guanine nucleotide exchange factor
GFP	Green fluorescence protein
GIGYF2	GRB-10 interacting GYF protein 2
GST-tag	Glutathion-S-Transferase-Tag
GTPase	Small guanosine triphosphate
GYF	Standing for conserved Gly, Trp, Phe motif
His-tag	Histidin-tag

HPRT	Hypoxanthin-Phosphoribosyl-Transferase
HSC	Hematopoietic stem cell
HSV	Herpes simplex virus
IFN-α	Interferon α
IGF-1	Insulin growth factor-1
IKMC	International Knockout Mouse Consortium
IL-7Rα	IL-7 receptor α
IP	Immunoprecipitation
IPTG	Isopropyl-β-D-thiogalactopyranosid
Kan	Kanamycin
kD	Kilo dalton
LDH	Lactate dehydrogenase A
LN	Lymph node
loxP sites	Locus of crossover (x) in P1
LRRK2	Leucine-rich repeat kinase 2
MAF	Murine Adult Fibroblasts
MALT	Mucosa-associated lymphoid- tissue
MEF	Murine Embryonic Fibroblasts
MFI value	Median fluorescence value
MHC I	Major histocompatibility complex I
miRNA	MicroRNA
MMLV	Moloney murine leukemia virus
MS	Mass Spectrometry
neo	Neomycin
NK cells	Natural killer cells
NLS	Nuclear localization signal

Npw38	38 kD nuclear protein containing a WW domain
NpwBP	Npw38 binding protein
OD	Optical density
P-bodies	Processing bodies
Pabp	Poly (A) binding protein
PAC	Bacteriophage P1 artificial chromosome
PBMCs	Peripheral blood mononuclear cells
PBS	phosphate buffer saline
PD	Parkinson's disease
PECAM-1	platelet endothelial cell adhesion molecules-1
PERQ2	PERQ amino acid-rich with GYF domain containing protein 2
pI	Isoelectric point
pI-pC	Polyinosinic poly-cytidylic acid
PP1	Protein phosphatase 1
PPII	Polyproline type II helices
PQBP-1	Polyglutamine-binding protein 1
PRD	Proline-rich sequence recognition domains
PRS	Proline-rich sequences
PTM	Post-translational modifications
RISC	RNA-induced silencing complex
RNA	Ribonucleic acid
RNP	Ribonucleoproteins
RT	Room temperature
S. pombe	Schizosaccharomyces pombe
SCA1	Spinocerebellar ataxia type 1
SDS-PAGE	Sodium dodecyl sulfate polyacrylamide gel electrophoresis

SG	Stress granules
SH3	Src homology 3
SILAC	Stable isotope labeling in cell culture
SIPP1	Splicing factor that interacts with PQBP-1 and PP-1
siRNA	Small interfering RNA
SMA	Spinal Muscular Atrophy
SMY2	Suppressor of myosin 2
SNP	Single nucleotide polymorphism
snRNPs	Small nuclear ribonulear particles
SP1	Transcription factor SP1
SS	Splice site
SSC	Sideward scatter
SSR	Site-specific recombination
Tamara	Tetramethylrhodamine
Tbc1d10b	TBC1 domain family member 10B
TCR	T cell receptor
T_H2	T helper cells
TK	Thymidine Kinase
UEV	Ubiquitin E2 variant
WT	Wildtype
WW	Standing for conserved Trp-Trp motif

Table X.0.1. Abbreviations used in this study

Sequence of pPNT4-CD2BP2

5’gctcgaaattaaccctcactaaagggaacaaaagctggagctccaccgcggtggcggcctaggcctcactggccgtcgagtttaaacggccggccaccaggtgcggccgcggtaccagcttttgaggtt
agtttggaacttgatgtgagagtactgatccagggttaggggcagatttgatgattgccatcttctgtactccccttaggcaacaggacctgtaccgaatcctgaaggcctataccatctacaggcctgacgaggg
ctactgtcaggcccaggccccagtggctgcggtgttgctaatgcacatgcctgctgaggtcagcataagtggacctgtttggggtgggggtgagaagatatagacataccatggtgaagggagagctgcata
ctccctgcttctcaggccccatccctgcctcttgttcttgcccttcttagcaagcgttttggtgcctggtacagatctgcgacaagtacctcccaggttactacagtgcagggctggtgagtgtctggaagctgggt
gcactggggctgccttaggaccttgccctgcctcatttgtccttctgtccctcgaccattgaggttaagacagcctcttaggtttgattgtaccctgaggggaccacagcaaaccagacccacttcttatagctcttc
ccaccgcctctaggaagccattcagttggatggagaaatctttttgcactcctgcgccgggtctctccgctggcacatcgtcaccttcggcggcagcgcattgaccctgtgctctacatgacagagtggttcatg
tgcatctttgcccgcaccctccccctgggcttcagtgctgcgtgtctgggacatgtttttctgtgaaggtatttcagtggctggccaggctgaggggggaggctaggatttgttacttactggtatcccatagacaagt
attgttgggcctaggcttcataataaactctgcagtttggaaaaacagggcctatcttggtttggccaccagcctagagtctgcttgccctccaagaaatcttcagctgtaaggctggcaggcatcagcagcagca
gggctgtttgcctccataagacagcggaggtcctggacctgatttctctttgcattcttctctgaccctgtaggcgttaagatcatcttccgagtggctctggttttactgcggcacacactgggttctgtggaaaagc

tgcgctcatgtcaaggcatgtatgaaaccatggagcagcttcgaaacctaccacaacagtgtatgcaggaggacttcctggtgcatgaggtaggccatgagcctcagcacaccctgacctgcttcagcccatt
cccacacaggtctacactctggcttccatgtctctgtctaggtaaccaacctcccagtgacagaagcatggattgagcgggagaatgcagcccaactgaagaagtggcgagaaactagaggagagctgcagt
atcggccctcacggcgactacacggctcccgagccatccatgaggaacgcaggcggcagcagccacccctgggcccttcctctagcctcctcagcctccctagtctcaagagcagaggctcccgggcagt
tggagggggctccttccccaccacctcctgtccgcagggctagtgctgggcccgtccctggggctgtcgtcattgctgagggactgcatccatccctttccttcacctactggtaacagcaccccactaggcacca
gcaaggagatcaggcggcaggagaaagagcggcagaaacaggagaaagatcgagagaaggagcggcagagacaagagaaggagcgggaaaggcaggagaaggagcggcagaagtgggaaaa
ggagcaagagaaggaacagcagaagcaggagaaggagcggcagaagctggagaagaaaggccaaggccggaaactgtccttgcgtcgaagggcagatgggccccggcatcccatgatggtgggg
acaggtcagcagctgaggcccggcaggatgcttacttttgacctctggttggatctggatggcatggccctcctccttccctcatcgagagcagccctggcaggctctcccagctccccttggcaggctcttcc
tttttctgaggaaagtggcttgattccctgactccttgccagctgctgatccgtacatggccaggacagccacagtgcaagggacagctgcattacctagggtaacagtgaccaagtctggagaccctttgtc
cagttaggctcagcttgggtctctgtcacacctatgaaatccttctggggtgctgtcttacactccggtggcttcccttagatggtggagctaggttccttttcctgtcttggggccctgcctgtcaccccactgccta
ctgggggccaaggctgttttctctcctggatatccttgtgttgtaattatgtacagaaggtcaggttggcctggggtgggtgctgtccttttccctctccacagcgctgcttcactccagtttatttaagaggatatgct
aggaagtgtcctccgtctccttcccacccgtgccctgctctctcctaactcacttgctttgtatgctcaggcctctctgctgcagtcacaaagtctgtcttcgattttgttcctttctagccatcaagccctctctgaata
agggtcttcccttgagtccaggggtggaacccaatgtttacattctcttctgtcttggtcccacctcagtggcagttttgtggcgctttgaggaaccggaaaatgaacctgctgttatatctgtctcccgccttgttattt
gaagagtgctgtagagtaagggggagtggggagggcaggcacaaagtctgactttccataggttcagtctgcaggtcttggcaggaacatctggaccactggttctcaatcttcctaatgctgtgaccctttaata
cagttctttatattgtggtgactccaaccataaaattattttcattattacttaataacagtatactactgctatgaatcataatgtacgtctctgttttctgatagtcttaggcaacctctgtgaatagtattcgaccccccaaa
aggagtcacagtaaacgctcacttcatctctcatcaacaaacatagtggtccagctccttcctcctcagctttgcctggattctgctgctcccactctcactggcctcctgggatcctctgcacagcttgcaggactg
ggatcgcctttccaatggcttcagcccccctggaagctgaaggaggggcctgagagtgtgtgcaaaaccaccatctttagattgggctgggttcttggtcagcagcttggtgcagttccctgggcgtctagggta
gactaactgcctggggttcatcccagcaggtacacacaaccaaactgcgcagctcttgttttctgtggctagatctttgccacacaccctctactccgggtcaggatgataaaggtgtgggcttctgtggccgtaa
agctccacttggcacttctcagcagaaaggggatcagggtgtgtggtctccaggtagagaaaaccccctccggatgaaccagcagtgctgagagctgctttcttcagggtcctgtctgtagcaagatgccctcc
tggtctagaacttgtgttctgtacccacagaagtgaagtttcatgattcacaatgggagaaaaccctggaggagaaaggcgtggtccatctggctgccctcttccaactctagtaggatcaccggagctatttagc
cgagggtggggacgggggtggaggcgttgaggtttgagttgttccccagagctccgtcgacggccgcataacttcgtatagcatacattatacgaagttatcgaagttcctattctctagaaagtataggaactt
caagctaattctaccgggtagggaggcgcttttcccaaggcagtctggagcatgcgctttagcagccccgctgggcacttggcgctacacaagtggcctctggcctcgcacacattccacatccaccggtag
gcgccaaccggctccgttctttggtggcccccttcgcgccaccttctactcctcccctagtcaggaagttcccccccgccccgcagctcgcgtcgtgcaggacgtgacaaatggaagtagcacgtctcactagtc
tcgtgcagatggacagcaccgctgagcaatggaagcgggtaggcctttggggcagcggccaatagcagctttgctccttcgctttctgggctcagaggctgggaaggggtgggtccgggggcgggctcag
gggcgggctcaggggcggggcgggcgcccgaaggtcctccggaggcccggcattctgcacgcttcaaaagcgcacgtctgccgcgctgttctcctccttcctcatctccgggcctttcgacctgcagccaat
atgggatcggccattgaacaagatggattgcacgcaggttctccggccgcttgggtggagaggctattcggctatgactgggcacaacagacaatcggctgctctgatgccgccgtgttccggctgtcagcg
caggggcgcccggttctttttgtcaagaccgacctgtccggtgccctgaatgaactgcaggacgaggcagcgcggctatcgtggctggccacgacgggcgttccttgcgcagctgtgctcgacgttgtcact
gaagcgggaagggactggctgctattgggcgaagtgccggggcaggatctcctgtcatctcaccttgctcctgccgagaaagtatccatcatggctgatgcaatgcggcggctgcatacgcttgatccggcta
cctgcccattcgaccaccaagcgaaacatcgcatcgagcgagcacgtactcggatggaagccggtcttgtcgatcaggatgatctggacgaagagcatcaggggctcgcgccagccgaactgttcgccag
gctcaaggcgcgcatgcccgacggcgaggatctcgtcgtgacccatggcgatgcctgcttgccgaatatcatggtggaaaatggccgcttttctggattcatcgactgtggccggctgggtgtggcggaccg
ctatcaggacatagcgttggctacccgtgatattgctgaagagcttggcggcgaatgggctgaccgcttcctcgtgctttacggtatcgccgctcccgattcgcagcgcatcgccttctatcgccttcttgacgag
ttcttctgaggggatcaattctctagagctcgctgatcagcctcgactgtgccttctagttgccagccatctgttgtttgcccctccccgtgccttccttgaccctggaaggtgccactcccactgtccttcctaata
aaatgaggaaattgcatcgcattgtctgagtaggtgtcattctattctgggggggtgggtggggcaggacagcaagggggaggattgggaagacaatagcaggcatgctggggatgcggtgggctctatgg
cttctgaggcggaaagaaccagctggggctcgatcgagatccgaagttcctattctctagaaagtataggaacttccgggatcctgcaggcacgagctccagatctaaacctcactattggggaagatctcac
ctggccccagctttgcaggagctggatcccagccctttggcagtttgctaagggatgaggtaggcttcgtgtaactgatgggcttctgcctggttacaggccacggacggaagccagtggcacctcctgtgatg
gttgtcccgctacagaaactaggaattaagtgggagaatagacatggtgcaaatgactcctgggttctaaaagggcttggtttggaaggtgcccgagcgcttataatcagaagcaggactcagagagaagag
caagacttttcttaaaaatagacggtctcatgttgtatcccagactgtcgtcaatctcgcgacaatcaatcctgtttcaatttcccgagtgttgggactgcgttaagatcggaagcccgggtgtctactgaaggccac
taggcgtacagaacccctatccatacatgcaaacggaagcccgaagcctctgttcggcctgtgcctctccatccaggccttgggaacctcttagcacaccacgctccttatcctcactgtagcctccatgtagagg
aataataaaacatttcccgccatcctcaagtcccgtgaggcaaggacgtagttcacgcgagtctttgcaggtcttgcgtcacttcctgccgcgagtcggccttggctaatggtatgcatccgccctttttgaataga
agtgaagccacttccgggtcctatgccggtctccacggttttttccgggtgatgaaggcgggtgccccggatgtaataccggcgaaagcatctttccttttcttccccgcctgaccctgggttcctaggtgagca
ccggcgggtaagattgtttgaatccccgcgggtttgcttcgccttagtttgtacgccaaggacatggccgagcaggtcgctacgtggtattcggggatctaggcagctccagctcttgggtccgaccggcctct
gtgagcactcgggtgggagaggtggttgagttcggtagctccggactggtaggggagtggtgacgtaggggaacctgactccccatccccgggtgggaatacccgcagggtccacgcgggggcggaga
tccttcccatcgcctctcctccgggcctcagaattgcccaaccaaccccggacgtcgtgcctgctagttctctcagatgctttagcgatctgtcctcgctcacatttaccaggaaaaatgttggtggcccctgcact
cccccgcggtcctctctccttacctcacttcctcactacatatcttttccgaggtccagctggaggaaatccacagccaatcatgccaaagaggaaagtgacttttcagggtgttggagatgaggatggtgaaga
tgaaatcagtgtgcccaaaaagaaggtgagatggccagatttcgaatttccgtggaggactgagaggaaagaaggaggaaatctgatgggaggaaagccgggaagccaaggaagtgttagttttccccg
gcgcactgggtttggaaagatttgtgtacagatcctggagtatctggggaactacccagttggctgcatttctcatttgcttcggcctcctcacagctggtggaccctgtggctgcagcaggtggtcctgggagcc
gcttcaaaggcaagcactctttagacagtgatgaagaggatgatgatgaggaagggtccagcaaatatgatatcctggcctcagaggatgtagaaggtgagctatgtccgaagcgttaacataacttcgtatag
catacattatacgaagttatgaattcgttaactgagttgggggacaagccttcaggatggaggtgggaggtgtgcctgcttccctttgcgtgtctagcatgccccaccccccaatgtcttcggtgcaggtcagga
agcagctactctccctagtgagggcggtgtgaggatcacaccccttcaacctgcaggaagagatggaggaaggccacttttgatgctgatggcaactacttcctgaaccaggatgcgcagatccgagacagctg
gctggacaacattgactgggtgtggcccagggactattctggctgaggcctgggagtgcaggtgcagggcctgggccctggtggaagtttgtaagaaattctaattatcttttccttgtaggtgaggatcaagga
acggcccccctgataagcaccaggtttcagactcggaggaggaagacagcctgggtcagactccaatgagcgcccaagcactcctggagggacttttggagttgttgttgccaagagagacagtggctgggg
cccttaggcggctgggggcccgaggaggaggcaaagggagcaacagcaaggggactggacggcccaattccccccagcggctagaccggctgtctgggttagctgaccaaatggtggcacgaggcaa
ccttggtgtgtaccaggaaacaagggaacggttggctatgcgactgaagggtttggggtgtcgggcccagggatccatgacccacacctccacccctccctggacatgtttgctgaggaagtagcagagg
gtgaactggaaacccaacccctacccaaagagagggtaagtttggagggcacgggtgggggcagtgtgggctggagactgagtgcttgaggcccaagtatcgttcattgtgttagaggcagagtcagc
aggagatggcctgatggatgtgatgtgggagtataaatgggagaacacgggggacgccgagctgtatggaccttcaccagtgcccagatgcaggtgagctgcccccgccgcgtctgtcccatctgtcca
gcccaccttctgtcagcttgcctgagttctgtcctctgttcttacagacgtgggtgagtgaaggttacttcccggatggtgtttattgtcggaagctggacccctccgggcggccagttctacaactccaagcgcatt
gattttgagctgtacacgtgagcccgctaagggccccatgcggcacggcagccccttctttcttgaacttggcagaggaagccccagctgctctgggcagtgaggatattggaggccactttaaagccattgttt
cccaataaaagccttgactgtgcgatggccaagagccaggcttctccatagctccttttggcttcacctggtaggtccctgagcgtttcttcccgagagacttcctcacttgcttctctctggtgtcttggaccacct
cagttttttttcccaccctggaggcagaggtagggcccatcagatgtcctgtgacttttcctacgtagacaacttctacttgctgtgtaaaattccctccatcactctttctccagtctcccttgcaagtccctgttctgc
tgatctttgacttttaggacctcaaatgctctgtcctggcagctcccttgtagctgggacattgggaagaccttgaaatcctattgagagattctcttaaacatgcattctcttcttccatagtctgatttttctaccctcg
ccccctgcagtagcttctgtagcttttaggtgaagtataaacttggtagcacttcaaggttgcttgagccaccatgtgacacagaggggggcaaagtgcagtggcttattggagatgccacagtaatagagagc
tggccatggagctaagtctcctgaccttttttggcataaagcttgtaccgagctcgtggcgccgcctgagaaattctaccgggtaggggaggcgcttttcccaaggcagtctggagcatgcgctttagcagccc
cgctgggcacttggcgctacacaagtggcctctggcctcgcacacattccacatccaccggtaggcgccaaccggctccgttctttggtggcccctttcgcgccaccttctactcctcccctagtcaggaagttc
ccccccgccccgcagctcgcgtcgtgcaggacgtgacaaatggaagtagcacgtctcactagtctcgtgcagatggacagcaccgctgagcaatggaagcgggtaggcctttggggcagcggccaatag
cagctttgctccttcgctttctgggctcagaggctgggaaggggtgggtccgggggcgggctcagggggcgggctcagggggcggggcgggcgcccgaaggtcctccggaggcccggcattctgcacgctt
caaaagcgcacgtctgccgcgctgttctcctccttcctcatctccgggcctttcgacctgcagcgacccgcttaacagcgtcaacagcgtgccgcagatcttggtggcgtgaaactcccgcacctcttcggccag
cgccttgtagaagcgcgtatggcttcgtaccccctgccatcaacacgcgtctgcgttcgaccaggctgcgcgttctcgcggccataacaaccgacgtacggcgttgcgccctcgccggcaacaaaaagccac
ggaagtccgcctggagcagaaaatgcccacgctactgcgggtttatatagacggtccccacgggatggggaaaaccaccaccacgcaactgctggtggccctgggttcgcgcgacgatatcgtctacgtac
ccgagccgatgacttactggcgggtgttgggggcttccgagacaatcgcgaacatctacaccacacaacaccgcctcgaccagggtgagatatcggccggggacgcggcggtggtaatgacaagcgccc
agataacaatgggcatgccttatgccgtgaccgacgccgttctggctcctcatatcgggggggaggctgggagctcacatgcccgcccccggcccctcaccctcatcttcgaccgccatccgcgccc
tcctgtgctaccccggccgcgcgataccttatgggcagcatgaccccccaggccgtgctggcgttcgtggccctcatcccgccgaccttgcccggcacaaacatcgtgttgggggcccttccggaggacaga
cacatcgaccgcctggccaaacgccagcgccccggcgagcggcttgacctggctatgctggccgcgattcgccgcgtttatgggctgcttgccaatacggtgcggtatctgcagggcggcgggtcgtggc
gggaggattggggacagctttcgggggcggccgtgccgccccagggtgccgagccccagagcaacgcgggcccacgacccatatcggggacacgttatttaccctgtttcgggccccgagttgctgg
ccccccaacggcgacctgtataacgtgtttgcctgggctttggacgtcttggccaaacgcctccgtcccatgcatgtctttatcctggattacgaccaatcgcccgccggctgccgggacgccctgctgcaactta
cctccgggatggtccagacccacgtcaccaccccaggctccataccgacgatctgcgacctggcgcgcacgtttgcccgggagatgggggaggctaactgaaacacggaaggagacaataccggaagg

aacccgcgctatgacggcaataaaaagacagaataaaacgcacgggtgttgggtcgtttgttcataaacgcggggttcggtcccagggctggcactctgtcgataccccaccgagaccccattgggaccaat
acgcccgcgtttcttccttttccccaccccaaccccccaagttcgggtgaaggcccagggctcgcagccaacgtcggggcggcaagccctgccatagccacgggccccgtgggttagggacggggtccccc
atggggaatggtttatggttcgtgggggttattattttgggcgttgcgtggggtcaggtccacgactggactgagcagacagacccatggtttttggatggcctgggcatggaccgcatgtactggcgcgacac
gaacaccgggcgtctgtggctgccaaacaccccgacccccaaaaaccaccgcgcggatttctggcgccgccggacgaactaaacctgactacggcatctctgccccttcttcgctggtacgaggagcgct
tttgttttgtattggtcaccacggccgagtttccgcgggaccccggccaggacctgcagaaattgatgatctattaaacaataaagatgtccactaaaatggaagtttttcctgtcatactttgttaagaagggtgag
aacagagtacctacattttgaatggaaggattggagctacgggggtgggggtggggtgggattagataaatgcctgctctttactgaaggctctttactattgctttatgataatgtttcatagttggatatcataattt
aaacaagcaaaaccaaattaagggccagctcattcctcccactcatgatctatagatctatagatctctcgtgggatcattgtttttctcttgattcccactttgtggttctaagtactgtggtttccaaatgtgtcagtttc
atagcctgaagaacgagatcagcagcctctgttccacatacacttcattctcagtattgttttgccaagttctaattccatcagaagcttggcactggccgtcgttttacaacgtcgtgactgggaaaaccctggcgt
tacccaacttaatcgccttgcagcacatccccctttcgccagctggcgtaatagcgaagaggcccgcaccgatcgcccttcccaacagttgcgcagcctgaatggcgaatggcgcctgatgcggtatttttctcc
ttacgcatctgtgcggtatttcacaccgcatatggtgcactctcagtacaatctgctctgatgccgcatagttaagccagccccgacacccgccaacacccgctgacgcgccctgacgggcttgtctgctcccg
gcatccgcttacagacaagctgtgaccgtctccgggagctgcatgtgtcagaggttttcaccgtcatcaccgaaacgcgcgagacgaaagggcctcgtgatacgcctatttttataggttaatgtcatgataataa
tggtttcttagacgtcaggtggcacttttcggggaaatgtgcgcggaacccctatttgtttatttttctaaatacattcaaatatgtatccgctcatgagacaataaccctgataaatgcttcaataatattgaaaaagga
agagtatgagtattcaacatttccgtgtcgcccttattcccttttttgcggcattttgccttcctgtttttgctcacccagaaacgctggtgaaagtaaaagatgctgaagatcagttgggtgcacgagtgggttacatc
gaactggatctcaacagcggtaagatccttgagagttttcgccccgaagaacgttttccaatgatgagcacttttaaagttctgctatgtggcgcggtattatcccgtattgacgccgggcaagagcaactcggtc
gccgcatacactattctcagaatgacttggttgagtactcaccagtcacagaaaagcatcttacggatggcatgacagtaagagaattatgcagtgctgccataaccatgagtgataacactgcggccaacttac
ttctgacaacgatcggaggaccgaaggagctaaccgcttttttgcacaacatgggggatcatgtaactcgccttgatcgttgggaaccggagctgaatgaagccataccaaacgacgagcgtgacaccacga
tgcctgtagcaatggcaacaacgttgcgcaaactattaactggcgaactacttactctagcttcccggcaacaattaatagactggatggaggcggataaagttgcaggaccacttctgcgctcggcccttccgg
ctggctggtttattgctgataaatctggagccggtgagcgtgggtctcgcggtatcattgcagcactggggccagatggtaagccctcccgtatcgtagttatctacacgacggggagtcaggcaactatggat
gaacgaaatagacagatcgctgagataggtgcctcactgattaagcattggtaactgtcagaccaagtttactcatatatactttagattgatttaaaacttcatttttaatttaaaaggatctaggtgaagatccttttg
ataatctcatgaccaaaatcccttaacgtgagttttcgttccactgagcgtcagaccccgtagaaaagatcaaaggatcttcttgagatcctttttttctgcgcgtaatctgctgcttgcaaacaaaaaaaccaccgct
accagcggtggtttgtttgccggatcaagagctaccaactctttttccgaaggtaactggcttcagcagagcgcagataccaaatactgtccttctagtgtagccgtagttaggccaccacttcaagaactctgtag
caccgcctacatacctcgctctgctaatcctgttaccagtggctgctgccagtggcgataagtcgtgtcttaccgggttggactcaagacgatagttaccggataaggcgcagcggtcgggctgaacgggggg
ttcgtgcacacagcccagcttggagcgaacgacctacaccgaactgagatacctacagcgtgagctatgagaaagcgccacgcttcccgaagggagaaaggcggacaggtatccggtaagcggcagggt
cggaacaggagagcgcacgagggagcttccagggggaaacgcctggtatctttatagtcctgtcgggtttcgccacctctgacttgagcgtcgatttttgtgatgctcgtcaggggggcggagcctatggaaa
aacgccagcaacgcggcctttttacggttcctggccttttgctggccttttgctcacatgttctttcctgcgttatcccctgattctgtggataaccgtattaccgcctttgagtgagctgataccgctcgccgcagccg
aacgaccgagcgcagcgagtcagtgagcgaggaagcggaagagcgcccaatacgcaaaccgcctctccccgcgcgttggccgattcattaatgcagctggcacgacaggtttcccgactggaaagcgg
gcagtgagcgcaacgcaattaatgtgagttagctcactcattaggcaccccaggctttacactttatgcttccggctcgtatgttgtgtggaattgtgagcggataacaatttcacacaggaaacagctatgaccat
gattacgccaa’3

Figure X.1. **Sequence of the final pPNT4-CD2BP2 vector**. The 5’Homology is shown in violet, the loxP site in yellow, the FRT site in grey, the Neo cassette in red, the 3’Homology in dark violet and the Thymidine cassette in green.

Acknowledgement

Zunächst möchte ich mich herzlich bei Prof. Christian Freund für vier Jahre finanzielle und mentale Unterstützung bedanken, der mich auch durch die tiefen Täler meines Projekts begleitet hat. Wenn ich nur ansatzweise so viel Freude und Motivation am Forschen behalte, wie Christian es bis heute hat wäre ich hoch zufrieden.

Des weiteren möchte ich mich bei meinem Kollegen bedanken. Ohne Kirill wäre mein Maus Targeting Vektor niemals entstanden- es leben die russischen Klonierungstricks. Katharina und Kathrin haben mich schon in frühen Morgenstunden unterstützt und waren immer für mich da, egal mit welchen Sonderwünschen ich kam, danke!

Bei meiner gesamten Gruppe möchte ich mich dafür bedanken, dass sie sich immer geduldig meiner Mausprobleme angenommen haben und trotz der Fachfremdheit mich mit guten Vorschlägen unterstützt haben. Andreas, Bernhard und Dani möchte ich herzlich für ihre Unterstützung beim Erzeugen dieser Arbeit danken. Bernhard, als Meister des Words und Andreas als kritischer Leser. Liebe Dani, tausend Dank für deine Hilfe und deine kulinarische Verköstigung!

Mein Dank gilt außerdem der Steglitz-Gang von 2007, als alles begann. Knobi, Nicolas, Ronny, Marcus und Philliph, danke für die tolle Zeit mit euch- auch wenns diese Maus dann doch nicht gewesen ist. Knobi, vielen Dank für deine Unterstützung und dass du mich immer wieder beruhigt und mir gut zugesprochen hast. Du hast mich gelehrt, dass der Kampf an der Bench gewonnen wird! Nicolas, ich danke dir sehr für die vielen Telefonate, bei denen du mich immer unterstützt und aufgebaut hast!

Einen riesiger Dank auch an die gesamte Arbeitsgruppe Müller/ Dechend am ECRC. Danke, dass ihr mich wie ein Gruppenmitglied aufgenommen habt und mir mit Rat und Tat zur Seite standet. Mein besonderer Dank gilt hier Florian, der mich in Zeiten unterstützt hat, als ich dachte, dass alles vorbei sei. Danke, dass du an mich geglaubt hast! Bei Basti möchte ich mich herzlichen für seine tierärztliche Weisheit bedanken. Es ist mir immer wieder eine Freude mit dir zu präppen. Und natürlich tausend Dank an Dominik, für die vielen anregenden Diskussionen und, dass du dich als Zweitgutachter zur Verfügung gestellt hast!

Bei Susann möchte ich mich für ihre Hilfe beim FACSen, bei Alexandra für ihre unendliche Geduld während der Embryonenpräpp bedanken. Johanna danke ich sehr für ihre zuverlässige Hilfe bei der Genotypisierung und der generellen Unterstützung im Labor.

Mein allergrößter Dank für technische Unterstützung gilt der gesamten transgenic core facility am MPI in Dresden, insbesondere Ronald Naumann. Es ist wohl nicht übertrieben zu sagen, dass es ohne dich, lieber Ronald, keine CD2BP2 KO Maus geben würde. Danke für die tolle Unterstützung in den letzten Jahren. Ich hoffe auf eine fruchtvolle Zusammenarbeit in der Zukunft.

Thanks a lot to all the reviewers of this script. Trent, thank you for great support for the introduction. Johannes Wilbertz, thanks a lot for your dedicating work on the mouse part. This part is definitely suitable for the transgenic society now! Jim Sudmeier, you followed my life since I was five years old and it really meant a lot to me that you helped me now, again, with my Thesis. Times with you in Boston are always the best. Thanks a lot!

Abschließend möchte ich mich bei meiner Familie und meinen engen Weggefährten bedanken. In eine Familie geboren zu sein, wo die Forschung zum Alltag dazu gehört ist wohl nicht jedem vergönnt. Ich hatte dieses Glück und weiß es sehr zu schätzen. Danke außerdem an Kathrin, Andrea, Harry und vor allem Yvonne, dass ihr mich in den letzten Monaten immer wieder auf andere Gedanken gebracht habt und immer ein Ohr für mich hattet.

Publications/ Posters/ Awards

Publications

Publications submitted during this study

Ash MR, Faelber K, Kosslick D, **Albert GI,** Roske Y, Kofler M, Schuemann M, Krause E & Freund C (2010) Conserved beta-hairpin recognition by the GYF domains of Smy2 and GIGYF2 in mRNA surveillance and vesicular transport complexes. *Structure* **18**, 944-954, doi: 10.1016/j.str.2010.04.020.

Searle J, Mockel M, Gwosc S, Datwyler SA, Qadri F, **Albert GI**, Holert F, Isbruch A, Klug L, Muller DN, et al. (2011) Heparin Strongly Induces Soluble fms-Like Tyrosine Kinase 1 Release In Vivo and In Vitro. *Arterioscler Thromb Vasc Biol*, doi: 10.1161/ATVBAHA.111.237784.

Publications submitted before this study

Albert GI, Hoeller U, Schierle J, Neuringer M, Johnson EJ & Schalch W (2008) Metabolism of lutein and zeaxanthin in rhesus monkeys: identification of (3R,6'R)- and (3R,6'S)-3'-dehydro-lutein as common metabolites and comparison to humans. *Comparative biochemistry and physiology Part B, Biochemistry & molecular biology* **151**, 70-78, doi: 10.1016/j.cbpb.2008.05.014.

Posters presented during this study

10th Transgenic Technology Meeting, St. Pete Beach, Florida (October 2011)

Poster: "Characterization of the GYF-domain containing protein CD2BP2"

FG806 Forschergruppensymposium in Kremmen, Germany (June 2009)

Poster: "Functional characterization of GYF domain containing proteins"

11th PhD Retreat of MDC and FMP, Kremmen, Germany (September 2009)

Poster: "Characterization of CD2BP2 and GIGYF2"

Joint Symposium of MDC and FMP, Berlin, Germany (April 2009)

Poster: "Creation of a conditional KO system of GYF domains"

10th PhD Retreat des FMP und MDC Berlin, Gross Dölln, Germany (September 2008)

Poster: ”Characterization of CD2BP2 and GIGYF2”

XX International Congress of Genetics, Berlin, Germany (July 2008)

Poster: “Functional characterization of GYF domain containing proteins”

Talks given during this study

Structural Biology Seminar, Biochemistry Department of Tufts University, Boston, USA (October 2011)

Talk: “Characterization of the GYF-domain containing protein CD2BP2”

Group seminar in Ellis Reinherz group at the Dana-Faber Institute, Boston, USA (October 2011)

Talk: “Characterization of the GYF-domain containing protein CD2BP2”

PhD Retreat of FG806 (November 2010)

Talk: “Conditional gene targeting of CD2BP2”

Awards

1. Registration Award of the 10th Transgenic Technology Meeting, St. Pete Beach, Florida (October 2011)

2. 3rd place Poster Award at the Joint Symposium of MDC and FMP, Berlin, Germany (April 2009)

Der Lebenslauf ist in der Online-Version aus Gründen des Datenschutzes nicht enthalten.